NASA/CP—2005-213655/VOL1

2004 NASA Seal/Secondary Air System Workshop

October 2005

The NASA STI Program Office . . . in Profile

Since its founding, NASA has been dedicated to the advancement of aeronautics and space science. The NASA Scientific and Technical Information (STI) Program Office plays a key part in helping NASA maintain this important role.

The NASA STI Program Office is operated by Langley Research Center, the Lead Center for NASA's scientific and technical information. The NASA STI Program Office provides access to the NASA STI Database, the largest collection of aeronautical and space science STI in the world. The Program Office is also NASA's institutional mechanism for disseminating the results of its research and development activities. These results are published by NASA in the NASA STI Report Series, which includes the following report types:

- TECHNICAL PUBLICATION. Reports of completed research or a major significant phase of research that present the results of NASA programs and include extensive data or theoretical analysis. Includes compilations of significant scientific and technical data and information deemed to be of continuing reference value. NASA's counterpart of peer-reviewed formal professional papers but has less stringent limitations on manuscript length and extent of graphic presentations.

- TECHNICAL MEMORANDUM. Scientific and technical findings that are preliminary or of specialized interest, e.g., quick release reports, working papers, and bibliographies that contain minimal annotation. Does not contain extensive analysis.

- CONTRACTOR REPORT. Scientific and technical findings by NASA-sponsored contractors and grantees.

- CONFERENCE PUBLICATION. Collected papers from scientific and technical conferences, symposia, seminars, or other meetings sponsored or cosponsored by NASA.

- SPECIAL PUBLICATION. Scientific, technical, or historical information from NASA programs, projects, and missions, often concerned with subjects having substantial public interest.

- TECHNICAL TRANSLATION. English-language translations of foreign scientific and technical material pertinent to NASA's mission.

Specialized services that complement the STI Program Office's diverse offerings include creating custom thesauri, building customized databases, organizing and publishing research results . . . even providing videos.

For more information about the NASA STI Program Office, see the following:

- Access the NASA STI Program Home Page at ***http://www.sti.nasa.gov***

- E-mail your question via the Internet to help@sti.nasa.gov

- Fax your question to the NASA Access Help Desk at 301–621–0134

- Telephone the NASA Access Help Desk at 301–621–0390

- Write to:
  NASA Access Help Desk
  NASA Center for AeroSpace Information
  7121 Standard Drive
  Hanover, MD 21076

NASA/CP—2005-213655/VOL1

2004 NASA Seal/Secondary Air System Workshop

Proceedings of a conference held at Ohio Aerospace Institute
sponsored by NASA Glenn Research Center
Cleveland, Ohio
November 9–10, 2004

National Aeronautics and
Space Administration

Glenn Research Center

October 2005

This work was sponsored by the Low Emissions Alternative Power Project of the Vehicle Systems Program at the NASA Glenn Research Center.

Available from

NASA Center for Aerospace Information
7121 Standard Drive
Hanover, MD 21076

National Technical Information Service
5285 Port Royal Road
Springfield, VA 22100

Available electronically at http://gltrs.grc.nasa.gov

Executive Summary
Volume 1

The 2004 NASA Seal/Secondary Air System workshop covered the following topics: (i) Overview of NASA's new Exploration Initiative program aimed at exploring the Moon, Mars, and beyond; (ii) Overview of the NASA-sponsored Ultra-Efficient Engine Technology (UEET) program; (iii) Overview of NASA Glenn's seal program aimed at developing advanced seals for NASA's turbomachinery, space, and reentry vehicle needs; (iv) Reviews of NASA prime contractor and university advanced sealing concepts including tip clearance control, test results, experimental facilities, and numerical predictions; and (v) Reviews of material development programs relevant to advanced seals development.

The NASA UEET overview illustrated for the reader the importance of advanced technologies, including seals, in meeting future turbine engine system efficiency and emission goals. For example, the NASA UEET program goals include an 8- to 15-percent reduction in fuel burn, a 15-percent reduction in CO_2, a 70-percent reduction in NO_x, CO, and unburned hydrocarbons, and a 30-dB noise reduction relative to program baselines.

The workshop also covered several programs NASA is funding to develop technologies for the Exploration Initiative and advanced reusable space vehicle technologies. NASA plans on developing an advanced docking and berthing system that would permit any vehicle to dock to any on-orbit station or vehicle, as part of NASA's new Exploration Initiative. Plans to develop the necessary mechanism and "androgynous" seal technologies were reviewed. Seal challenges posed by reusable re-entry space vehicles include high-temperature operation, resiliency at temperature to accommodate gap changes during operation, and durability to meet mission requirements.

Contents

OVERVIEW OF NASA GLENN SEAL DEVELOPMENTS

Bruce M. Steinetz, Margaret P. Proctor, and Patrick H. Dunlap, Jr.
National Aeronautics and Space Administration
Glenn Research Center
Cleveland, Ohio

Irebert Delgado
U.S. Army Research Laboratory
Glenn Research Center
Cleveland, Ohio

Joshua Finkbeiner
National Aeronautics and Space Administration
Glenn Research Center
Cleveland, Ohio

Jeffrey J. DeMange and Christopher C. Daniels
University of Toledo
Toledo, Ohio

Scott B. Lattime
Ohio Aerospace Institute
Brook Park, Ohio

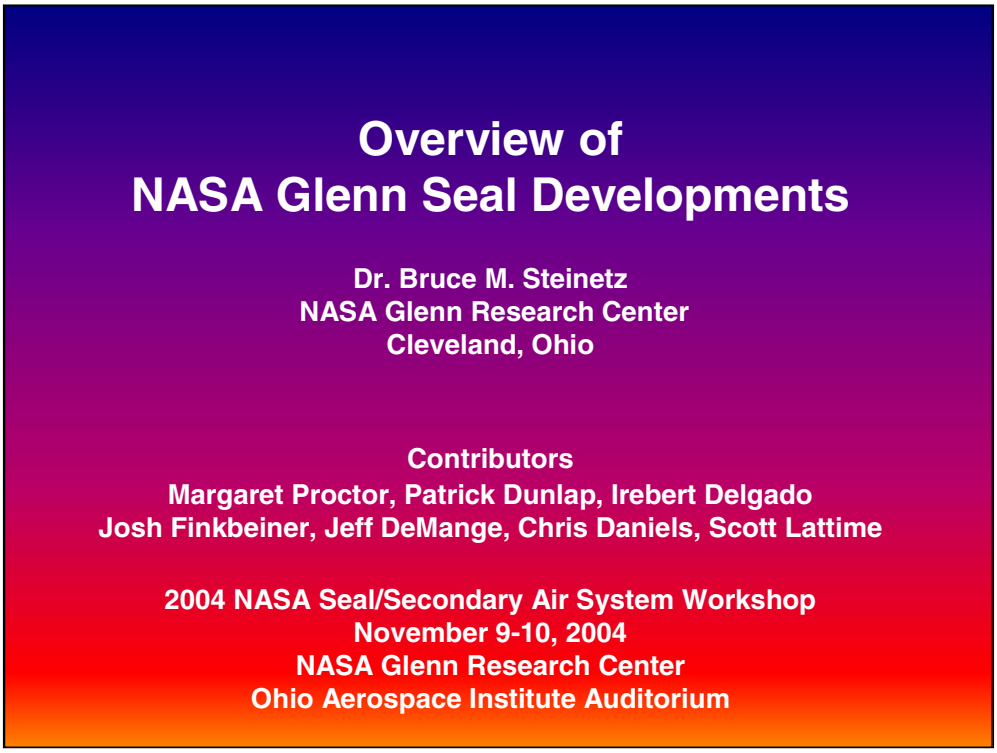

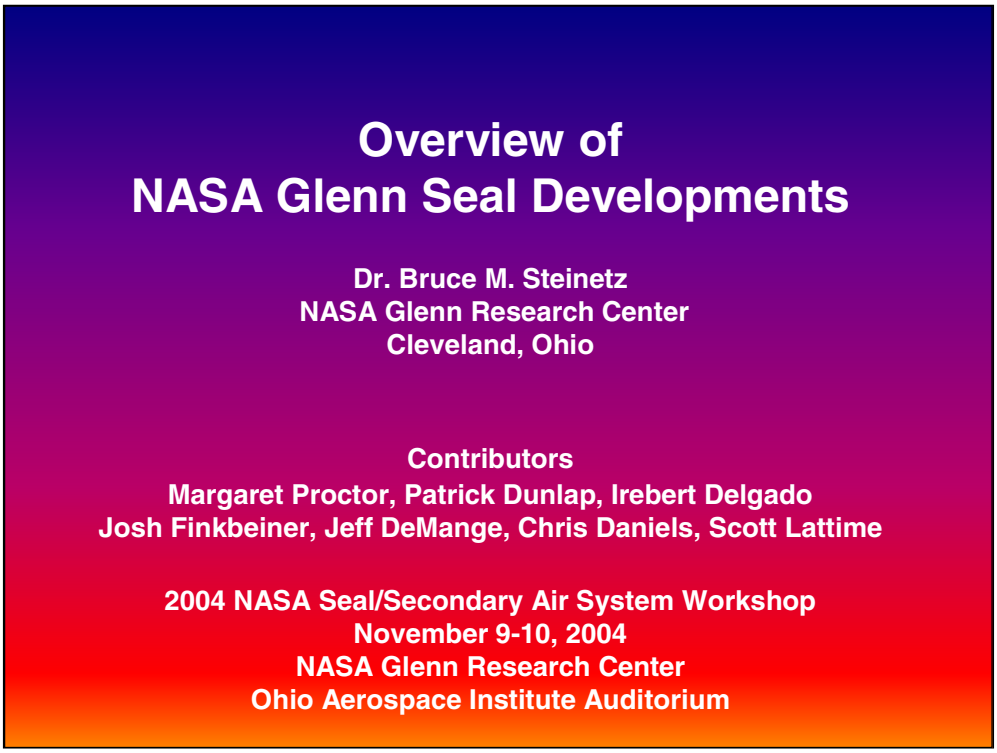

NASA Glenn hosted the Seals/Secondary Air System Workshop on November 9-10, 2004. At this workshop NASA and our industry and university partners shared their respective seal technology developments. We use these workshops as a technical forum to exchange recent advancements and "lessons-learned" in advancing seal technology and solving problems of common interest. As in the past we are publishing the presentations from this workshop in two volumes. Volume I will be publicly available and individual papers will be made available on-line through the web page address listed at the end of this chapter. Volume II will be restricted under International Traffic and Arms Regulations (I.T.A.R.).

The first day of presentations included overviews of NASA programs devoted to the President's new Space Exploration Initiative and advancing the state-of-the-art in turbine engine technology. Ms. Ginty presented an overview of the Ultra-Efficient-Engine Technology (UEET) and Quiet Aircraft Technology (QAT) programs. The UEET program is aimed at developing highly-loaded, ultra-efficient engines that also have low emissions (NOx, unburned hydrocarbons, etc.). Mr. Naininger of NASA's Exploration Project office summarized key elements and long range plans for exploring the Moon and Mars through both robotic and manned missions.

Dr. Steinetz presented an overview of NASA seal developments. Representatives from GE provided insight into their advanced seal developments for both aircraft engines and ground power. Mr. Shaughnessy presented an overview of the work P&W and Stein Seal are doing on the development of high misalignment carbon seals for a geared fan application. Mr. Delgado of NASA Glenn presented an overview of turbine testing at NASA GRC. Ms. Proctor presented a comparison of leakage and power loss results for brush and finger seals NASA GRC obtained using the turbine seal rig.

Turbine engine studies have shown that reducing high pressure turbine (HPT) blade tip clearances will reduce fuel burn, lower emissions, retain exhaust gas temperature margin and increase range. Mr. Ruiz, of General Electric Aircraft Engines, presented results of their Propulsion 21 HPT advanced clearance control study contract. Mr. Watts of Allison Advanced Development Co. presented plans to develop an innovative SMART-Track clearance control mechanism to actively control HPT clearances in the AE30XX series of engines. Mr. Geisheimer of Radatech presented an overview of their microwave blade tip sensor technology. Microwave tip sensors show promise of operation in the extreme gas temperatures present in the HPT location. Dr. Lattime presented the design and development status of a new Active Clearance Control Test rig aimed at demonstrating advanced ACC approaches and sensors. Mr. Turnquist of General Electric Global Research Center presented an overview of wear studies of strip seals used extensively in the ground based power industry.

Dr. Zheng, of PerkinElmer Centurion Mechanical Seals, discussed a non-contacting seal for main shaft locations and component attributes of 2-D and 3-D modeling programs. Dr. Braun presented investigations into a non-contacting finger seal under development by NASA GRC and University of Akron. Mr. Justak presented an overview of non-contacting hybrid seal that combines flexible-beam supported seal pads with a brush secondary seal. Dr. Stango presented analytical assessments of the role of inter-bristle friction force on brush seal hysteresis.

Mr. Richard Thomas of the Bentley Pressurized Bearing Co. presented an overview of a successful program to replace the improperly designed magnetic bearings and brush seals with pressurized bearings and labyrinth seals in a liquid natural gas turboexpander allowing the machine to operate at the required 70,000rpm.

Mr. Robertson of NASA Johnson Space Center presented an overview of a novel docking and berthing mechanism being developed by NASA JSC with support from NASA Glenn Research Center and Marshall Space Flight Center for future space vehicles as part of NASA's new Exploration Initiative. This androgynous docking/berthing system would enable any vehicle to dock or berth with any other on-orbit vehicle. To meet this requirement, a seal-on-seal interface is required posing several interesting challenges. Dr. Chen of Boeing-Huntington Beach presented an overview of the X-37 vehicle development status and seal needs. Mr. Ed Pendleton of Wright-Patterson Air Force Base presented a summary of the goals and objectives of the Air Force Scramjet Engine Demonstrator (SED) program.

Mr. Dunlap presented promising flow and high temperature durability results for a ceramic wafer seal being considered for a variety of applications including engine ramps of future hypersonic airbreathing engines. Mr. DeMange presented recent flow and high temperature scrub results for several seals and counter-face materials being considered for the X-37's control surfaces.

Mr. Finkbeiner presented an overview of an unique arc jet test apparatus being developed to evaluate control surface seals for next generation re-entry and hypersonic vehicles. Mr. Taylor presented high temperature resiliency test results for candidate knitted spring tubes being evaluated for future re-entry vehicle seal needs. Mr. Taylor demonstrated the temperature and resiliency benefits of Rene'41 over the baseline Inconel X-750 wire material.

In the afternoon session, Mr. Oswald presented finite element analysis results for two candidate seal preloaders: the canted coil spring and the knitted spring tube. Mr. Oswald's results are providing useful insight into the stress states that exist under load helping guide seal preloader design and selection.

Advanced structural seals and preloading elements require application of advanced high temperature materials. The closing session of the workshop presented seal concepts and materials being developed at several locations. Mr. Paquette presented Refractory Composites' efforts to develop a refractory metal canted coil spring seal preloader, under contract to NASA GRC. Mr. More (Advanced Products) and Dr. Datta (Advanced Components and Materials) presented recent progress in their high temperature (1600-1800°F) metallic seal development.

Another Seal Team goal is to increase the temperature capability of our braided hybrid seal. The hybrid seal combines the features of a lightweight braided ceramic core with an abrasion resistant metallic core outer sheath. Formerly the outer sheath was made of Haynes 188 wires limiting use to <1800°F. Ms. Opila investigated the oxidation behavior of several promising wire materials (e.g. Kanthal and PM2000) for service potentially to 2200°F.

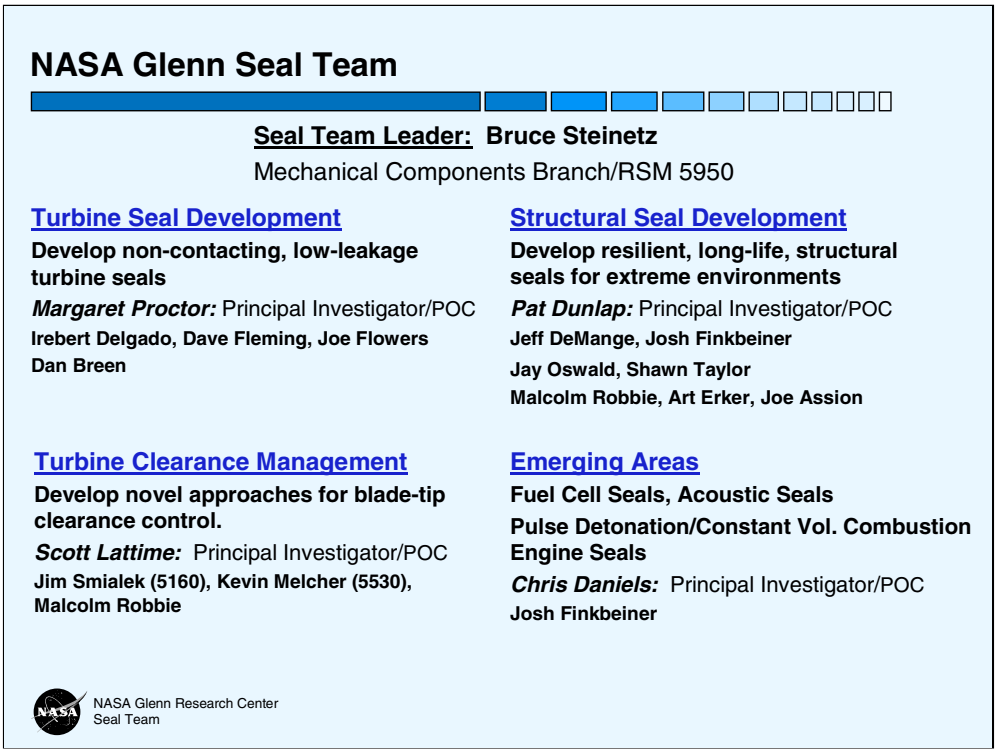

The Seal Team is divided into four primary areas. The principal investigators and supporting researchers for each of the areas are shown in the slide. These areas include turbine seal development, structural seal development, turbine clearance management, and seals for emerging areas. The first area focuses on high temperature, high speed shaft seals for turbine engine secondary air system flow management. The structural seal area focuses on developing resilient structural seals required to accommodate and seal structural distortions in extreme space- and aero-applications. Our goal in the turbine clearance management project is to develop advanced sealing approaches for minimizing blade-tip clearances and leakage. We are planning on applying either rub-avoidance or regeneration clearance control concepts (including smart structures and materials) to promote higher turbine engine efficiency and longer service lives.

We are also contributing seal expertise in a range of emerging areas. These include acoustic seals (a GRC innovation, see Daniels et al, 2004), fuel cell seals, and seals for pulse detonation/constant volume combustion engines. The fuel cell power and pulse detonation engine applications would see significant efficiency gains through the improvement of their sealing systems.

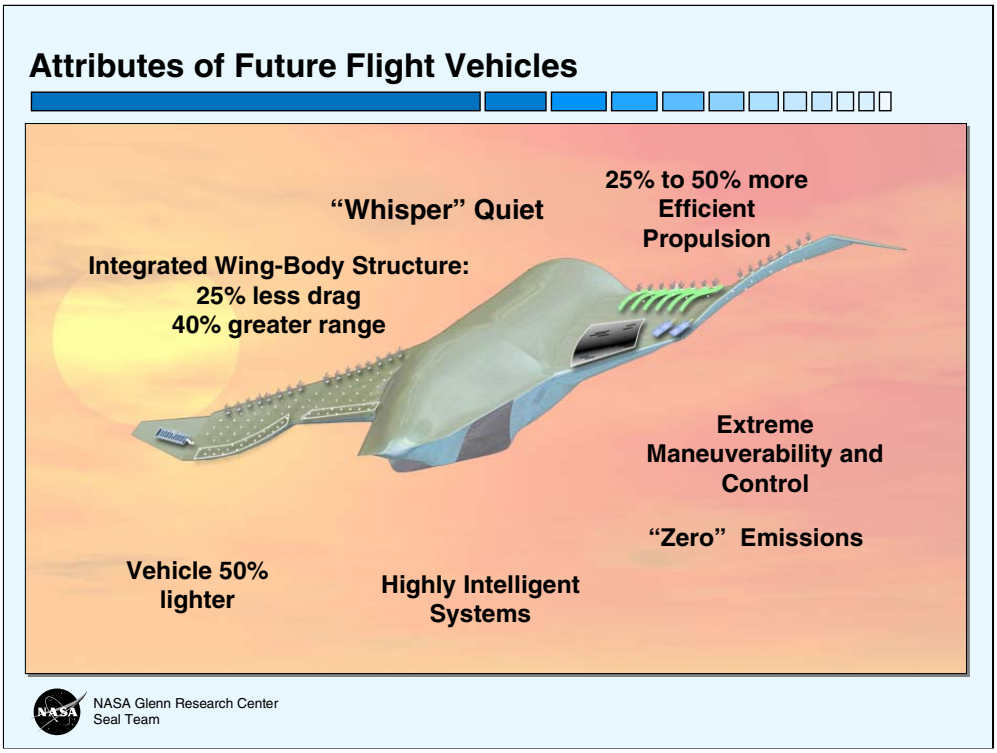

Attributes of future aircraft are illustrated here. Future vehicles will incorporate advanced materials to reduce weight and drag. Future aircraft will also use highly efficient quiet propulsion systems to reduce fuel burn, reduce emissions and reduce noise in and around airports.

One might ask: What role would advanced seals play in these future vehicles? Lower leakage engine seals reduce engine fuel burn and as a result reduce aircraft emissions. Cycle studies have shown the benefits of increasing engine pressure ratios and cycle temperatures to decrease engine weight and improve performance in next generation turbine engines (Steinetz and Hendricks, 1998). Advanced seals have been identified as critical in meeting engine goals for specific fuel consumption, thrust-to-weight, emissions, durability and operating costs. NASA and the industry are identifying and developing engine and sealing technologies that will result in dramatic improvements and address each of these goals.

Aspirating Seal Development: GE90 Demo Program

Funded UEET Seal Development Program

Goal:

Complete aspirating seal development by conducting full scale (36 in. diameter) aspirating seal demonstration tests in GE90 engine.

Payoffs:

- Leakage ~1/4th labyrinth seal
- Decrease SFC by 1.86% for three locations
- Operates without contact under severe conditions:
  + 10 mil TIR
  + 0.25°/0.8 sec tilt maneuver loads (0.08" deflection!)
-

Schedule:

– Complete engine assembly: 4Q CY03
– GE90 engine test **(completed):** 1Q CY04

Partners:

GE/Stein Seal/CFDRC/NASA GRC

NASA Glenn Research Center
Seal Team

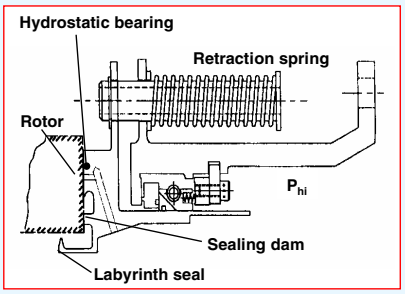

General Electric GE90

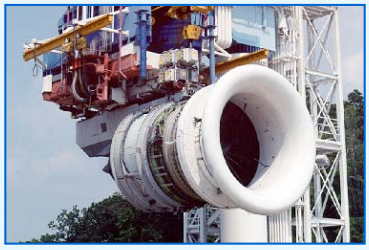

General Electric is developing a low leakage aspirating face seal for a number of locations within modern turbine applications. This seal shows promise both for compressor discharge and low-pressure turbine balance piston locations.

The seal consists of an axially translating mechanical face that seals the face of a high speed rotor (Turnquist et al, 1999). The face rides on a hydrostatic cushion of air supplied through ports on the seal face connected to the high pressure side of the seal. The small clearance (0.001-0.002 in.) between the seal and rotor results in low leakage (1/4th that of new labyrinth seals). Applying the seal to 3 balance piston locations in a GE90 engine can lead to >1.8% SFC reduction. GE Corporate Research and Development tested the seal under a number of conditions to demonstrate the seal's rotor tracking ability. The seal was able to follow a 0.010 in. rotor face total indicator run-out (TIR) and could dynamically follow a 0.25˚ tilt maneuver (simulating a hard maneuver load) all without face seal contact. The NASA GRC Ultra Efficient Engine Technology (UEET) Program funded GE to demonstrate this seal in a ground-based GE-90 demonstrator engine in 2003-2004. More details can be found in Boyle and Albers, 2005 in this Seal Workshop Proceedings and Turnquist, et al 1999.

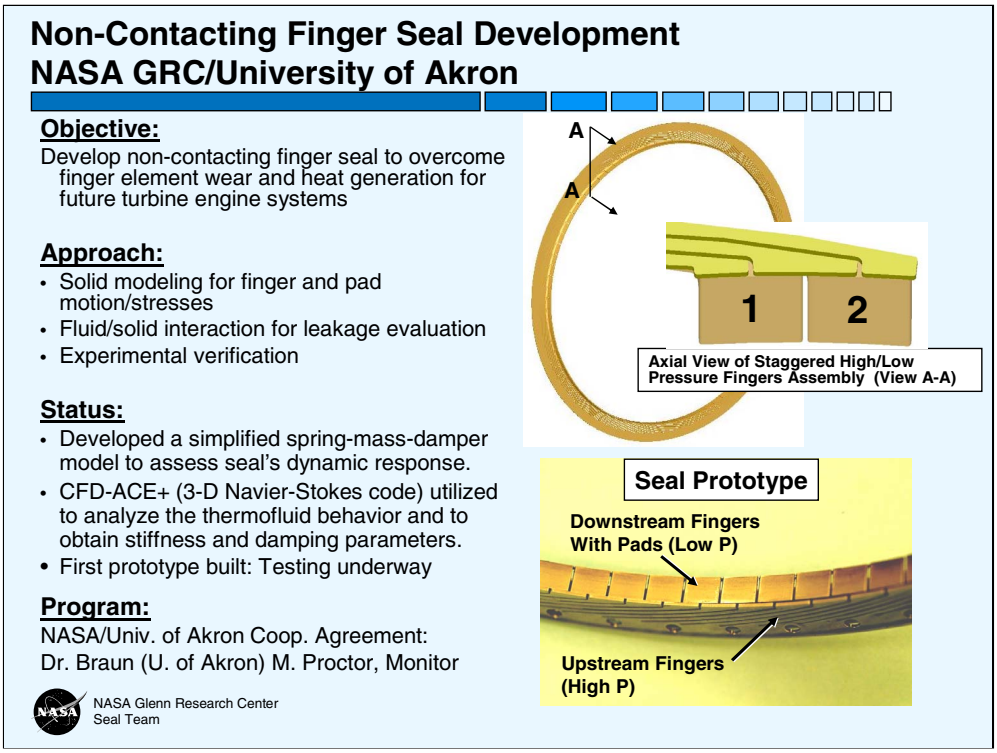

Conventional finger seals like brush seals attain low leakage by operating in running contact with the rotor (Proctor, et al, 2002). The drawbacks of contacting seals include wear over time, heat generation, and power loss (Proctor and Delgado, 2004).

NASA Glenn has developed several concepts for a non-contacting finger seal. In one of these concepts the rear (low-pressure, downstream) fingers have lift pads (see pads 1 & 2 in inset figure) and the upstream (high pressure side) fingers are pad-less, and are designed to block the flow through the slots of the downstream fingers. The pressure-balance on the downstream-finger lift-pads cause them to lift. The front fingers are designed to ride slightly above the rotor preventing wear. Pressure acts to hold the upstream fingers against the downstream fingers. It is anticipated that the upstream/downstream fingers will move radially as a system in response to shaft transients. The NASA Glenn non-contacting finger seal was recently awarded a U.S. patent No. 6,811,154. (Proctor and Steinetz, 2004)

Dr. J. Braun of University of Akron is performing analyses and tests of this GRC concept through a cooperative agreement (Braun et al, 2003). University researchers developed an equivalent spring-mass-damper system to assess lift characteristics under dynamic excitation. Fluid stiffness and damping properties were obtained utilizing CFD-ACE+ (3-D Navier-Stokes code) and a perturbation approach. These stiffness and damping properties were input into the dynamic model expediting the solution to aid in the design of the finger and pod configurations. Dr. Braun and his team subsequently fabricated a first generation non-contacting finger seal based on this design. Early test results showed that the finger seal operates without contact with the shaft at pressures up to 15 psid. Non-contact operation was proven via both electric-circuit continuity and high magnification photo-imagery. More details can be found in Braun et al, 2005 in this Seal Workshop Proceedings. After feasibility tests are complete at the University, seals will be tested under high speed and high temperature conditions at NASA GRC.

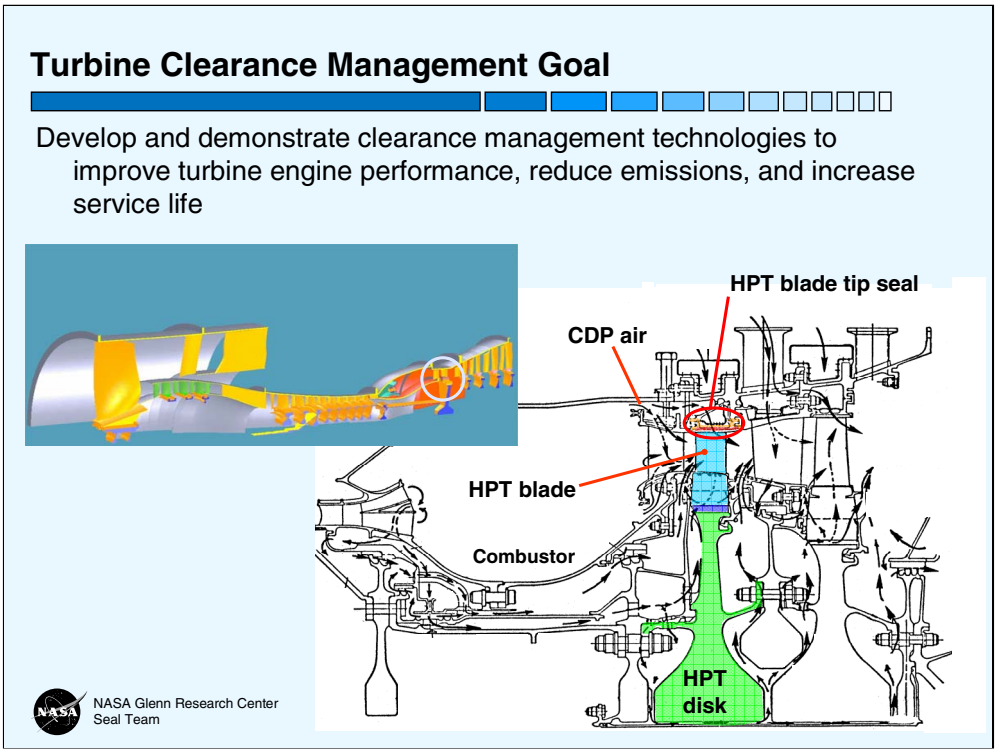

System studies have shown the benefits of reducing blade tip clearances in modern turbine engines, especially the high pressure turbine. Minimizing blade tip clearances throughout the engine will contribute materially to meeting NASA's Ultra-Efficient Engine Technology (UEET) turbine engine project goals of reducing fuel burn and emissions. NASA GRC is examining two candidate approaches including rub-avoidance and regeneration.

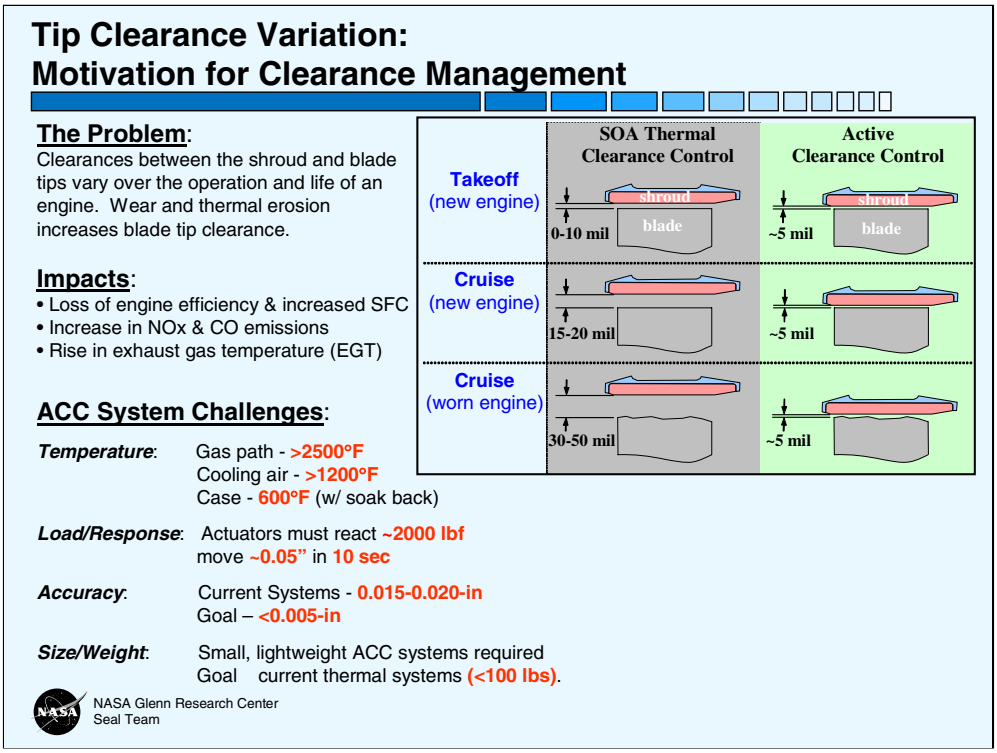

Clearances between the shroud and blade tips vary over the operation and life of an engine. During operation, variations in tip clearance occur primarily due to differences in thermal growth of the case and thermal-mechanical growth of the rotor. Wear of the shroud and blade tips due to rubs and thermal erosion increases over the engine's life and contributes to permanent increases in blade tip clearance. As clearances increase, the engine runs hotter (less efficient) to achieve the same thrust and speed.

Current ACC systems use fan and compressor air to contract the HPT case flanges, varying the shroud diameter, and hence blade-tip clearance during cruise (see thermal clearance control illustration above). These systems cannot respond to fast transient events such as takeoff, re-accel, and sudden step altitude changes. Adequate cold-build clearances are chosen to prevent rubbing between the blade tips and shroud seals during minimum clearance events. As such, tip clearances are larger than desired throughout the flight profile causing greater fuel burn and emissions and shorter range. Utilizing our proposed fast-response, mechanical systems will minimize clearances throughout flight operation, including fast transient events. (See active clearance control illustration above)

There are a number of challenges that must be overcome in developing a successful active clearance control (ACC) system. One of the largest challenges of those listed above is the extreme thermal environment the ACC system must operate in. Gas path temperatures exceed 2500°F and shroud cooling temperatures exceed 1200°F.

Benefits of Blade Tip Clearance Control

- Fuel Savings/ Reduced Emissions (HPT)
  - 0.010-in tip clearance is worth ~0.8-1% SFC
  - Emissions Reduction (Landing/Takeoff – Ref. GE Propulsion 21 Study)
    - » NOx
    - » CO
- Increased Cycle Life (Reduced Maintenance Costs)
  - Deterioration of exhaust gas temperature (EGT) margin is the primary reason for aircraft engine removal from service
  - 0.010-in tip clearance is worth ~10 ºC EGT
  - Allows turbine to run at lower temperatures, increasing cycle life of hot section components and engine time-on-wing (~1000 cycles)
- Increased Efficiency/Operability
  - Increased payload and mission range capabilities
  - Increased high pressure compressor (HPC) stall margin

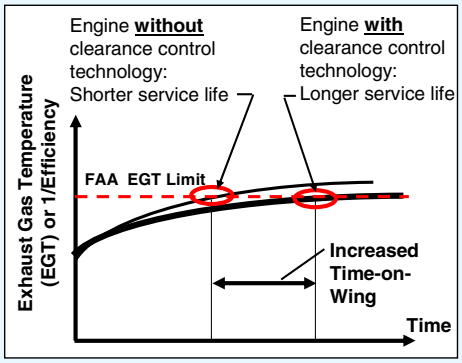

Clearance Control Technology Promotes High Efficiency and Long Life

NASA Glenn Research Center
Seal Team

Blade tip clearance opening is a primary reason for turbine engines reaching their FAA certified exhaust gas temperature (EGT) limit and subsequent required refurbishment. As depicted in the chart on the right, when the EGT reaches the FAA certified limit, the engine must be removed and refurbished. By implementing advanced clearance control measures, the EGT rises slower (due to smaller clearances) increasing the time-on-wing.

In summary, benefits of clearance control in the HPT turbine section include lower specific fuel consumption (SFC), lower emissions (NOx, CO), retained exhaust gas temperature (EGT) margins, higher efficiencies, longer range (because of lower fuel-burn) (see General Electric Report, 2004 and Lattime et al, 2002). Benefits of clearance control in the compressor include better compressor stability (e.g. resisting stall/surge), higher stage efficiency, and higher stage loading. All of these features are key for future NASA and military engine programs.

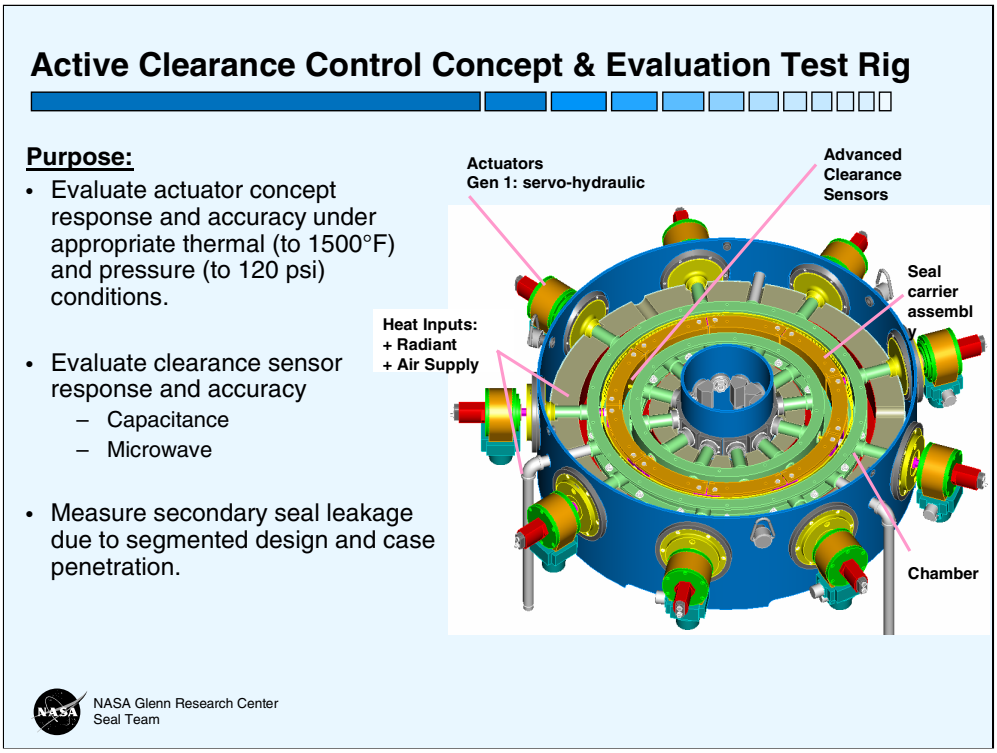

NASA GRC is developing a unique Active Clearance Control (ACC) concept and evaluation test rig. The primary purpose of the test rig is to evaluate actuator concept response and accuracy under appropriate thermal (to 1300+F) and pressure (up to 120 psig) conditions. Other factors that will be investigated include:

•Actuator stroke, rate, accuracy, and repeatability

•System concentricity and synchronicity

•Component wear

•Secondary seal leakage

•Clearance sensor response and accuracy

The results of this testing will be used to further develop/refine the current actuator design as well as other advanced actuator concepts. More details regarding this test rig can be found in Lattime and Steinetz 2005 in this Seal Workshop Proceedings, and Lattime et al, 2003.

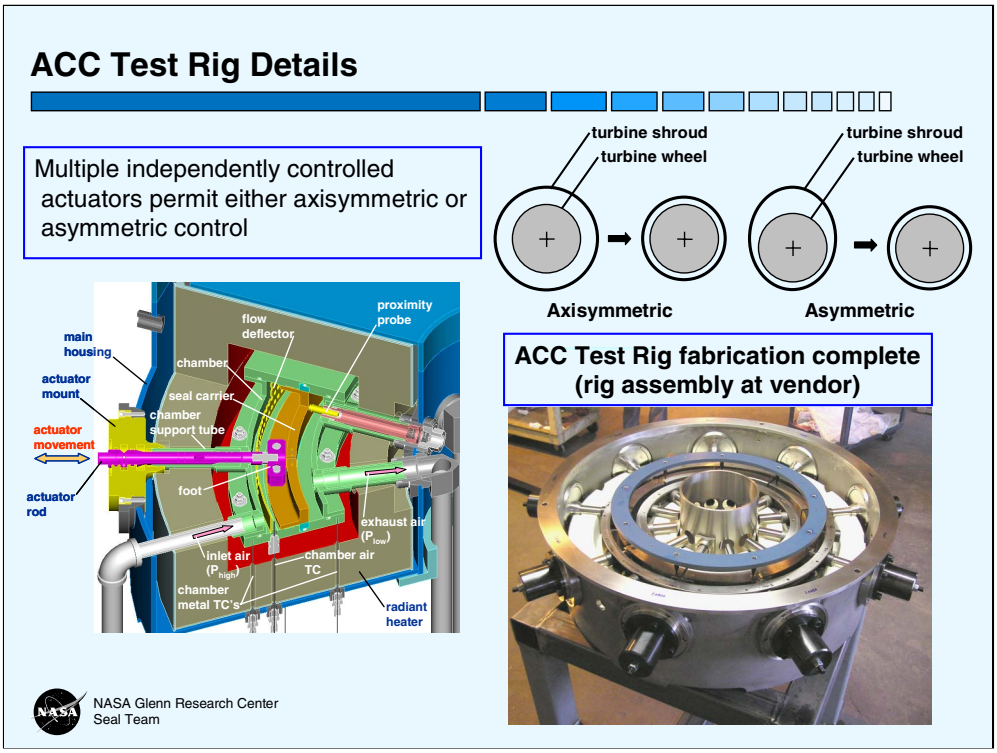

The ACC test rig under development utilizes nine independently controlled actuators. This will permit assessment of both axisymmetric control and asymmetric control. Because of engine thermal and structural non-uniformities, engine case structures can become egg-shaped. Under these circumstances, asymmetric control strategies would permit more uniform clearances around the circumference.

The ACC test rig fabrication has been completed, as shown in the lower right figure. However, the hydrotest performed revealed some weld cracks that are currently being investigated.

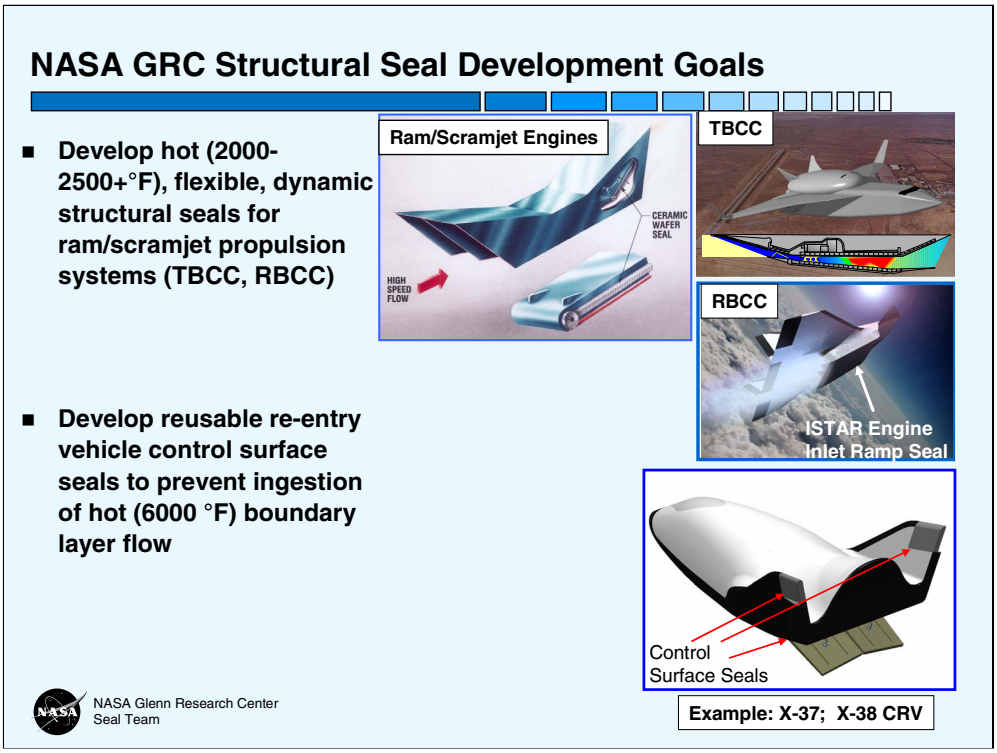

NASA GRC is developing advanced structural seals for both propulsion and vehicle needs by applying advanced design concepts made from emerging high temperature ceramic materials and testing them in advanced test rigs. See Dunlap 2005, et al, and Finkbeiner 2005, et al in this Seal Workshop Proceedings and Dunlap 2004a, b, et al and DeMange 2004, et al for further details.

FALCON Hypersonic Vehicle Seal Development

- Objective: Develop high temperature seals for control surfaces and access doors on future hypersonic vehicles
- Requirements
  - Temperature: Extreme
  - Life: Reusable
  - Mission duration: Less than 2 hrs
- Approach
  - Identify and develop high temperature seals and preload devices
  - Perform critical function performance tests at GRC
  - Perform arc jet tests on leading concepts at JSC
- Partner organizations: DARPA, Lockheed Martin

NASA Glenn Research Center
Seal Team

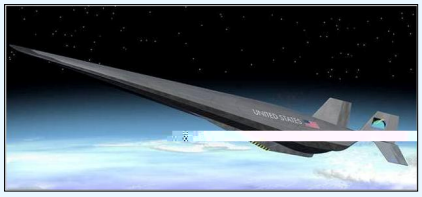

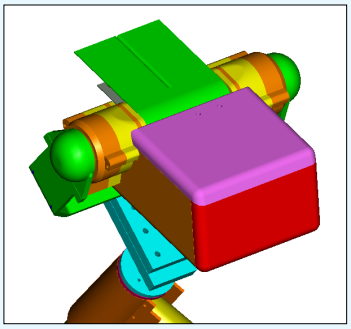

Model of GRC seal arc jet test fixture

NASA GRC is working under DARPA sponsorship to develop control surface seals for future hypersonic weapon systems under a program known as FALCON.

In this program we plan on identifying and developing seals and preloader system that can meet the expected temperatures and pressures. We will perform critical function performance tests utilizing our new test capabilities described on the next chart. Those concepts that meet functional requirements will then be tested in an arc jet environment at NASA JSC. We will use an arc jet test fixture that can subject candidate seals and ceramic matrix composites to simulated hypersonic flight conditions.

A unique feature of this new test fixture is the ability to asses the effects of flap motion on seal performance during arc jet testing. More detail regarding this fixture can be found in Finkbeiner, et al, 2004 and Finkbeiner, et al 2005 in this Seal Workshop Proceedings.

Example Structural Seals Being Investigated

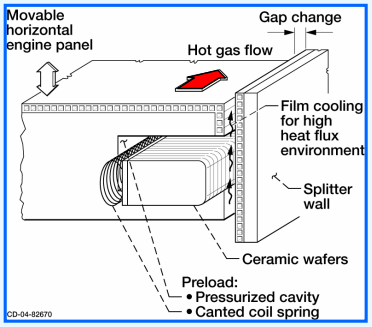

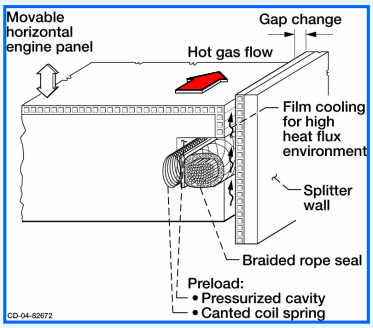

Ceramic Wafer Seal

- High temperature operation: 2500+˚F
- Low Leakage
- Flexibility: Relative sliding of adjacent wafers conforms to wall distortions
- Ceramic material lighter weight than metal system
- Tandem seals permit central cavity purge (cooling)

Braided Rope Seal

- High temperature operation: 2400+°F
- Flexible: seals & conforms to complex geometries
- Hybrid design (ceramic core/superalloy wire sheath) resists abrasion
- Tandem seals permit central cavity purge (cooling)

NASA Glenn Research Center
Seal Team

NASA GRC's work on high temperature structural seal development began in the late 1980's during the National Aero-Space Plane (NASP) project. GRC led the in-house propulsion system seal development program and oversaw industry efforts for propulsion system and airframe seal development for this vehicle.

Two promising concepts identified during that program included the ceramic wafer seal (Dunlap, 2004a et al and Steinetz, 1991) and the braided rope seal (DeMange, 2004 et al, Steinetz and Adams, 1998) shown here. By design, both of these seals are flexible, lightweight, and can operate to very high temperatures (2400+˚F). Both types of seals require some form of high temperature preload system. A high temperature canted coil spring is shown behind the seals shown. More information on the features and benefits of the canted coil spring can be found in Dunlap et al, 2004b and Oswald et al 2004 and Oswald 2005, et al in this Seal Workshop Proceedings. Refractory metals and oxygen resistant coatings being considered for the spring can be found in Paquette, 2005 in this Seal Workshop Proceedings.

A second type of preload system is also under development at GRC for textile based thermal barriers. A spring tube knitted out of Rene '41 shows greater resiliency at both 1500° and 1750°F than if made of the conventional Inconel X-750 material. (Taylor et al, 2004 and in Taylor et al, 2005 in this Seal Workshop Proceedings.)

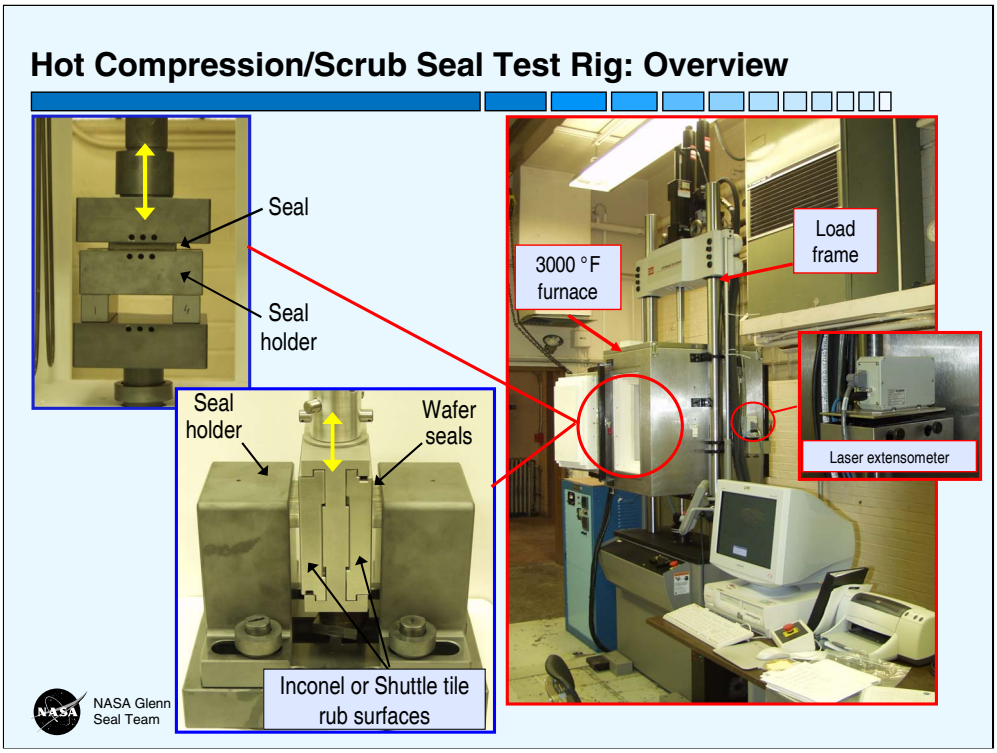

NASA GRC has installed state-of-the-art test capabilities for evaluating seal performance at temperatures up to 3000 °F (1650 °C). This one-of-a-kind equipment is being used to evaluate existing and new seal designs by simulating the temperatures, loads, and scrubbing conditions that the seals have to endure during service. The compression test rig (upper left photo) is being used to assess seal load vs. linear compression, preload, & stiffness at temperature. The scrub test rig (middle photo) is being used to assess seal wear rates and frictional loads for various test conditions at temperature. Both sets of fixtures are made of silicon carbide permitting high temperature operation in air.

The test rig includes: an MTS servo-hydraulic load frame, an ATS high temperature air furnace, and a Beta LaserMike non-contact laser extensometer, and the special purpose seal holder hardware. Unique features of the load frame include dual load cells (with multi-ranging capabilities) for accurate measurement of load application, dual servo-valves to permit precise testing at multiple stroke rates (up to 8 in./s.), and a non-contact laser extensometer system to accurately measure displacements.

Shuttle Main Landing Gear Door Seal Tests

- Objective: Perform flow and compression tests on Shuttle main landing gear (MLG) door environmental seal at different compression levels
- Why important?
  - JSC using data to determine acceptable seal gap range that can be verified each time MLG doors are closed for flight
  - Concerned about long term seal creep; need way to predict when to change out seals
- Two phases of testing
  - Phase I (Summer 2004): Flow tests on "as-received" seals
  - Phase II (1Q FY05):
    - » Flow tests on "flown" seals
    - » Compression tests on "flown" and "as-received" seals including 30-day compression test

NASA Glenn Research Center
Seal Team

At the request of NASA Johnson Space Center (JSC), a series of tests are being conducted by the Seal Team at GRC on the Shuttle main landing gear (MLG) door environmental seal in support of the Shuttle Return-to-Flight Program. This includes both flow tests and compression tests on the seals at different compression levels. JSC is using the data to determine an acceptable seal gap range that can be verified each time the MLG doors are closed for flight. They are also concerned about the effects of long-term creep when the seal is compressed for extended periods of time. The seal takes on a permanent set under these conditions and may not stay in contact with the opposing sealing surface at all times. JSC would like to determine a way to predict when the seals need to be replaced to avoid possibly dangerous situations that could occur if they take on too much permanent set.

This work has been divided into two phases of testing. This past summer the Seal Team completed a series of flow tests for JSC on samples of the "as-received" seal that had not yet flown on the Shuttle. Upon recently inspecting the MLG door environmental seals installed on several of the Shuttle orbiters, JSC discovered that they had taken on a set and were permanently compressed. JSC asked the Seal Team to repeat the sequence of leakage tests on these "flown" seals to determine how much flow gets past them if the seals do not stay in contact with the sealing surfaces in their permanently-compressed state. JSC has also requested that a series of compression tests be performed on as-received and flown seals to determine how much resiliency they have in each condition. A 30-day compression test will also be performed to evaluate the effects of long-term seal creep on seal resiliency.

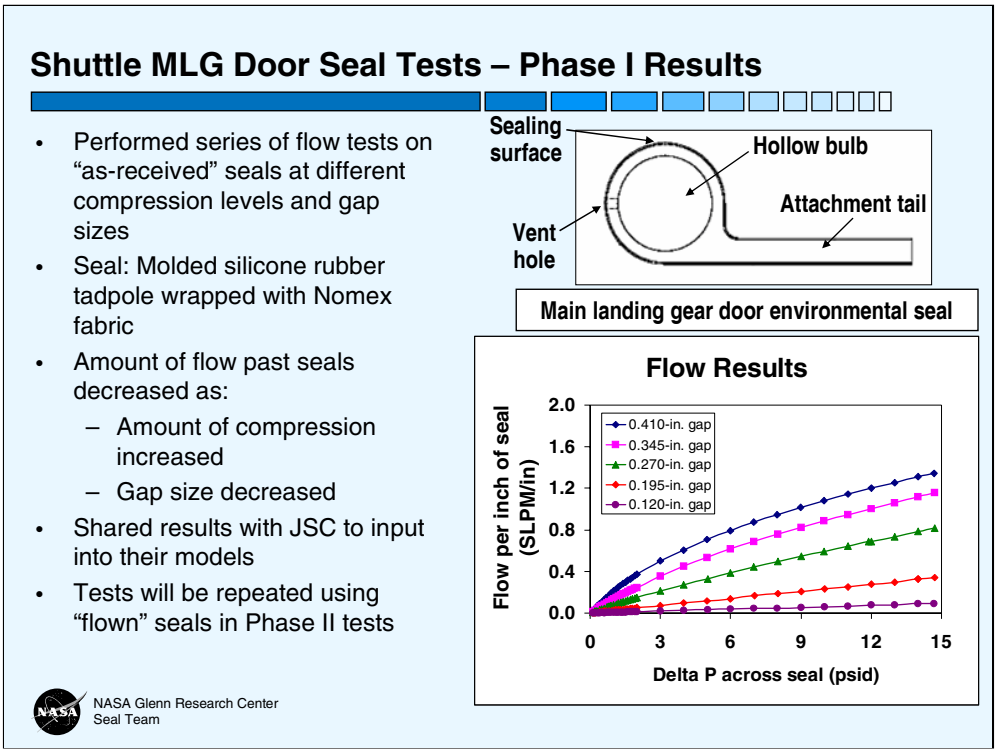

In Phase I, a series of successful flow tests were conducted on the "as-received" seals at different compression levels and gap sizes. Samples were leak tested at pressures up to 14.7 psid. This seal is currently produced by Northrop Grumman and consists of a silicone (ZZ-R-765, Class IIIa, Grade 50) core and tail which are wrapped with Nomex fabric. As expected, the amount of flow past the seals decreased as the amount of compression on the seals was increased and the gap size decreased. A final report was completed and forwarded to JSC for review and further analysis. These flow tests will be repeated in Phase II using "flown" seals that were removed from the Shuttle.

Shuttle RCC Leading Edge Permeability Tests

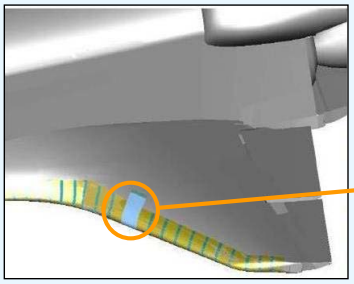

Individual leading edge panel

- Objective: Measure permeability of Shuttle leading edge reinforced carbon/carbon (RCC) material (coated & uncoated) in support of Return-to-Flight program
- Why important?
  - Material permeability determines amount of hot gas that can pass through leading edge and into cavity behind it
  - JSC using permeability values for carbon/carbon oxidation calculations under reentry conditions

NASA Glenn Research Center
Seal Team

The GRC Seal Team is also supporting the Return-to-Flight program by measuring the permeability of the reinforced carbon/carbon (RCC) material that makes up the Shuttle leading edges. This material is being evaluated in both coated and uncoated states to determine how the coating affects RCC permeability. These tests are important because the permeability of this material determines how much hot gas is able to pass through the leading edge and into the cavity behind it where lower-temperatures structures are located. JSC is also planning to use the permeability values that GRC records to calculate oxidation of the RCC material under reentry conditions.

Shuttle RCC Leading Edge Permeability Tests

- New test fixture used to measure permeability of porous and semi-porous materials based on data recorded during leak decay testing
- Automated data system tracks pressure decay vs. time
- Data used to calculate mass flow and permeability
- Initial results for coated RCC specimen show good correlation in mass flow vs. ΔP between GRC data and data recorded by Vought in 1980

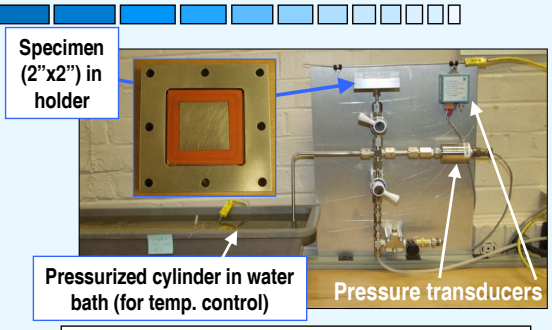

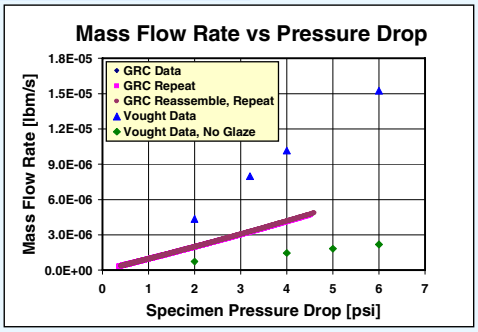

NASA Glenn Research Center
Seal Team

To perform these tests, GRC has installed a new test fixture that is being used to measure material permeability based on data recorded during leak decay tests. During these tests, a cylinder upstream of the test specimen is pressurized to a desired pressure. This pressure is then allowed to decay as air flows through the test specimen. An automated data acquisition system monitors the pressure decay versus time, and this data is then used to calculate the amount of mass flow through the specimen and the permeability of the material. Initial results for a coated RCC specimen have shown good correlation in the amount of mass flow through the specimen versus the pressure drop across the specimen when comparing GRC data to data presented in a report by Vought in 1980. The next step is to test an uncoated specimen and compare its permeability to that of the coated specimen.

Seal Development for Advanced Docking/Berthing System

Space Exploration Initiative

- Objective: Support NASA JSC by developing seals for advanced docking/berthing system
- Requirements
  - Seal diameter: 54 in.
  - Near hermetic seal
  - Seal-on-seal interface for androgynous system
  - Survive space environment (atomic oxygen, UV, thermal cycling) for long duration (est. 3-5+ yrs)
- Approach
  - Identify candidate elastomeric and metallic seals
  - Perform coupon-level and small-scale environmental exposure and flow tests
  - Perform mid-scale flow tests before and after environmental exposure (incl. variable gap, offset, hot and cold, seal-on-seal)
  - Down-select between competing concepts
  - Support scale-up and thermal-vacuum system-level tests at MSFC

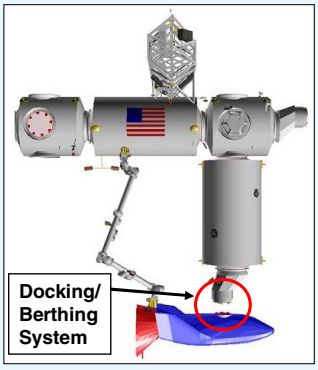

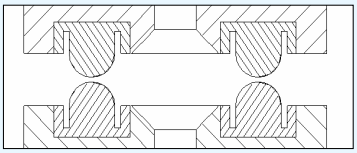

Seal-on-seal interface

NASA Glenn Research Center
Seal Team

NASA plans on developing an advanced docking and berthing system that would permit any vehicle to dock to any on-orbit station or vehicle, as part of NASA's new Exploration Initiative. (More detail on this new docking and berthing system can be found in Robertson 2005, in this Seal Workshop Proceedings.) To meet this "androgynous" operational goal, a seal-on-seal interface is required, as depicted in the lower graphic.

GRC will be supporting JSC in developing seal technology for this seal interface. Any seal developed must meet the stringent requirements identified including near-hermetic operation, prevent seal pull-out and resist space environments (atomic oxygen, UV, radiation and thermal cycling) for five plus years, amongst others. An evolutionary development approach has been identified as outlined above.

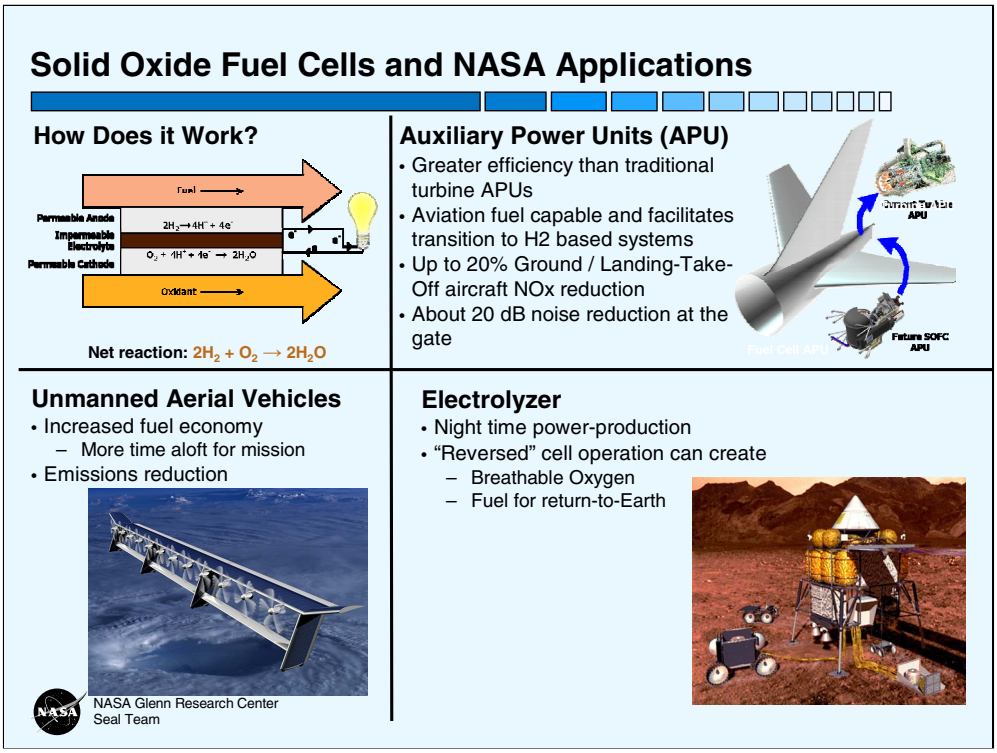

A fuel cell is an energy conversion device that generates electricity and heat by electrochemically combining fuel and oxidizer via an ion-conducting electrolyte. The electrochemical reaction is more attractive than combustion since the process is more efficient and less polluting. Solid Oxide Fuel Cells (SOFCs) are unique in that they are fuel flexible, using hydrogen, carbon monoxide, natural or coal gas, or low-sulfur jet fuel as the reactant.

NASA has three potential applications for SOFCs... (1) Commercial aircraft would benefit greatly by the substitution of SOFC-powered auxiliary power units (APUs) with (a) increased efficiency at both ground idle and in cruise, (b) reduced emissions of NOx, SOx, and particulates, (c) potentially greater power generating capability at altitude, and (d) gate noise reduction. (2) A hydrogen powered unmanned aerial vehicle (UAV) capable of flying for up to 10 days and solar-electric aircraft capable of multiple-week duration flights are both candidates for SOFC propulsion power. (3) A reversible SOFC could provide Space Exploration Initiative missions with power generation for base operations, fuel generation for the return trip, and breathable oxygen for astronaut explorers.

Fuel Cell Seal Development

What are the problems with SOFC seals?

- Coefficient of Thermal Expansion (CTE) mismatch between the adjacent components causes relative displacements and seal damage
- Loss of seal integrity reduces SOFC performance due to
  - Fuel/air leakage
  - Electrode poisoning

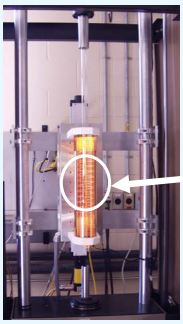

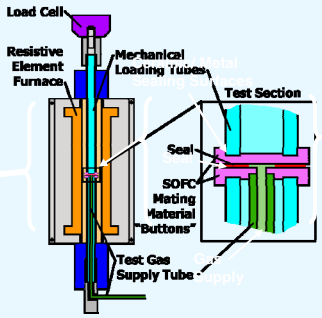

Approach: Pursue a multidisciplinary development effort including:

- Thermo-structural analyses
- Novel seal design concepts
- Advanced materials
- Experimentation

Test Apparatus Capabilities:

- Temperatures (up to 1100°C)
- Temperature transients (approx. 1°C/second)
- Gases (helium, air, and other non-combustibles)
- Gas pressures (up to 2.5 psig)
- Mechanical loads (up to 1000 lbf)

NASA Glenn Research Center
Seal Team

Planar SOFCs require high temperature hermetic seals to (1) prevent mixing of the fuel and oxidant within the stack, (2) prevent parasitic leakage of the fuel from the stack, (3) prevent contamination of the anode by air leaking into the stack, (4) electrically isolate the individual cells within the stack, and (5) mechanically bond the cell components. The sealing challenges are aggravated by the need to maintain hermetic boundaries between the different flow paths during transient (heating / cooling) operation with vibration loads.

NASA GRC is taking a multidisciplinary approach to developing SOFC seals. Thermo-structural analyses, novel seal concept development, advanced materials development, and experimental leakage determination are being simultaneously pursued to solve the sealing challenges.

A leakage facility has been built at NASA GRC to accurately measure any leakage through SOFC seals while simultaneously exposing the seal to an environment that closely resembles that of an operating fuel cell. Capable of heating to temperatures as high as 1100 Celsius at ramp rates of approximately 1 degree Celsius per second, the system measures the leakage of any non-combustible gas while maintaining compressive mechanical loads on the seal.

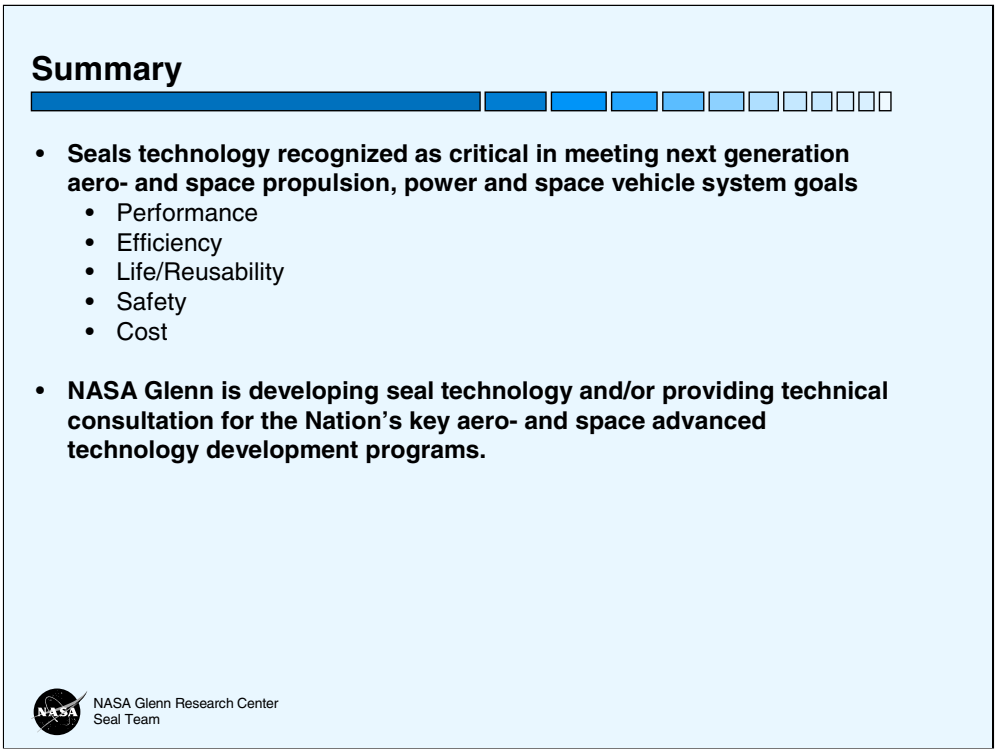

NASA Glenn is currently performing seal research supporting both advanced turbine engine development and advanced space vehicle/propulsion system development. Studies have shown that decreasing parasitic leakage through applying advanced seals will increase turbine engine performance and decrease operating costs.

Studies have also shown that higher temperature, long life seals are critical in meeting next generation space vehicle and propulsion system goals in the areas of performance, reusability, safety, and cost.

NASA Glenn is developing seal technology and providing technical consultation for the Agency's key aero- and space technology development programs.

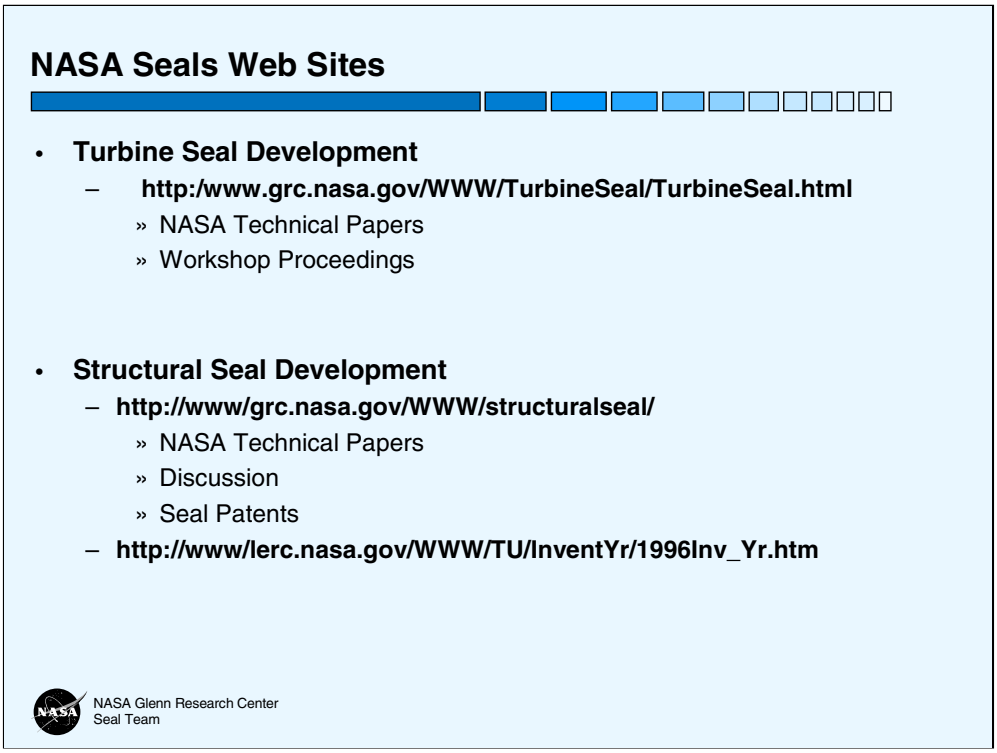

The Seal Team maintains three web pages to disseminate publicly available information in the areas of turbine engine and structural seal development. Please visit these web sites to obtain past workshop proceedings and copies of NASA technical papers and patents.

References

- Braun, M.J., Choy, F.K., Pierson, H.M., 2003, “Structural and Dynamic Considerations Towards the Design of Padded Finger Seals”, AIAA-2003-4698 presented at the AIAA/ASME/SAE/ASEE conference, July, Huntsville, AL.
- Daniels, C., Finkbeiner, J, Steinetz, B.M., Li, Xiaofan, Raman, G, 2004, “Non-linear Oscillations and Flow of Gas Within Closed and Open Conical Resonators,” AIAA-2004-0677. To be presented at the 82nd AIAA Aerosciences Meeting, Reno, NV, January.
- DeMange, J.J., Dunlap, P.H., Steinetz, B.M., 2004,“Advanced Control Surface Seal Development for Future Space Vehicles,” Presentation and Paper at 2003 JANNAF Conference, Dec. 1-5, Colorado Springs, CO. (NASA TM-2004-212898).
- Dunlap, P.H., Steinetz, B.M., DeMange, J.J., 2004a, “Further Investigations of Hypersonic Engine Seals,” NASA TM-2004-213188, AIAA-2004-3887, August. Presented at the 2004 AIAA/ASME/SAE/ASEE Joint Propulsion Conference, July 2004, Ft. Lauderdale, FL.
- Dunlap, P.H., Steinetz, B.M., DeMange, J.J., 2004b, “High Temperature Propulsion System Structural Seals for Future Space Launch Vehicles,” Presentation and Paper at 2003 JANNAF Conference, Dec. 1-5, Colorado Springs, CO. (NASA TM-2004-212907).
- Finkbeiner, J.R., Dunlap, P.H., Steinetz, B.M., Robbie, M., Baker, F., and Erker, A., 2004, “On the Development of a Unique Arc Jet Test Apparatus for Control Surface Seal Evaluations,” NASA TM-2004-213204, AIAA-2004-3891, August. Presented at the 2004 AIAA/ASME/SAE/ASEE Joint Propulsion Conference, July 2004, Ft. Lauderdale, FL.
- General Electric Aircraft Engines, 2004, “HPT Clearance Control (Intelligent Engine Systems) – Phase 1 – Final Report,” NASA Contract NAS3-01135, April.
- Lattime, S.B., Steinetz, Bruce M., Robbie, M., 2003, “Test Rig for Evaluating Active Turbine Blade Tip Clearance Control Concepts,” NASA TM-2003-212533, also AIAA-2003-4700, presented at the AIAA/ASME/SAE/ASEE conference, July, Journal of Propulsion and Power, 2004, Huntsville, AL.
- Lattime, S.B., Steinetz, B.M., 2002, “Turbine Engine Clearance Control Systems: Current Practices and Future Directions, “ NASA TM-2002-211794, AIAA 2002-3790.

NASA Glenn Research Center
Seal Team

References (cont'd)

- Oswald, J.J., Mullen, R.H., Dunlap, P.H., and Steinetz, B.M., 2004, "Modeling and Evaluation of High Temperature Canted Coil Springs as Seal Preloading Devices," NASA TM-2004-213189, AIAA-2004-3889, August. Presented at the 2004 AIAA/ASME/SAE/ASEE Joint Propulsion Conference, July 2004, Ft Lauderdale, FL.
- Proctor, M.P., Delgado, I.R., 2004, "Leakage and Power Loss Test Results for Competing Turbine Engine Seals," ASME GT2004-53935, Proceedings of ASME Turbo Expo, Vienna Austria, June.
- Proctor, M.P., Steinetz, B.M., 2004, "NonContacting Finger Seal," U.S. Patent 6,811,154, Issued 11/02/04, (LEW 17,129-1).
- Proctor, M.P; Kumar, A.; Delgado, I.R., 2002, "High-Speed, High Temperature, Finger Seal Test Results," NASA TM-2002-211589, AIAA-2002-3793.
- Steinetz, B.M., Hendricks, R.C., and Munson, J.H., 1998, "Advanced Seal Technology Role in Meeting Next Generation Turbine Engine Goals," NASA TM-1998-206961.
- Steinetz, Bruce M.; Adams, Michael L., 1998, "Effects of Compression, Staging and Braid Angle on Braided Rope Seal Performance", J. of Propulsion and Power, Vol. 14, No. 6, also AIAA-97-2872, 1997 AIAA Joint Propulsion Conference, Seattle, Washington, July 7-9, 1997, NASA TM-107504, July 1997.
- Steinetz, B.M., 1991, "High Temperature Performance Evaluation of a Hypersonic Engine Ceramic Wafer Seal," NASA TM-103737
- Taylor, S.C., DeMange, J.J., Dunlap, P.H., Steinetz, B.M., 2004, "Evaluation of High Temperature Knitted Spring Tubes for Structural Seal Applications," NASA TM-2004-213183, AIAA-2004-3890. Presented at the 2004 AIAA/ASME/SAE/ASEE conference, July, Ft Lauderdale, FL.
- Turnquist, N.A.; Bagepalli, B; Lawen, J; Tseng, T., McNickle, A.D., Kirkes; Steinetz, B.M., 1999, "Full Scale Testing of an Aspirating Face Seal", AIAA-99-2682.

NASA Glenn Research Center
Seal Team

OVERVIEW OF NASA'S EXPLORATION INITIATIVE

Joseph Nainiger
National Aeronautics and Space Administration
Glenn Research Center
Cleveland, Ohio

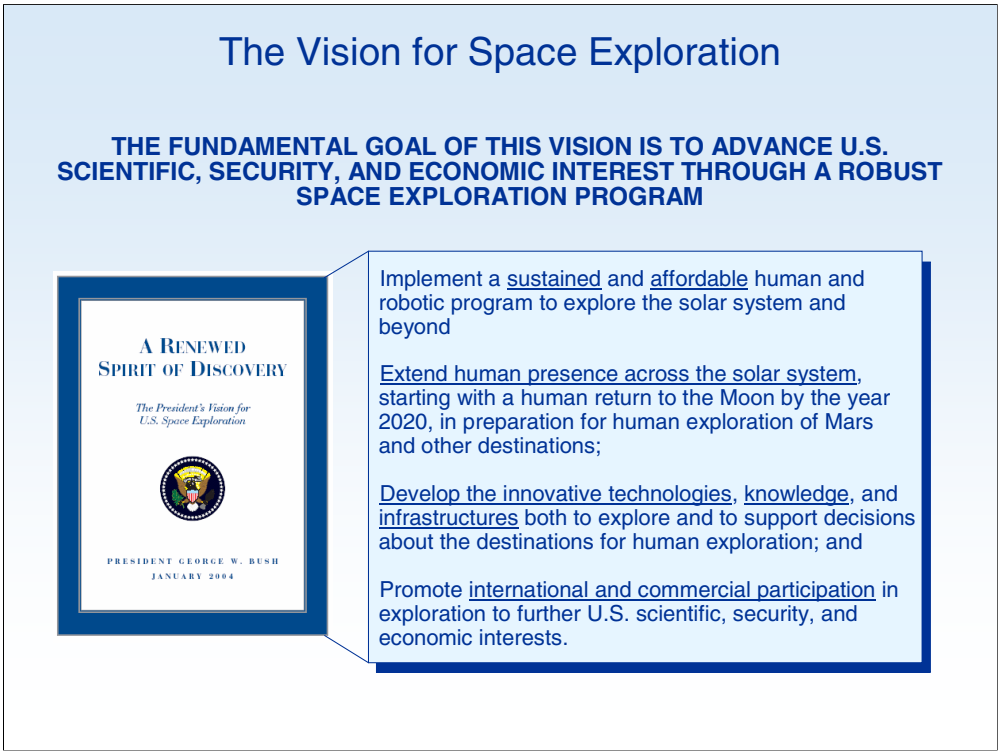

• On January 14th, the President announced that we were going back to the moon, continuing to Mars and Beyond.

• The plan to accomplish this is laid out in the Vision document

• Read "Fundamental Goal" Statement on chart

• Scientific – From a scientific standpoint, exploration and science leads to discovery, which is what drives us

• Security – Security in this sentence is not homeland security, but rather allowing other gov't agencies to leverage our technologies to further their objectives.

• Economic Interest - For less than 1% of the budget, we have improved the quality of life and the aerospace industry has a major economic impact on the nation. We know we will have the same type of return through exploration and discovery in the future, we just can't define what specifically it will be.

• The key word here is sustainability – we are in it for the long haul – we have to get through 30 budget cycles, 8 presidential elections and multiple congresses. We need to be credible. When you have credibility and affordability, you have sustainability.

Key Elements of the Vision

- **Objectives**
  - Implement a sustained and affordable human and robotic program
  - Extend human presence across the solar system and beyond
  - Develop supporting innovative technologies, knowledge, and infrastructures
  - Promote international and commercial participation in exploration

- **Major Milestones**
  - 2008: Initial flight test of CEV
  - 2008: Launch first lunar robotic orbiter
  - 2009-2010: Robotic mission to lunar surface
  - 2011 First Uncrewed CEV flight
  - 2014: First crewed CEV flight
  - 2015: Prometheus 1 - Jupiter Icy Moon Orbiter (JIMO)
  - 2015-2020: First human mission to the Moon

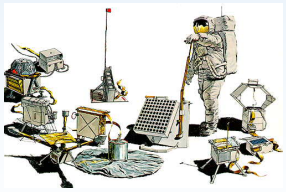

- We have identified a number of transforming changes discussed in our Strategic Plan that are important ingredients for fulfilling our Vision & Mission
- Highlight SUSTAINED being through the future not just for set amount of years.
- Establish credibility by achieving these milestones
- On time and within budget
- Sept 04 a RFI was sent out and over 1000 concepts were received for CEV and 11 selections have been made
- Talk to timeline (major milestones)
- 2012 -2015 Maintaining the importance of Nuclear propulsion research through JIMO

Other questions if asked:

Difference from OSP to CEV is that OSP was low orbit crew return vehicle to ISS, but CEV is planned to travel to the moon and mars.

Realizing the Future
Earth, Moon, Mars, and Beyond

Foster and sustain the exploration culture across generations

- Open new frontiers
- Continuing and inspiring
- A constant impetus to educate and train

Identify, develop, and apply advanced technologies to…

- Enable exploration and discovery
- Allow the public to actively participate in the journey
- Translate the benefits of these technologies to improve life on Earth

Harness the brain power

- Engage the nation's science and engineering assets
- Motivate successive generations of students to pursue science, math, engineering and technology
- Create the tools to facilitate broad national technical participation

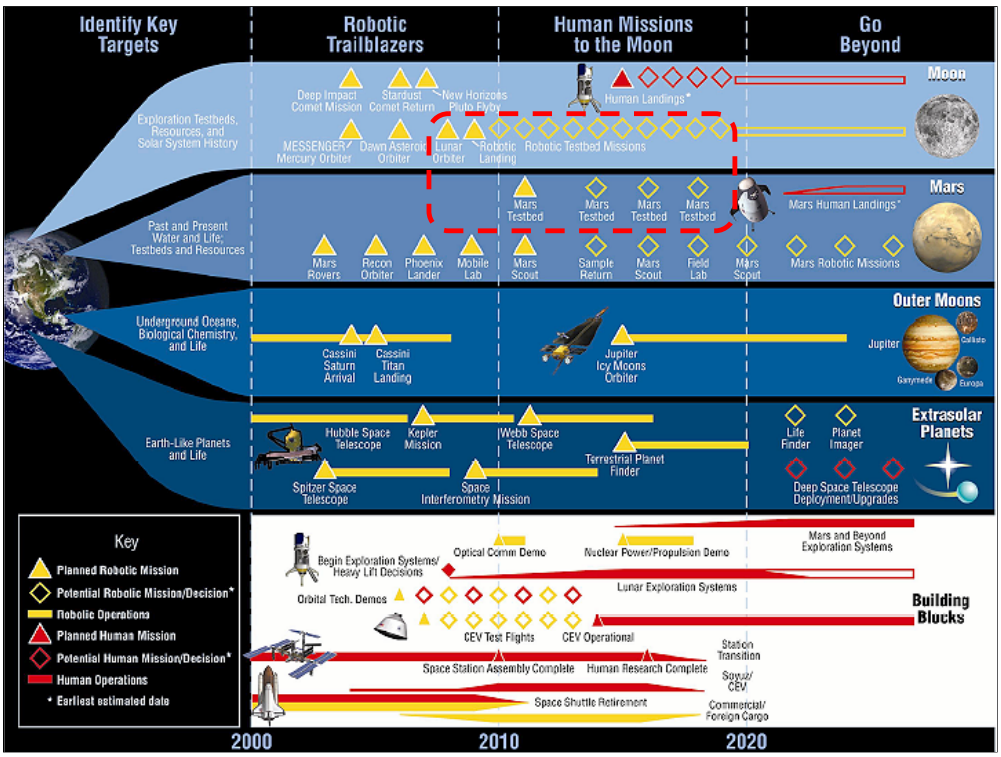

-This is a snap shot of the activities that NASA is engaged in across the agency

-Across the Agency everyone is involved and an intricate part of the success for the Vision

*Possible tailoring to the centers as what piece of the plan each center is involved with

This chart shows how comprehensive the Vision is. It encompasses Science, missions – human and robotic – and includes the Exploration Systems Mission Directorate's portion.

Preparing for Mars Exploration

Moon as a test bed to reduce risk for future human Mars missions

- **Technology advancement** reduces mission costs and supports expanded human exploration
- **Systems testing** and technology test beds to develop reliability in harsh environments.
- **Expand mission and science surface operations** experience and techniques
- **Human and machine collaboration**: Machines serve as an extension of human explorers, together achieving more than either can do alone
- **Breaking the bonds of dependence on Earth**: (e.g./Life Science/Closed loop life support tests)

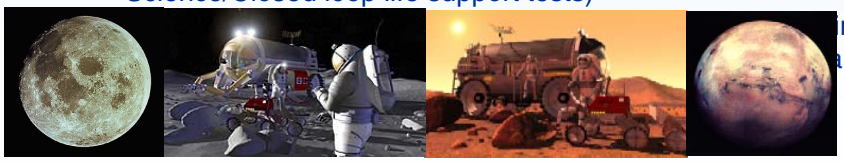

-Traveling to the Moon is important as it enables us to set test beds to go to Mars to minimize risk.

-Establishing an infrastructure by going to the Moon will build sustainability, affordability, and establish credibility.

-Reiterates points outlined

Questions:

Why are we going to the Moon and Mars? Resources. Life Science.

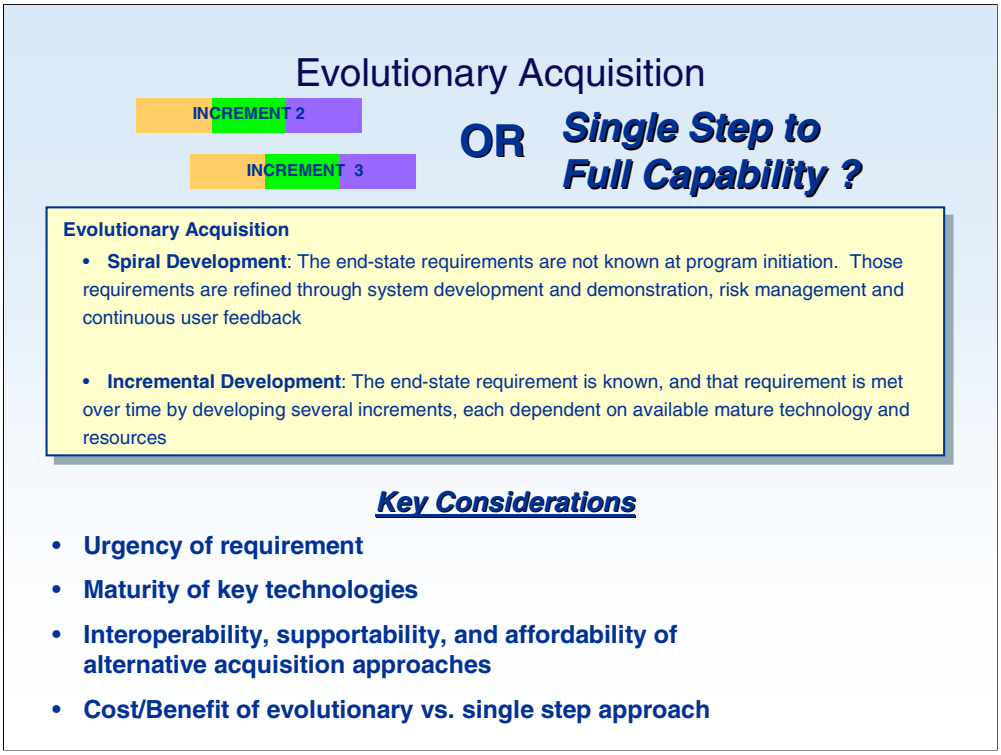

Evolutionary Acquisition allows us to deliver a capability in increments, understanding that there is a need for future capability improvements. It allows us to time phase our requirements and integrate matured technologies into future increments to provide ever increasing capabilities. It is a method that allows for requirement uncertainty due to the inherent phasing of the development.

Evolutionary Acquisition directly contrasts the single step acquisition processes. In the single step acquisition process all of the requirements and the end state must be known up front. This has led to long lead acquisitions and changing requirements that are not able to benefit from maturing technology.

The two approaches utilized in evolutionary acquisition include Spiral Development and Incremental Development. These two approaches need not be used in separation from each other. In our case we are using the two in combination. We are acquiring the systems necessary to go to Mars using spiral development. We do not know the end point of the system capabilities required to go to Mars, but we do know that we need to have crewed flight, which is the first spiral. Within that spiral we have an increment to develop a CEV. We also know we will have a spiral to take us to the moon between 2015 and 2020. The capabilities required for this spiral are still being defined. Once they are defined one or more increments that are managed as unique acquisitions will be used.

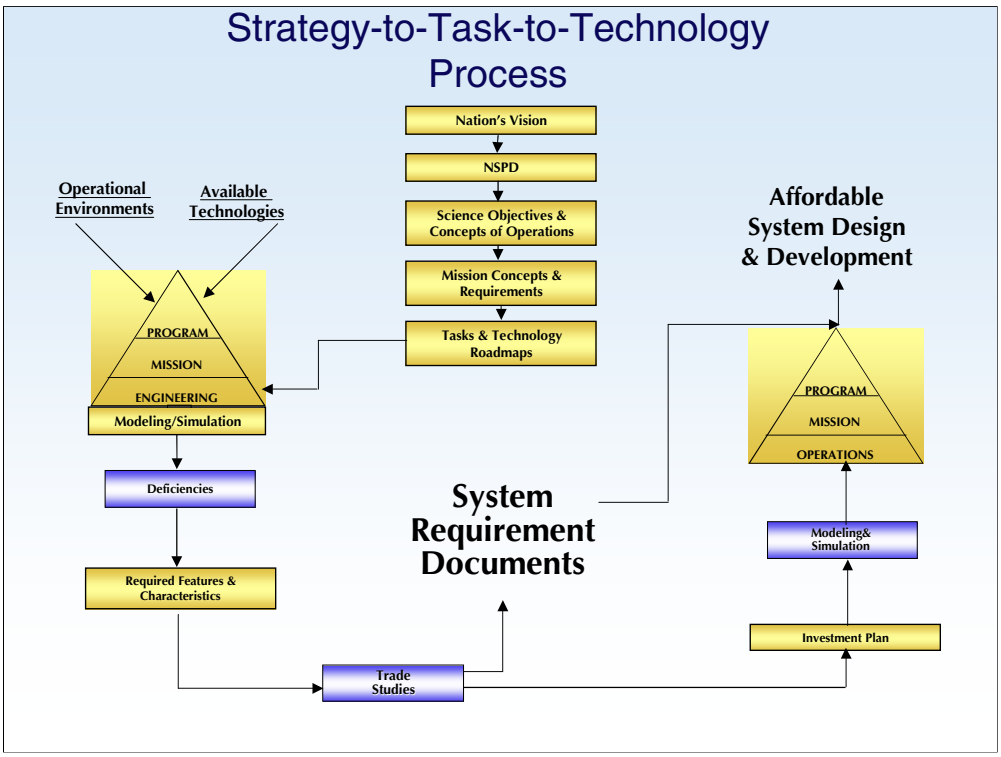

Specific program tasks derive from management rigor – a disciplined approach to management that includes an acquisition and investment plan targeted toward building new capabilities and engaging in essential research and development. The process of flowing from our strategy to program tasks is iterative. Our strategy for ensuring affordable and sustainable design and development requires extensive modeling and simulation of concepts and their interactions within a range of anticipated operational environments. Cost, performance, and risk data are evaluated iteratively to determine the optimal:

•Requirements set and priorities

•Design for desired capabilities

•Acquisition plan for new capabilities

•Investment plan for research and technology development.

Like our overall efforts, this strategy-to-task process is spiral in nature in that, through repeated cost analysis and performance options, trends and results – including progress in developing specific capabilities and progress in maturing essential technologies – we spiral towards the deployment of new transformational capabilities in a manner that is safe, effective, and affordable.

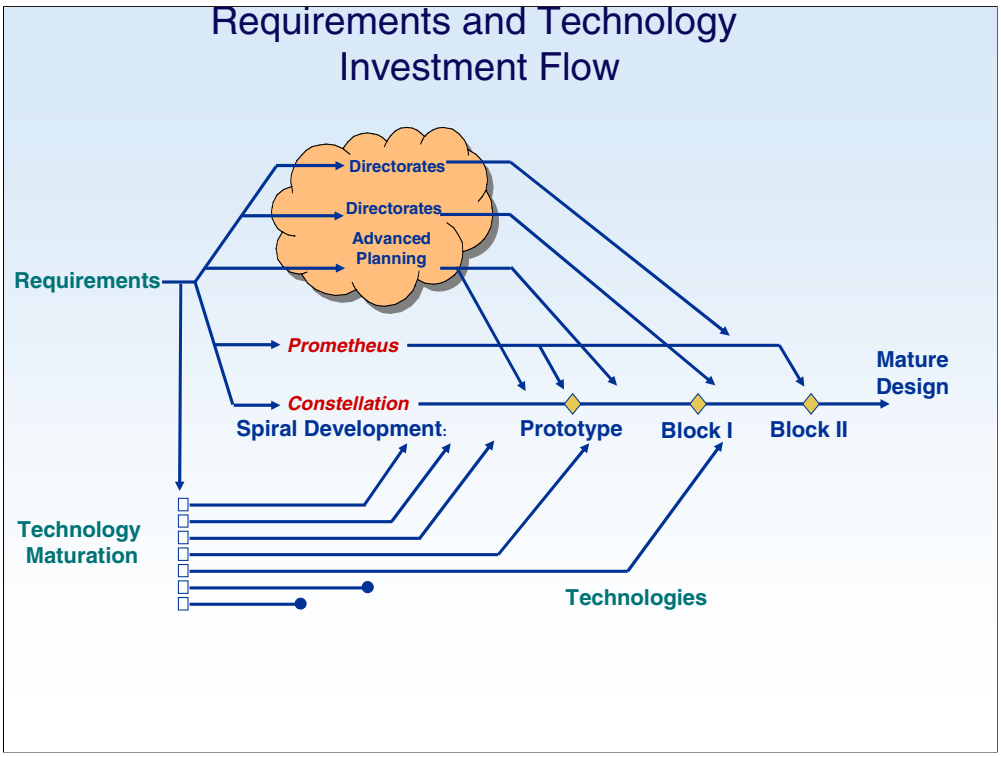

Slide shows the process and flow kicked off by requirements definition. The other directorates and advance planning will provide requirements. This flow helps develop and identify the technology in which we need to invest. Once the technologies are to a point of maturity, they can be integrated.

Analogy: If a car company wants to release a new model, they first build a prototype to be used as their concept car. When the concept is ready for manufacture, it moves to Block 1, which is similar to the first release of the car to the general public – say, a 2005. After gathering data on things that can be added, improved, repaired, or streamlined, the car manufacturer begins work on the next model, most likely to be released in 2006. This continuous improvement helps bring the design closer to maturity in a logical, controlled fashion based upon solid data. In addition, consumers who get a positive feeling from the 2005 model will tell friends and family and the market will be more willing to invest additional funds in a new, improved 2006 model. This allows the manufacturer to add more features and options to their car, just as NASA will be able to add more and more technology to projects as they evolve.

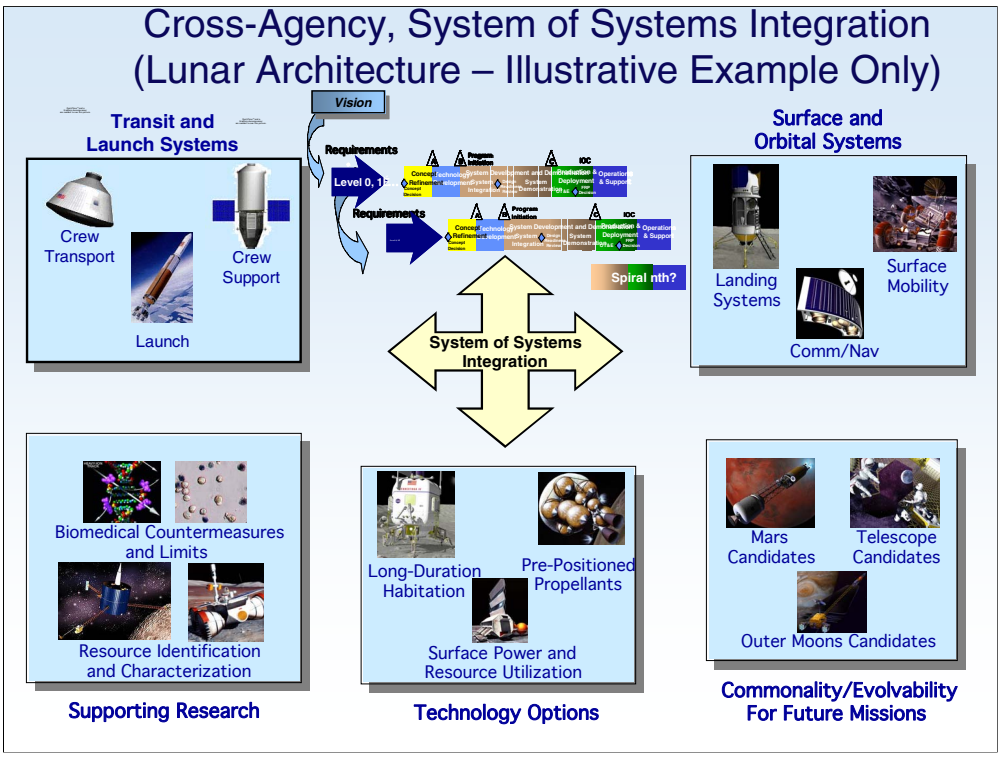

Explain that each of the areas mentioned are subject to their own individual spirals, such as the phases involved in creating the CEV.

This slide exhibits the system of systems approached in ESMD, but for all of the technology and technical prowess, it is missing one key element. (*Note: recommend adding picture of human using animation on this slide.)* Humans are a key piece of functionality in any NASA system of systems.

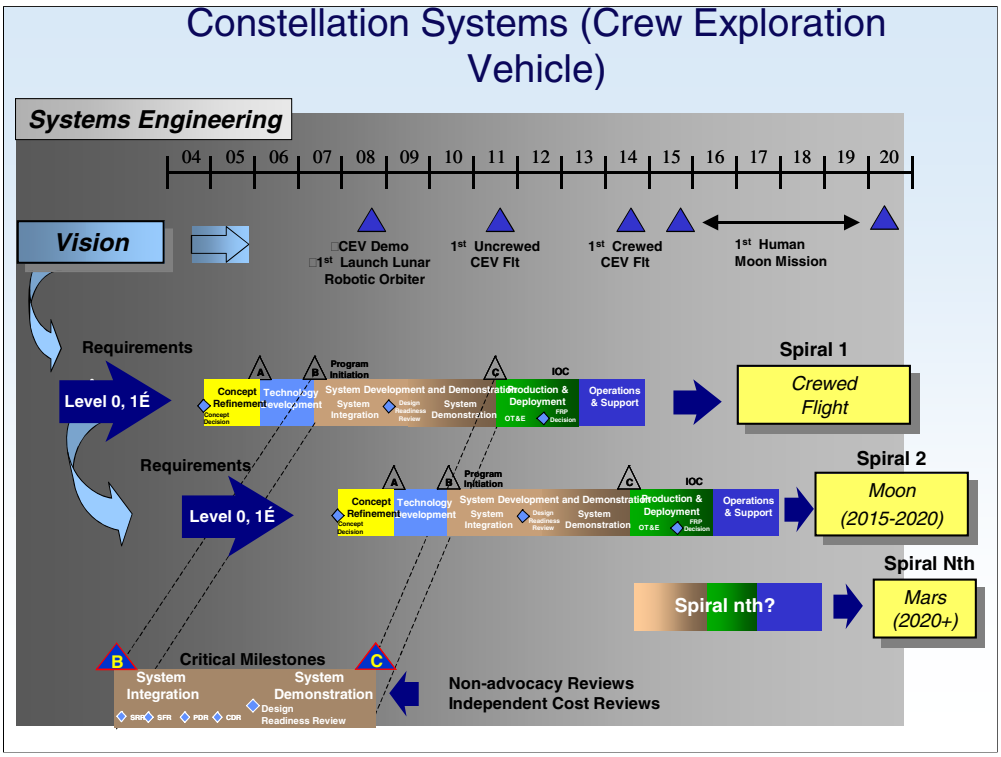

Shows the systems engineering rigor of the program

Shows overall integration of all spirals

Spiral develop and milestones within each spiral, rigorous implementation plans

How systems engineering permeates throughout each spiral and between spirals

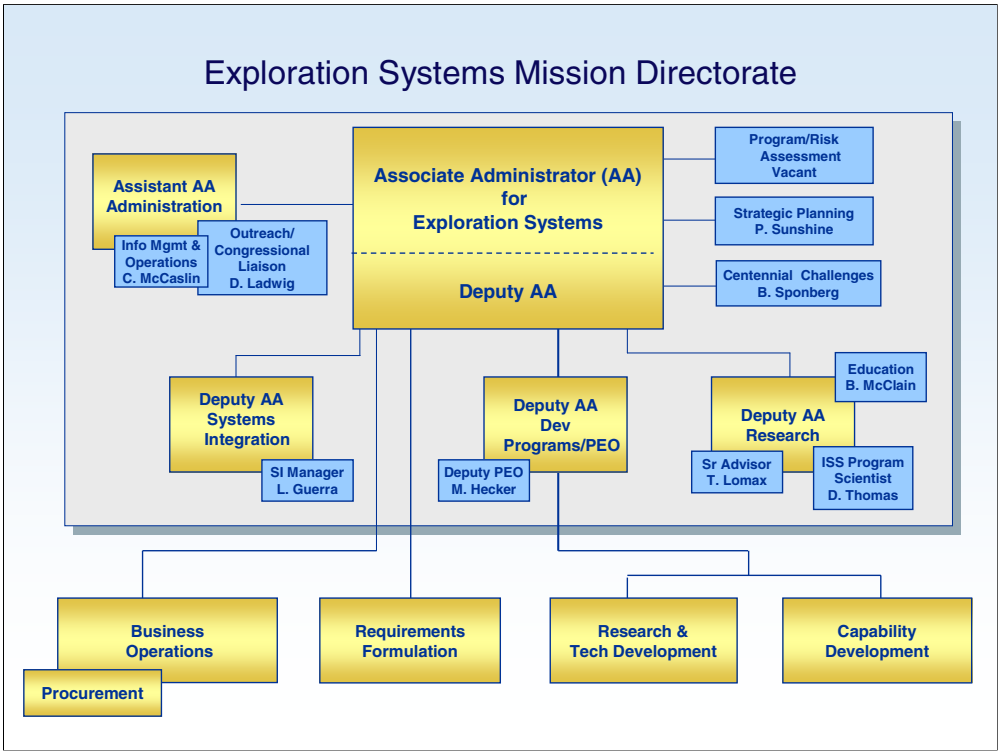
Exploration Systems Mission Directorate
Assistant AA Administration
Info Mgmt & Operations C. McCaslin
Outreach/ Congressional Liaison D. Ladwig
Associate Administrator (AA) for Exploration Systems
Deputy AA
Program/Risk Assessment Vacant
Strategic Planning P. Sunshine
Centennial Challenges B. Sponberg
Deputy AA Systems Integration
SI Manager L. Guerra
Deputy AA Dev Programs/PEO
Deputy PEO M. Hecker
Deputy AA Research
Education B. McClain
Sr Advisor T. Lomax
ISS Program Scientist D. Thomas
Business Operations
Procurement
Requirements Formulation
Research & Tech Development
Capability Development

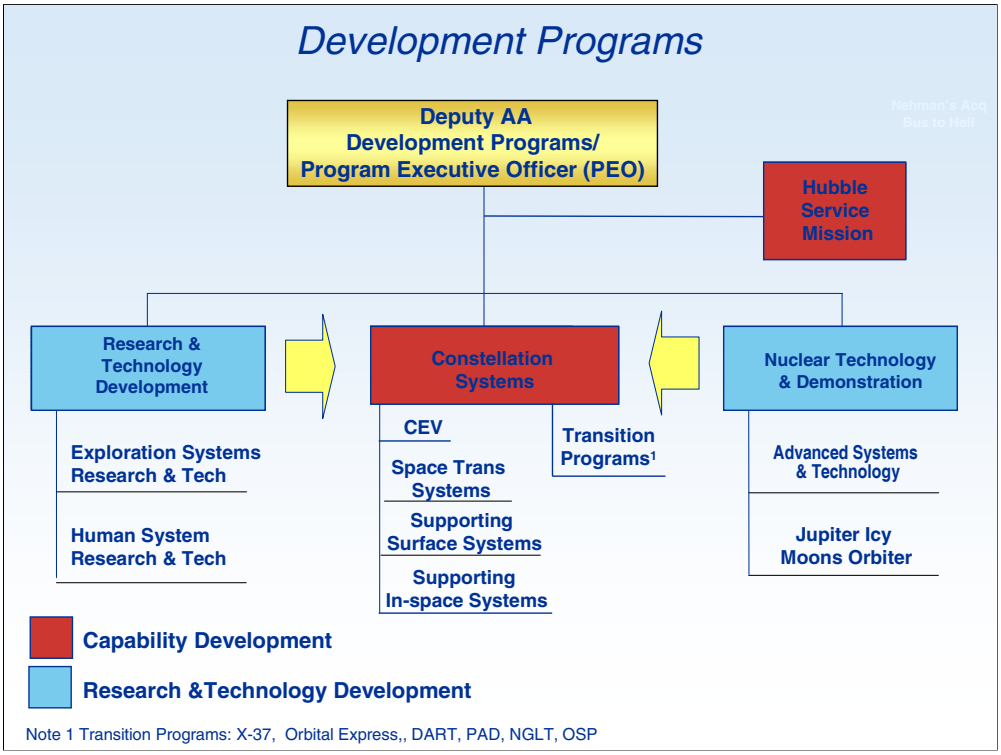

Our Development Programs Division develops capabilities and their supporting technologies to sustained and affordable human and robotic exploration. Our Development team is responsible for implementing the requirements and developing the systems to realize the Vision.

This chart demonstrates that the things that we are working in the Research & Technology Development and Nuclear Technology & Demonstration directly feed into Constellation System

We are implementing the Vision one step at a time

Major Challenges

- Integration of pieces
  BAAs / Trades / RFP / Acq Plan / Budget / International
  Detailed Plan - Disciplined Execution
- Refinement of Organization to Execute
  Identify Needs -- Recruit
- IT Tools to Manage
  Support In-House / Buy
- Cross Agency Integration with Industry
  Stick to Plan -- Communicate
- Maintain Credibility with all Shareholders
- Sustainability with Budget Changes
  Plan Contingencies

Thoughts

- We Have a Great Team – Greater Than the Sum of Its Parts
- We Are Putting Together “World Class” Programs and Processes
- We Are Substantially Changing the Way NASA Does Business by Infusing Management Rigor, Consistency of Purpose, and Disciplined Processes
- Tremendous Support From Our Administrator, the White House and Growing Support in Our Congress
- Great Enthusiasm From US and International Industry to Participate
- We Have the Privilege to Be Working on Programs of High National Importance on Behalf of All Americans
- We Are Inspiring Our Children - the Next Generation of Americans That Will Pick up the Baton of Exploration
- United Support of Vision will Ensure Sustainability

OVERVIEW OF THE ULTRA-EFFICIENT ENGINE TECHNOLOGY AND QUIET AIRCRAFT TECHNOLOGY PROJECTS

Carol Ginty
National Aeronautics and Space Administration
Glenn Research Center
Cleveland, Ohio

Vehicle Systems Program – VSP Vision and Mission

- **Provides technology foundation for future aerospace vehicles**
- **Develops and demonstrates advanced concepts**
  - Airframe
  - Advanced validated tools and techniques
  - Conceptual design and systems analyses
  - Aerodynamic and structure design and development
  - Advanced propulsion system concepts and installations
  - Airborne systems design and testing
  - Flight and systems demonstrations

History

- **VSP was originally composed of several focused programs and a number of base research activities across four Centers**
  - NASA Glenn-UEET, base R&T
  - NASA Langley-TCAT, QAT and base R&T
  - NASA Dryden-base R&T such as as AAW, IFC, etc.
  - NASA Ames-support to other programs such as in nanomaterials, advanced controls
- **Specific guidance was given to better focus the VSP technology development portfolio in 2003-2004**
  - OMB guidance
  - Specific external reviews and recommendations from the NRC, ATAC and IRG
  - Future needs of key customers and stakeholders also considered in the reformulated program
- **Changes at NASA HQ-from Aerospace Technology Enterprise *to* Aeronautics Enterprise *to* Aeronautics Research Mission Directorate (ARMD)**

Vehicle Systems Restructuring

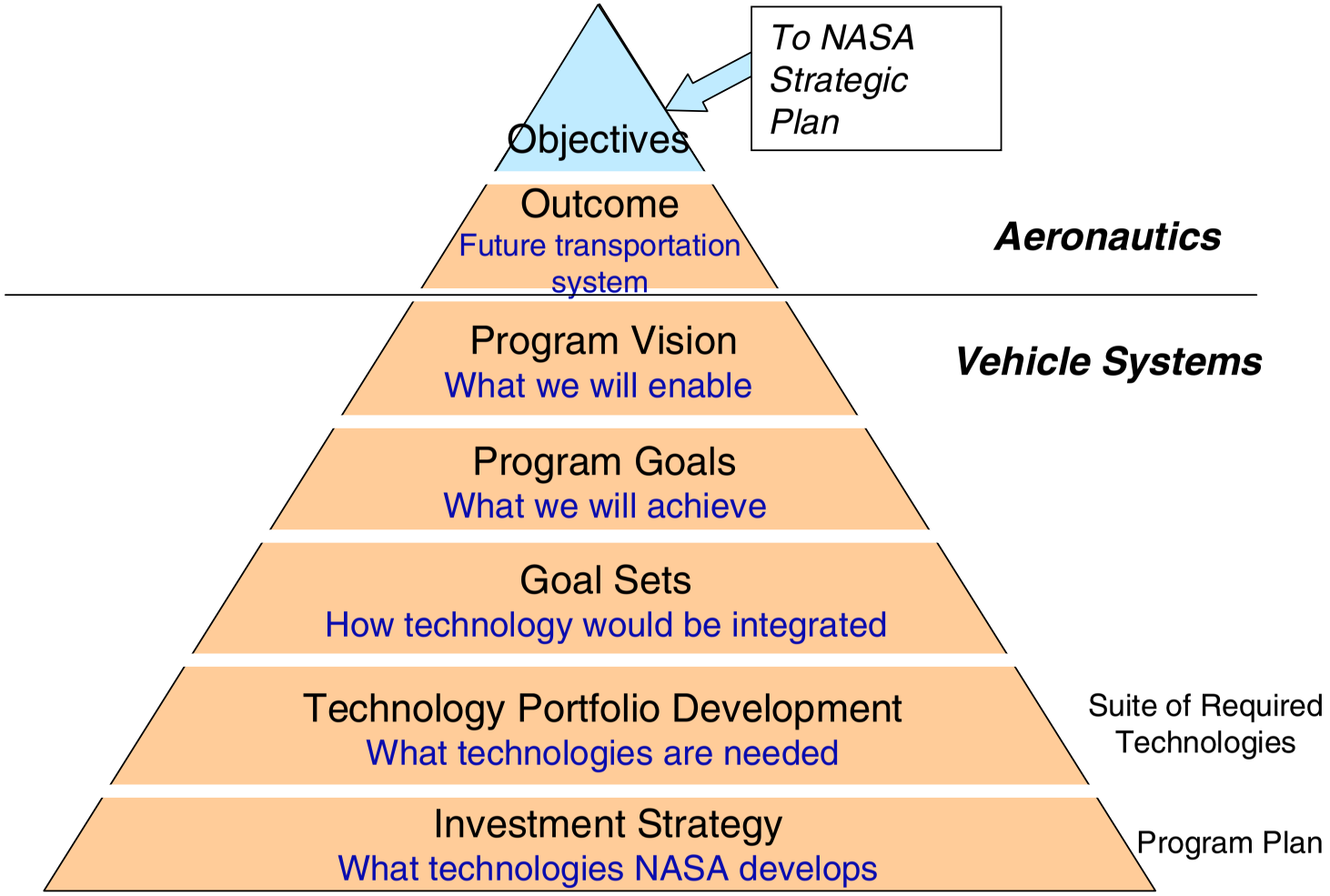

VEHICLE SYSTEMS
Where Innovation Soars

Program Structure

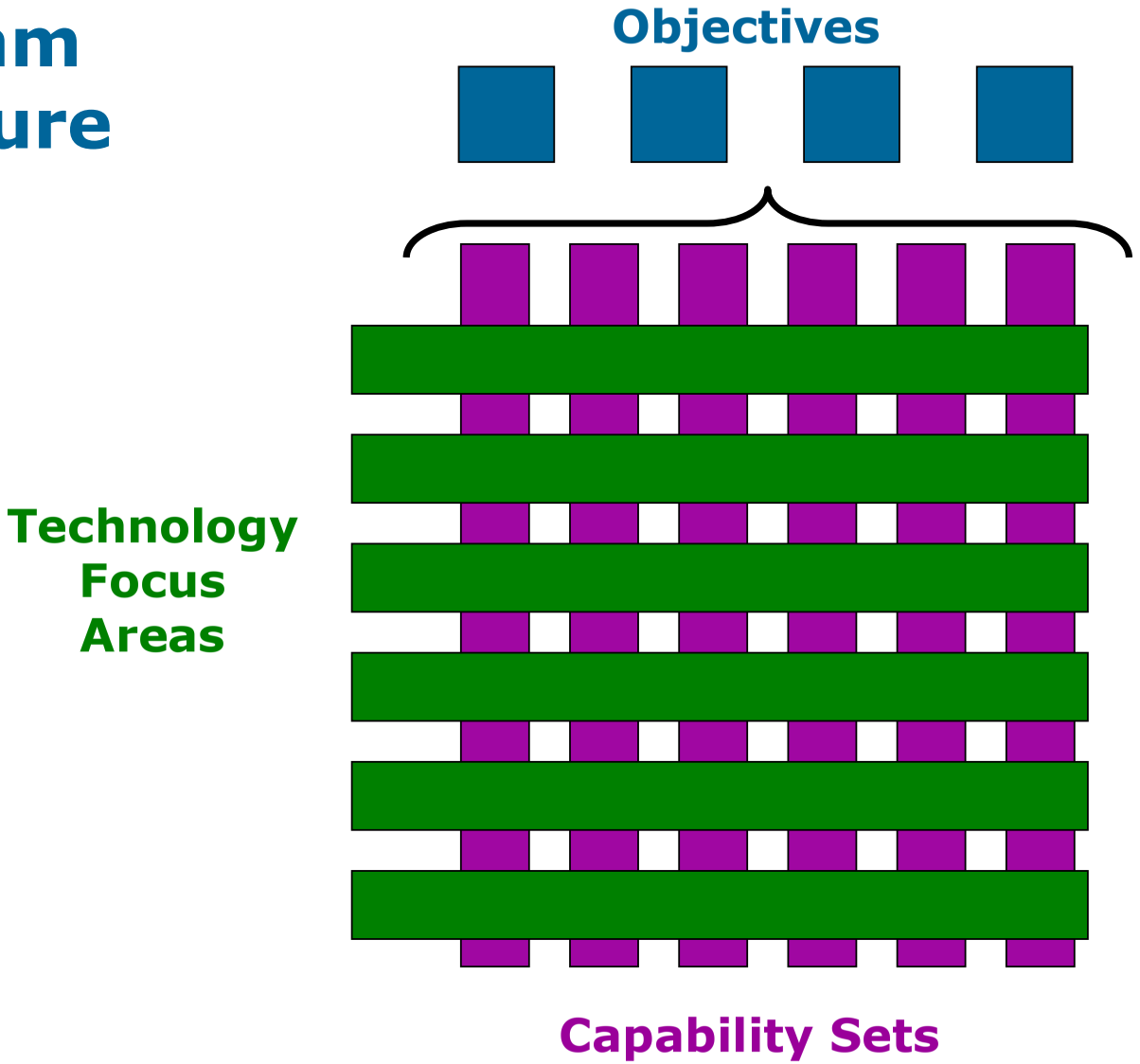

Objectives for the Public Good

Protect the Environment

Protect local and global environmental quality by reducing aircraft noise and emissions.

Increase Mobility

Enable more people and goods to travel faster and farther, with fewer delays

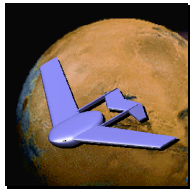

Explore New Aerospace Missions

Pioneer novel aeronautical concepts and technologies to support science missions and terrestrial and space applications

Partnerships for National Security

Enhance the Nation's security through aeronautical partnerships with DOD, DHS, and other U.S. or international government agencies

Strategic Technology Focus Areas

- ***Environmentally Friendly, Clean Burning Engines***
  - Develop innovative technologies to enable intelligent turbine engines with significantly reduced harmful emissions while maintaining high performance and increasing reliability
- **New Aircraft Energy Sources and Management**
  - Investigate new energy sources and intelligent management techniques for zero emissions and enable new vehicle concepts for public mobility and new science missions
- ***Quiet Aircraft for Community Friendly Service***
  - Develop airframe and engine noise reduction technology and operational concepts to bring objectionable noise within the airport boundary
- **Aerodynamic Performance for Fuel Efficiency**
  - Improve aerodynamic efficiency, structures and materials technologies, and design tools and methodologies to reduce fuel burn and minimize environmental impact and enable new vehicle concepts and capabilities for public mobility and new science missions

Strategic Technology Focus Areas *(cont.)*

- **Aircraft Weight Reduction and Community Access**
  - Develop ultralight smart materials and structures, aerodynamic concepts, and lightweight subsystems to enable advanced configurations for public mobility, high altitude long endurance vehicles, and planetary aircraft
- **Smart Aircraft and Autonomous Control**
  - Enable aircraft to fly with reduced or no human intervention, to optimize flight over multiple regimes, and to provide maintenance on demand towards the goal of a feeling, seeing, sensing, sentient air vehicle

Cross-cutting the Six Technology Focus Areas

- **Flight and System Demonstrations**
  - Mature and validate new aircraft capabilities in relevant flight environment in partnership with industry and other government agencies
- **Strategic Technical Directions (VISTA)**
  - Gather data and perform strategic analysis to provide guidance on future program directions

Capability Sets Based on Conceptual Vehicles

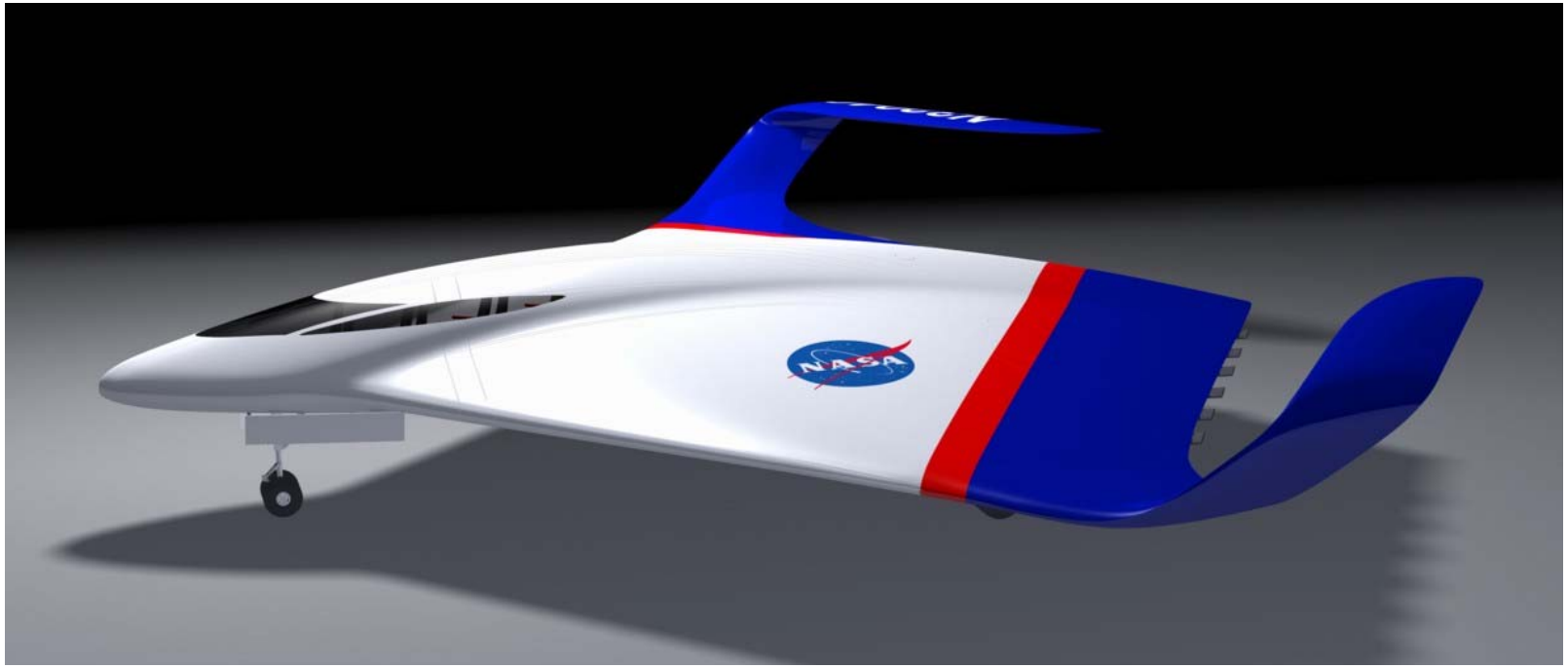

VEHICLESYSTEMS
Where Innovation Soars

Vehicle Sectors

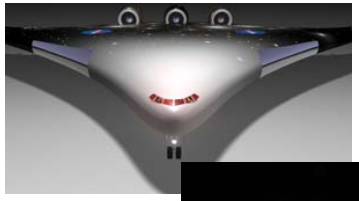

Subsonic Transports

Associate Program Manager for VISTA

Supersonic Aircraft

Rotorcraft

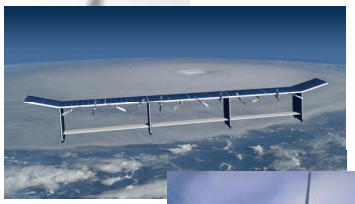

Uninhabited Air Vehicles

Personal Air Vehicles

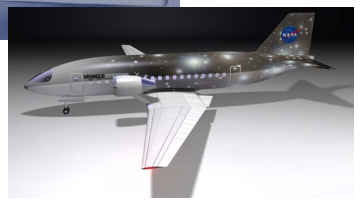

Extreme STOL

VEHICLE SYSTEMS
Where Innovation Soars

Vehicle System Program Structure

Program Manager — Dr. Rich Wlezien
Deputy PM — Herb Schlickenmaier

Program Office

Associate Program Manager for Operations
Vacant

Associate Program Manager for Technology
Vacant

Associate Program Manager for Strategy
Bob McKinley
Teresa Kline

Vehicle Sector Managers

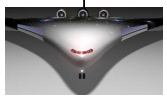

Subsonic Transports
Fay Collier
Ruben Del Rosario

Supersonic Aircraft
Peter Coen
Jon Seidel

Rotorcraft
Gloria Yamauchi
Mike Watts

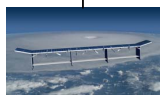

Uninhabited Air Vehicles
Larry Camacho
Jeff Yetter

Personal Air Vehicles
Mark Moore
Andy Hahn

Extreme STOL
John Zuk
Doug Wardell

Project Managers

LaRC
Roy Bridges

Quiet Aircraft Technology (QAT)
Mike Marcolini and Linda Bangert

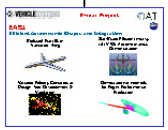

Efficient Aerodynamics Shapes and Integration (EASI)
Jim Pittman and Dave Hahne

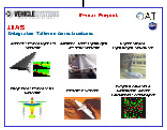

Integrated Tailored AeroStructures (ITAS)
Long Yip and Jeff Jordan

Autonomous Robust Avionics (AuRA)
Jim Burley and Dave Richwine

GRC
Julian Earls

Ultra-Efficient Engine Technology (UEET)
Kestutis "Kaz" Civinskas and Mary Jo Long-Davis

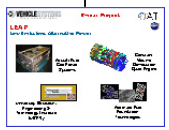

Low-Emission Alternative Power (LEAP)
Mark Klem and Barb Esker

DFRC
Kevin Petersen

Flight & Systems Demonstration (F&SD)
Eddie Zavala

Linkage: the Whole Picture

The President's Management Agenda

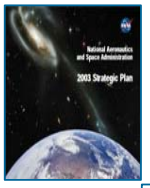

The NASA Strategic Plan

The Systems Vee

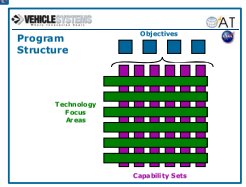

Vehicle Systems Structure

Vehicle Systems GOTChA's

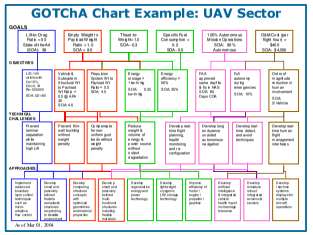

Vehicle Systems Roadmaps

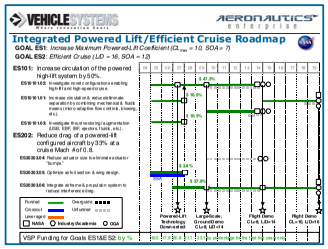

Level 3 Sub-Project Plans

Project Deliverables

Flight Demos
Hardware
Software
Methods
Tools
Data
...
+ Spinoffs

Level 1 Program Plan

VS: Program Outcomes, FY05-09

Environment:

- 70% NO_x Reduction for subsonic transports
  - Plus foundation technologies for an additional 10% reduction
- 25% CO_2 Reduction for subsonic transports
  - Plus foundation technologies for an additional 25% reduction
- 10 dB Noise Reduction for subsonic transports
  - Plus foundation technologies for an additional 10 dB reduction
- 24 dB noise reduction for advanced general aviation aircraft
- Define “acceptable sonic boom” for overland super-cruising aircraft

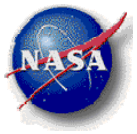

UEET - Ultra-Efficient Engine Technology Project

UEET Overview

- **Strategic Focus: Environmentally Friendly, Clean Burning Engines**
  - Develop innovative technologies to enable intelligent turbine engines that significantly reduce harmful emissions while maintaining high performance and increasing reliability.
- **Cross-cutting technology development & maturation focused on the Subsonic, Supersonic and Rotorcraft**
  - ST, "Reduced NOx and Improved TSFC & T/W"
  - SSA, "High Performance Inlets"
  - RC, "Advanced Drive Systems"

Purpose(s)

- **Develop and demonstrate propulsion technologies that address the goals of the Subsonic, Supersonic, and Rotorcraft Sectors in the Vehicle Systems Program.**
- **Develop propulsion technologies to reduce Thrust Specific Fuel Consumption (TSFC) and to increase Thrust/Weight (T/W) that will result in fuel burn reductions of up to 15%, equating to 15% reductions in CO_2.**
- **Develop combustor technologies (configuration and materials) that will enable reductions in Landing/Take-Off (LTO) NO_x of 70% relative to 1996 ICAO (International Civil Aviation Organization) standards.**

VEHICLESYSTEMS
Where Innovation Soars

UEET

5-year Project

Ultra Efficient Engine Technology

Low Emissions Combustor

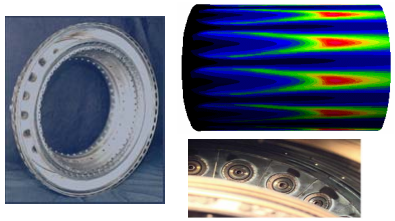

Systems Integration and Demonstration

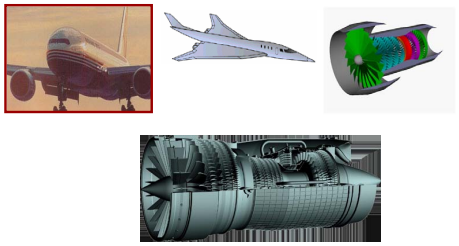

Highly Loaded. Light Weight Compressor & Turbines

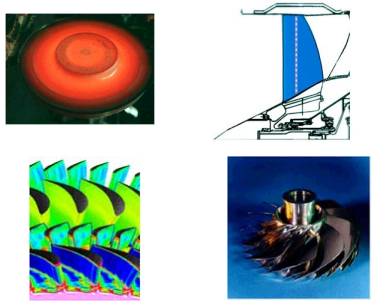

Highly Integrated Inlet

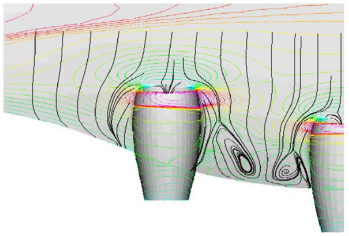

Advanced Drive Systems for Heavy-lift Rotorcraft

Intelligent Propulsion System Foundation Technologies

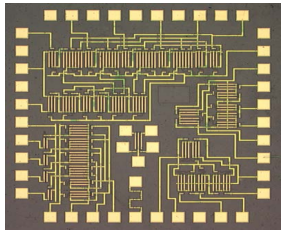

Organizational Breakdown Structure

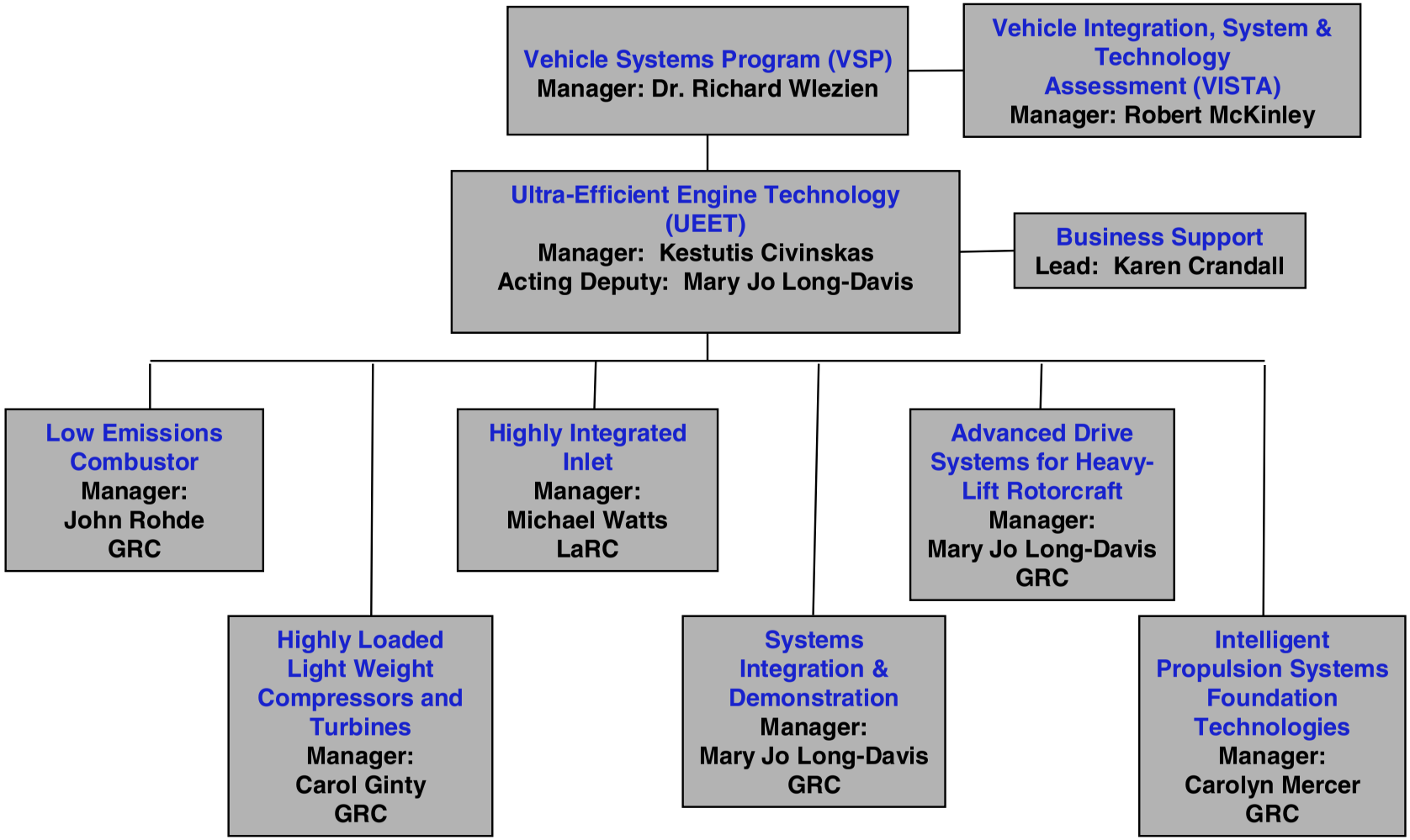

Vehicle Sectors Supported (1 of 2)

WBS	Sector	Approaches
2.7.2 Low Emissions Combustor	Subsonic (ST)	ST61932.41 - Advanced combustor techniques to reduce NOx ST61932.43 - Advanced materials for reduced combustion liner cooling ST61932.45 - Validated combustion codes for design and control of low emissions combustors
2.7.3 Highly Loaded Light Weight Compressors and Turbines	Subsonic (ST) Supersonic (SS)	ST41220.30 - Advanced materials and cooling technologies for reduced cooling ST41424.34 - Improved materials with higher temperature capability and strength per weight ST41220.31 - Advanced engine components ST41220.29 - Measurement tools and validated physics-based codes for highly loaded turbomachinery SS51119.29 - High temperature light weight materials, structural assemblies and thermal/environmental barrier coatings SS71623-34 - Creep resistant high temperature materials
2.7.4 Highly Integrated Inlets	Subsonic (ST) Supersonic (SS)	ST41423.32 - Flow management and control techniques SS10202.03 - Variable fidelity integrated MDO tools for innovative low boom configurations with high L/D

Vehicle Sectors Supported (2 of 2)

WBS	Sector	Approaches
2.7.5 System Integration and Demonstration	Subsonic (ST) Supersonic (SS)	ST41220.29 - Measurement tools and validated physics-based codes for highly-loaded turbomachinery ST61727.38 - Measurement tools and validated global and local models to improve cycle designs ST41426.36 - Highly reliable light weight mechanical systems SS51015.23 - Inlet distortion and fan dynamic control SS51116.24 - Inlet operability and viscous loss reduction
2.7.6 Advanced Drive Systems for Heavy-lift Rotorcraft	Rotorcraft (RC)	RC60911.26 - Methods to automatically detect failure of power train
2.7.7 Intelligent Propulsion Systems Foundation technology	Subsonic (ST) Supersonic (SS)	TBD- Specific approaches will be identified pending the results of a competitive procurement process

VEHICLESYSTEMS
Where Innovation Soars

UEET Technologies

TURBINE TIP CLEARANCE SENSOR
- Microwave sensor
- Control gaps to improve efficiency

LOW NOx COMBUSTOR TECHNOLOGIES
- Lean Burn Injection
- Rich Burn Injection
- Coatings for metallic liners

HIGH-LOADED LOW PRESSURE TURBINE (Regional)
- Hub endwall bleed
- LP stage reduction

HIGH-LOADED AXIAL COMPRESSOR
- 3D aero
- Inverse design
- Recirculating casing treatment

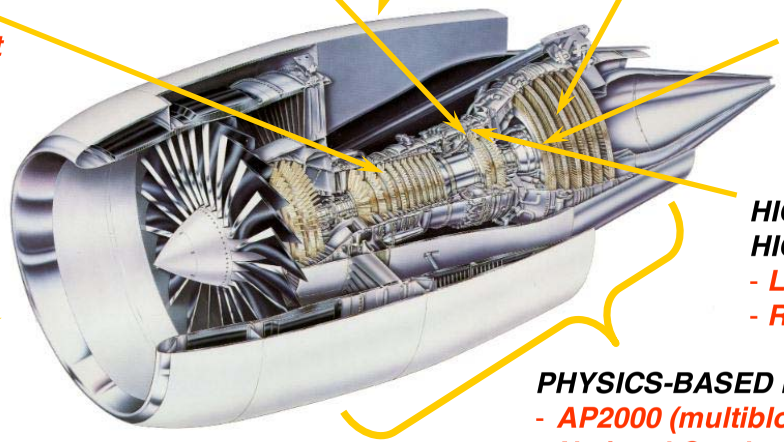

HIGH-LOADED HP/LP TURBINE SYSTEM
- Reduced interaction loss
- System weight reduction

ADVANCED MATERIALS
- Ceramic Matrix Composite Vanes
- Low Conductivity TBC
- Polymer Matrix Composite Components
- Advanced Alloys

HIGH-WORK SINGLE-STAGE HIGH-PRESSURE TURBINE
- Low shock loss design
- Reduced cooling losses

ACTIVE FLOW CONTROL FOR BWB INLETS
- Synthetic jets

PHYSICS-BASED MODELING & CFD
- AP2000 (multiblock APNASA)
- National Combustion Code
- MSU-TURBO
- Glenn-HT

MECHANICAL COMPONENTS
- Advanced Non-Contacting Seals
- Lightweight Gearbox Components for Large Geared Turbofan Engine

UEET Technology Portfolio Derived to Support Vehicle Systems Program Goals for Improved TSFC and T/W and Reduced NOx

Budget: % by Sector

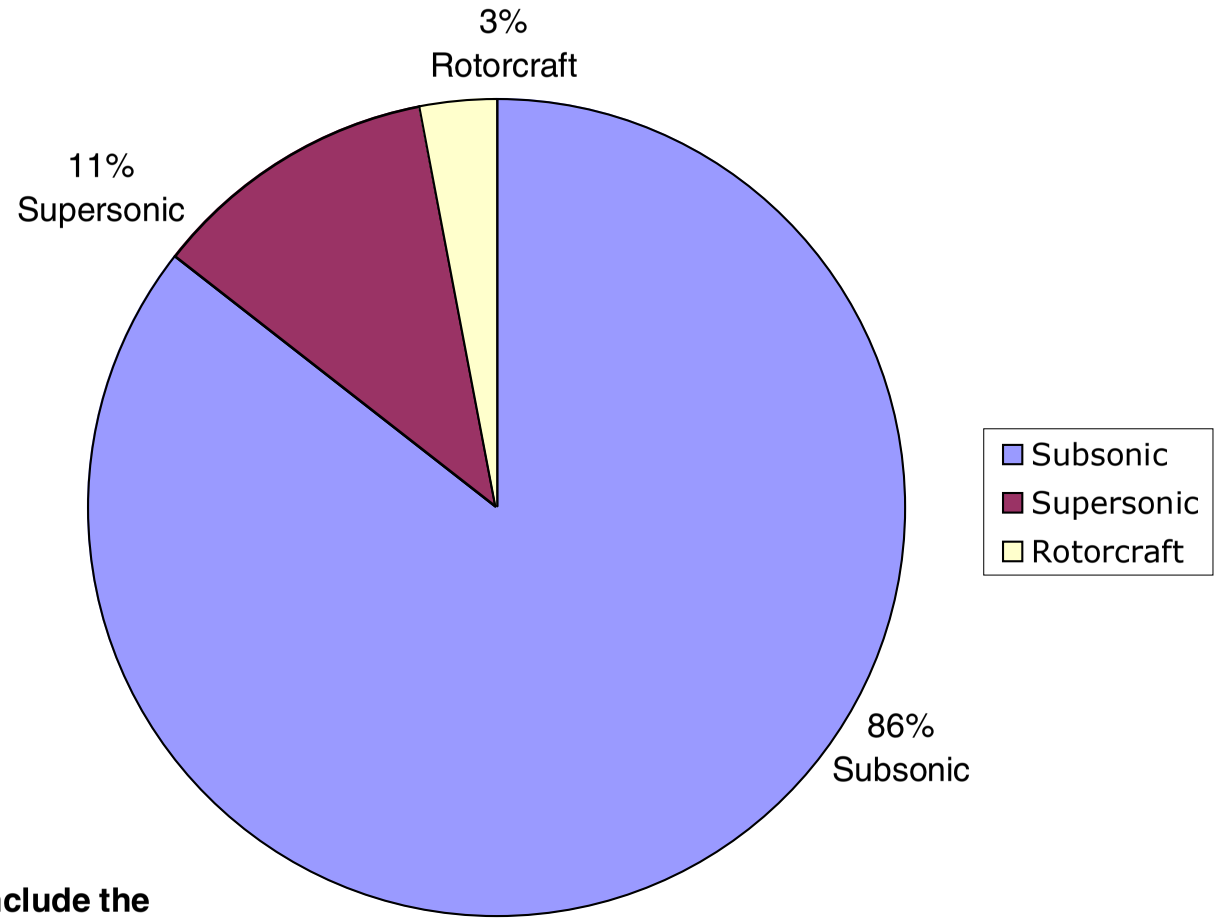

Total does not include the UEET Project's 20% funding of foundational technologies.

VEHICLE SYSTEMS
Where Innovation Soars

UEET L2 Plan

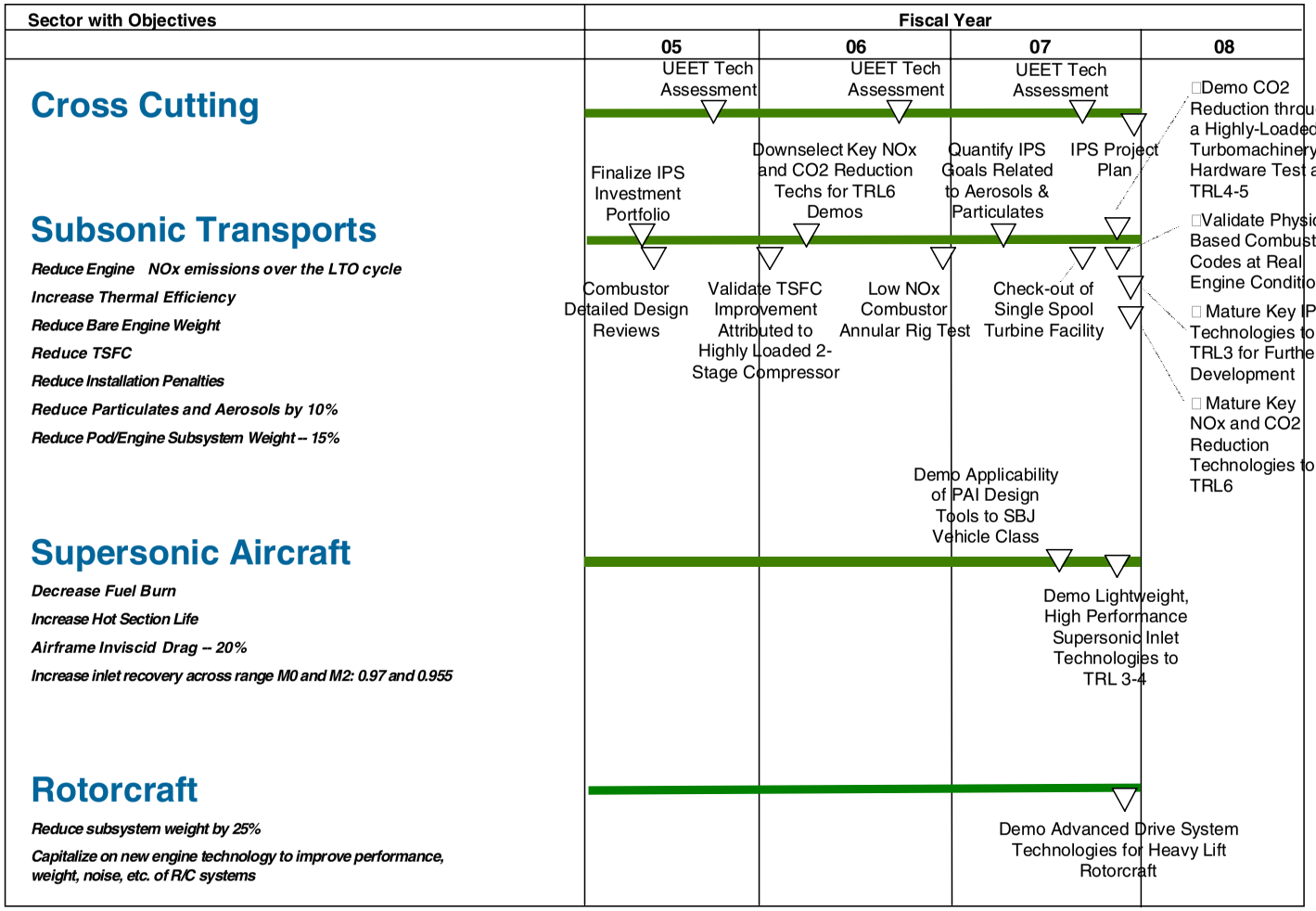

UEET L2 Plan V.1a 09Sep04

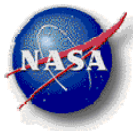

QAT - Quiet Aircraft Technology Project

QAT Overview

- **Strategic Focus: Quiet aircraft for Community Friendly Service**
  - Develop and integrate noise reduction technologies to enable unrestricted air transportation service to all communities
- **Focused primarily on the Subsonic Transport (ST) sector, with some support of the Rotorcraft (R/C), Supersonic, and Personal Air Vehicle (PAV) sectors**
  - ST, "Reduce Community Noise by 20 EPNdB" and "Reduce Empty Weight Fraction by 20%"
  - RC, "Reduce Community Noise" and "Reduce Cabin Noise and Vibration Throughout Flight Envelope"
  - SSA, "Sonic Boom Annoyance Reduced to Allow Supersonic Flight Overland"
  - PAV, "Reduce Community Noise"

Purpose of QAT

- **Strategic Focus: Noise Reduction Technology**
- **15-year goals**
  - Subsonic Transport, "Reduce Community Noise by 20 EPNdB"
  - Rotorcraft, "Reduce Community Noise by 14 EPNdB" and "Reduce Cabin Noise by 11 dBA and Vibration by 0.1g's Throughout Flight Envelope"
  - Supersonic, "Sonic Boom Annoyance Reduced to Allow Supersonic Flight Overland" and "Takeoff and Landing Noise Impact: Stage 4 - 4+EPNdB"
  - Personal Air Vehicles, "Reduce Community Noise by 24 dBA at Takeoff and Landing"

VEHICLE SYSTEMS
Where Innovation Soars

QAT

Quiet Aircraft Technology

7-year Project ending in FY07

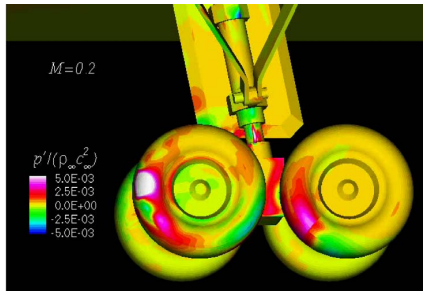

Airframe System Noise Reduction

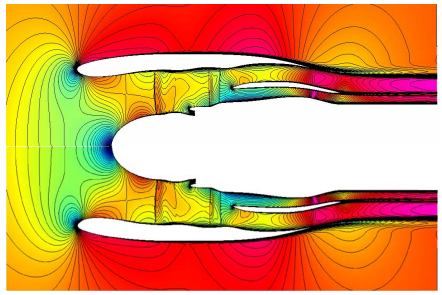

Engine System Noise Reduction

Community Noise Impact and Modeling

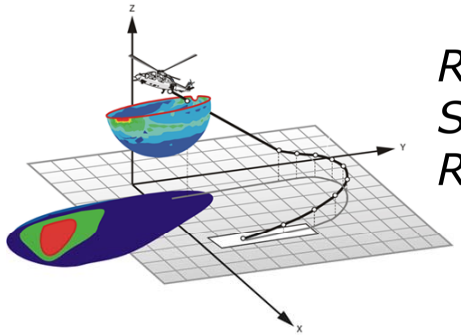

Rotorcraft System Noise Reduction

Organizational Breakdown Structure

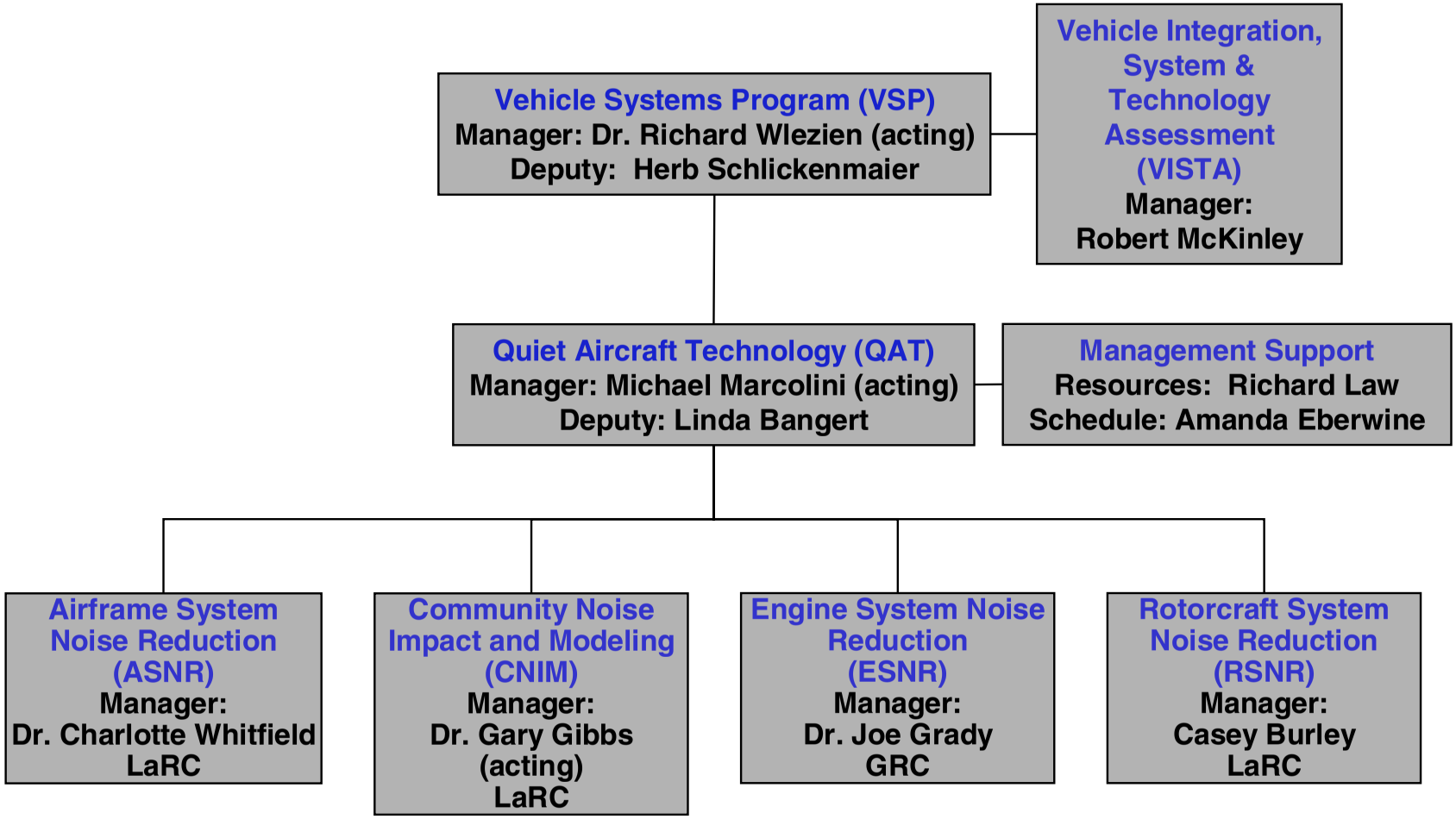

Vehicle Sectors Supported

WBS	Sector	Approaches
2.6.2 Airframe System Noise Reduction	Subsonic (ST)	ST205/20608.15 - Multifunctional structural design accounting for thermal, acoustic loads ST205/20608.16 - Active interior noise control for lightweight fuselage designs ST30710/30711.18 - Reduce identified noise sources through methods derived from physics-based understanding ST30913.22 - Identify, account for and reduce noise via propulsion/airframe interactions
	Personal Air Vehicle (PA)	PA60606.11 - Develop integrated and shielded ducted propeller system with active wake control, and acoustical suppression.
2.6.3 Community Noise Impact and Modeling	Subsonic (ST)	ST30812.20 Real-time calculation of noise minimal trajectories and pilot/controller tools to fly noise minimal trajectories ST30913.21 - Develop and validate tools to aircraft level system assessments for conventional and unconventional configurations
	Supersonic (SS)	SS30712.19 - Boom acoustic and structural response studies, simulator and in home studies

Vehicle Sectors Supported (continued)

WBS	Sector	Approaches
2.6.4 Engine System Noise Reduction	Subsonic (ST) Personal Air Vehicle (PA)	ST11115.24 - Advanced low noise fan designs, liner concepts and active control ST11115.25 - Reduce jet noise sources through methods derived from physics PA60606.11 - Develop integrated and shielded ducted propeller system with active wake control, and acoustical suppression.
2.6.5 Rotorcraft System Noise Reduction	Rotorcraft (RC)	RC40606.14 - Develop and validate source noise prediction and propagation capabilities. RC40606.15 - Develop and validate system/source noise and propagation prediction capabilities. RC40707.17 - Develop and demonstrate low noise operations and capabilities with acceptable handling qualities.

Technology Highlights

Airframe Noise Reduction
(Slats, flaps, gears)

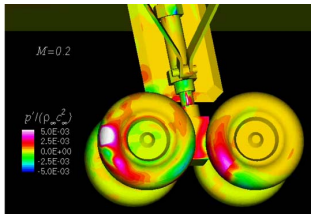

Landing gear

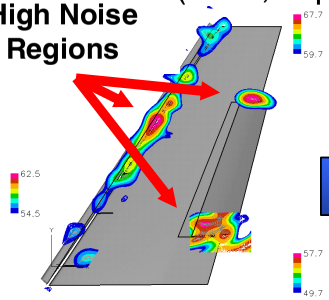

Baseline

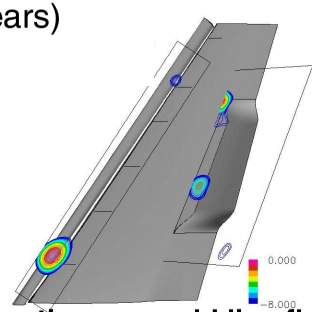

Continuous mold line flap and slat cove filler

Low Noise Flight Procedures
(Continuous descent approach, low noise guidance)

Fan Noise Reduction
(Forward swept fan, porous stators, variable area fan nozzle)

Jet Noise Reduction
(Advanced chevrons, vortex breakdown control, offset fan flow)

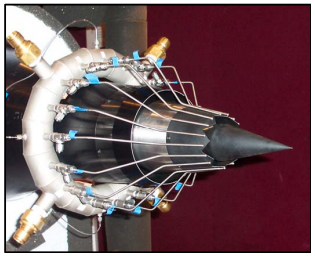

Baseline

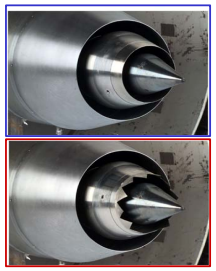

Chevron

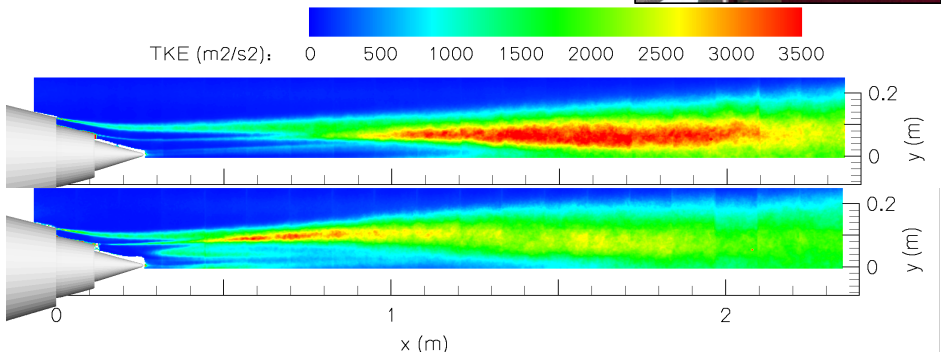

VEHICLE SYSTEMS
Where Innovation Soars

Budget: % by Sector (FY05-07)

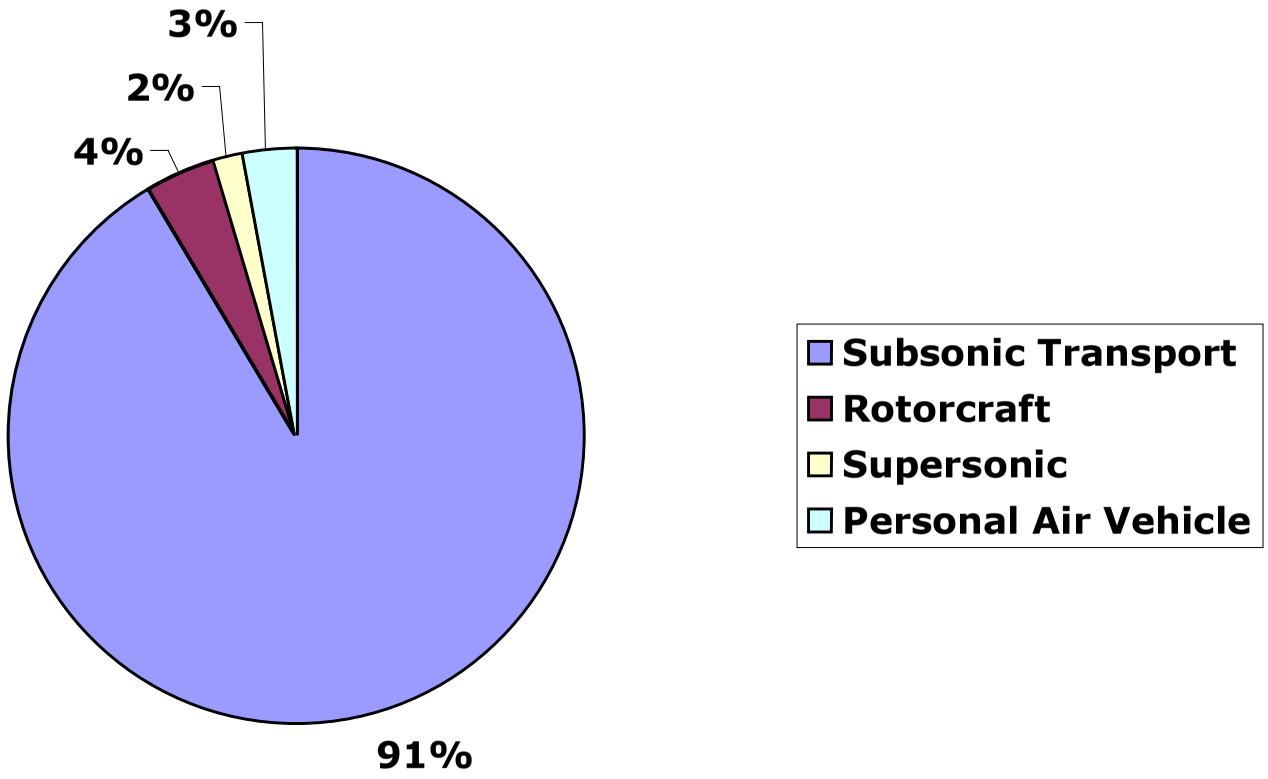

QAT L2 Plan

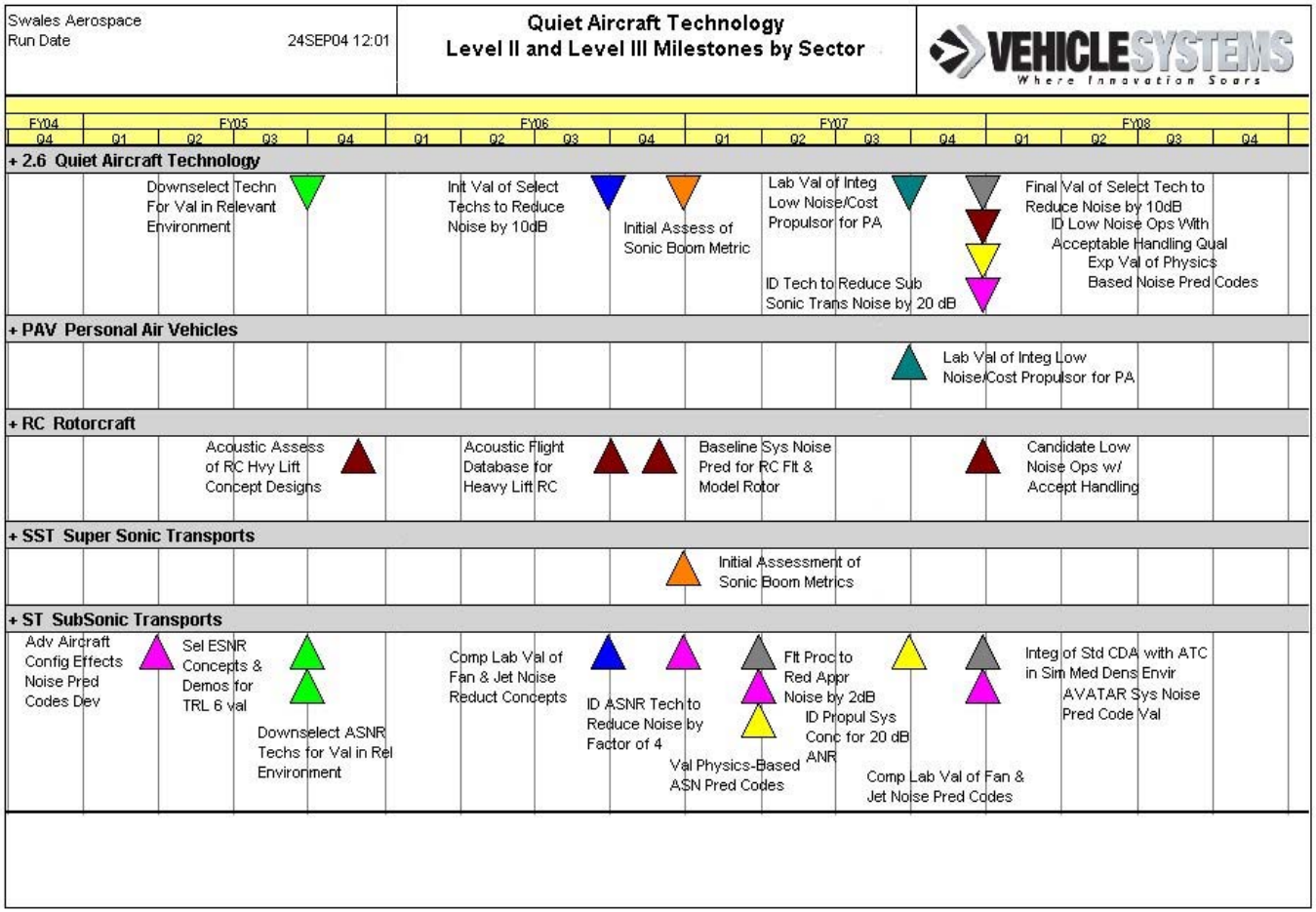
Swales Aerospace
Run Date 24SEP04 12:01
Quiet Aircraft Technology
Level II and Level III Milestones by Sector
FY04 FY05 FY06 FY07 FY08
Q4 Q1 Q2 Q3 Q4 Q1 Q2 Q3 Q4 Q1 Q2 Q3 Q4 Q1 Q2 Q3 Q4 Q1 Q2 Q3 Q4
+ 2.6 Quiet Aircraft Technology
Downselect Techn For Val in Relevant Environment
Init Val of Select Techs to Reduce Noise by 10dB
Initial Assess of Sonic Boom Metric
Lab Val of Integ Low Noise/Cost Propulsor for PA
ID Tech to Reduce Sub Sonic Trans Noise by 20 dB
Final Val of Select Tech to Reduce Noise by 10dB
ID Low Noise Ops With Acceptable Handling Qual
Exp Val of Physics Based Noise Pred Codes
+ PAV Personal Air Vehicles
Lab Val of Integ Low Noise/Cost Propulsor for PA
+ RC Rotorcraft
Acoustic Assess of RC Hvy Lift Concept Designs
Acoustic Flight Database for Heavy Lift RC
Baseline Sys Noise Pred for RC Flt & Model Rotor
Candidate Low Noise Ops w/ Accept Handling
+ SST Super Sonic Transports
Initial Assessment of Sonic Boom Metrics
+ ST SubSonic Transports
Adv Aircraft Config Effects Noise Pred Codes Dev
Sel ESNR Concepts & Demos for TRL 6 val
Downselect ASNR Techs for Val in Rel Environment
Comp Lab Val of Fan & Jet Noise Reduct Concepts
ID ASNR Tech to Reduce Noise by Factor of 4
Val Physics-Based ASN Pred Codes
Flt Proc to Red Appr Noise by 2dB
ID Propul Sys Conc for 20 dB ANR
Comp Lab Val of Fan & Jet Noise Pred Codes
Integ of Std CDA with ATC in Sim Med Dens Envir
AVATAR Sys Noise Pred Code Val

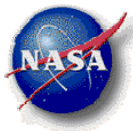

Technical Spotlights

Ultra Efficient Engine Technology Project

Aspirating Seal Demonstration

GE90-94B Engine Test Completed

- Aspirating seal tested on a ground-based GE90 test engine for 33 hours
- Testing conducted at the GEAE Test Operation Facility in Peebles, Ohio
- Cyclic test consisting of 250 B-Cycles
- Flow measurement repeatability within 5% at high power (15% at ground idle)

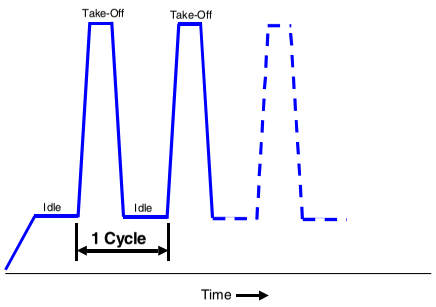

B-Cycle

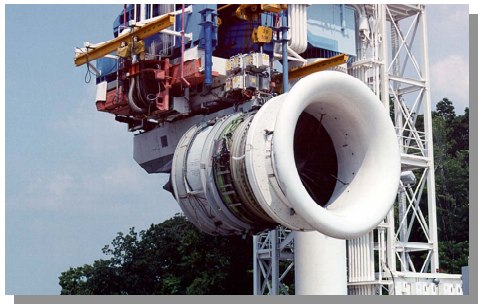

GE90 Test Stand
Peebles, OH

GE90-94B Turbine Rear Frame/Aspirating Seal Assembly

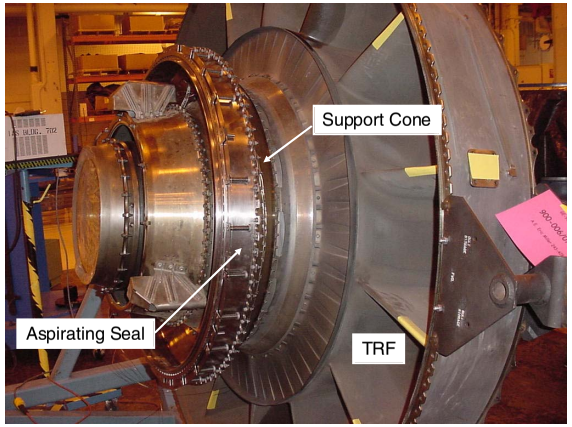

Aspirating Seal Hardware

Outer Diameter View of the Aspirating Seal Stator Assembly

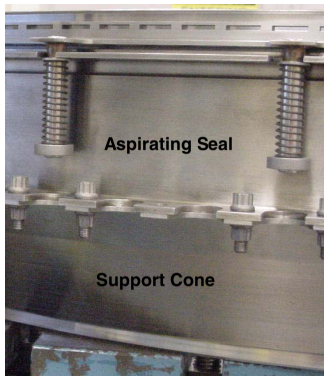

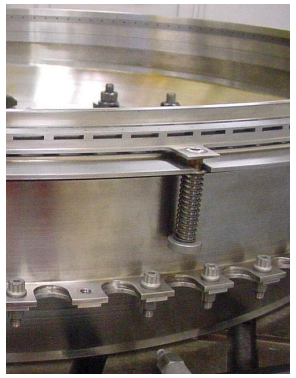

EVNERT Phase 1- AADC

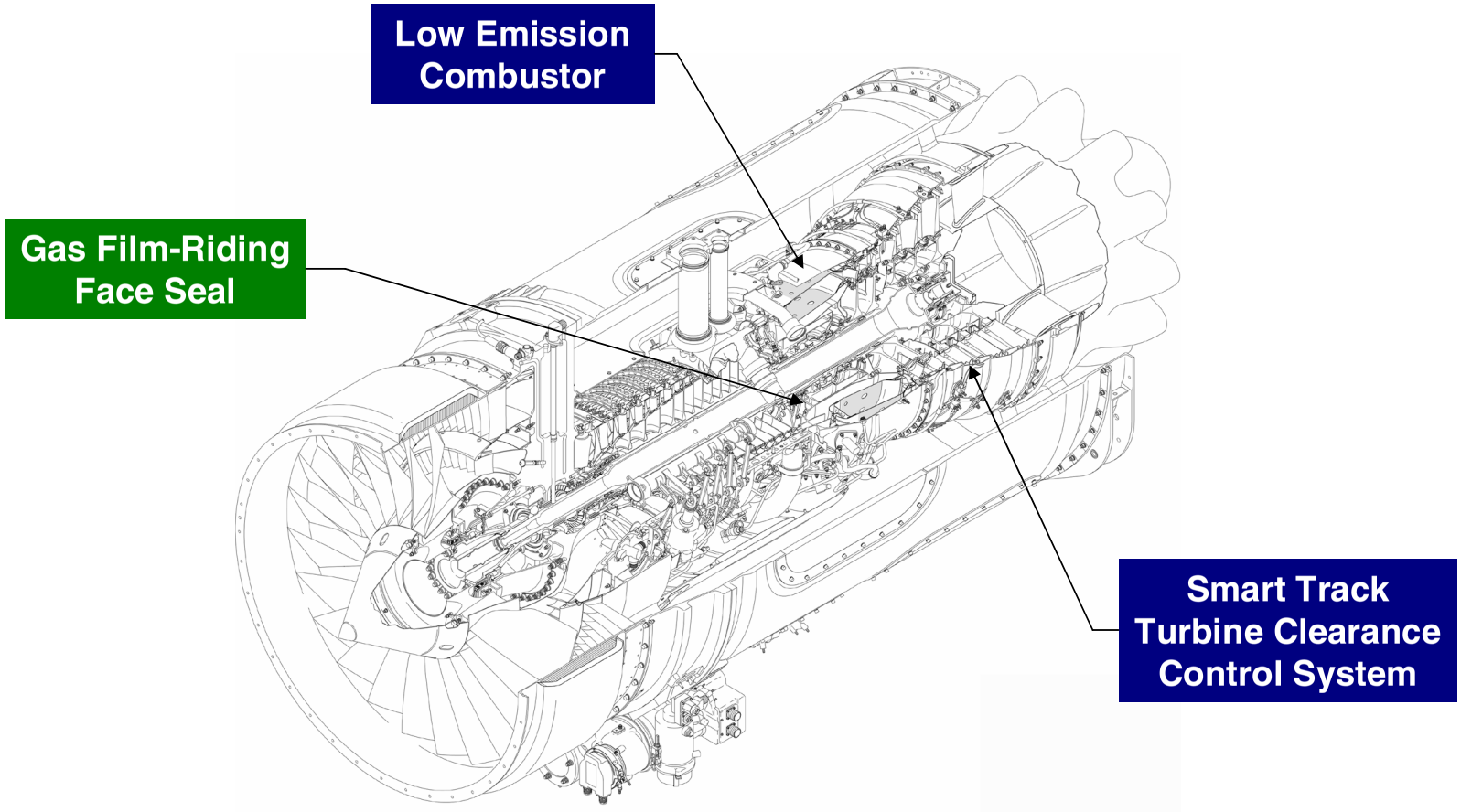

Proposed testbed engine is 7,000- to 9,000-lb thrust class

EVNERT Phase 1- GEAE

Integrated Multifunction Acoustic Composite Fan Case

Shape Memory Alloy Chevron Technology

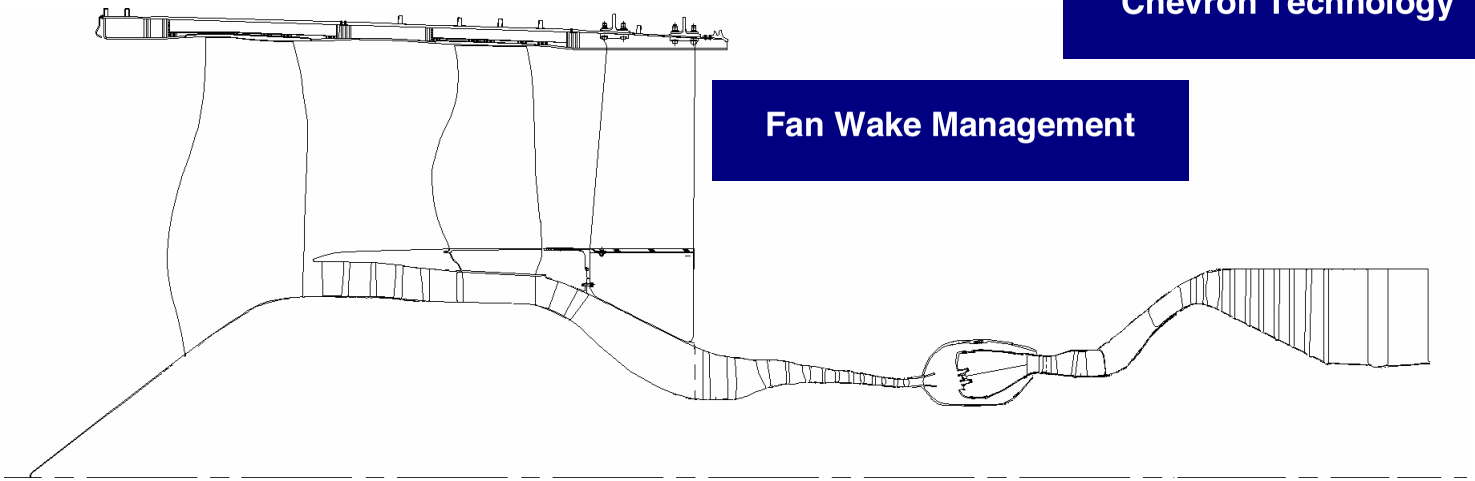

Fan Wake Management

Counter Rotating Fan and LP System

Vortex Stabilizing Jets

Proposed testbed engine is 35,000-lb thrust class

EVNERT Phase 1- Honeywell

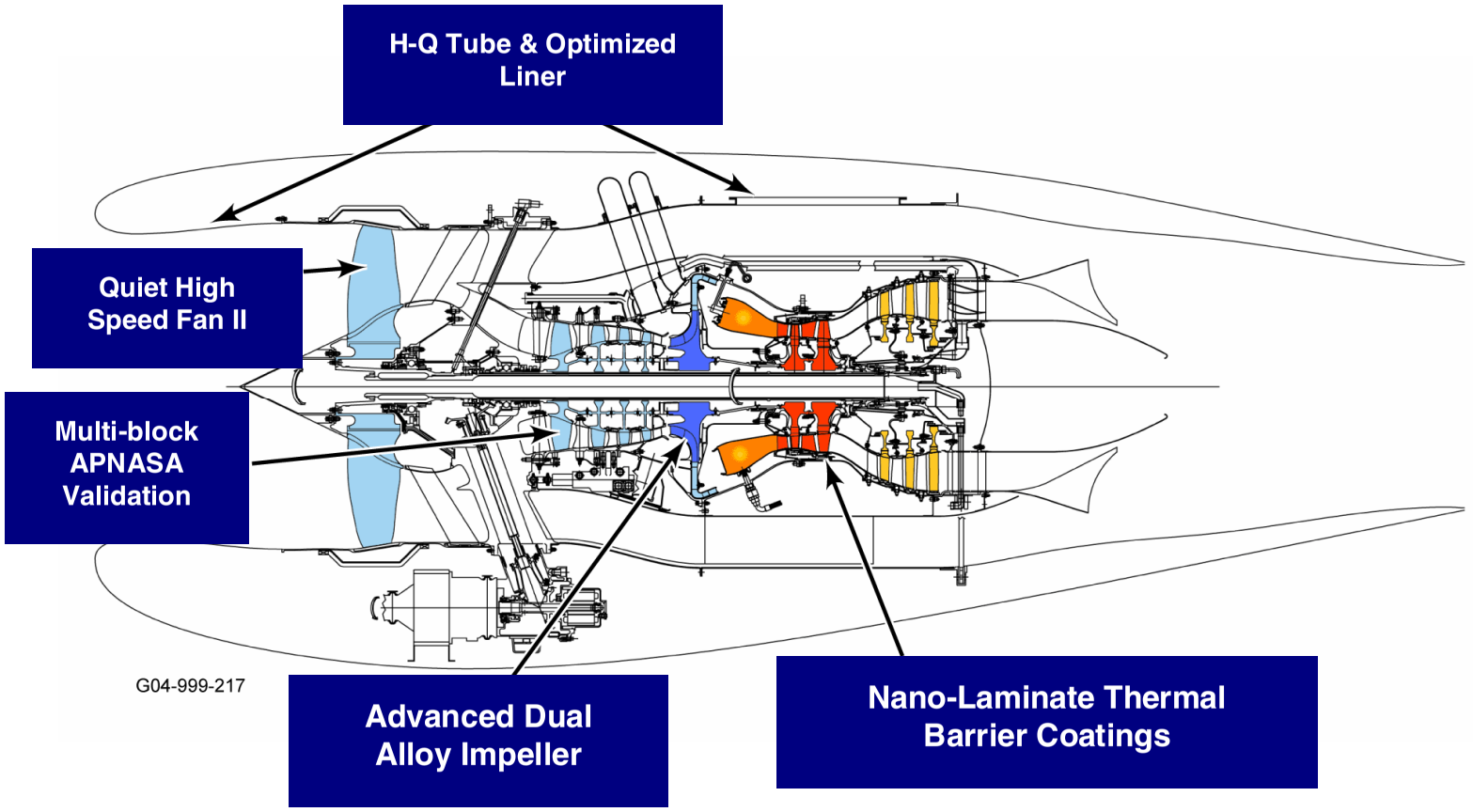

Proposed testbed engine is 8,000-lb thrust class

EVNERT Phase 1- P&W

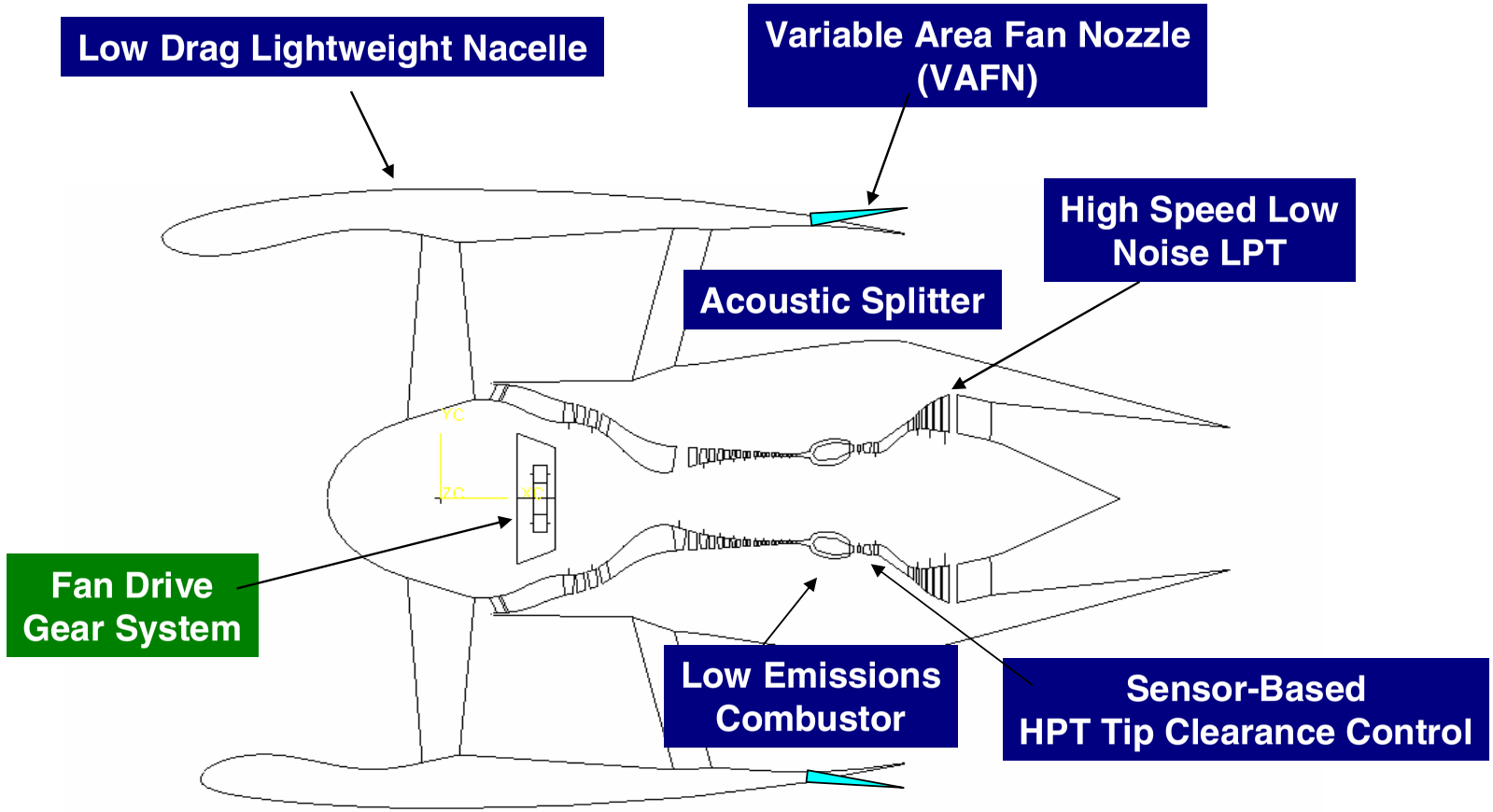

Proposed testbed engine is 35,000-lb thrust class

UEET Mechanical Components

OBJECTIVE: Mature mechanical component technologies for turbine engines to support Subsonic Sector goal of increased T/W; Develop enabling technologies for a large geared turbofan engine

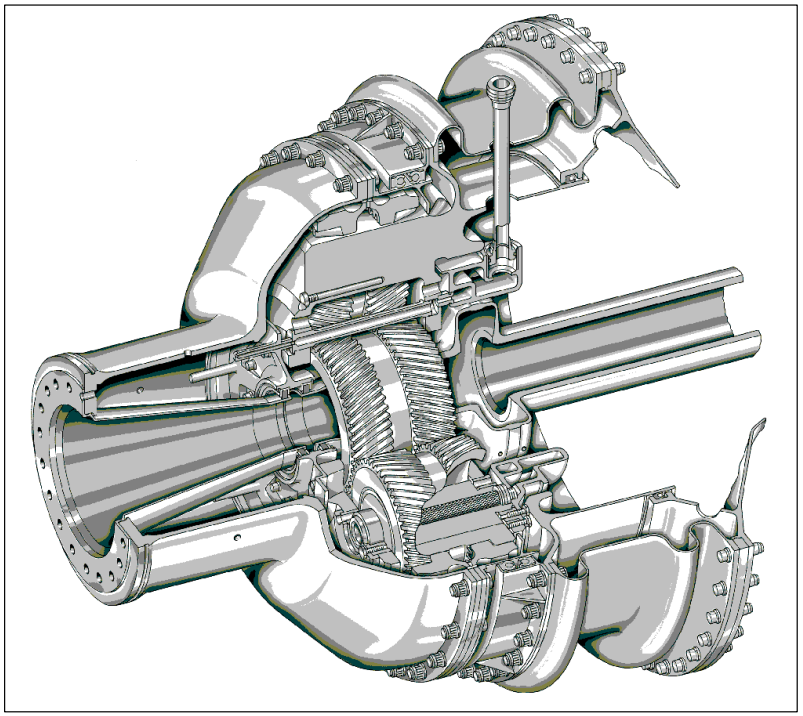

Advanced Planetary Transmission

Benefits:

- Efficiency is increased by allowing fan to operate optimum speed

Enabling Technologies:

- Uninterruptible lubrication system for highly loaded journal bearings of geared engines
- Bearing compartment seals with high misalignment capabilities
- Wave bearings for a lighter and more stable system

Lube System and High Misalignment Seal

Uninterruptible Lubrication System

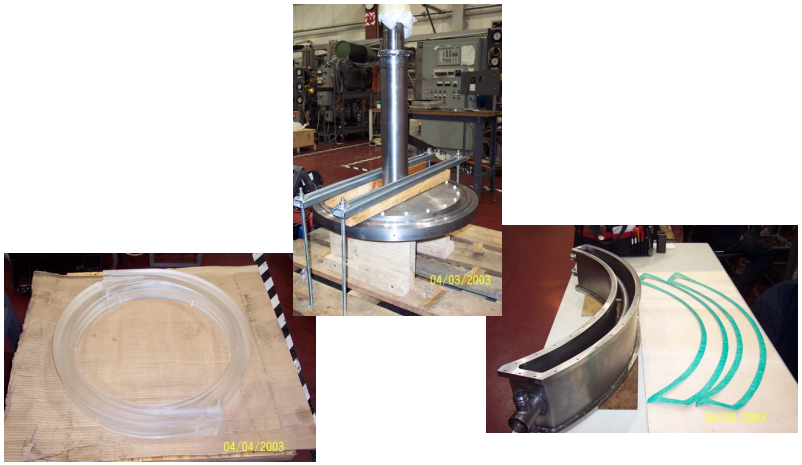

High Misalignment Seals Technical Results

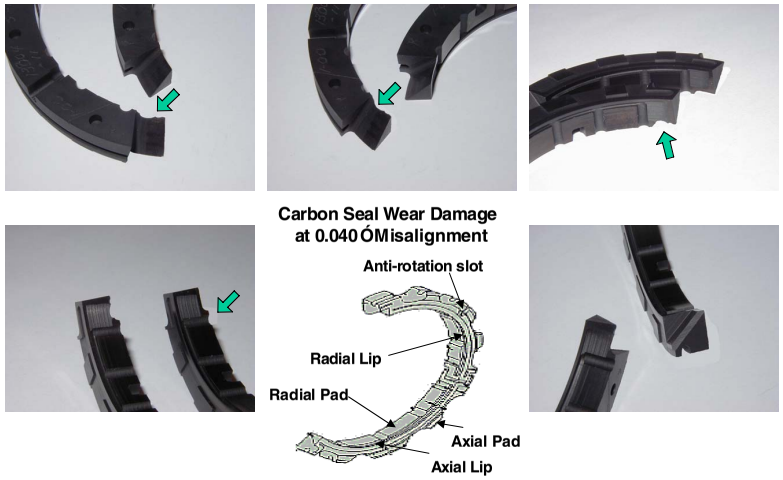

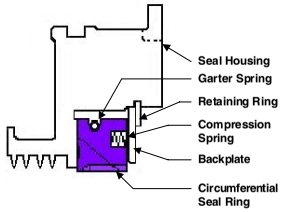

1-Piece Segmented Circumferential (Baseline - Tested)

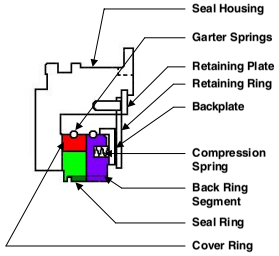

3-Piece Segmented Circumferential (Manufacturing in Process)

Summary Comments

- Vehicle Systems Program has passed the Non-Advocate Review and is proceeding onto implementation
- Ultra-Efficient Engine Technology and Quiet Aircraft Technology projects have been reformulated to support the goals of the Vehicle Systems Program
- Numerous technologies are being matured including seals which will enable the projects to successfully meet the emissions and noise reduction goals

HIGH MISALIGNMENT CARBON SEALS FOR THE FAN DRIVE GEAR SYSTEM TECHNOLOGIES

Dennis Shaughnessy and Lou Dobek
United Technologies
Pratt & Whitney
East Hartford, Connecticut

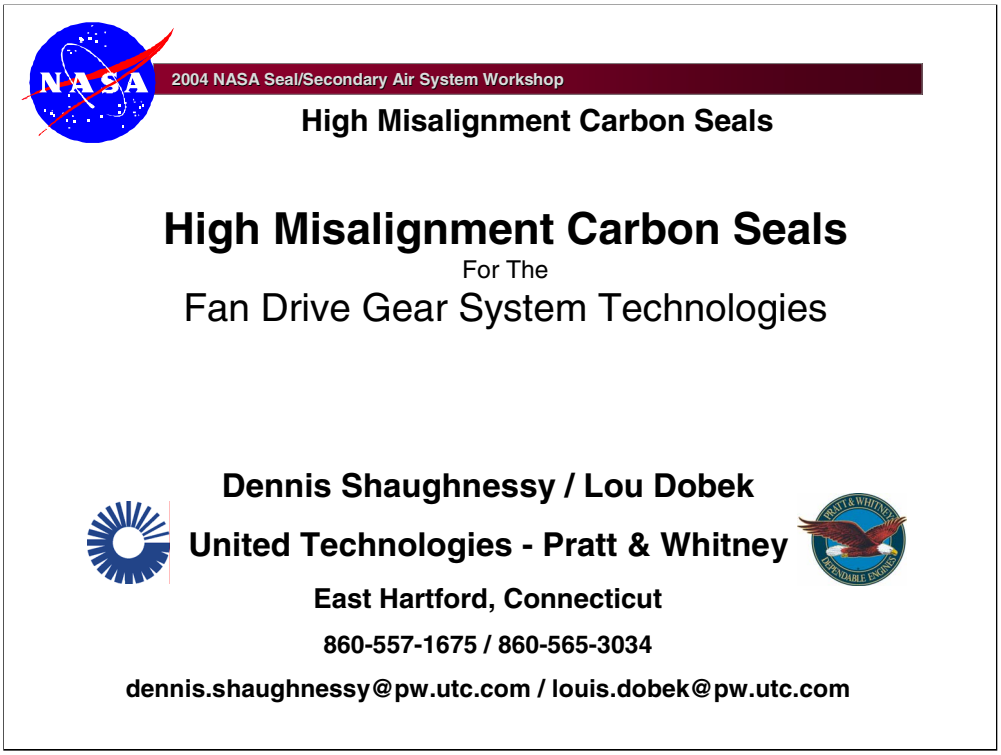

The Ultra Efficient Engine Technology (UEET) program is a NASA supported program to develop and demonstrate technology for quiet, fuel-efficient, low-emissions next generation commercial gas turbine aircraft engines. An essential role for achieving lower noise levels and higher fuel efficiencies is played by the power transmission gear system connected to the fan. Reduction geared systems driving the fan will be subjected to inertia and gyroscopic forces resulting in extremely high angular and radial misalignments. Because of the high misalignment levels, compartment seals capable of accommodating angularities and eccentricities are required. Pratt & Whitney and Stein Seal Company selected the segmented circumferential carbon seal as the best candidate seal type to operate at highly misaligned conditions and developed a test program to determine misalignment limits of current segmented circumferential seals. The long-term goal is to determine a seal design able to withstand the required misalignment levels and provide design guidelines. A technical approach is presented, including design modification to a “baseline” seal, carbon grade selection, test rig configuration, test plan and data acquisition. Near term research plans are also presented.

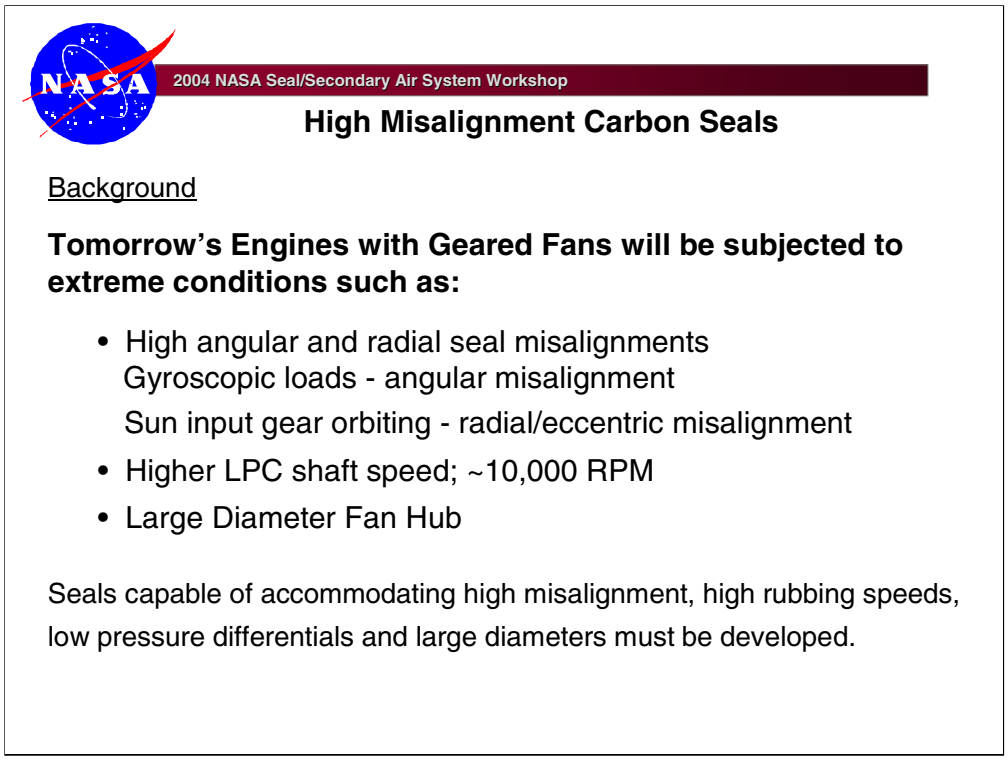

Background information on principal causes of extreme conditions in Advanced Commercial Engines. Such conditions impose on seals high misalignment, high rubbing speed, large diameters and low pressure differentials.

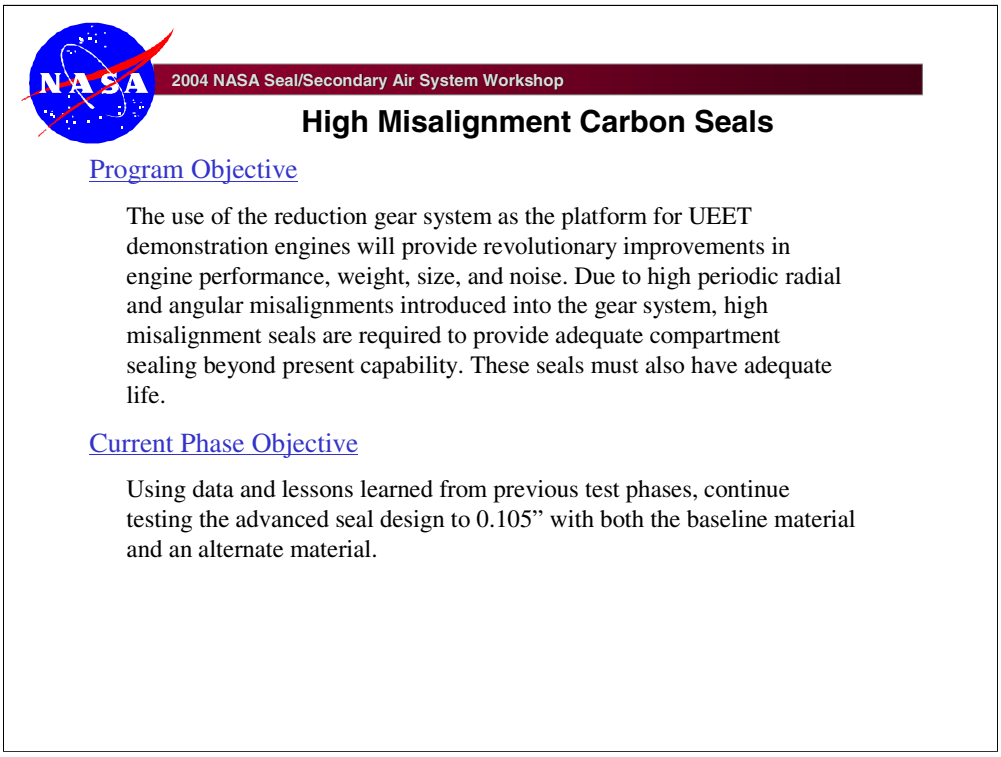

Overall program objective identifies the need for seals capable of periodic high radial and angular misalignment.

The current phase objective is to test an advanced seal design up to 0.105” of total misalignment using both the baseline material as well as an alternate material.

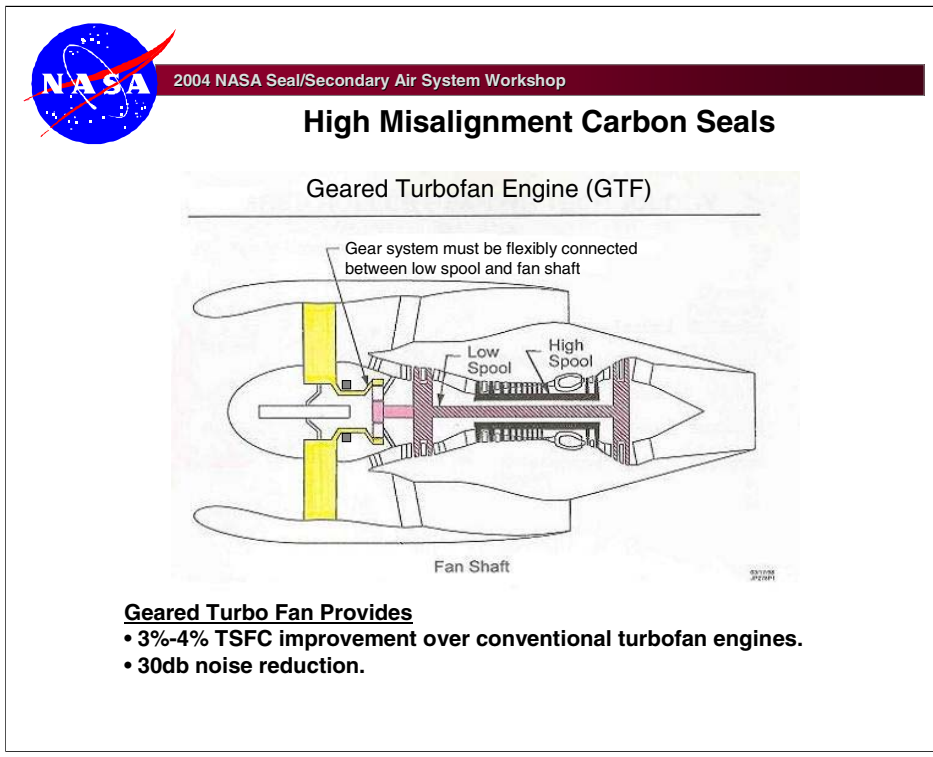

Misalignment seals are located along the flexible shaft between the low spool and fan shaft.

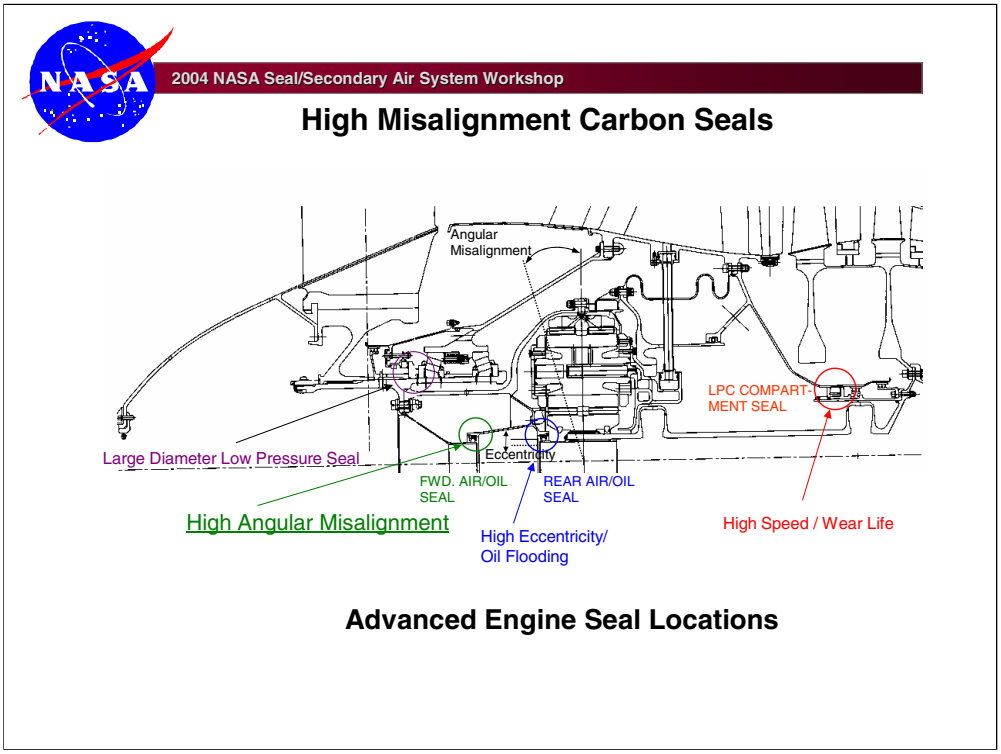

Seal locations within the forward compartments of the fan drive geared engine. Forward air/oil seal represents the location of the highest source of angular and radial misalignment.

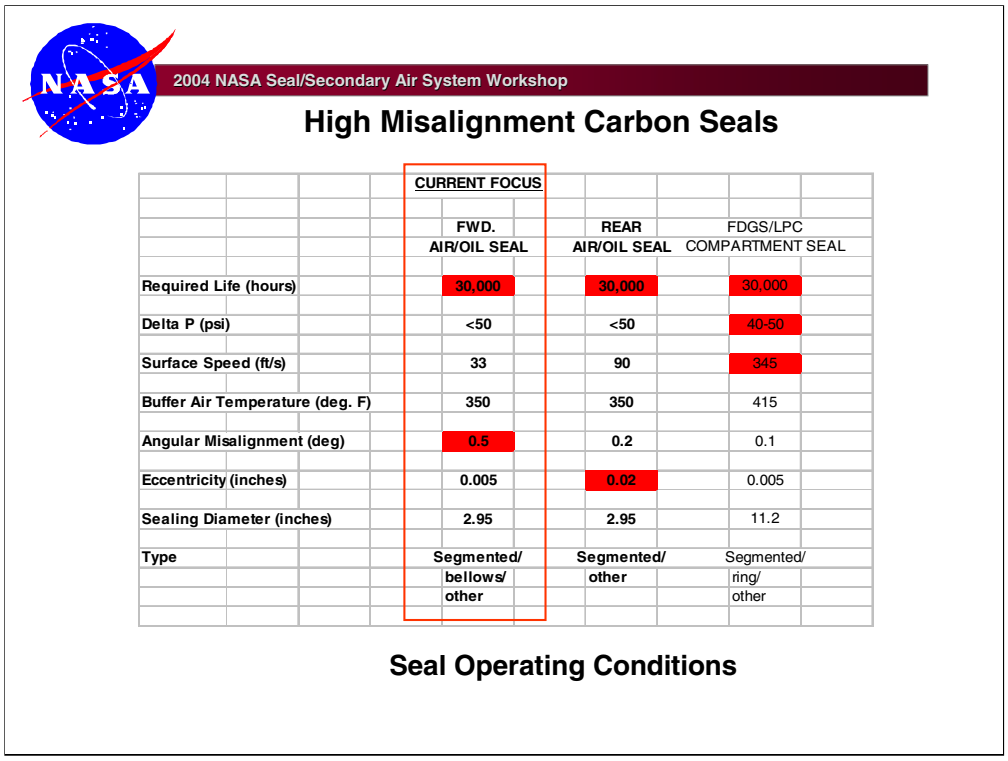

Seal operating conditions (required life, pressure differentials, speeds, misalignment levels and others).

Critical requirements are highlighted.

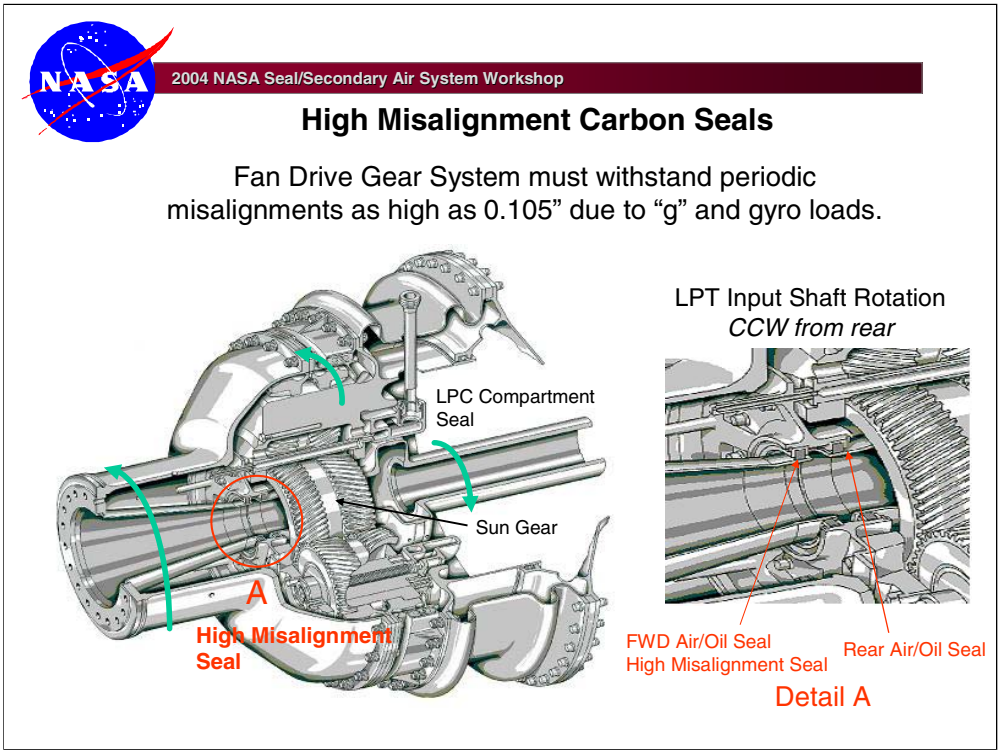

Fan drive gear systems must withstand periodic misalignments as high as 0.105" due to "g" and gyro loads.

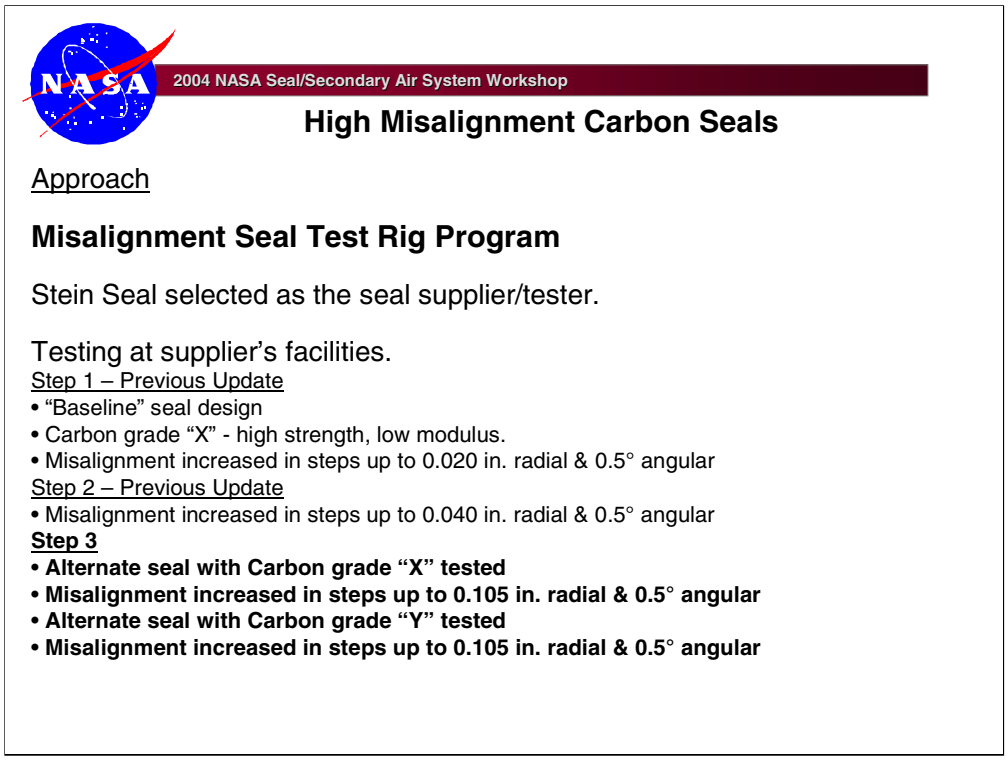

Technical approach of misalignment seal development program. Three main steps will be followed starting from "baseline" seal testing.

High Misalignment Test Rig

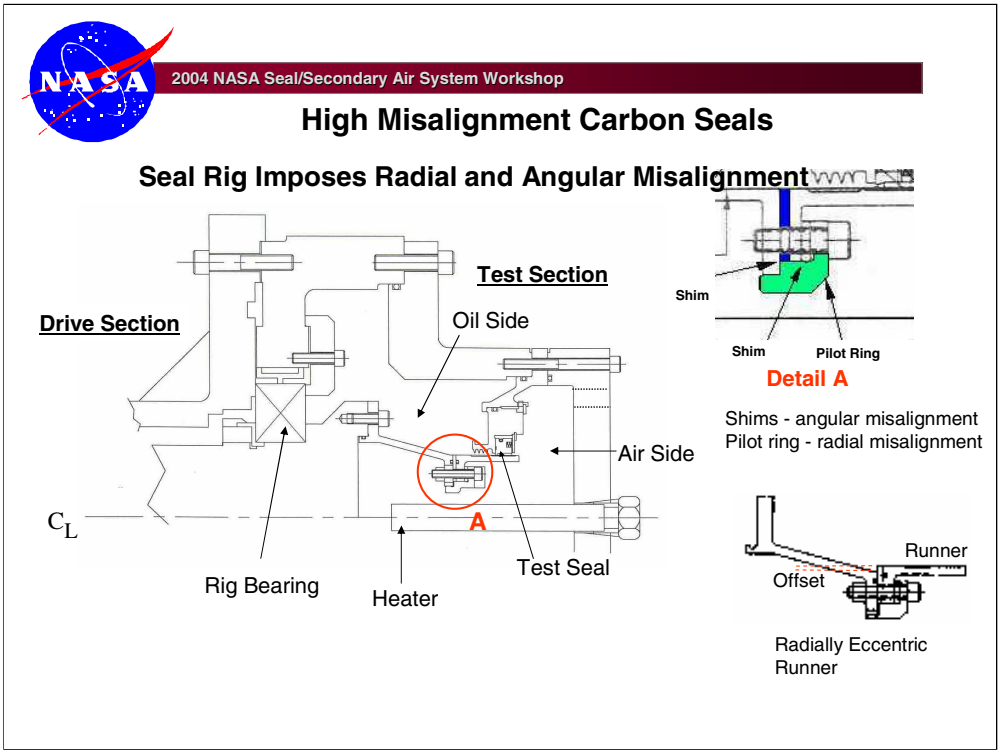

Seal test rig schematics used to impose radial and angular misalignment. Shims are used to impose angular misalignment and pilot rings are used to impose radial misalignment.

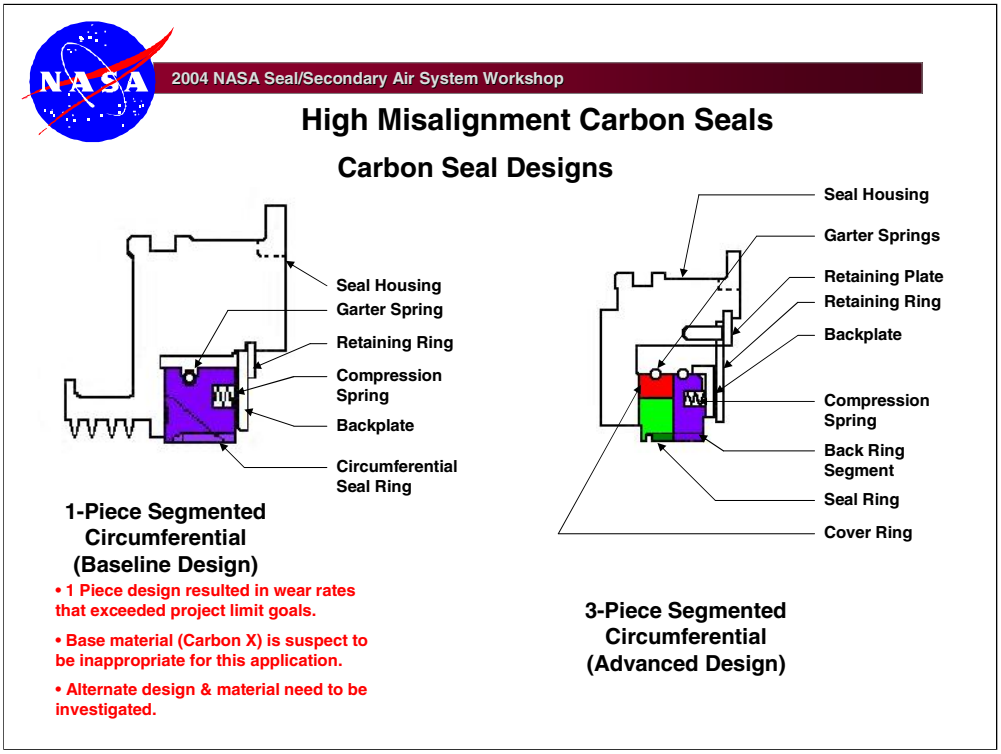

Baseline seal is compose of a one-piece 4 segmented seal. Alternate design is composed of a three-piece design, each piece consisting of four segments.

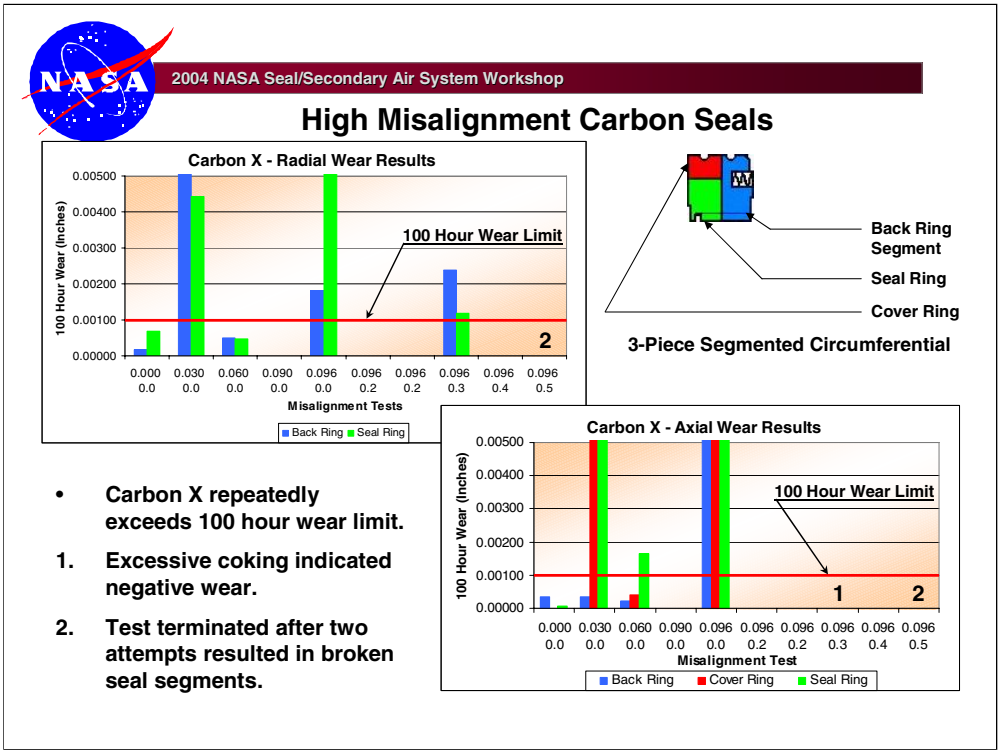

Carbon X repeatedly exceeds the 100 hour wear limit goal and testing was terminated after multiple failures.

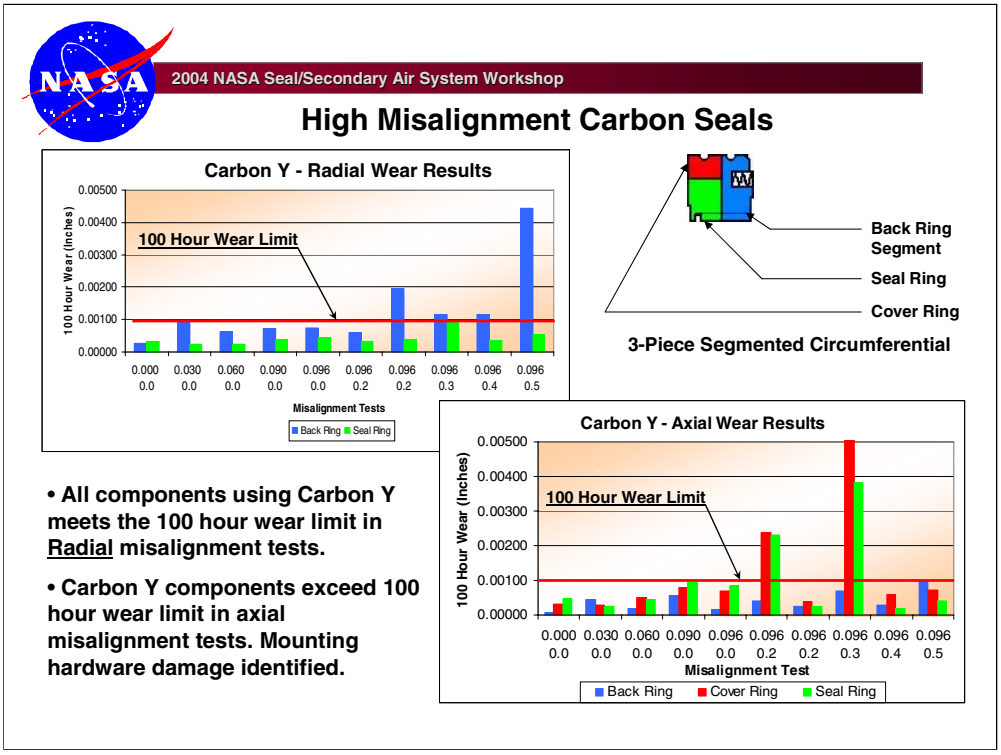

Carbon Y meets the 100 hour wear limit under purely radial misalignment conditions. Seal retaining hardware suffered fatigue and failure during combination radial & angular misalignment tests. These failures are to be investigated at the potential reasons for the 100 hour wear limit to be exceeded.

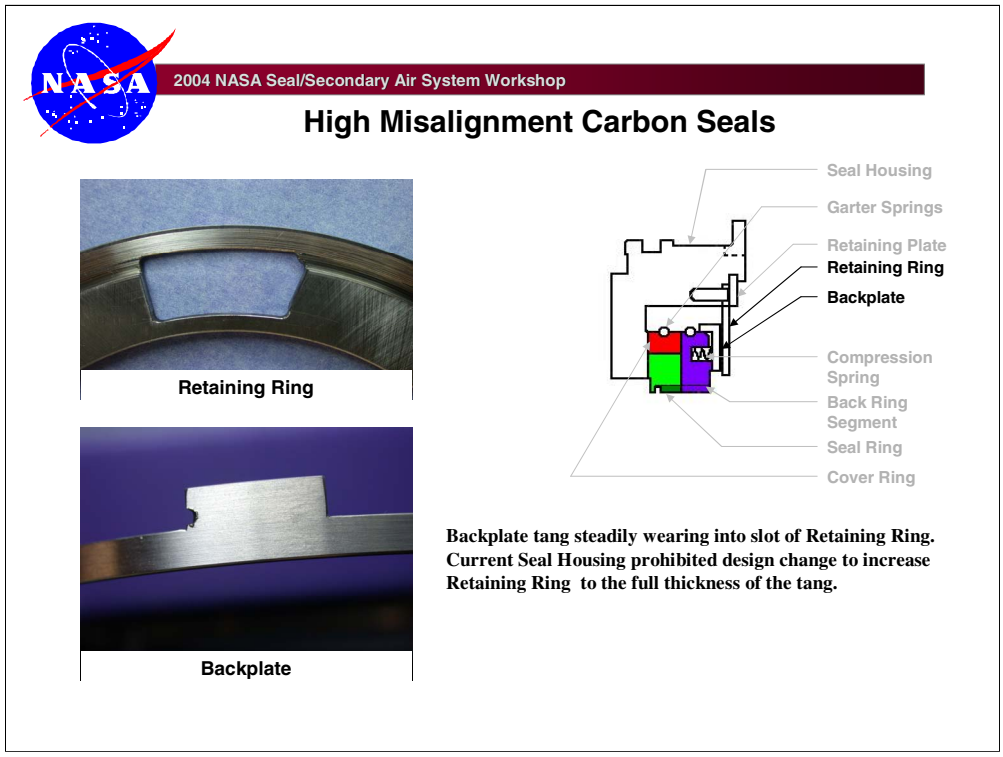

Photos of seal retaining hardware show the wear the occurred during misalignment testing.

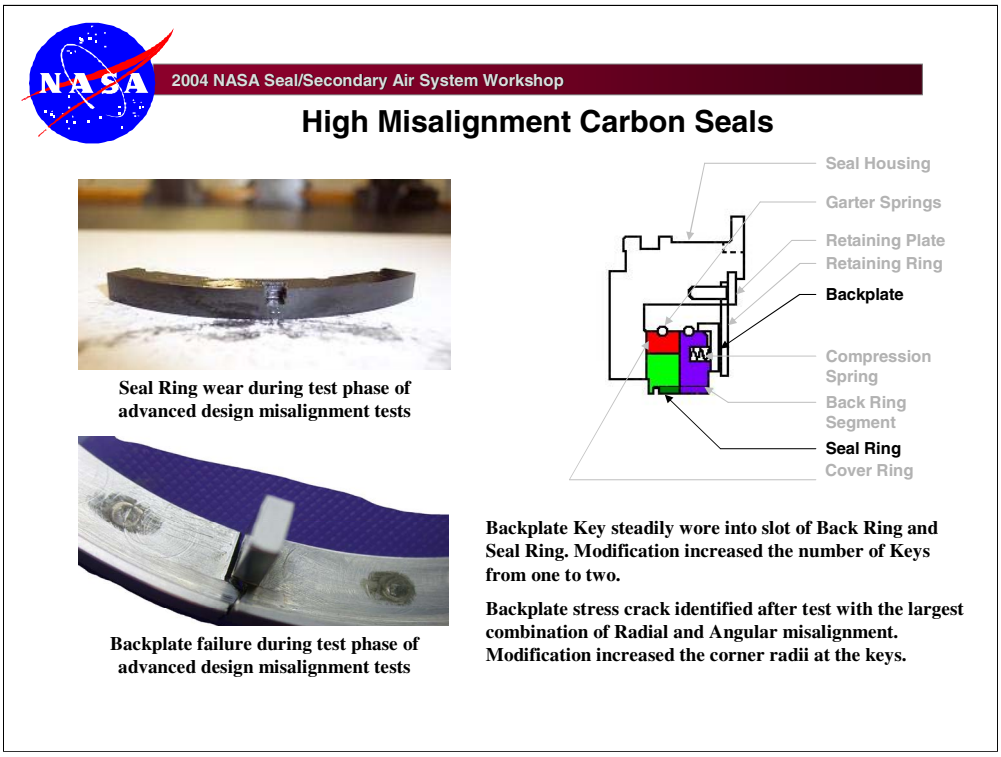

Photos of seal and associated retaining hardware show the wear and stress fracture that occurred during misalignment testing.

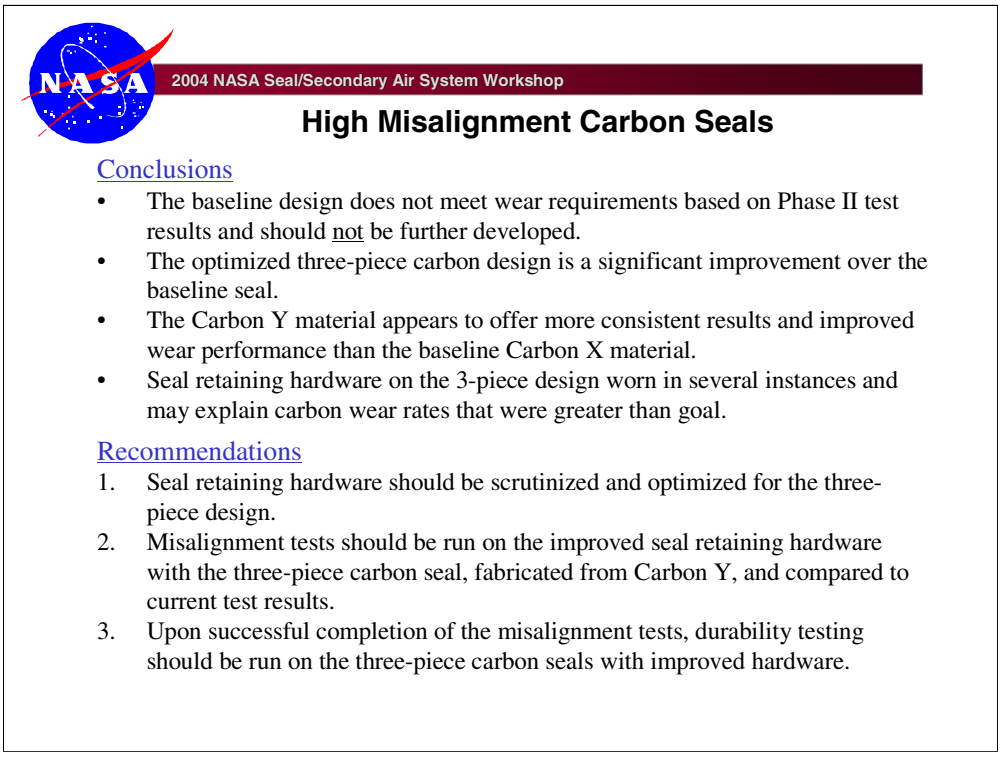

Conclusions identify that baseline seal design should not be further developed. Also the 3-piece design is a significant improvement over the baseline design. Carbon Y material appears to offer improved wear results from that of Carbon X. Further work is needed to improved the seal retaining hardware.

Recommendations are to investigate seal retaining hardware and improve. Another battery of tests utilizing Carbon Y and improved retaining hardware should be run and compared to the current results.

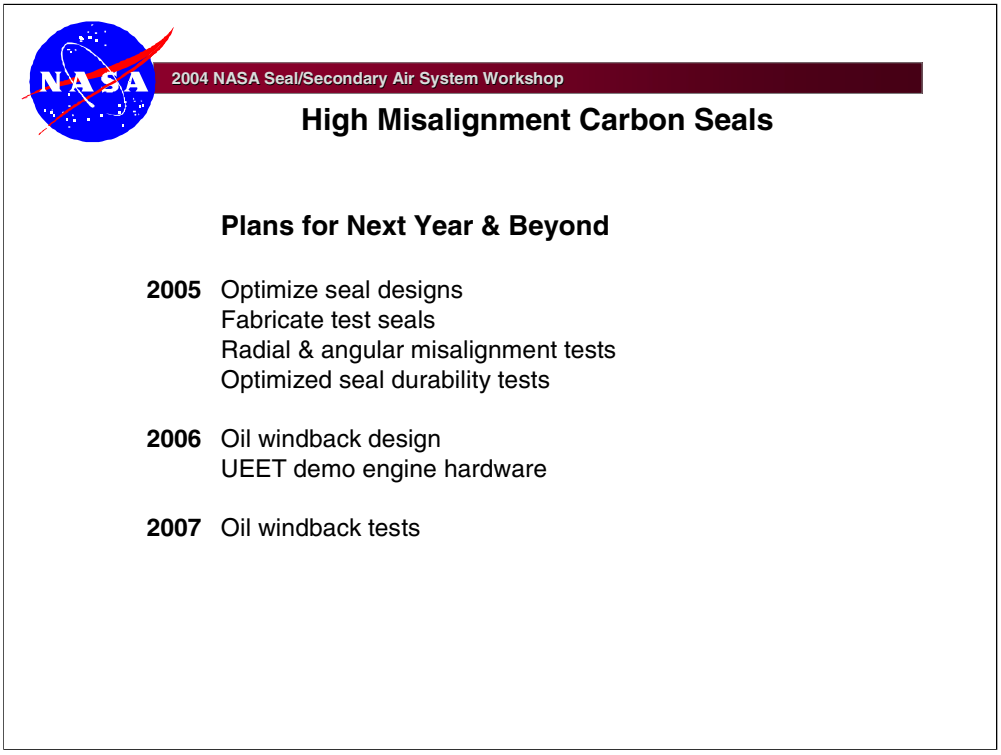

Plans for continuation include design optimization, durability testing, and windback design and testing.

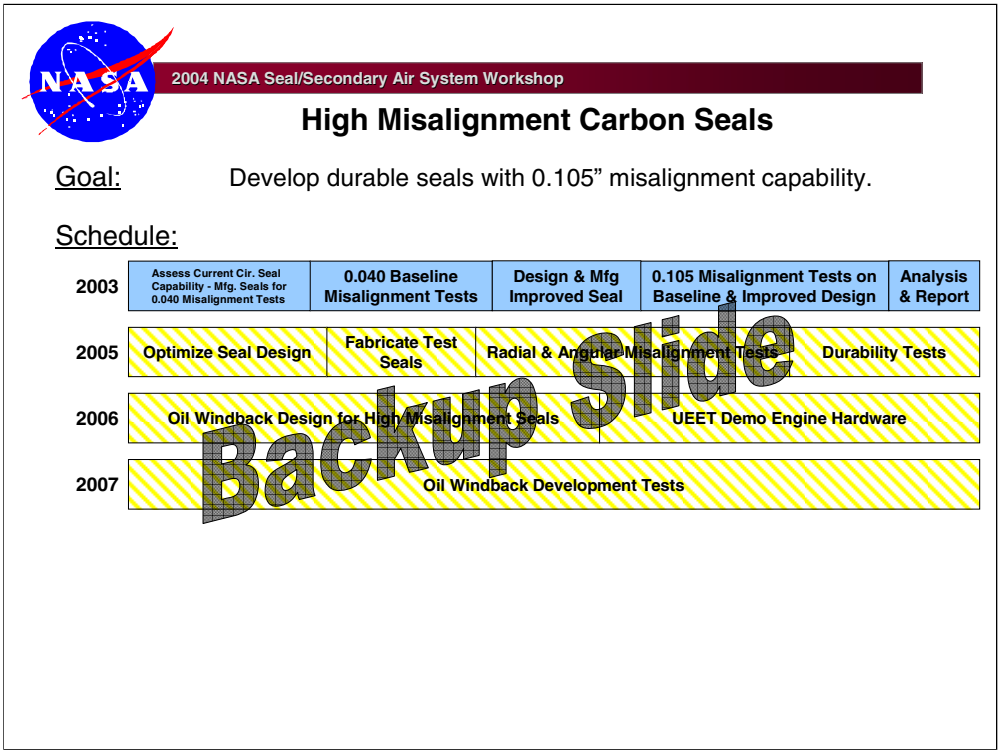

Objective – Development of seals capable of 0.105” misalignment for use in the Pratt & Whitney reduction gear system.

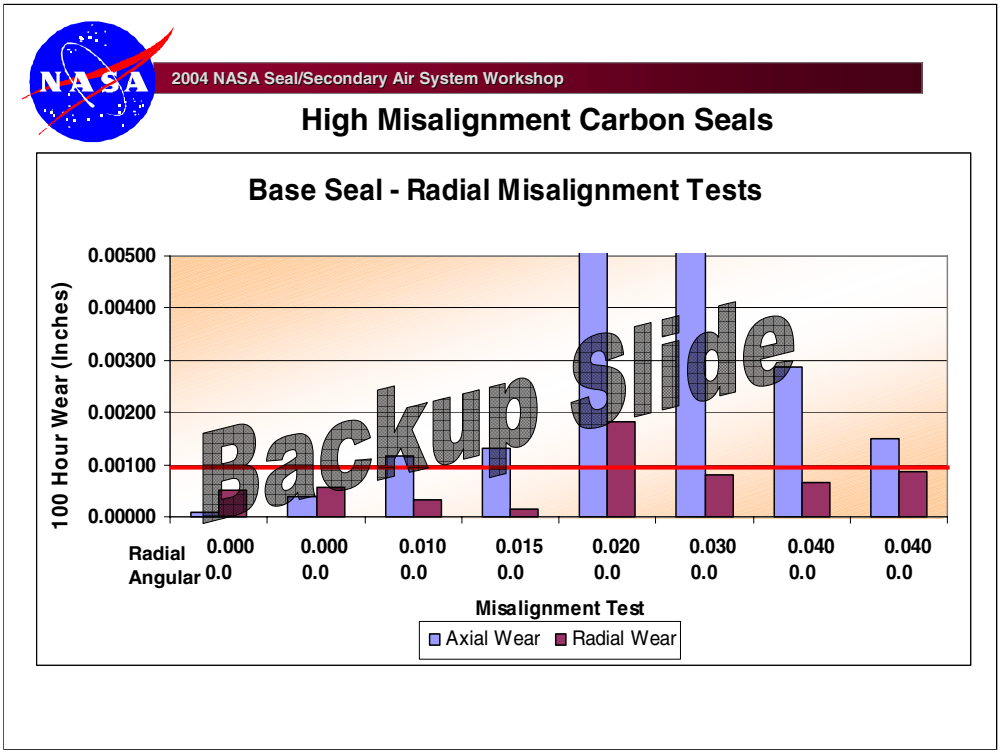

Step one and two test results indicate wear rates in excess of those desired. Unexpected reduction in wear rates at higher levels of misalignment under investigation.

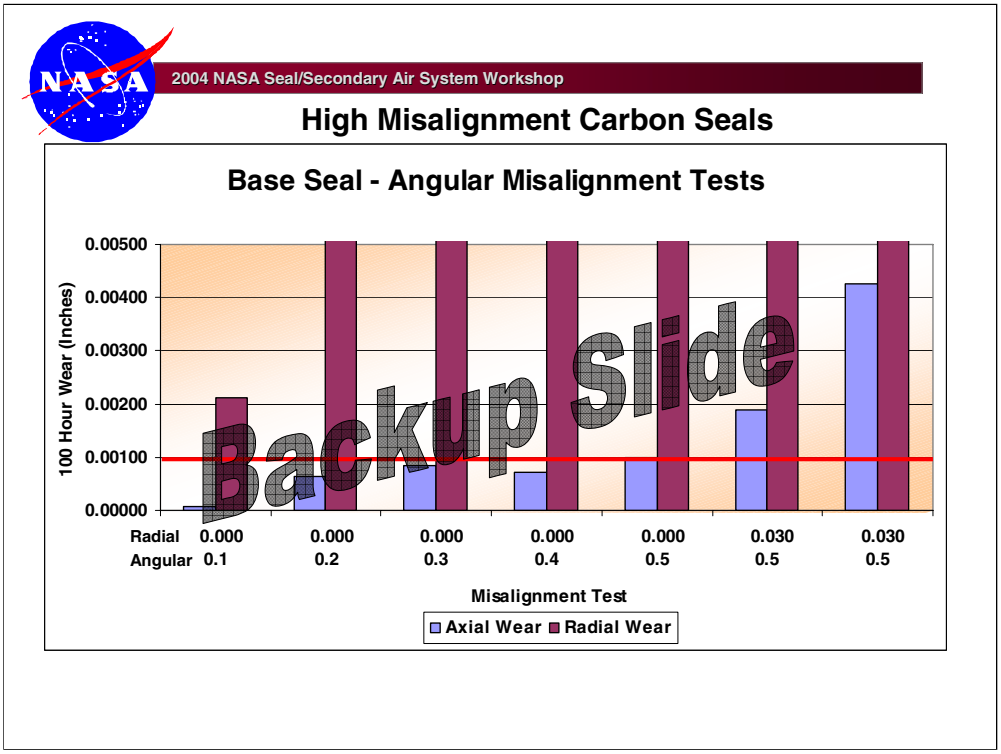

Step one and two test results indicate wear rates in excess of those desired. Unexpected reduction in wear rates at higher levels of misalignment under investigation.

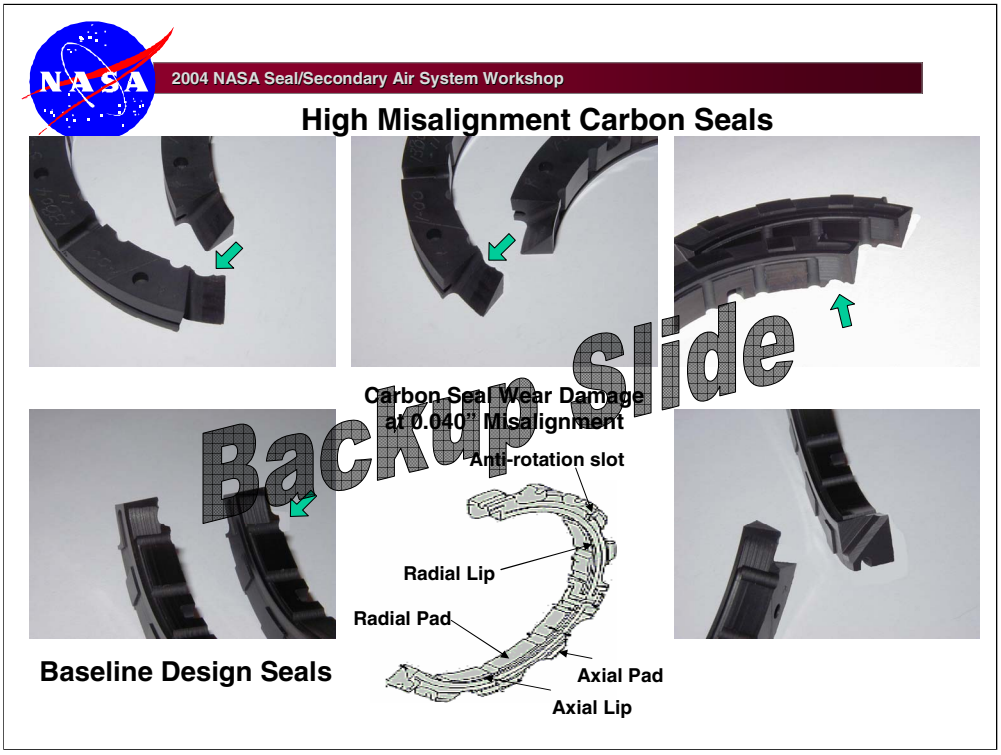

Step one Carbons indicate excessive wear and chipping along the tongue and sockets of the segments.

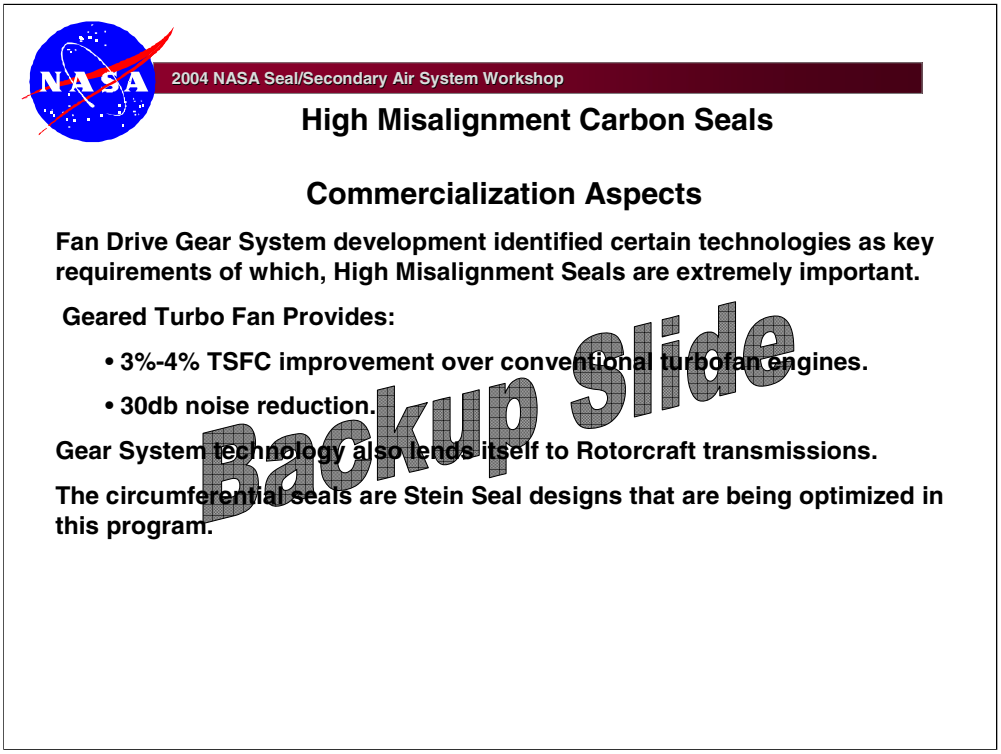

The Fan Drive Gear System offers significant advances in the areas of weight reduction, noise reduction and fuel consumption.

LEAKAGE AND POWER LOSS TEST RESULTS FOR COMPETING TURBINE ENGINE SEALS

Margaret P. Proctor
National Aeronautics and Space Administration
Glenn Research Center
Cleveland, Ohio

Irebert R. Delgado
U.S. Army Research Laboratory
Glenn Research Center
Cleveland, Ohio

Advanced brush and finger seal technologies offer reduced leakage rates over conventional labyrinth seals used in gas turbine engines. To address engine manufacturers' concerns about the heat generation and power loss from these contacting seals, brush, finger, and labyrinth seals were tested in the NASA High Speed, High Temperature Turbine Seal Test Rig. Leakage and power loss test results are compared for these competing seals for operating conditions up to 922 K (1200 °F) inlet air temperature, 517 KPa (75 psid) across the seal, and surface velocities up to 366 m/s (1200 ft/s).

The authors acknowledge contributions of:

Arun Kumar – Development of finger seal tested.

NASA GRC – conducted all testing.

Bruce Steinetz – guided the design, procurement, and fabrication of the High Temperature, High Speed Turbine Seal Test Rig

For the complete story please see "Leakage and Power Loss Test Results for Competing Turbine Engine Seals" paper by M. P. Proctor and I. R. Delgado presented at Turbo Expo 2004 sponsored by the American Society of Mechanical Engineers in Vienna, Austria, June 14-17, 2004, GT2004-53935, NASA/TM-2004-213049, ARL-TR-3157.

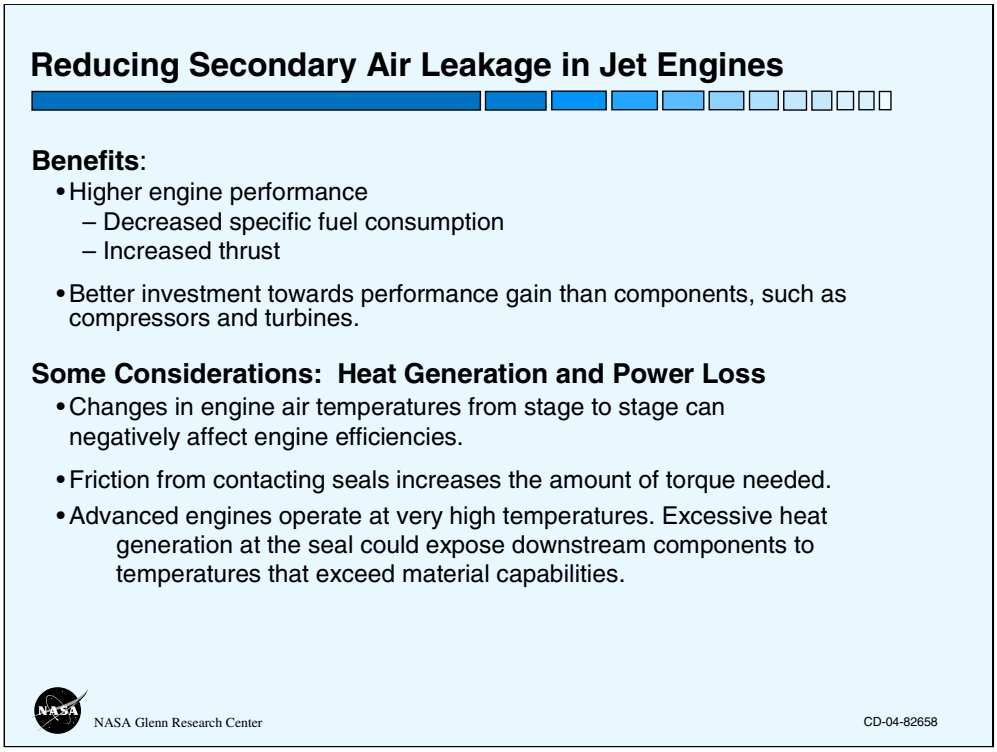

Self-explanatory

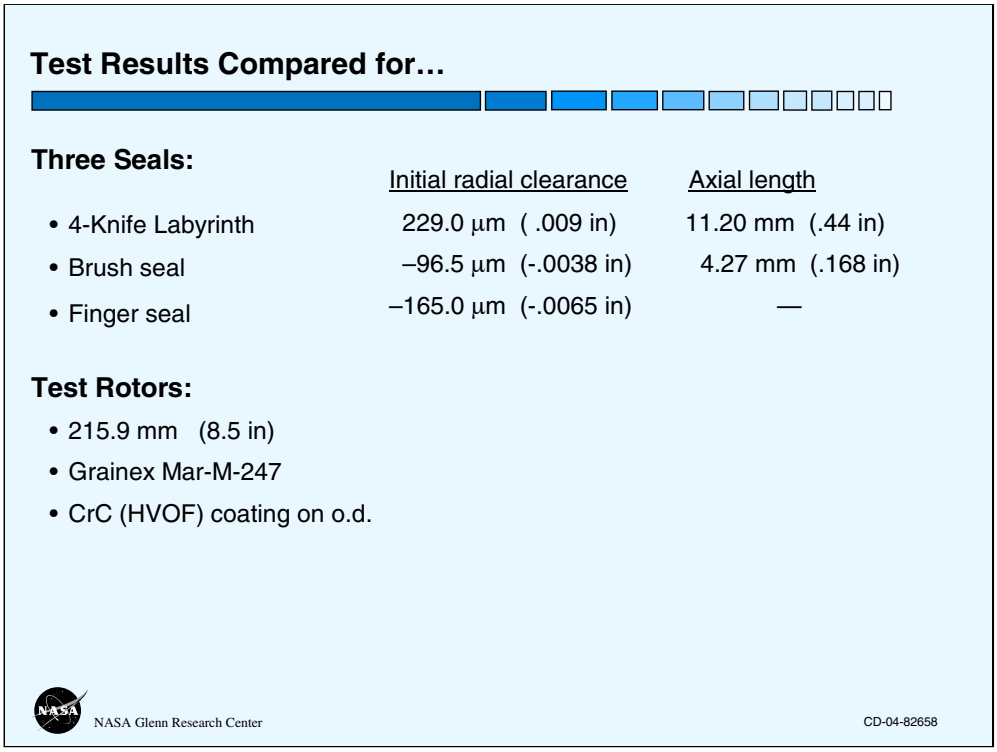

Leakage rate, power loss and wear results are compared for 3 seals: 4-knife labyrinth seal, a brush seal, and a finger seal.

The labyrinth seal had an initial radial clearance of 229 microns.

Both the brush seal and the finger seal initially had an interference with the rotor.

The radial interference of the brush seal was 96.5 microns.

The radial interference of the finger seal was 165 microns.

The finger seal has an axial length similar to the brush seal.

The axial length of the brush seal is 38 percent of the labyrinth seal.

The 216 mm test rotors used are made of Grainex Mar M-247 and have a chrome carbide coating on the o.d.

Four-Knife Labyrinth Seal

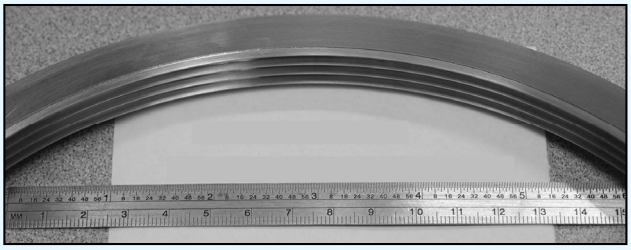

Labyrinth Seal Design Parameters

Material	Inconel 625
Type	Straight
Number of knives	4
Rotor outer diameter	215.9 mm
Tooth height	2.286 mm
Tooth taper angle	7.5 degrees
Land thickness	305 μm
Tooth pitch	3.175 mm
Radial clearance	229 μm
Seal inner diameter	216.154 mm

NASA Glenn Research Center

CD-04-82658

4 knife labyrinth seal has straight thru knife-edges and a radial clearance of 229 microns.

It is made of Inconel 625.

Only static tests were conducted.

It was determined that for safe operation at maximum speed and temperature that the labyrinth seal would need radial clearance of 305 microns at build.

KTK, an labyrinth seal analysis code, was used to predict the flowrates of this larger clearance seal.

Brush Seal With Flow Deflector

- **Inconel-625 sideplates**
- **Bristles are:**
  - Haynes-25
  - 102 μm diameter
  - At 50° angle to radius
  - 675 bristles/cm of circumference at seal i.d.
- **Fence height: 1.27 mm**
- **Total axial thickness: 4.27 mm**

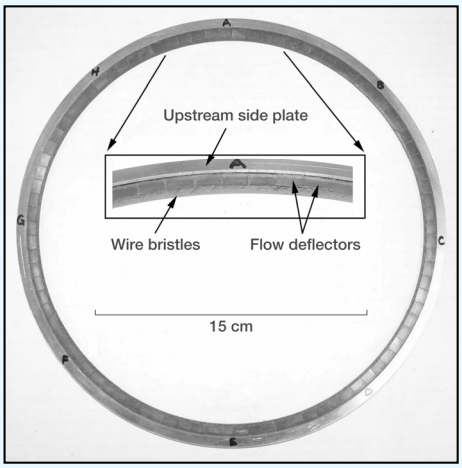

NASA Glenn Research Center

CD-04-82658

This is the brush seal we tested.

A brush seal is simply an annular pack of bristles sandwiched between two annular plates. This brush seal has a flow deflector on the upstream side to prevent the flow from jetting thru the bristles.

The sideplates are made of Inconel 625 and the bristles are made of Haynes-25.

The 102 micron (.004 in) diameter wire bristles are at a 50 degree angle to the radius allowing them to deflect away from the rotor as cantilever beams to accommodate rotor growth or deflections.

There are 675 bristles/cm of circumference at the seal id and the seal has a fence height of 1.27 mm (.050 in).

Fence height is the distance from the bristle i.d. to the i.d. of the seal backplate.

Total axial thickness is 4.27 mm (.168 in).

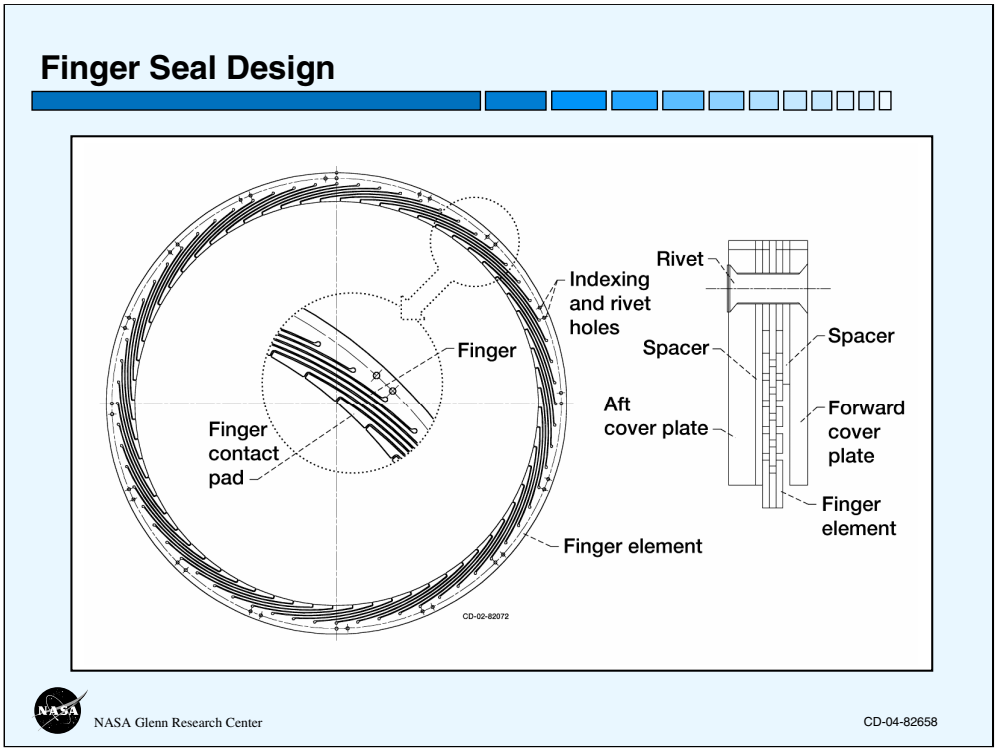

The finger seal functions similarly to the brush seal.

It is made of AMS 5537, a cobalt-base alloy.

It is comprised of forward and aft coverplates, 2 spacers, and 3 finger elements.

The annular finger elements are made of sheet stock and have a series of cuts along the inner diameter to create the fingers.

These fingers deflect as cantilever beams when loaded by rotor interference due to design, thermal or centrifugal growth or rotordynamics.

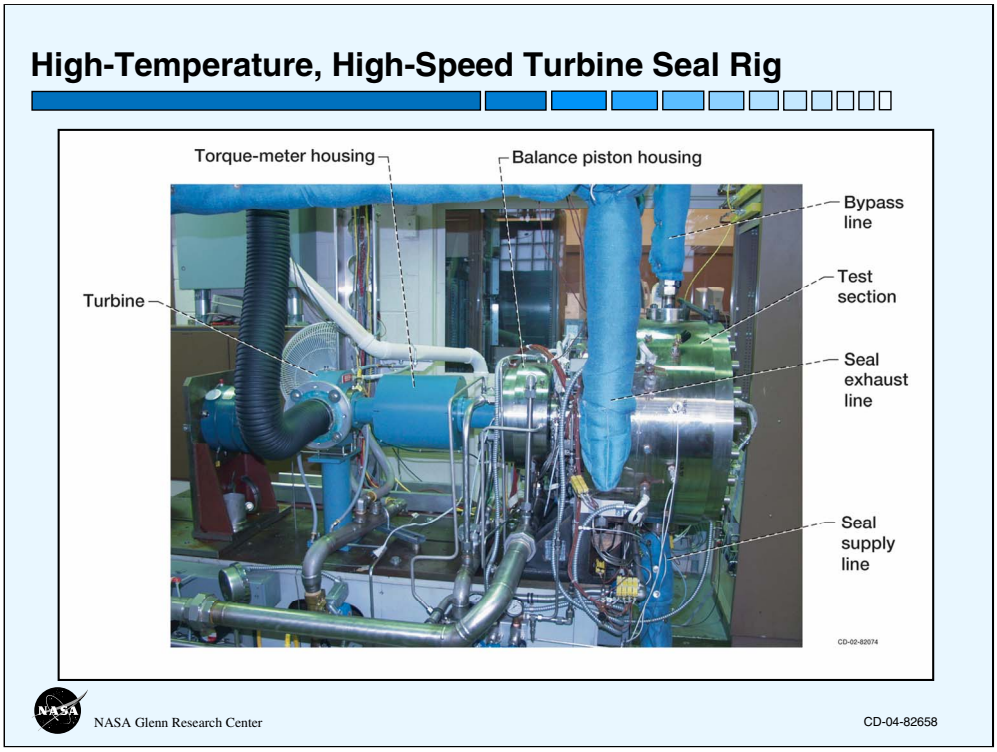

All the seals were tested in the High Temperature, High Speed Turbine Seal Rig at NASA Glenn Research Center.

Hot air enters the bottom of the test section, passes thru the seal and exits thru the 2 exhaust lines.

Under some conditions it is necessary to bypass the seal to maintain the test temperature.

Seal supply and bypass flow rates are measured. The difference of these 2 flows is the seal leakage rate.

An air turbine is used to power the rig.

The torquemeter is located between the turbine and the test rig.

A balance piston is used to control the thrust loads on the bearings due to the pressure differential acting on the seal test rotor.

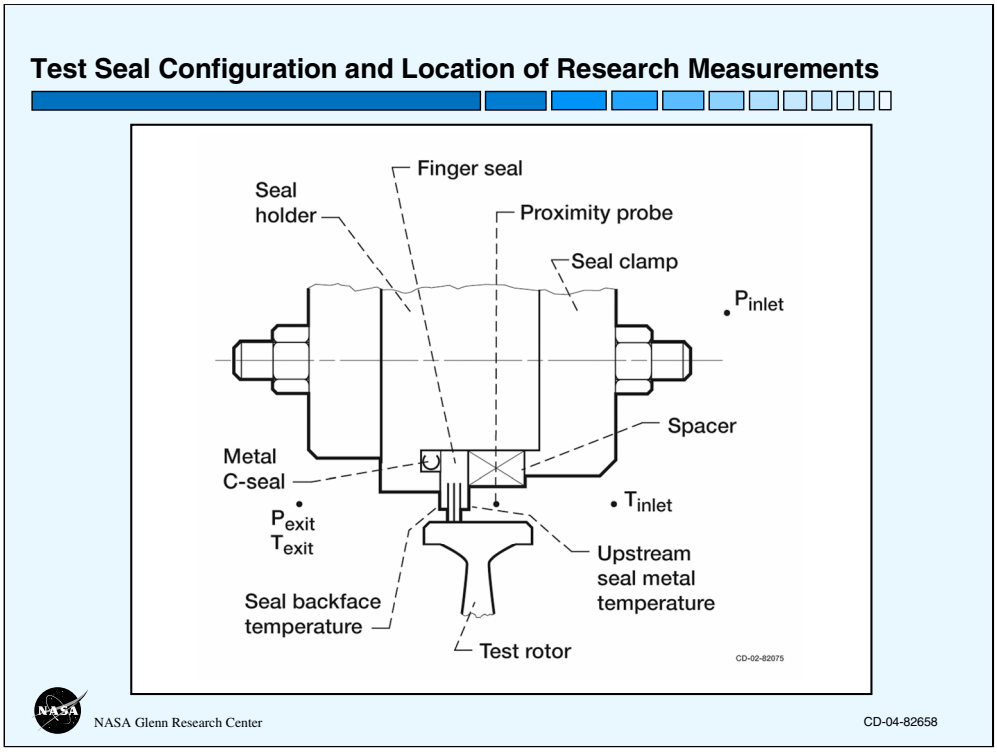

Here is the (Point out) the Test Rotor, Seal holder, and test seal.

The test seal is held in place by the spacer and the seal clamp.

For some tests proximity probes were mounted in the spacer to measure changes in clearance.

A metal c-seal is used to prevent flow from bypassing the test seal.

Inlet and exit pressures and temperatures are measured as well as the seal backface temperature.

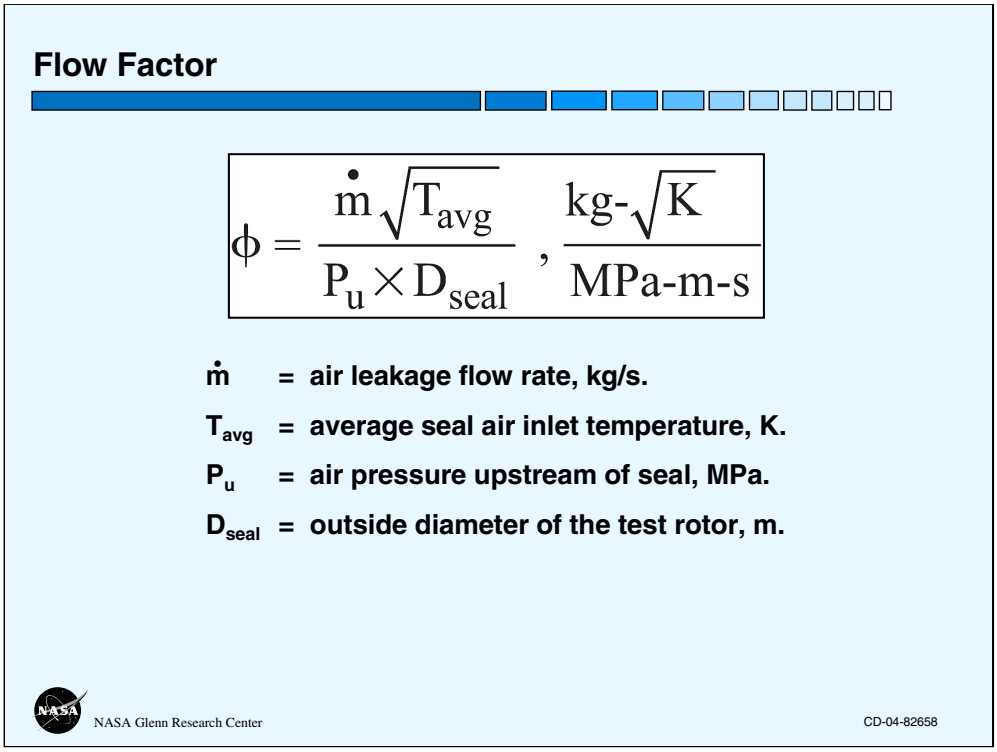

We present the leakage performance of the seals in terms of flow factor. Use of flow factor allows comparison of data taken at different test conditions and between seals of different diameters.

Flow factor is a function of:

the mass leakage rate

average seal air inlet temperature and upstream pressure

and seal diameter

Tests Conducted

Seal	Test Type	Temp., K	Pressure, kPa	Speed, m/s
Brush	Static	294, 533, 700, 811, 922	0 - 517 - 0	0
Brush	Performance	294, 533, 700, 811, 922	69, 276, 517	0, 183, 274, 366, 274, 183, 0
Brush	Endurance	922	517	366
Brush	Post-endurance Performance	294, 533, 700, 811, 922	69, 276, 517	0, 183, 274, 366, 274, 183, 0
Brush	Static	294, 533, 700, 811, 922	0 - 517 - 0	0
Finger	Static	294, 700, 922	0 - 517 - 0	0
Finger	Performance	700, 866, 922	69, 276, 517	0, 183, 274, 366, 274, 183, 0
Finger	Endurance	922	517	366
Finger	Post-endurance Performance	700, 866, 922	69, 276, 517	0, 183, 274, 366, 274, 183, 0
Labyrinth	Static	294	0 - 483 - 0	0

- **4 hour endurance test: inspections after 1, 2, and 4 hours**

NASA Glenn Research Center

CD-04-82658

This is a table showing the tests conducted.

4 tests were conducted on both the brush seal and finger seal: a static test, a performance test, an endurance test, followed by a post-endurance performance test. For the brush seal, the static test was repeated too.

Data was taken at five temperature conditions up to 922 K.

For the static tests, at each temperature the pressure differential was increased to 517 kPa (75 psid) and then decreased to 0.

In the performance tests, at each temperature, and at each of three pressure levels of 69, 276, and 517 kPa, the speed was stepped up to 366 m/s (1200 ft/s) and the stepped back down.

The 4 hour endurance test was conducted at the maximum conditions of 922 K, 517 kPa, and 366 m/s with inspections after hours 1, 2, and 4.

Only a room temperature static test was conducted for the labyrinth seal.

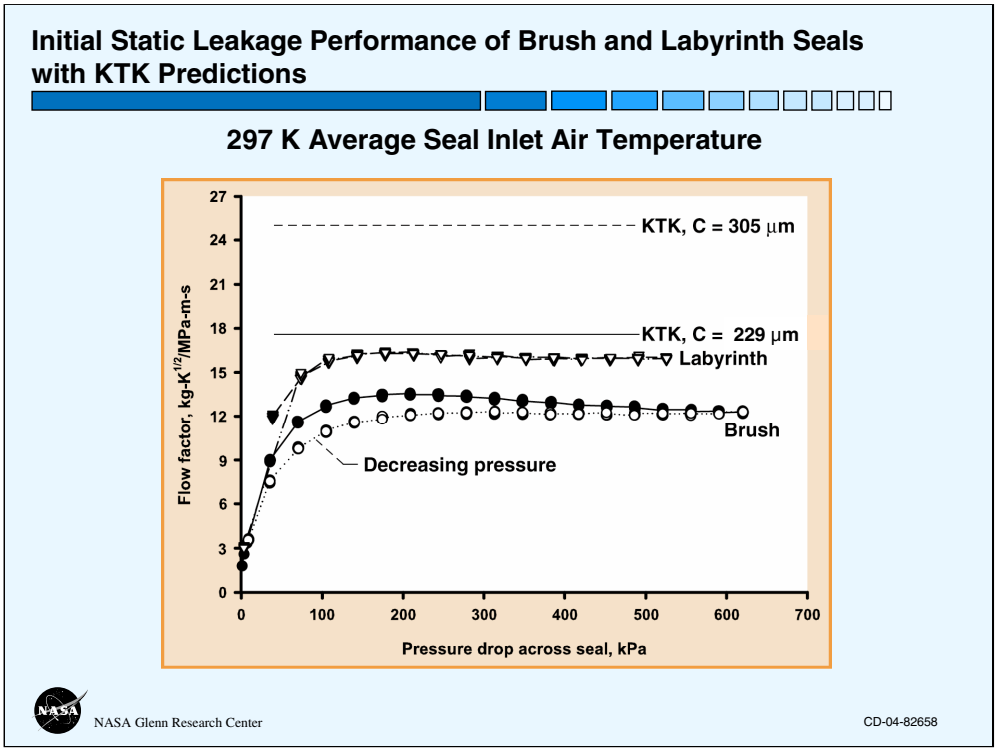

This is a comparison of the initial static leakage performance data measured for the brush seals and the labyrinth seal at room temperature. The plot shows flow factor versus pressure drop across the seal.

Brush seal leakage is 24% less than the labyrinth seal and uses only 38% of the axial space the labyrinth seal requires.

The KTK predicted leakage rate for the seal tested is shown by the solid line.

The measured labyrinth seal leakage is 91% of KTK predicted flow factor of 17.6 kg–$\sqrt{K}$/MPa-m-s.

For safe operation to 922 K and 366 m/s a labyrinth seal with a 305 μm radial clearance is required.

At that clearance, the KTK predicted flow factor is 25 which is twice the brush seal leakage.

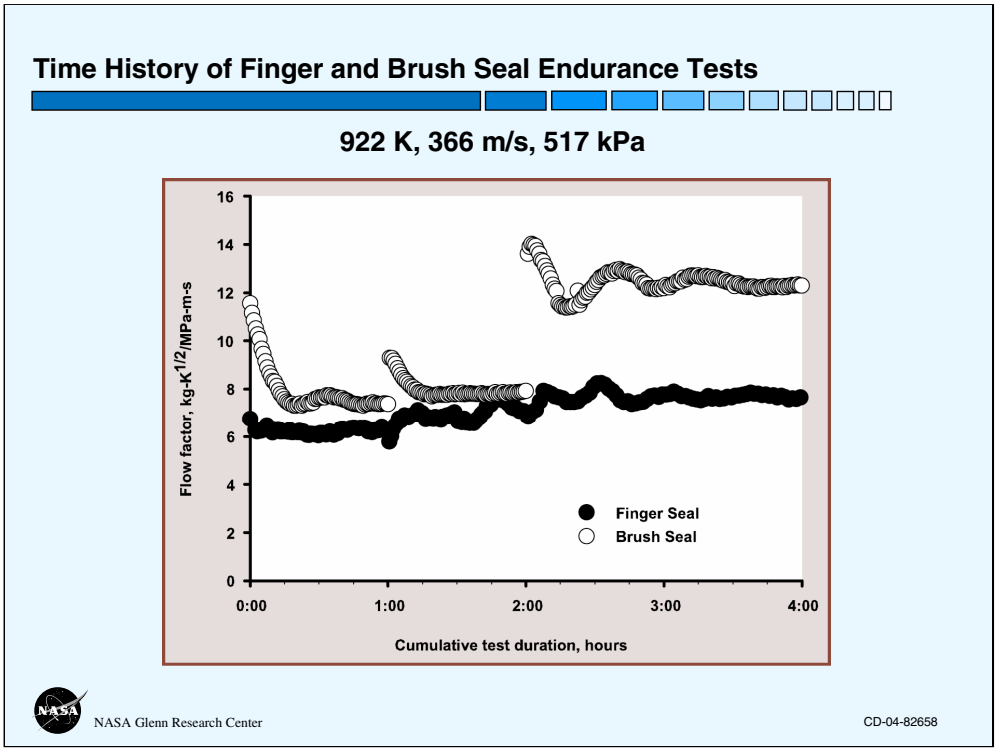

This is a time history of the leakage performance of the brush and finger seals during the endurance test conducted at 922 K, 366 m/s and 517 kPa.

The finger seal flow factor shown by the solid symbols is less than the brush seal through out the test.

Initially the brush seal leakage is only slightly higher than the finger seal.

However, after 4 hours of testing the finger seal leakage flow factor was 36% less than the brush seal flow factor.

• The predicted flow factor for 305 μm radial clearance labyrinth seal at these conditions is 26.1 kg–√K/MPa-m-s, which is 2.16 × brush seal, 3.38 × finger seal.

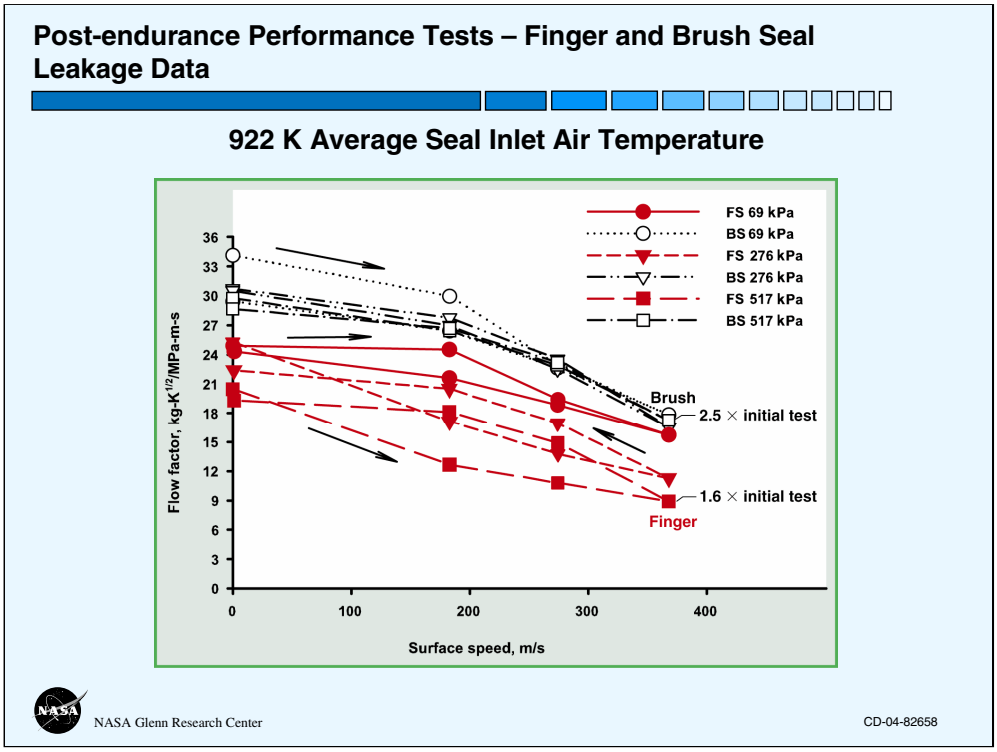

After the endurance test the performance test was repeated. This is a comparison of the brush and finger seal leakage performance data at 922 K.

The brush seal flow factor data shown in black is higher than the finger seal data in red.

The finger seal shows a definite pressure closing effect as the flow factor is lower at higher pressure differentials.

At 922 K, 366 m/s, 517 kPa, the flow factors are greater than in the initial performance test by a factor of 1.6 for the Finger Seal and 2.5 for the Brush Seal.

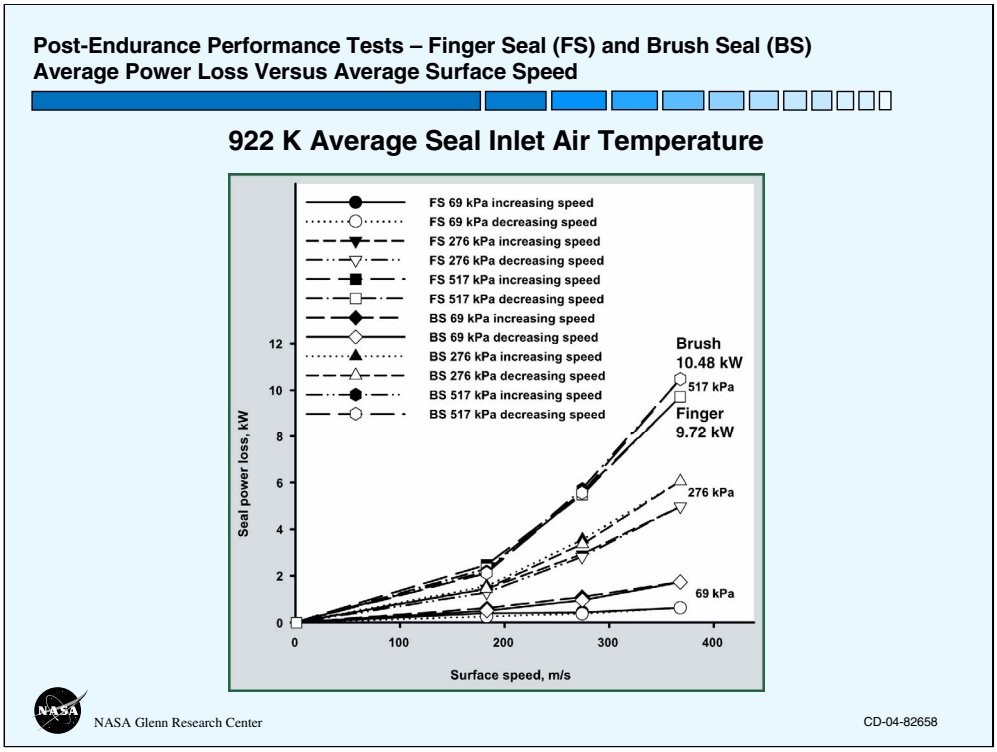

Seal power loss was calculated by measuring the torque with a seal and subtracting the tare torque measured without a seal to determine the seal torque and then multiplying the seal torque by the speed.

This is a comparison of the finger and brush seal power loss at 922 K (1200 ºF). The data shown here is from the post-endurance performance test, which is very similar to the first performance test.

As expected the power loss increases with speed and with pressure differential across the seal.

At all three pressure conditions the brush seal power loss is slightly higher than the finger seal power loss.

At the maximum speed and pressure of 366 m/s and 517 kPa the power loss for the brush seal is 10.5 kW and for the finger seal it is 9.72 kW.

We recognize that these seal power loss values may be substantially higher than the true seal power loss since the tare torque was measured at ambient pressure.

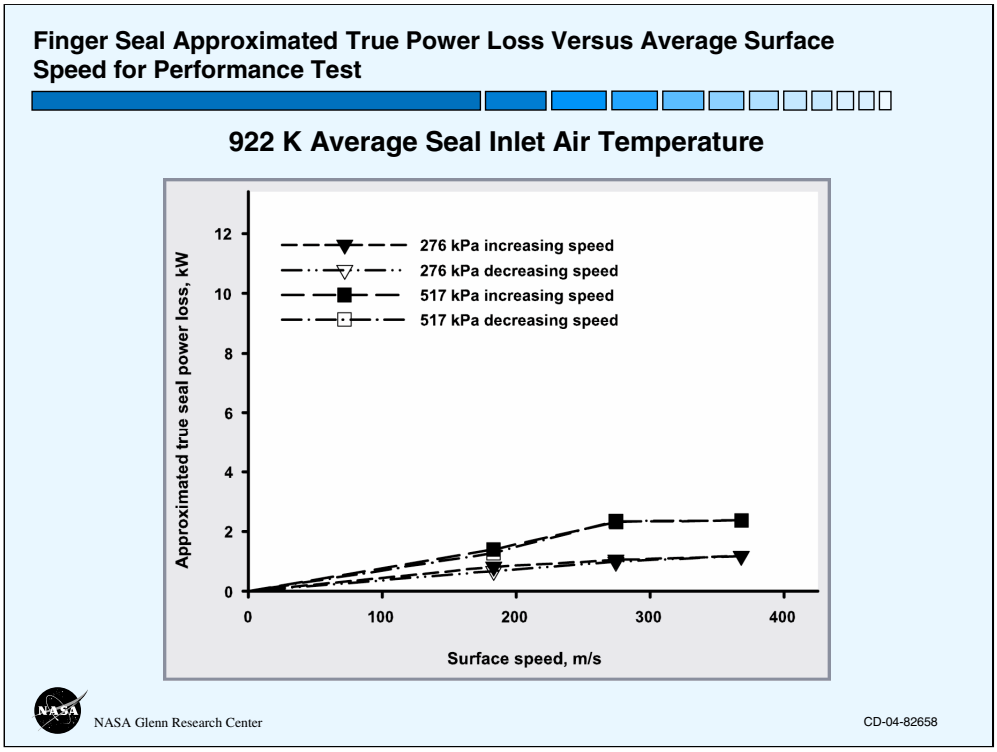

Windage losses on the high pressure side of the test rotor and balance piston were approximated using a solution provided by Schlicting. The additional torque on the bearings due to the thrust loads was also estimated. These estimations were then used to determine the approximated true power loss for the finger seal shown here.

The approximated true power loss increases with speed and with pressure, but not to the same degree as the data based on the ambient pressure tare torque.

At the maximum conditions of 922 K, 366 m/s, and 517 kPa the approximated true seal power loss is 2.36 kW. This is 1/4 of the seal power loss based on the ambient pressure tare torque.

Hence, this finding suggests that additional testing with a straight cylindrical seal or labyrinth seal is needed to establish tare torque data that accounts for pressure differentials across the test seal.

Using the ambient pressure tare torque is adequate for comparing performance, however.

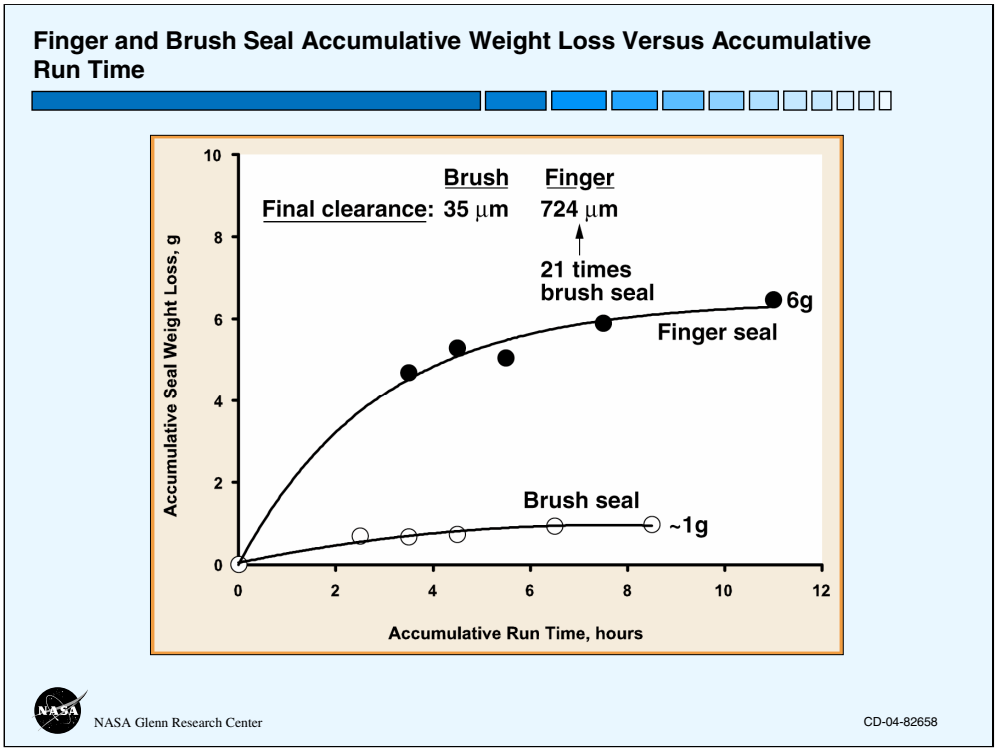

This is a comparison of the finger and brush seal accumulative weight loss versus accumulative run time.

The finger seal had a final weight loss of 6 g and the brush seal lost ~1g.

70–71% of the seal weight loss occurred in the initial performance tests.

Weight loss was used to calculate change in seal inner radius and final static, room temperature clearance.

The brush seal had a final clearance of 34.5 microns and the finger seal final clearance was 724 microns, which is 21 times greater than the brush seal.

	Brush seal	Finger seal
• Calculated radius change	131 μm	889 μm
• Final clearance	34.5 μm	723.9 μm

Rotor Wear

Average rotor wear track measurements for finger seal

Seal:	Finger	Finger
Test type	Width, μm	Depth, μm
Baseline	0	0
Performance	2413	6.22
First hr endurance	2108	4.47
Second hr endurance	2642	4.19
Fourth hr endurance	2313	6.32
Last performance	2438	5.49

- **Rotor wear due to brush seal was very minimal.**
- **Rotor wear due to finger was measurable, but small.**

NASA Glenn Research Center

CD-04-82658

Rotor wear was measured using a profilometer at 8 circumferential locations around the rotor od to measure wear track depth and width.

The average wear track measurements for the finger seal are shown here and are quite small with a maximum track depth of about 6 microns.

Rotor wear due to the brush seal was minimal.

The Chrome Carbide coating performed well.

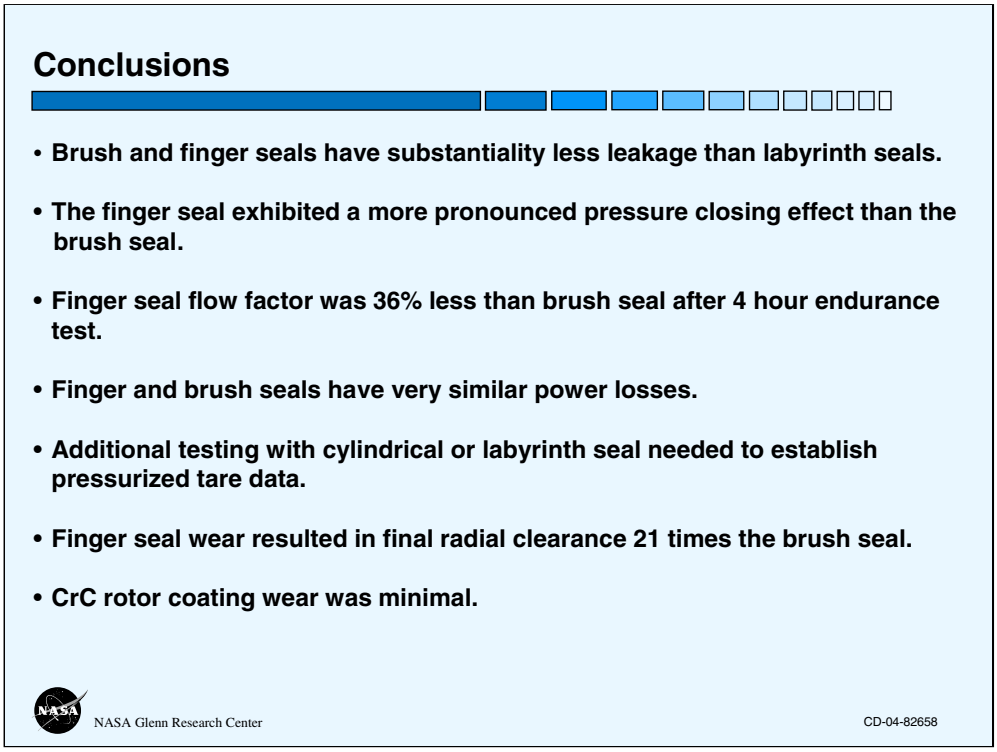

Self-Explanatory.

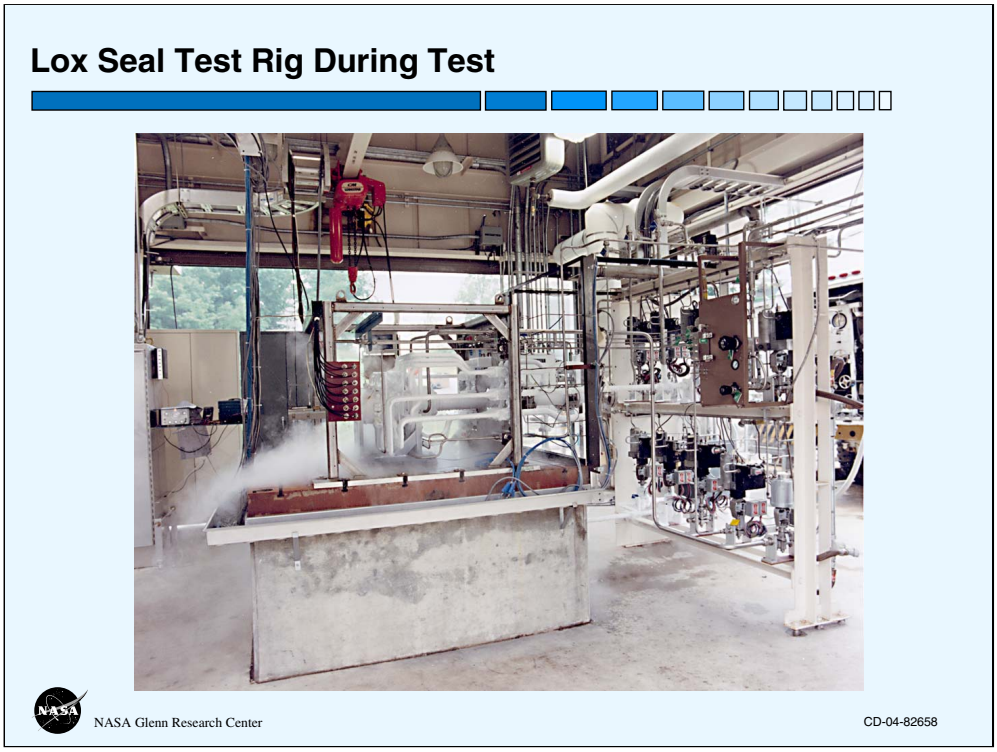

This photograph shows the Lox Seal Test Rig during a test at the old Rocket Engine Test Facility.

As you may recall our cryogenic seals testing has been on hold due to the airport expansion.

Our cryogenic component laboratory has been re-located to Plum Brook Station in Sandusky, Ohio. The facility systems verification testing is beginning as we speak and should be completed by March 1, 2005. The facility has LN2, LH2, LOX, GN2, GH2, and GHe capabilities. We are working to get resources to re-establish the cryogenic seal test rigs at Plum Brook. If you have any need for cryogenic seals testing or testing of other cryogenic components, please let me know. We'd like to put this new facility to good use. You can contact me, Margaret Proctor, at 216-977-7526 or speak with me over lunch or at a break while you are here.

TEST RIG FOR EVALUATING ACTIVE TURBINE BLADE TIP CLEARANCE CONTROL CONCEPTS: AN UPDATE

Scott B. Lattime
Ohio Aerospace Institute
Cleveland, Ohio

Bruce M. Steinetz and Kevin Melcher
National Aeronautics and Space Administration
Glenn Research Center
Cleveland, Ohio

Jonathan A. Decastro
QSS Group
Cleveland, Ohio

Malcolm G. Robbie and Arthur H. Erker
Analex Corporation
Cleveland, Ohio

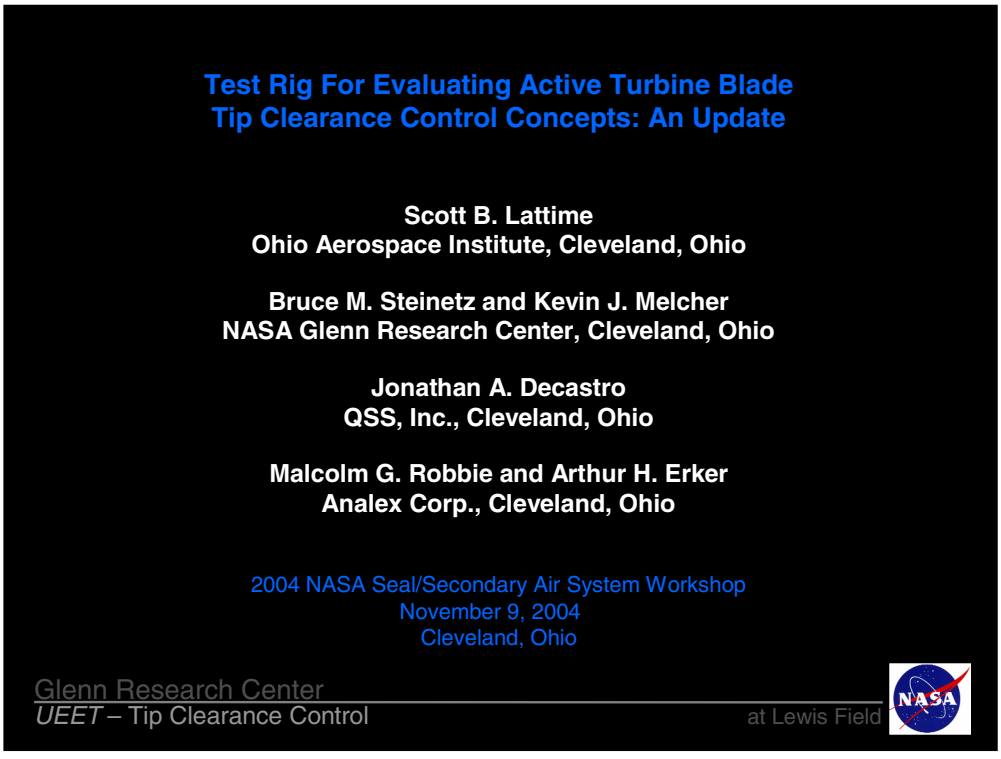

Objectives

- **Design a fast mechanical ACC system for HPT tip seal clearance management**
  - Improve upon slow thermal response of “case cooling” methods used today.
  - Provide continuous ACC throughout entire flight profile.

- **Design a test rig to evaluate ACC system concepts.**
  - Evaluate actuator concept response and accuracy under appropriate thermal and pressure conditions in a non-rotating environment.
  - Evaluate clearance sensor response and accuracy in a non-rotating “hot“ environment.
  - Measure secondary seal leakage due to segmented shroud design, shroud actuation, and case penetration.

- **Test Rig Capabilities:**
  - Chamber temperatures up to 1500 °F.
  - Seal carrier backside pressure up to 120 psi (simulate cooling air Δp).
  - Sized for actual seal hardware (20” diameter turbine).
  - Simulate realistic tip seal clearance changes due to mechanical and thermal loading (electronically).
  - Positioning feedback sensing, rig construction, and actuation system designed to achieve positioning accuracy 0.004-in.

Test Rig/ ACC System Specifications

- **Temperature**
  - The backside of the HPT shroud (blade outer-air-seal) is generally cooled with compressor discharge air (P3 air: **1200 to 1300 ºF**)
- **Pressure**
  - The cooling air is also used to purge the leading and trailing edges of the shroud segments, providing a positive backflow margin from the hot rotor inlet flow.
  - P3 is highest during maximum thrust events such as takeoff and re-accel. For large commercial engines this translates to a maximum cooling air pressure differential of up to **150-psid** across the shroud.
- **Actuation Range and Rate**
  - Maximum tip clearance changes due to axisymmetric and asymmetric loads on the rotor and stator components are on the order of 0.050-in.
  - FAA requires that engines have the ability to reach 95% rated takeoff power from flight idle (or from 15% rated takeoff power) in 5.0 seconds.

  → **0.01-in/s**

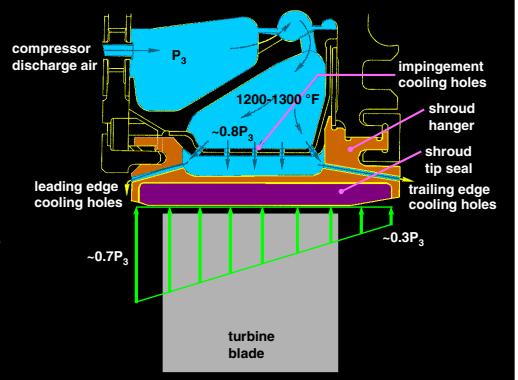

HPT shroud hanger and seal w/ cooling and purge flow

Glenn Research Center
UEET – Tip Clearance Control
at Lewis Field

The design was concentrated on simulating the temperature and pressure conditions that exist on the backsides of the seal segments, without the need for a rotating turbine. This greatly simplified the rig design. We plan to assess the response of the ACC system to the effects of a turbine wheel (i.e., rapid clearance closures due to mechanical and thermal loads) by simulating closures electronically, as will be discussed in a later.

Design Criteria

- **The substantial diameter of the segmented shroud structure (~20-in), under moderate pressures (~120-psi), gives rise to significant loads, and hence stresses, to which the actuation system and components must react.**
- **These stresses coupled with high temperatures (1200 to 1300 °F) can significantly reduce component cycle life due to creep.**
- **Managing these stresses with adequate materials and geometry to improve component cycle life was a driving factor in the rig component design.**
- **Larson-Miller parameter data for a variety of high temperature, super alloys was utilized to design components to achieve a desired minimum cycle life.**
  - Inconel 718 utilized for most of the hot section components.
  - Components were designed for less than 0.5% creep strain, resulting in a 15-ksi limiting stress.
  - **15-ksi stress level corresponds to over 100,000 hours life at 1300 ˚F and approximately 300 hours life at 1500 ˚F.**

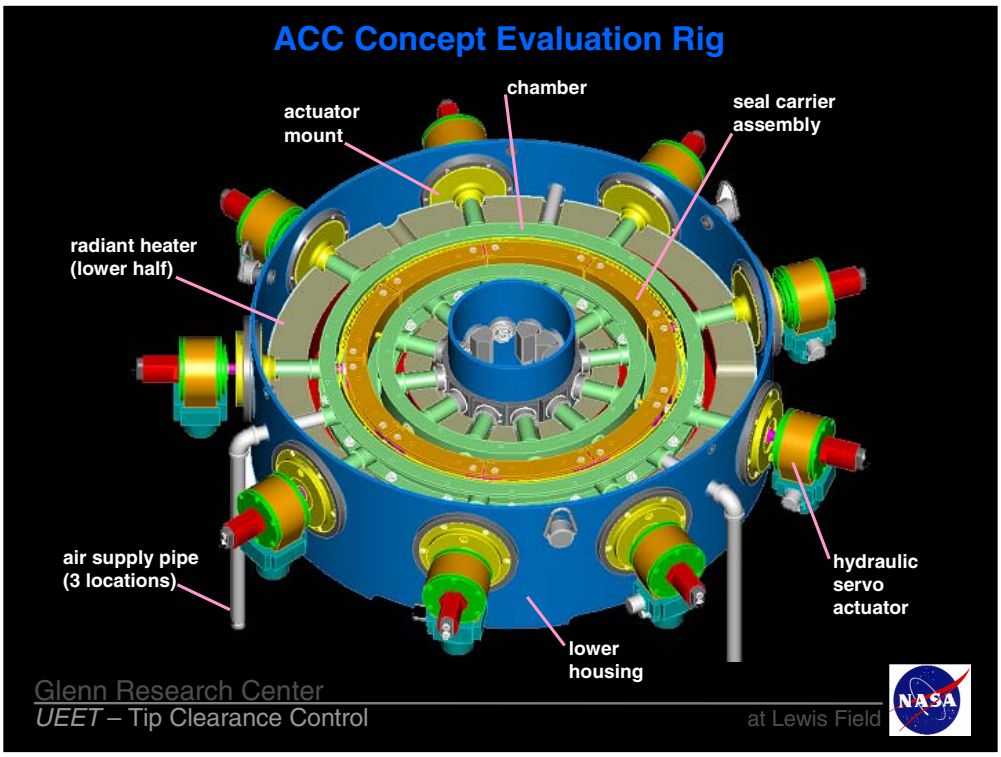

Here we see the Gen 1 ACC System Concept and Test rig.

The test rig comprises six main components: the housing, the radiant heater, the pressurized chamber, the seal carrier assembly, the actuator rod assemblies, and the hydraulic actuators.

At the heart of the rig is a segmented shroud structure (seal carrier) that would structurally support the tip seal shroud segments in the engine. Radial movement of the seal carriers controls the effective position/diameter of the seal shroud segments, thereby controlling blade tip clearance.

The rig housing consists of two concentric cylinders, which form an annular cavity. An annular radiant heater made of upper and lower halves surrounds the segmented seal carrier structure to simulate the HPT tip seal backside temperature environment. A pressurized chamber encloses the carrier segments inside the annular heater through which heated pressurized air is supplied to simulate the P3 cooling/purge air pressure on the seal backsides. Heated air enters the chamber via three pipes that are fed from a manifold at the air heater exhaust through radial inlet ports as shown.

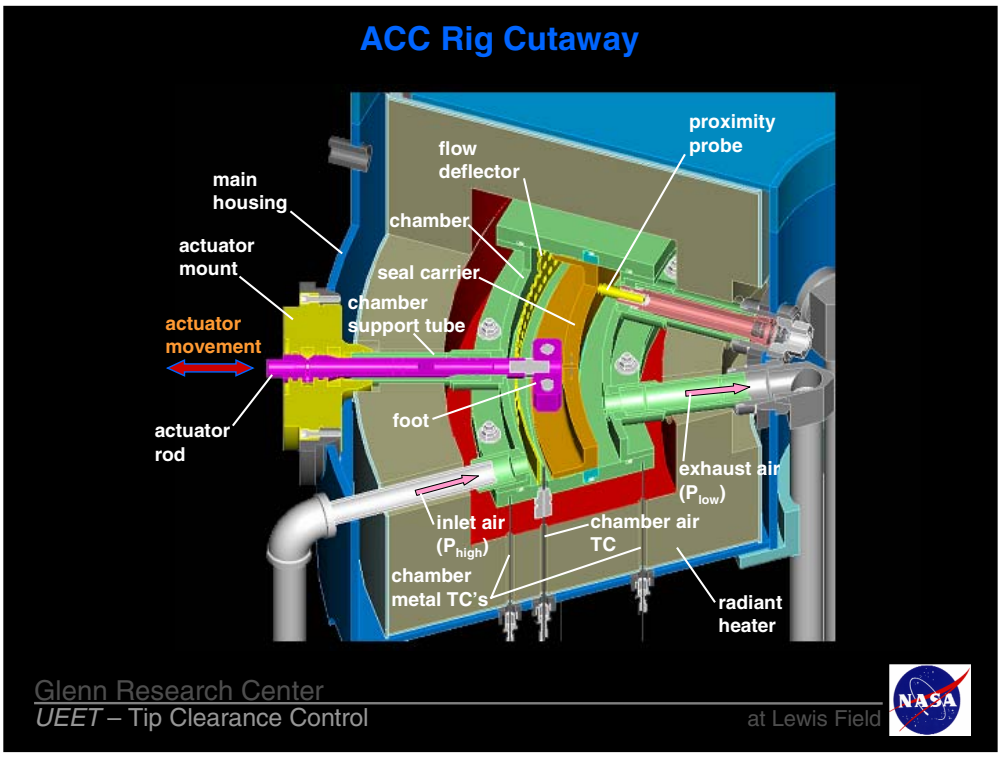

The carrier segments are connected to independent hydraulic actuators through an actuator rod assembly. The foot of the actuator rod assembly positions the carrier segments in the radial direction, while allowing relative circumferential movement or dilation of the seal carrier segments through a pinned and slotted arrangement.

A series of radial tubes projecting outward from the chamber's inner and outer side walls serve as supports, air supply and exhaust ports, probe fixtures, and the actuator rod guides. The chamber functions to support and align the carrier segments and actuator rods, as well as to house instrumentation and to seal the pressurized air from the radiant heater which is not designed to carry any pressure loading.

The inlet flow is baffled circumferentially around the outer chamber wall by a flow deflector to achieve uniform heating of the seal carrier assembly. The pressurized air is sealed along the sides of the seal carrier segments by contacting face seals that are energized via metal "E"-seals imbedded in the upper and lower chamber plates. The joints between adjoining carrier segments are sealed with thin metal flexures. Air that escapes over and between the carrier segments is vented out of the rig through a number of exhaust pipes that protrude radially along the inner chamber wall. The number and inner diameter of exhaust pipes were chosen to eliminate the possibility of backpressure at the exhaust ports.

High temperature proximity probes measure the radial displacement of the seal carriers at various circumferential locations. These measurements provide direct feedback control to the independent actuators and allow the desired radial position (clearance) to be set. The direct feedback control system allows for simulation of realistic transient tip clearance changes in lieu of a rotating turbine wheel. Superimposing a mission-clearance-profile over the actual clearance measurement input to the actuator controllers will allow researchers to assess the system's response to the most dramatic transient events such as mechanical and thermal loading of the rotor during takeoff and re-accel.

The proximity probes are held at a constant standoff to the chamber inner wall via a spring-loaded piston arrangement. The spring-loaded mounting keeps the proximity sensor at a relatively constant position to the chamber inner sidewall during the initial heating of the rig. This arrangement also allows for easy removal of the probes without dismantling the housing.

The chamber air temperatures will be measured at three circumferential locations on the high-pressure side of the carriers to show how well the pressurized air is mixed by the chamber baffle. The chamber flange metal temperatures will be measured via two surface thermocouples attached to the inner and outer flange on the lower cover plate.

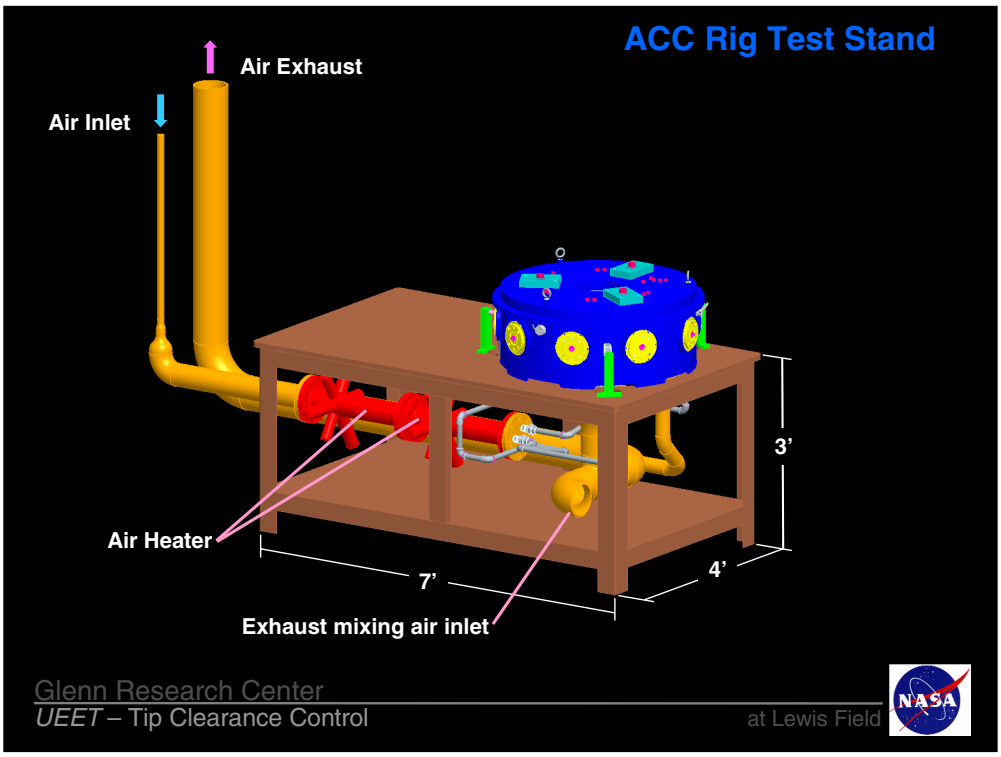

This slide shows the rig’s air supply and exhaust plumbing layout as well as the test stand dimensions.

The air heater system comprises two 36-kW, inline, flanged heaters, manufactured by Osram Sylvania. It is designed to supply up to 75-scfm of air at 120-psi and 1500 °F.

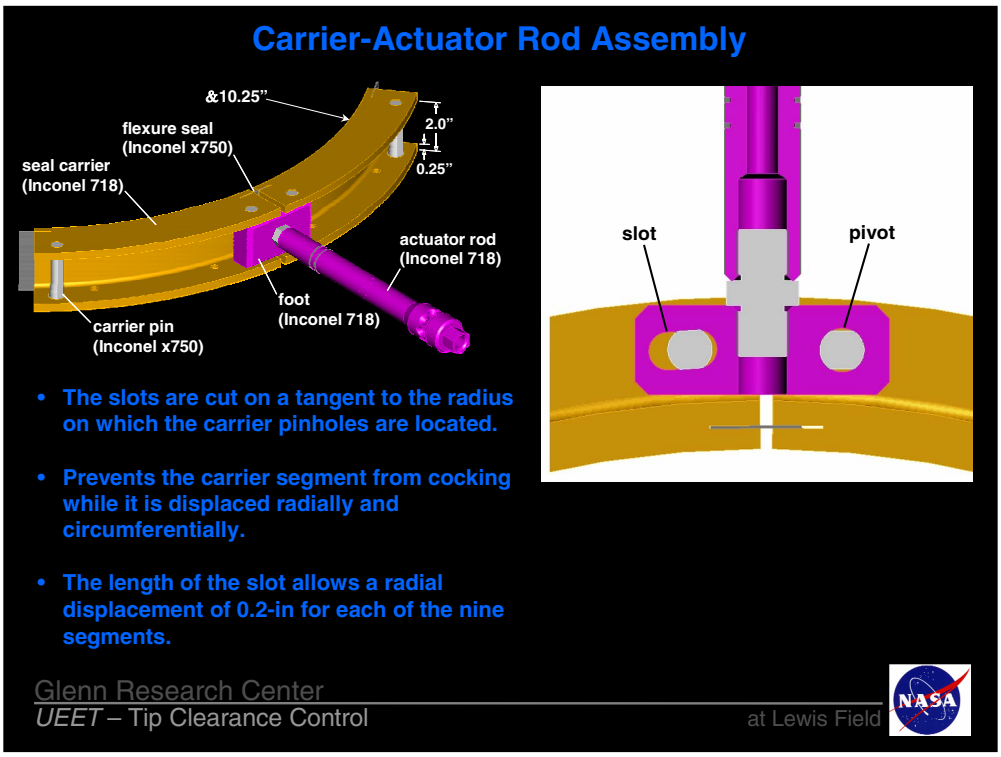

Because the carriers are constrained by a pinned connection at one end and a slotted connection at the other, the segments must shift circumferentially as they are displaced in the radial direction. The slots in the feet are cut on a tangent to the radius on which the carrier pinholes are located. This keeps the carrier segments from cocking while it is displaced in both the radial and circumferential directions. The circumferential length of the carrier segments as well as the length of the slot in the actuator rod foot allows a radial displacement of 0.2-in for each of the nine segments. The slots for the flexure seals have adequate clearance to prevent the segments from becoming arch-bound as the segments are moved radially inward.

The pins are made of Inconel X750. This material was selected to help minimize galling against adjacent Inconel 718 components. The pins have flats machined on the diameter that contacts the slots, providing a bearing surface and reducing the contact stress developed between the pin and foot

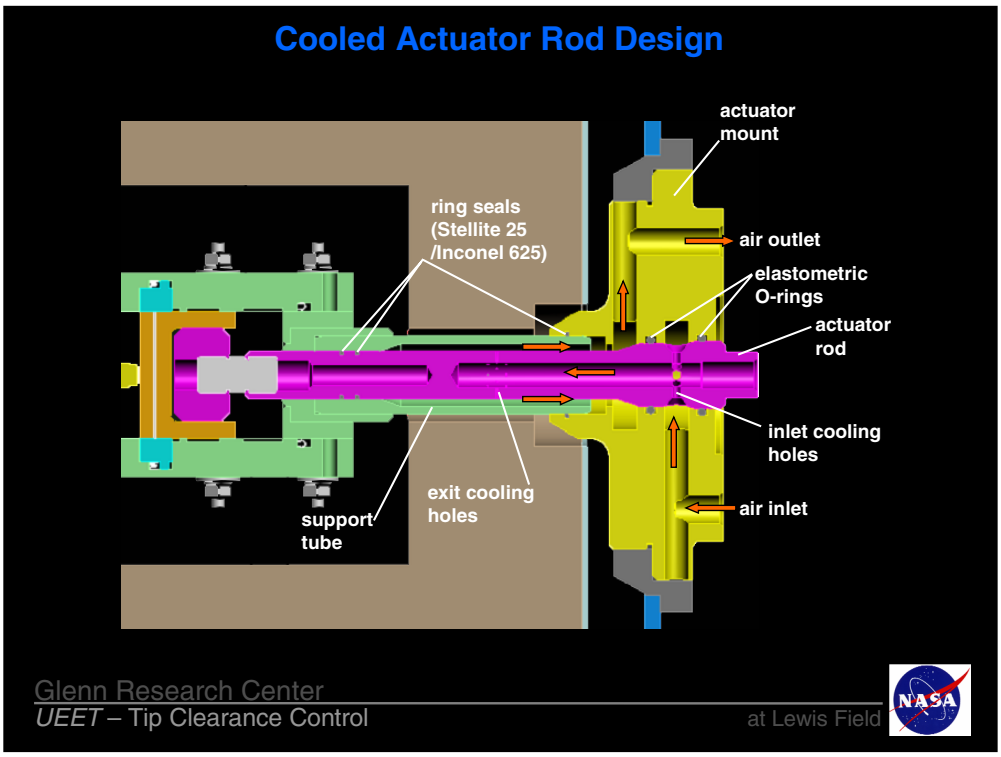

The cooling scheme allows the actuator rod and support tube to function as a tube-in-tube heat exchanger using a small flow rate of ambient air to cool the assembly.

The cooling holes were made from three sets of six, 0.03-in diameter holes drilled around the circumference of the hollow rod. Ambient air, supplied at the rod end through features in the actuator mount, travels axially through the center of the rod, passes radially through the cooling holes, and exits between the support tube and outer diameter of the rod.

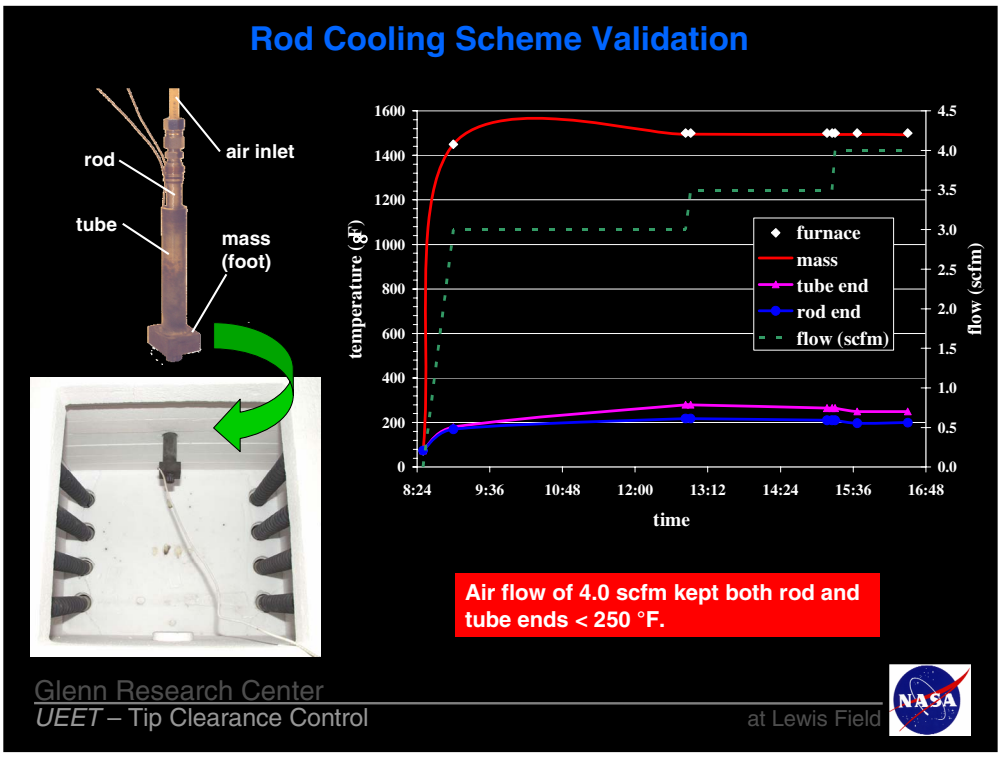

A mockup of the cooled actuator rod design was built to validate the design. A solid steel block (simulating the actuator foot) was bolted to one end of a stainless steel tube (simulating the rod). Another larger tube was welded to the block (simulating the support tube) in a concentric arrangement. An air supply line was attached to the end of the inner tube from which the assembly was supported and inserted into a box furnace. The insulation thickness of the furnace closely approximated that of the radiant heater designed for the rig. A plastic supply line was used minimize heat loss through the supply tube. Thermocouples were attached to measure the temperatures of the mass, the end of the inner rod, and the end of the outer tube. The furnace was heated to 1500 °F and after the mass temperature stabilized at 1500 °F, ambient air at approximately 70 °F was supplied to the assembly. Temperatures of the furnace, mass, tube end, and rod end are shown as a function of time on the left vertical axis. The cooling air volumetric flow is shown on the right vertical axis. The chart shows that for minimal air flow (3.0 to 4.0-scfm) both the tube and rod end temperatures were kept below 250 °F. Thus the cooling scheme design was successfully validated and implemented into the rig design to allow the use of conventional actuators.

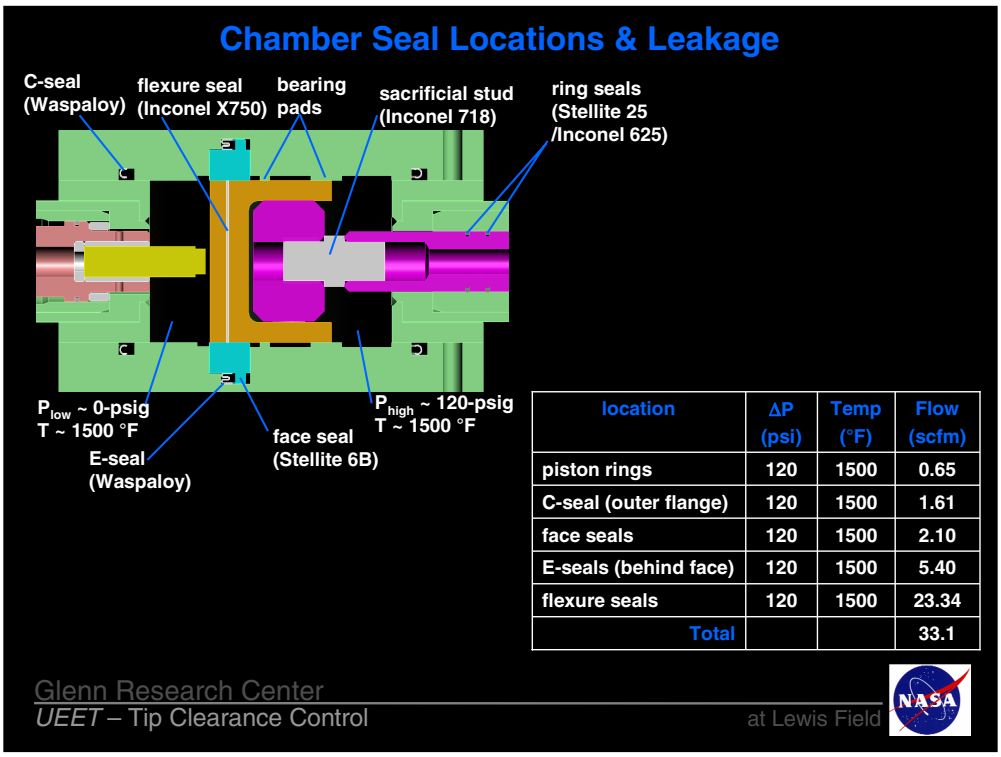

The nature of this ACC concept with its segmented shroud design and case penetration requires multiple high temperature seals. The test rig will allow the development and evaluation of these seals that will eventually be required in an engine. Obviously the leakage created by the use of these secondary seals must be minimized to gain the benefits of the ACC system. For the test rig, the secondary seal leakage drove the design of the air heater.

Flexure seals are used to prevent the radial flow of pressurized air between the carrier segment joints. The 2.0-in wide by 0.9-in long flexures are made of 0.02-in Inconel X750 sheet stock. This material was chosen for its galling resistance to the carrier material. The carrier slits that contain the flexures are designed with a 0.01-in clearance.

The chamber contains four “C-seals”, two on the upper and lower outer diameter flanges and two on the upper and lower inner diameter flanges of the cover plates. The seals are made of Waspalloy and have a cross sectional thickness of 0.015-in. The seals were designed by Perkin-Elmer to seal against a 120-psi pressure at 1500 °F and they require a 150-lbf/in seating load per seal at assembly.

The upper and lower cover plates also house a metal face seal assembly. These seals act to block the pressurized air from flowing between the cover plates and carrier segments. The face seal, made of Stellite 6B, is a pressure balanced design and utilizes an “E-seal” as a preload and secondary seal device. Stellite 6B was selected for the face seal material due to its high temperature properties and anti-galling performance against Inconel 718. The E-seals, also designed by Perkin-Elmer Fluid Sciences and made of Waspalloy, provide a closing force to the face seal on the carrier segments and prevent air from leaking between the face seal and cover plate. Each E-seal provides about 10-lbf/in preload to its corresponding face seal. The face seal was designed with a generous cross section, due to its large diameter, to provide stiffness for operation as well as manufacturing.

The actuator rod contains two pairs of expanding concentric ring seal sets on its bearing surface. Each pair is made of an outer Stellite 25 ring and an inner Inconel 625 ring. The seals were designed by Precision Rings, Inc. (Indianapolis, IN) for a 120-psi at 1500 °F.

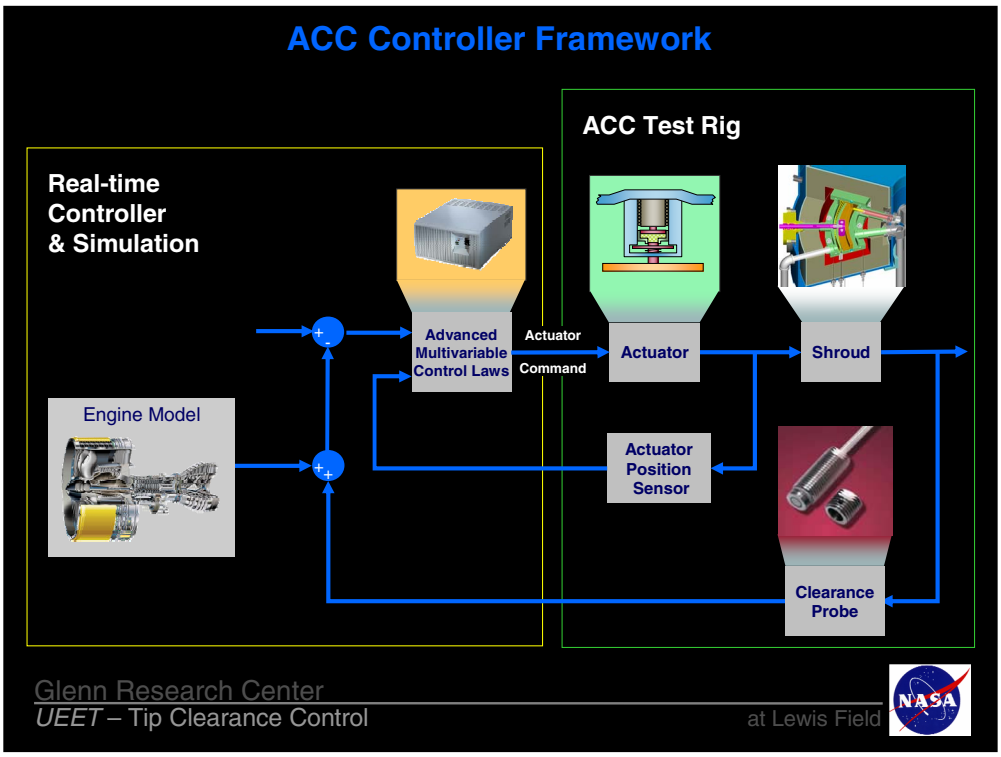

This slide shows a diagram of the control system strategy that will employed to operate and evaluate this first generation ACC system as well as future systems. Each of the nine independent hydraulic actuators will have its own feedback control allowing the positioning of each cylinder or actuator. An outer loop will be monitoring the position of the carrier segments. The outer loop will determine the minimum clearance off of which the desired clearance will be measured. The control system will be used to evaluate the accuracy and response of the ACC system to both steady state and transient clearance profiles.

Our next speaker, Mr. Kevin Melcher of the Controls and Instrumentation Branch at NASA GRC, will provide a more in depth discussion on his development of this control system and his work on defining control system requirements and architecture for advanced ACC systems.

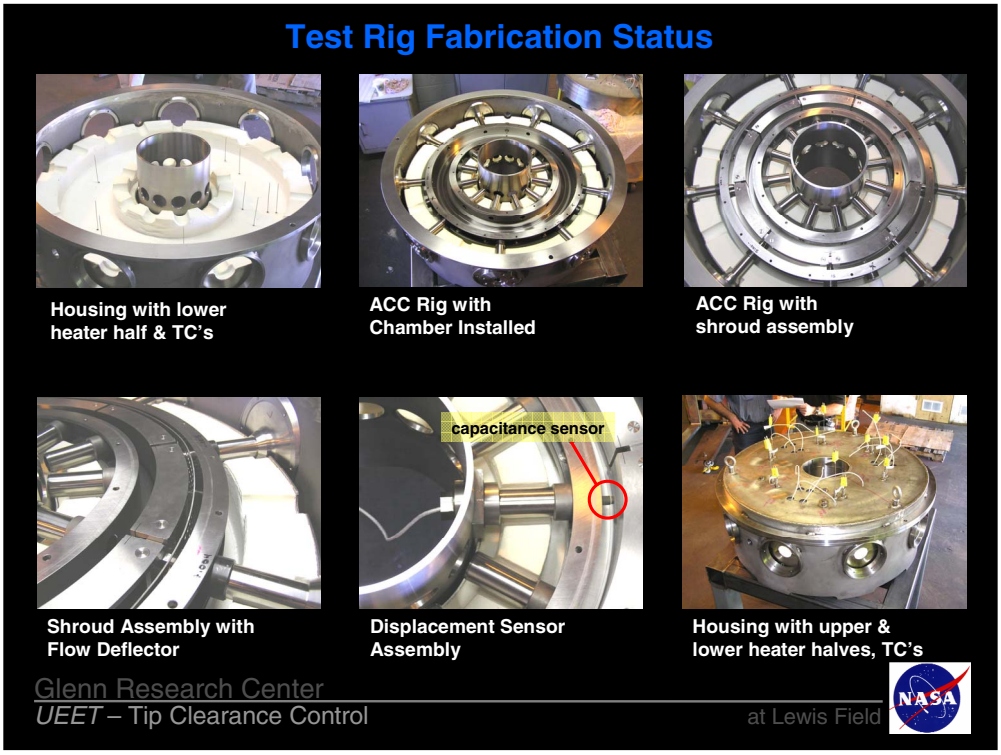

Here we can see some of the main components of the test rig as they are currently being fabricated. The components are about 75% complete. We expect assembly to occur at the end of the month, with rig check out occurring towards the end of December.

Rig Assembly w/ Mechanical Checkouts & Gage Plate

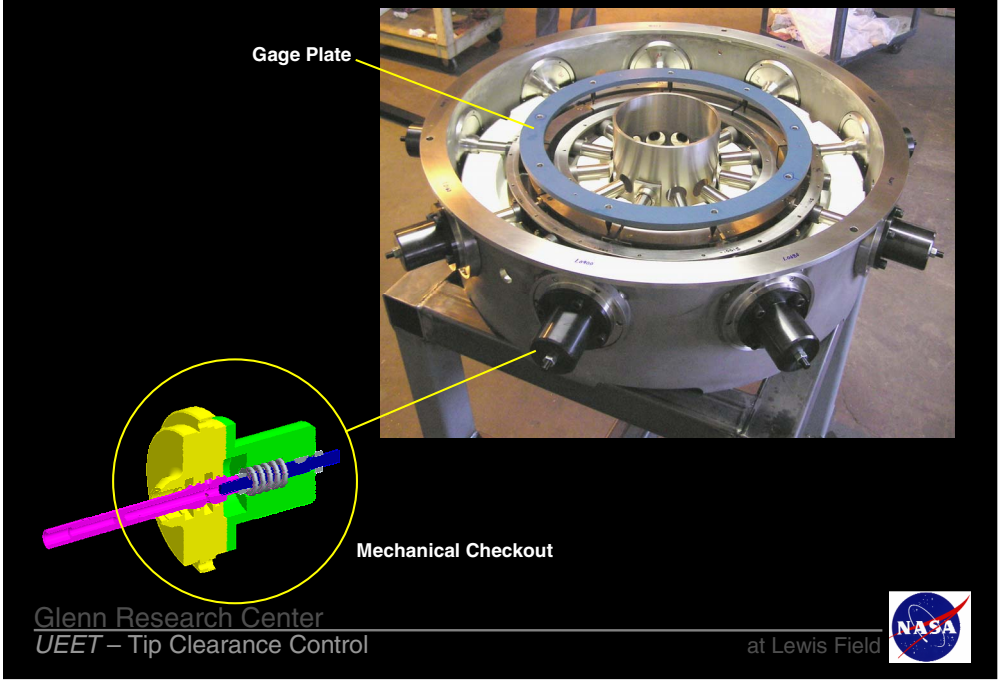

Glenn Research Center
UEET – Tip Clearance Control
at Lewis Field

Carrier Segments Cycled Through 0.2”

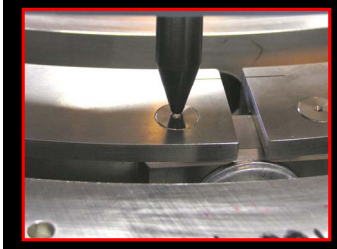

Segments at + 0.1”
($\&_{max}$)

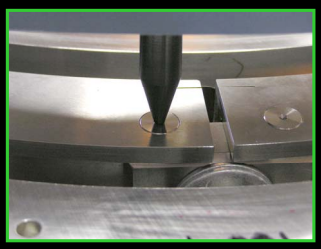

Gage Plate Pin Captured
at Neutral Diameter

Segments at - 0.1”
($\&_{min}$)

Glenn Research Center
UEET – Tip Clearance Control
at Lewis Field

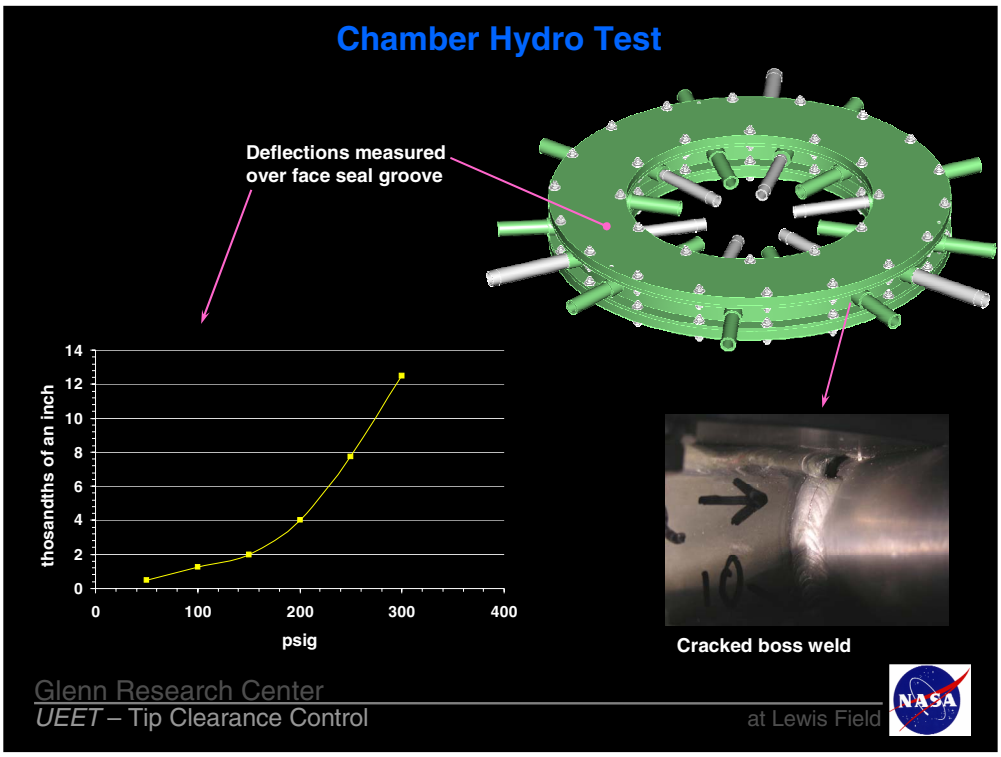
Chamber Hydro Test
Deflections measured over face seal groove
thousandths of an inch
14
12
10
8
6
4
2
0
0
100
200
300
400
psig
Cracked boss weld
Glenn Research Center
UEET – Tip Clearance Control
at Lewis Field
NASA

Schedule

Complete Assembly/ Facilities	Q1 FY05
Complete Rig Checkout	Q1 FY05
Evaluate Gen 1 ACC Concept (Ambient)	Q2 FY05
Evaluate Gen 1 ACC Concept (~1300 °F)	Q2 FY05
Evaluate AADC SMART Track Concept (Ambient)	Q1-2 FY06
Evaluate AADC SMART Track Concept (~1300 °F)	Q1-2 FY06

Plans

- **The ACC Test Rig will be used to evaluate the performance of GRC's 1st Gen ACC system and others (AADC –SMART Track). Performance will be evaluated under a series of HPT simulated temperature and pressure conditions.**
  - Actuator stroke, rate, accuracy, repeatability
  - System concentricity, synchronicity
  - Component wear
  - Secondary seal leakage
  - Clearance sensor response and accuracy
- **The results of this testing will be used to further develop/refine the current actuator designs as well as other actuator concepts.**
  - SMA's, piezoelectric, magnetostrictive, other
- **Optimization of ACC system components for future flight hardware development.**
  - increased cycle life
  - reduced size and weight

WEAR PREDICTION OF STRIP SEALS THROUGH CONDUCTANCE

Norman Turnquist and Farshad Ghasripoor
GE Global Research
Niskayuna, New York

Mark Kowalczyk and Bart Couture
GE Energy
Schenectady, New York

Advanced Sealing Technology at GE Global Research

Team

Shorya Awtar
Nitin Bhate
Bruce Briel
Bruce Brisson
Ray Chupp
Biao Fang
Farshad Ghasripoor
Chuck Golden
Mohsen Salehi
Omprakash Samudrala
Norman Turnquist
Kripa Varanasi
Chris Wolfe




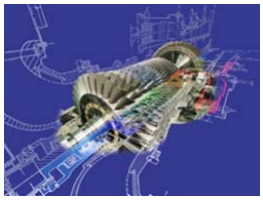
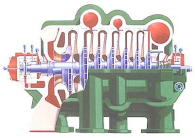

imagination at work

Advanced Seal team at GE Global Research

-Developing advanced seal technologies for GE Aircraft Engines, Land-Based Gas Turbines, Steam Turbines, Industrial Compressors, etc.

-Developing seals for both new products and retrofits into existing equipment

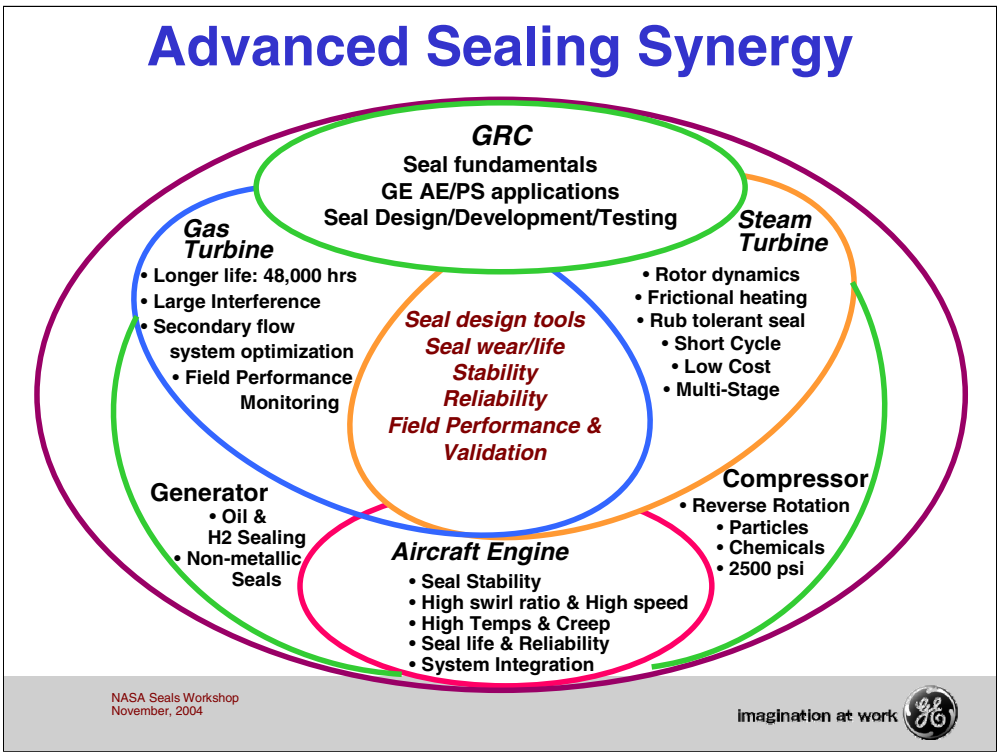

Different applications have different design considerations for advanced seals.

Seals are developed for each application, analytical design tools are developed, and the design tools can be applied across the spectrum of applications.

GE Global Research is a “hub” for Advanced Seals development across GE.

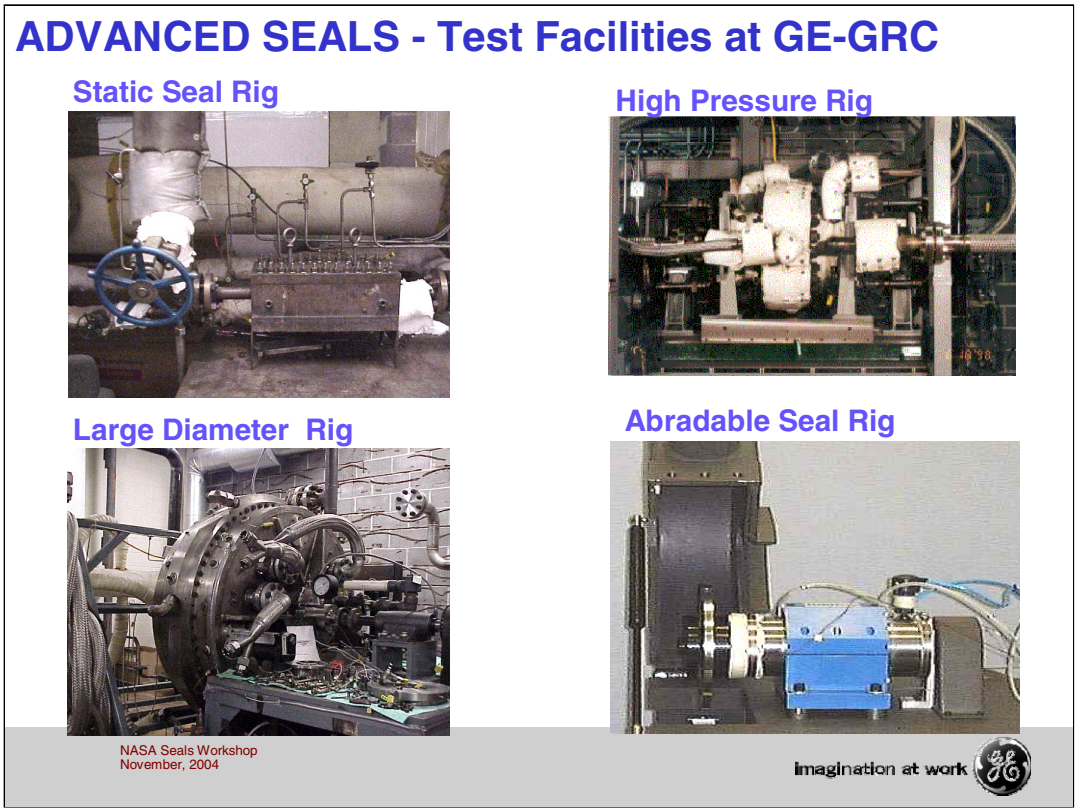

Several experimental rigs are used to quantify performance and characteristics of advanced seals. A **static rig** is employed for testing both static and dynamic seals. It is a high pressure, high temperature rig that gives comparative leakage performance data for various seals types, i.e., cloth, labyrinth, brush, honeycomb, C-, E-, etc. A **smaller rotary rig** (High Pressure Rig) is used for testing in air or steam of dynamic seals. This rig is used to test subscale seals at full turbine conditions. A **larger rotary rig** is used for testing full-scale dynamic seals at subscale conditions. This rig is the one that has been used to test aspirating face seals as well as brush seals. An **abradable rub rig** is a versatile rig for testing candidate abradable shroud materials rubbing against tipped and untipped blades. It can simulate turbine blade-tip rotation and incursion rates, and has heating capability to operate at turbine environment temperatures. Wear characteristics are determined from measured level of shroud and blade-tip wear.

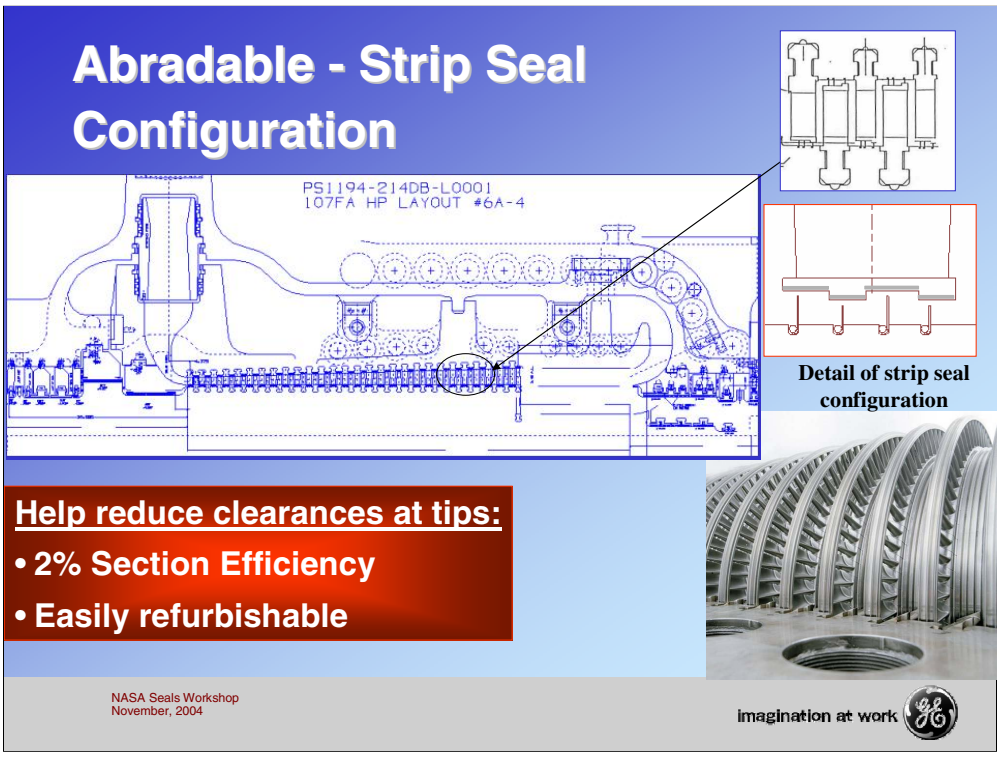

GE HEAT Steam Turbine has 28 stages.

Caulked-in strip seals used in drum rotor turbine construction; strips caulked directly into rotor.

Strips used in conjunction with abradable coating on shrouded nozzle tips.

Strips can be replaced if damaged.

Abradable coating permits tight assembly clearances without risk of hard metal-to-metal rubs.

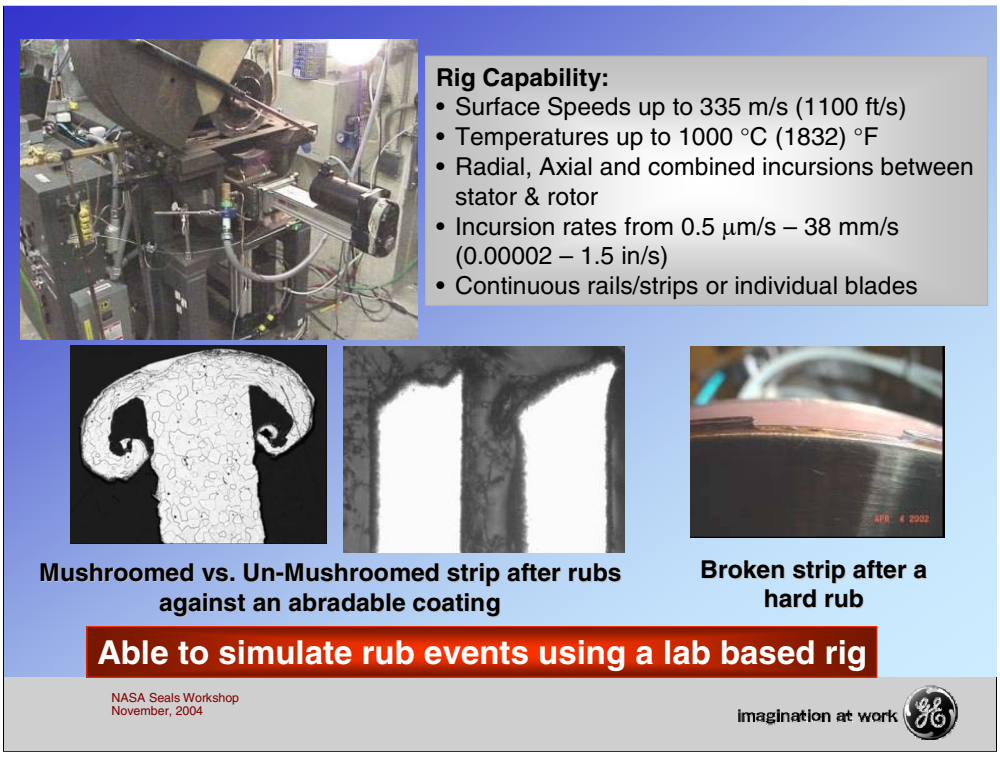

Subscale rub tests demonstrate effectiveness of abradable coating in preventing strip damage during rub events test rig also used to investigate rub behavior of various strip materials.

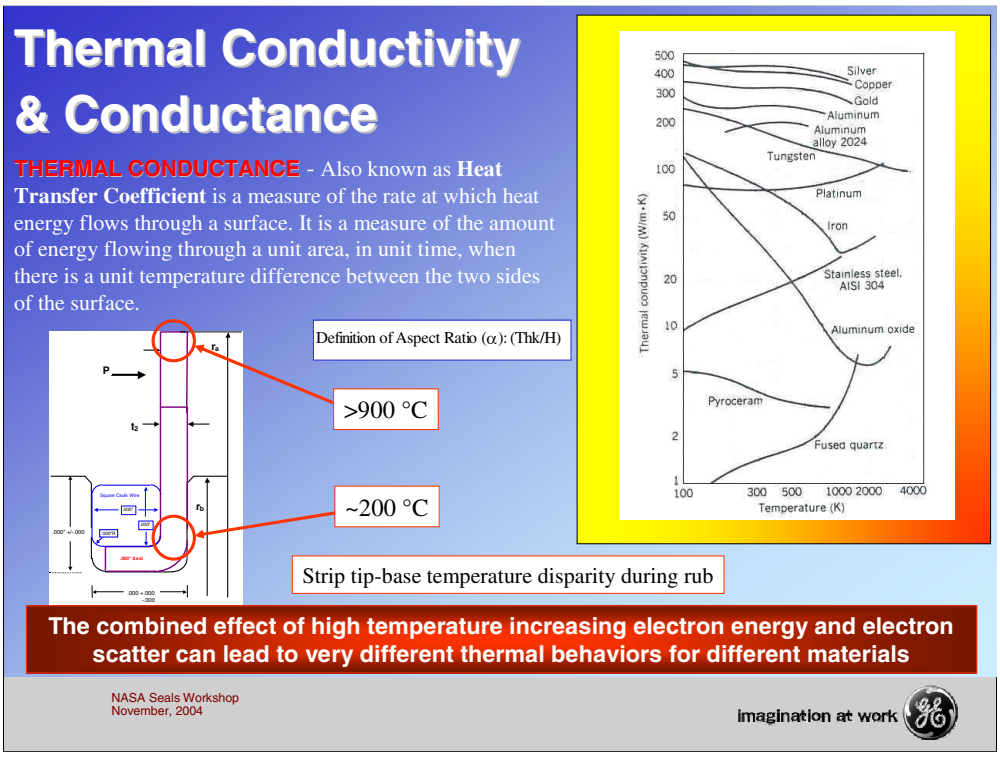

Conductance accounts for strip geometry as well as conductivity of the strip material. Ability of strips to draw away heat from rub event is key to minimizing strip wear.

Aspect ratio is an important variable that is purely a function of the strip geometry.

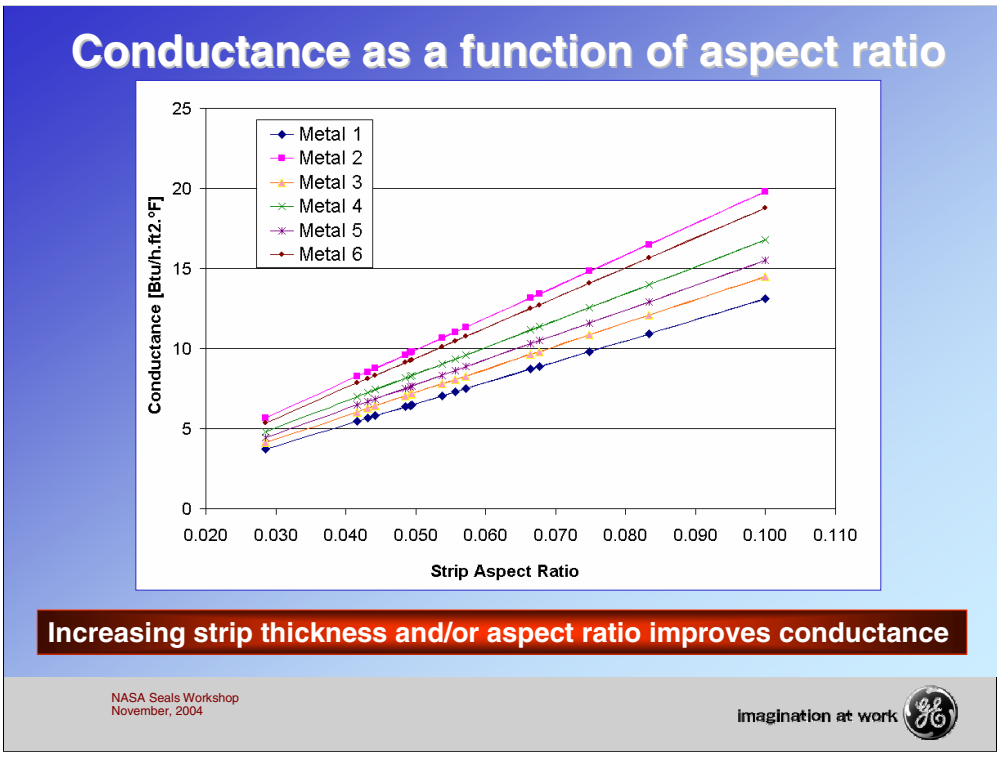

Conductance increases linearly with increasing aspect ratio.

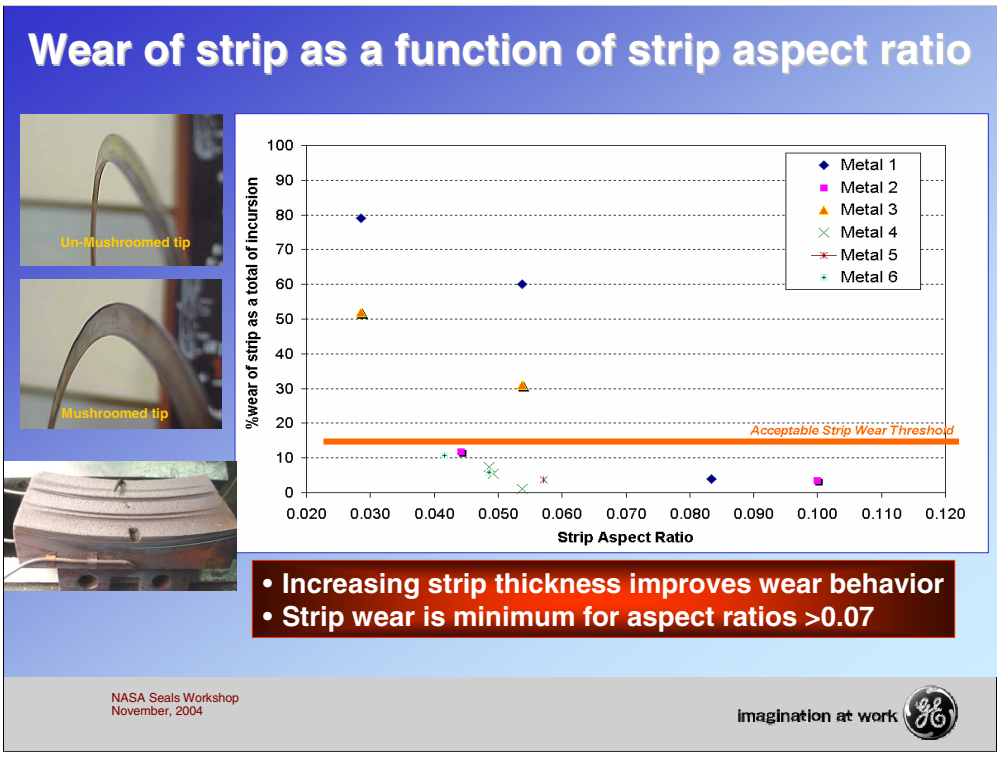

Increasing strip thickness increases Aspect Ratio, and therefore Conductance.

For the cases considered, Aspect Ratio = 0.07 is the cutoff between excessive and acceptable strip wear.

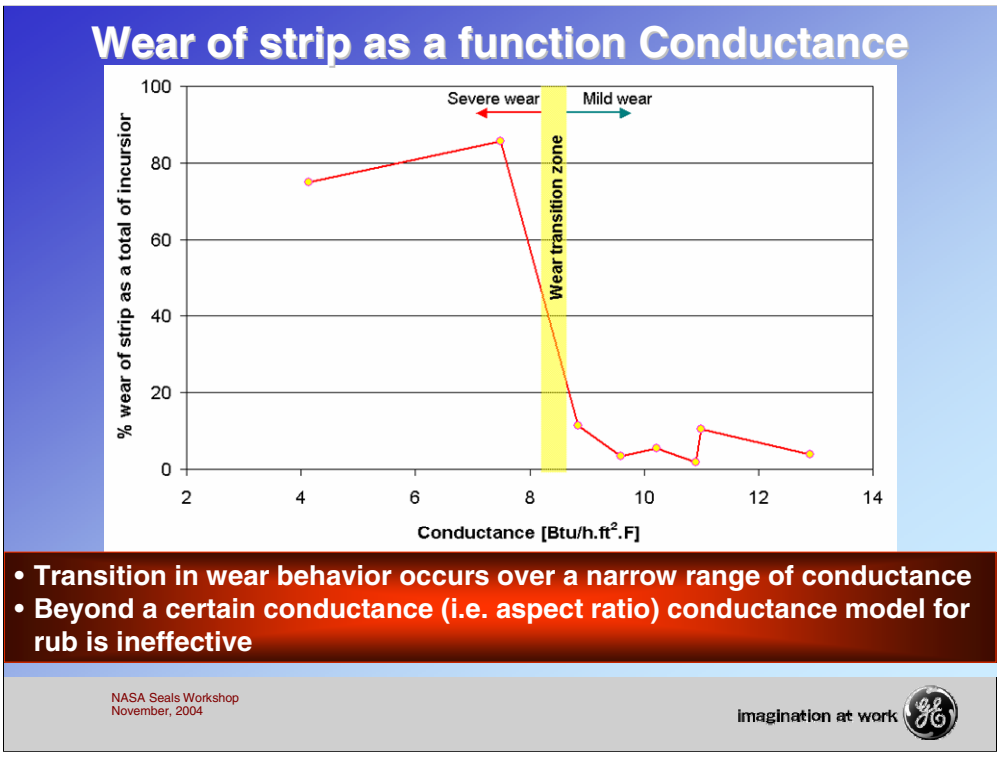

The transition from Severe Wear to Mild Wear is abrupt, and occurs when the heat transferred away by Conductance is inadequate to prevent melting at the tip.

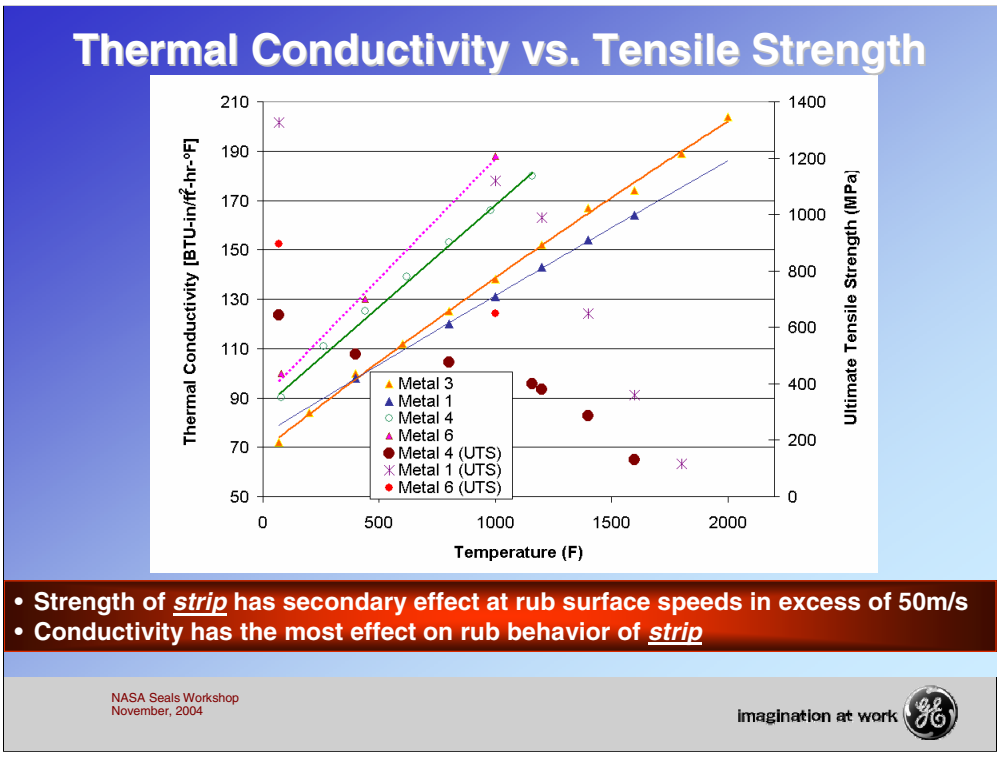

Tensile strength of the strip material has only a secondary effect on wear behavior; the wear is primarily driven by conductance.

The implication is that high strength superalloys are not necessarily good strip materials from a wear standpoint.

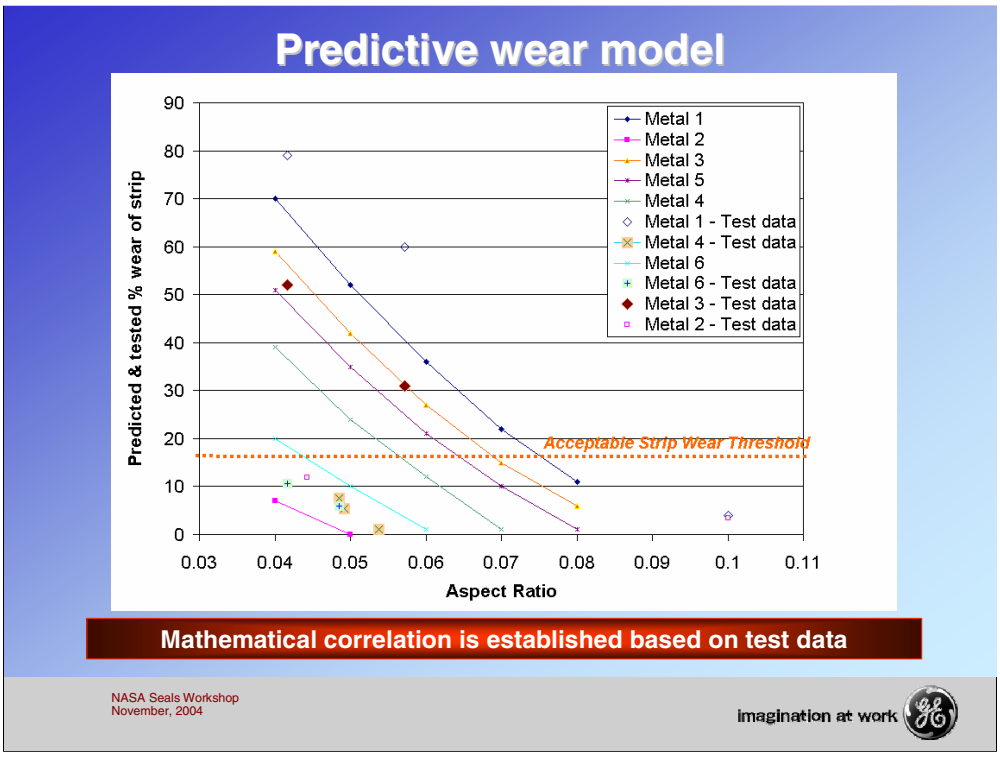

A predictive model for strip wear has been developed and validated with subscale rig tests.

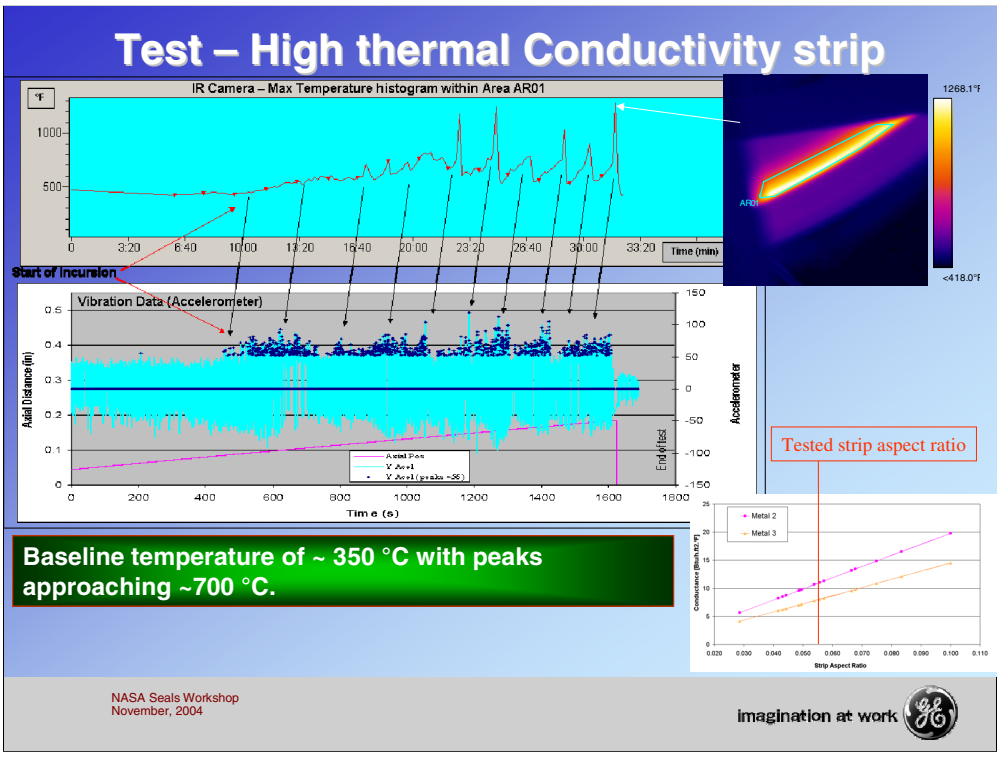

Strip temperatures measured using thermal imaging show peak temperatures of ~700C for a high conductivity strip

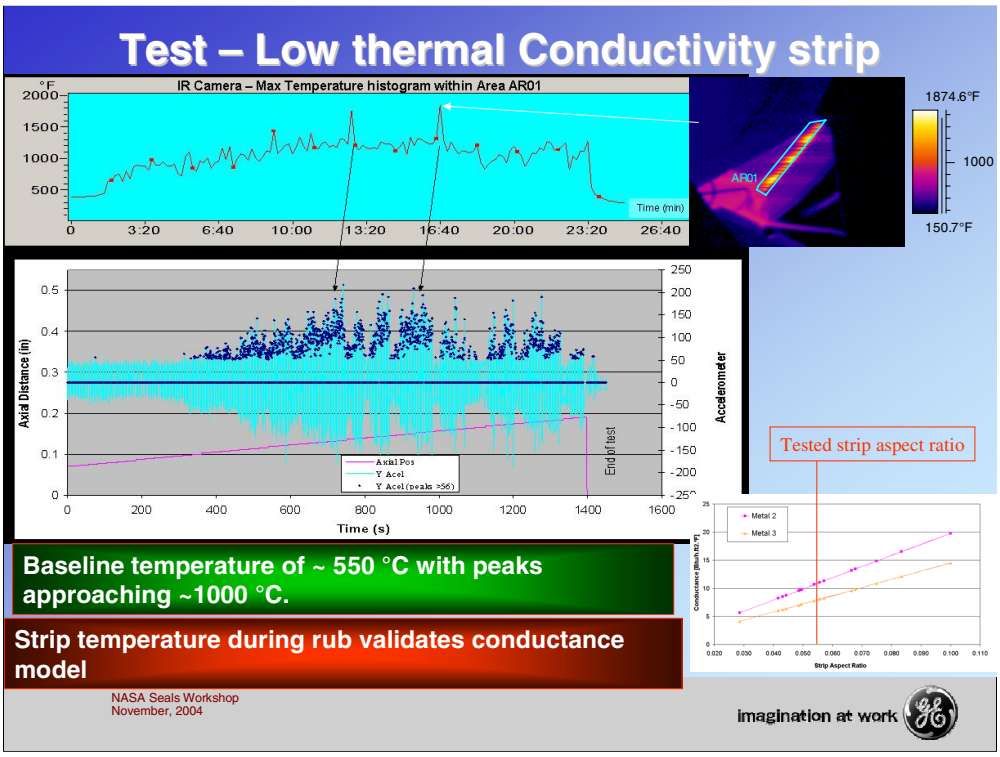

Strip temperatures measured using thermal imaging show peak temperatures of ~1000C for a low conductivity strip.

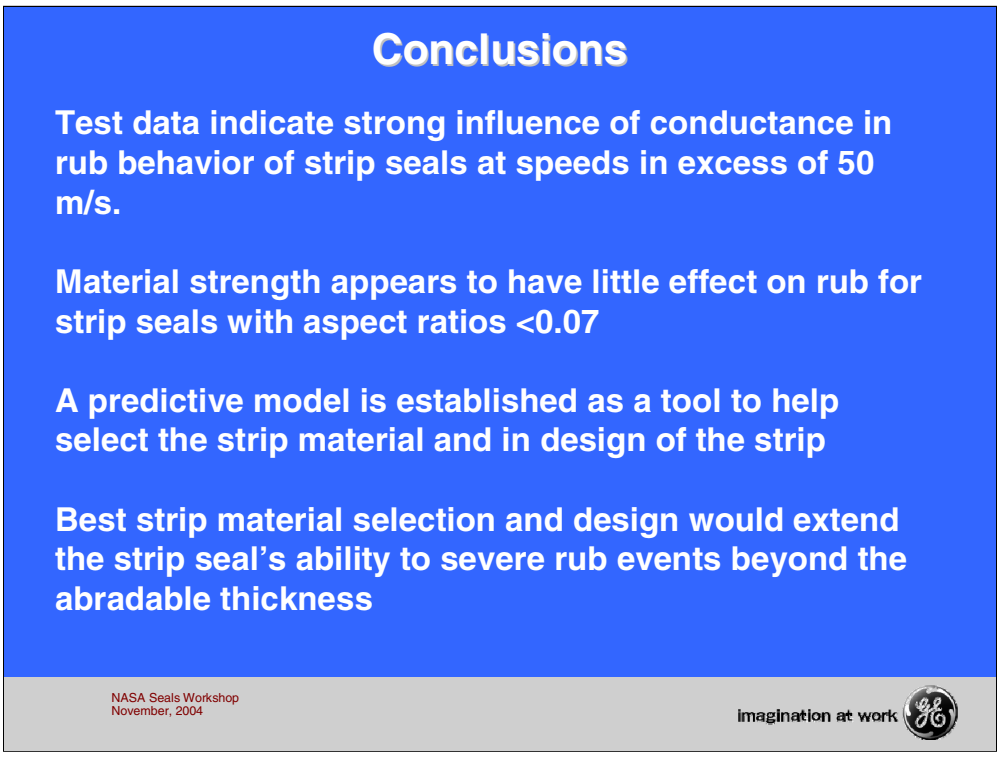

Conclusions

Page intentionally left blank

PARAMETRICAL STUDY OF HYDRODYNAMIC SEAL USING A 2D DESIGN CODE AND COMPARING WITH A 3D CFD MODEL

Xiaoqing Zheng
Perkin Elmer Centurion Mechanical Seals
Warwick, Rhode Island

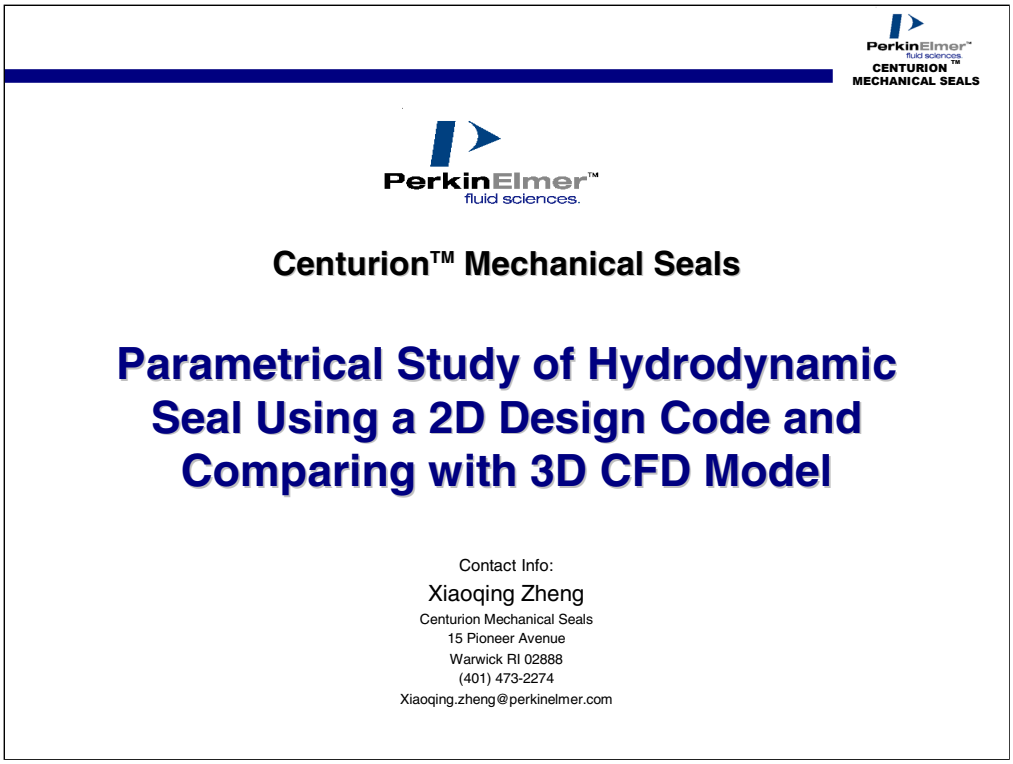

Hydrodynamic film-riding gas seal, having been successfully used in industrial pump and compressor applications for decades, is now finding way into aero-engines. Aerospace applications require the seal work robustly under various speeds and constantly changing pressures. Maintaining seal face flatness is also more challenging in aerospace than in industrial applications because of the seal size and the rapid thermal transition in aero-engines. Another difficulty in aerospace application comes from the altitude condition, where air is thin, not enough opening force may be generated to separate the seal faces from touching. Therefore, the hydrodynamic groove design is more critical in aerospace application. In order to maximize the seal performances, the groove shape and depth are optimized for the worst application condition, such as at the altitude, with using a 2D model coupled with a non-linear optimization procedure.

Seals designed in this way have been found working well both in rig test and in on-flight evaluation. However, two recently designed seals based on full optimization were found not working during rig test. These two seals features very fine grooves that is thinner than the other seals that worked well. The 2D code from time to time predicted that seals work better if more grooves were engraved. The under-performed two seals indicted there might be something missing in the 2D model. It was speculated that the entrance losses and 3D effects for narrow grooves become significant, resulting in reduction of hydrodynamic opening force. In order to quantify the influences of 3D effect, a three-dimensional model is therefore developed to calculate the fluid flow between the seal faces, and then the results are compared with the 2D solution. The model solves a circumferential section of seal face that consists one land and one groove region. A small region outside the sealing face is also included to simulate the flow entrance and exit. It was found that the 3D CFD model generally agrees with the 2D model in determining the optimum groove dimensions. The 3D code gives similar trend predictions of seal opening force under the influences of groove depth, number of grooves, land to groove ratio and groove angle, although there exist differences in the absolute value levels. The 3D CFD results forced a re-examination of hardware and further re-test the seal. It is concluded that the problems were due to manufacture tolerance with such fine grooves. The design code is correct, but manufacture capability should be incorporated. CFD results and test data are reported in this paper.

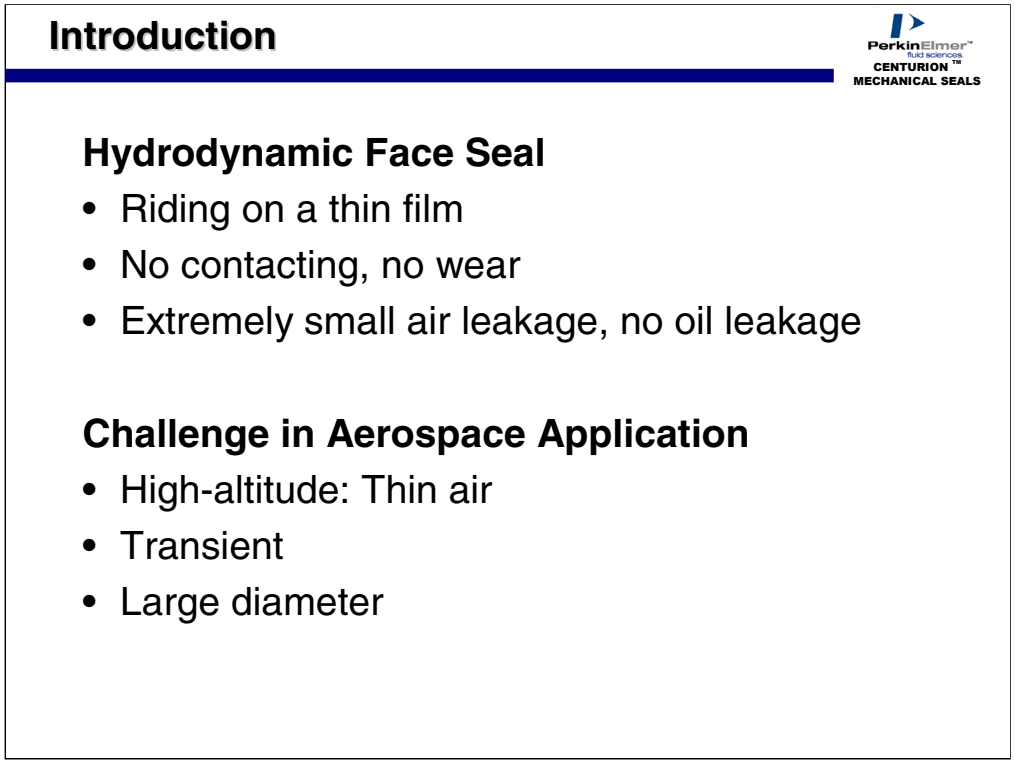

Hydrodynamic film-riding gas seal, having been successfully used in industrial pump and compressor applications for decades, is now finding way into aero-engines. Aerospace applications require the seal work robustly under various speeds and constantly changing pressures. Maintaining seal face flatness is also more challenging in aerospace than in industrial applications because of the seal size and the rapid thermal transition in aero-engines. Another difficulty in aerospace application comes from the altitude condition, where air is thin, not enough opening force may be generated to separate the seal faces from touching. Therefore, the hydrodynamic groove design is more critical in aerospace application. In order to maximize the seal performances, the groove shape and depth are optimized for the worst application condition, such as at the altitude, with using a 2D model coupled with a non-linear optimization procedure.

Film Riding Hydrodynamic Face Seal

PerkinElmer fluid sciences
CENTURION ™
MECHANICAL SEALS

PKI "State Of The Art" Design Code Solves The Seal Equations

1. **Seal Equation:** $\vec{\nabla}\bullet\{ph^3\vec{\nabla}p-6\mu ph\omega r\theta\}=0$

2. **Code uses CFD to solve groove equations**
3. **Code is coupled with ADINA to analyze face deflections**
4. **Optional Dam Section Hydrostatic Equation: (for high pressure drop)**

$$\frac{dM^2}{dr}=\frac{2(1+\frac{\gamma-1}{2}M^2)M^2}{1-M^2}(\frac{1}{r}+\frac{dh}{hdr})+\frac{2\gamma M^4(1+\frac{\gamma-1}{2}M^2)f}{(1-M^2)h}$$

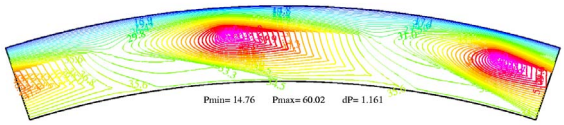

Automatic 6 design parameters Non-linear optimization

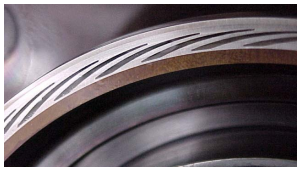

The 2D seal code has been validated against rig test data including high-altitude conditions. It is then incorporated into the powerful ADINA program for 3D dynamic analysis. A non-linear procedure has been developed on top of the program. Each design is optimized based on the worst operating condition. Therefore each design is a result of full DOE analysis with direct simulations. As shown here, each design is distinctive in the shape, depth, and number of grooves.

Design Tool Reliability ?

PerkinElmer fluid sciences
CENTURION ™
MECHANICAL SEALS

- When seal failed
- When seal contacts / wears
- When certain kind of seal under-performed

Is the design tool reliable?

If not sure, what is missing?

- 2D simplification in fluid simulation?
- Entrance loss (inadequate computational domain)?

Seals designed in this way have been found working well both in rig test and in on-flight evaluation. However, two recently designed seals based on full optimization were found not working during rig test. These two seals features very fine grooves that is thinner than the other seals that worked well. The 2D code from time to time predicted that seals work better if more grooves were engraved. The under-performed two seals indicted there might be something missing in the 2D model. It was speculated that the entrance losses and 3d effects for narrow grooves become significant, resulting in reduction of hydrodynamic opening force.

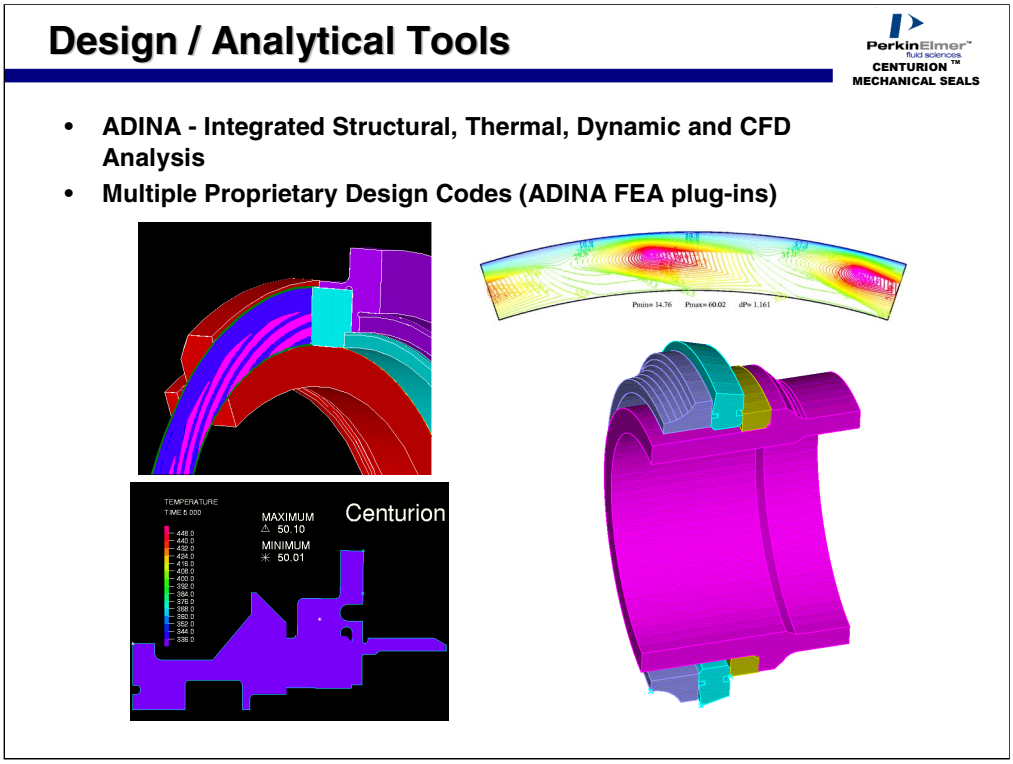

ADINA, a multi-physics engineering program specialized in Fluid-Structure Interaction simulation is used in our seal design and optimization. Uniquely, we have plugged our seal code into the ADINA system, therefore 3D CFD, Structural, Thermal dynamic analysis can be done efficiently for hydrodynamic seal design.

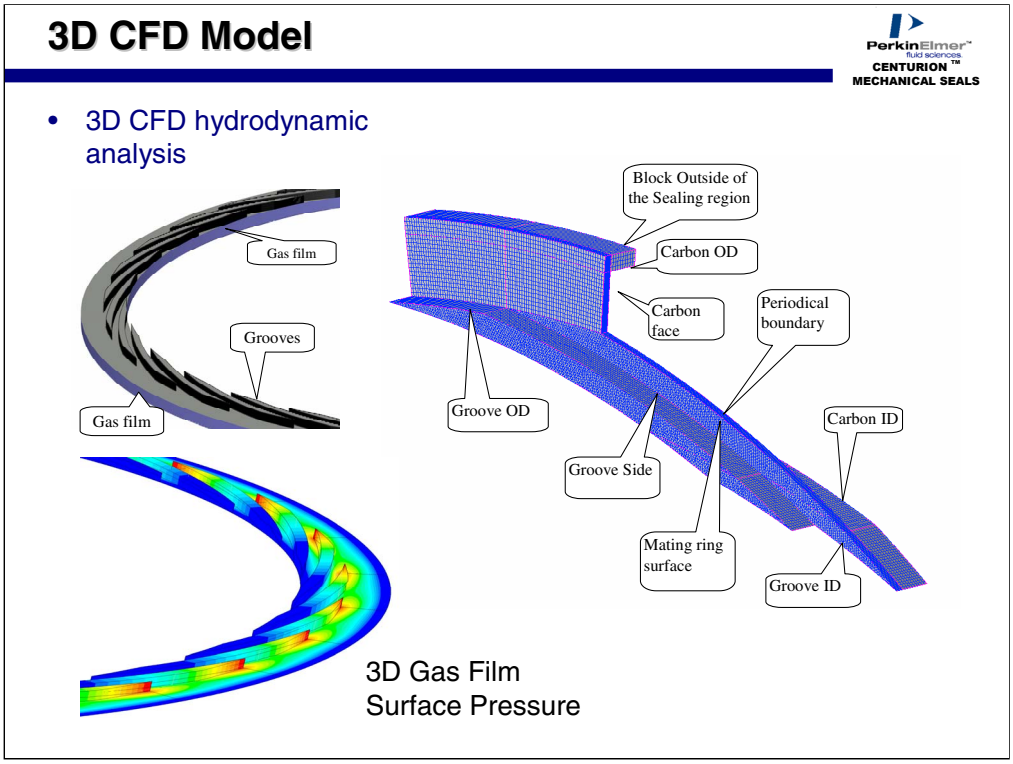

The fluid flow domain includes the groove that extends beyond the carbon ID, the land area, dam area and areas outside of the sealing faces to include entrance losses in the model. One slice consisting of one groove and one land area is actually solved.

Governing Equations

PerkinElmer fluid sciences
CENTURION ™
MECHANICAL SEALS

Governing Equations

- The equations solved are 3D Navier-Stokes Equations. No simplification is made.

Boundary conditions

1. The mating ring surface and grooves are rotating at a constant speed and the seal ring is stationary. The seal OD and ID are exposed to ambient pressure and room temperature.
2. Stationary and rotating walls are treated as non-slipping
3. Periodical boundary condition for section interfaces

Model Seal

PerkinElmer fluid sciences
CENTURION ™
MECHANICAL SEALS

Parameter	Value	Notes
Groove profile radius	1.47	
Film thickness	0.000100	
Number of grooves	20-70	While land to groove ratio is kept 0.75
Land to groove ratio	0.25-2	Number of groove is fixed
Groove depth	100-750	groove number and angle are fixed
Groove angle	6-30	Groove depth, number of grooves and land to groove ratio are fixed
Shaft speed	10,000 and 20,000 rpm	
Pressure	Ambient for ID and OD	

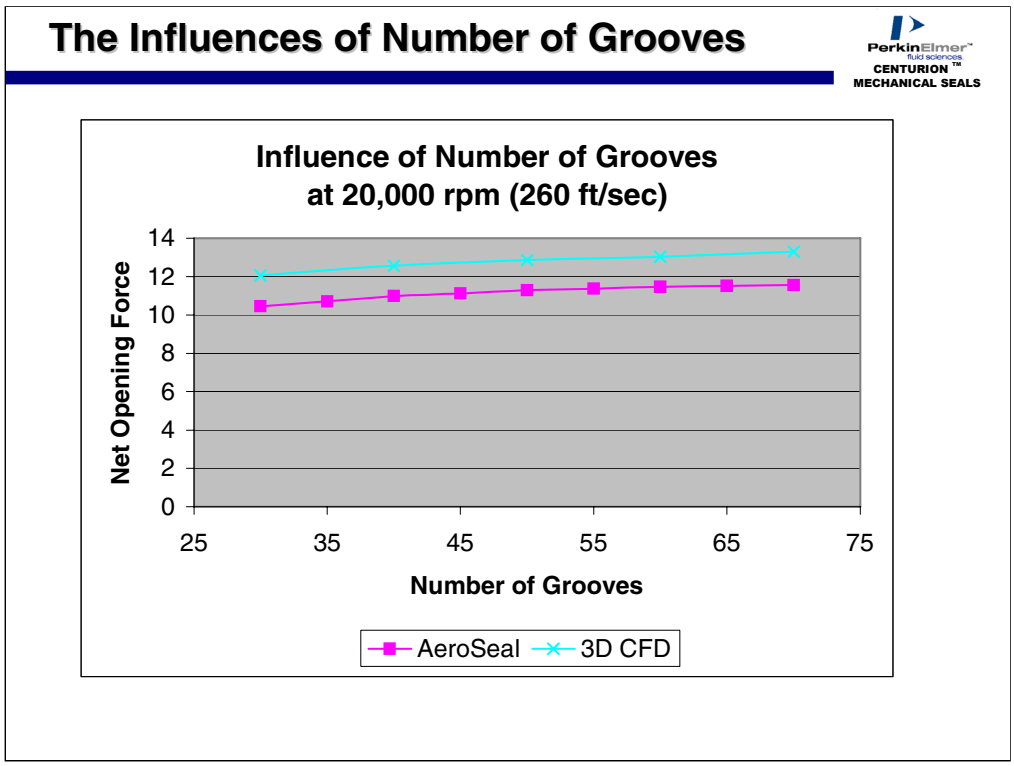

The influences of number of grooves for this seal are studied at 10,000 rpm and 20,000 rpm. The groove depth is set to 0.000350 inches more than the design value, the land to groove ratio is 0.75, and the groove angle is set to the design value. Both 2D and 3D models predict that more grooves, more opening force. Despite the difference of absolute opening force between the 3D and 2D results, the trend is parallel for both models.

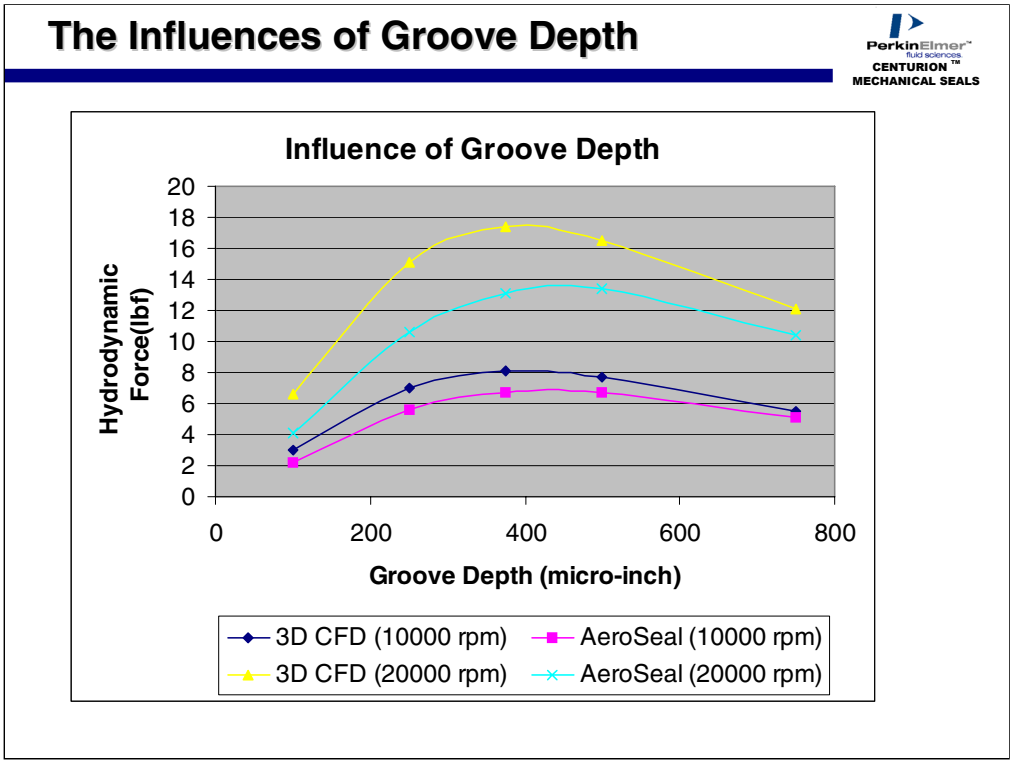

The groove number, the land to groove ratio and the groove angle are set to the design values in this study. Both 2D and 3D models show strong dependency of hydrodynamic force on the groove depth. It is also interesting to note the difference between 2D and 3D model becomes smaller at the groove depth gets shallower or getting very deep.

In this case, the optimal groove depth under seal level pressure condition is close to the design value, predicted by both 2D and 3D models

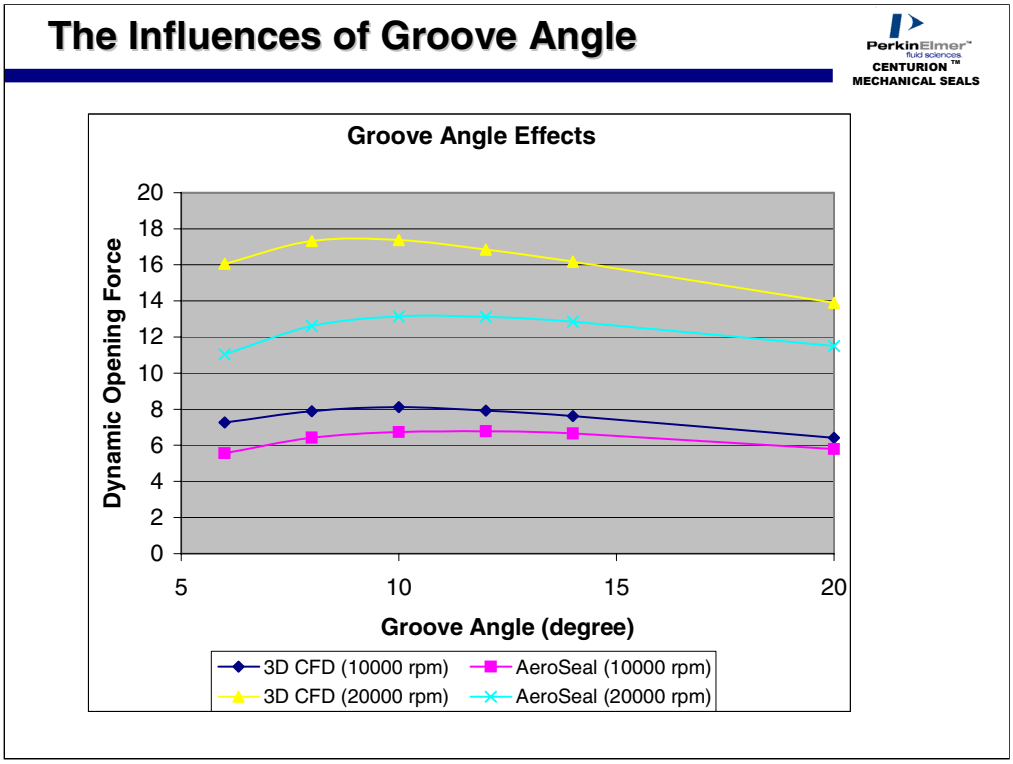

The groove depth and the land to groove ratio are fixed with design values. The groove radius of curvature is 1.470 inches representing a spiral groove at the initial angle of groove.

Both 2D and 3D models show considerable dependency of hydrodynamic force on the groove angle. In this study, the groove profile curvature is fixed; only angle is changed to isolate the influence. For real spiral grooves, the curvature is a function of the groove angle.

In this case, the optimal groove angle predicted by the 2D model is only one degree higher than that by the 3D model.

The Influences of Land to Groove Ratio

PerkinElmer fluid sciences
CENTURION ™
MECHANICAL SEALS

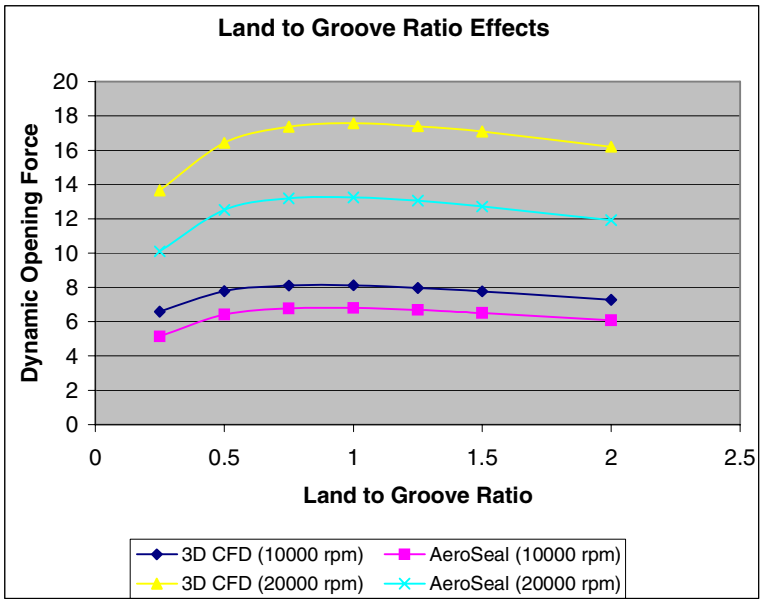

Revisit Tested Seal

PerkinElmer fluid sciences
CENTURION ™
MECHANICAL SEALS

- Both 2D and 3D models suggest more grooves work better within the range that we are looking

Manufacture Discrepancy

- The designed land to groove ratio is 0.75.
- The made is only 0.5. The grooves were made too wide.
- If the land to groove ratio is set to 0.5, rerun the 2D seal analysis confirms rig observation.

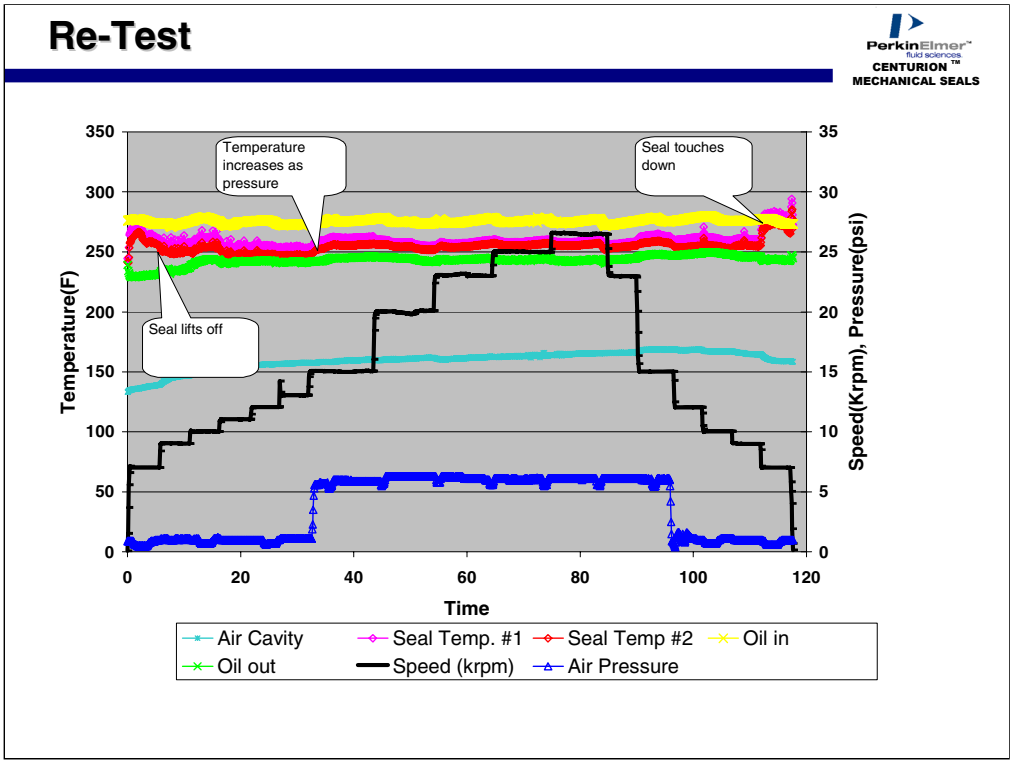
Re-Test
PerkinElmer fluid sciences
CENTURION ™
MECHANICAL SEALS
Temperature increases as pressure
Seal touches down
Seal lifts off
Temperature(F)
Speed(Krpm), Pressure(psi)
Time
0
20
40
60
80
100
120
0
50
100
150
200
250
300
350
0
5
10
15
20
25
30
35
Air Cavity
Seal Temp. #1
Seal Temp #2
Oil in
Oil out
Speed (krpm)
Air Pressure

Conclusion

PerkinElmer fluid sciences
CENTURION ™
MECHANICAL SEALS

1. The 3D CFD model generally agrees with the 2D model.
2. The physical model of the 3D code is more accurate than that of the 2D code.
3. However, the 2D model is solved numerically more accurately than the 3D model is.
4. In most cases, At least theoretically, seals with more grooves work better.
5. 3D CFD simulation also supports the groove design from the 2D model.

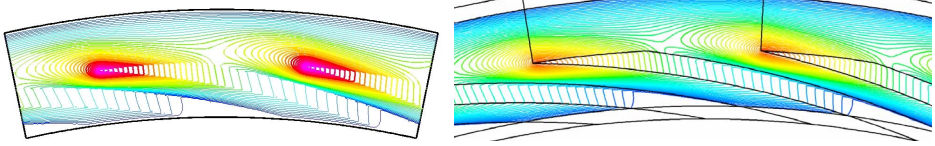

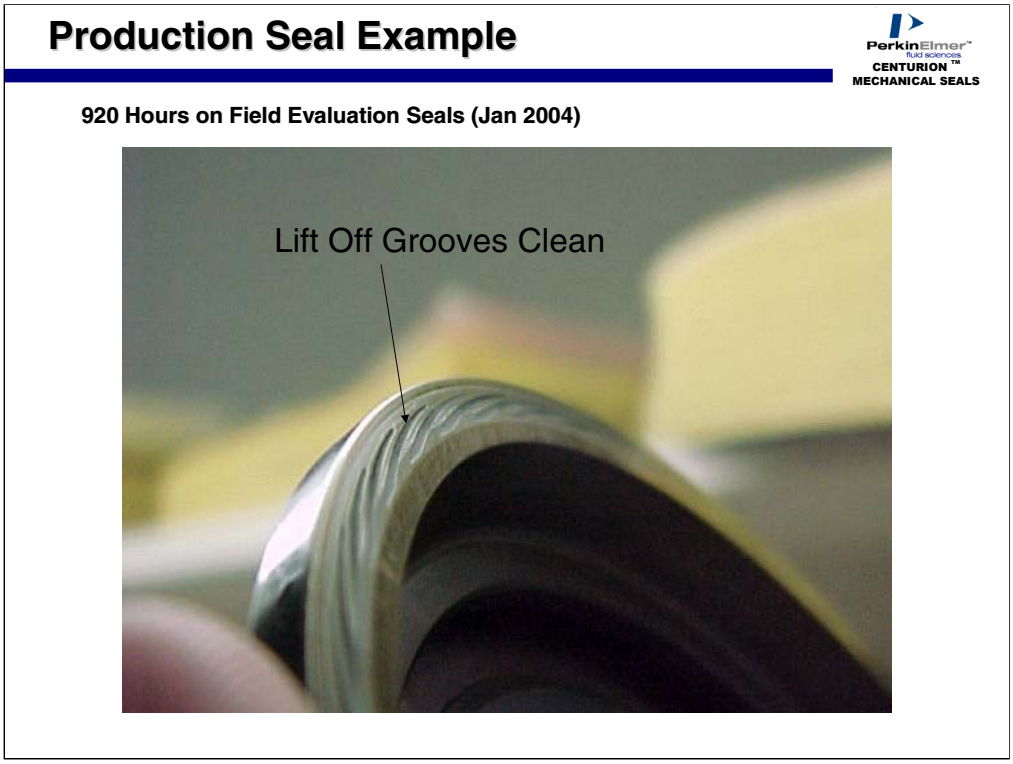

This is a picture we obtained from Honeywell earlier this year. It shows the hydrodynamic grooves still clean and there is no oil leakage. The seal has been qualified for production and has accumulated more than 51,000 hours in field with no failure.

NON-CONTACTING FINGER SEAL DEVELOPMENTS AND DESIGN CONSIDERATIONS: THERMOFLUID AND DYNAMICS CHARACTERIZATION, EXPERIMENTAL

M. Jack Braun, Hazel M. Pierson, and Dingeng Deng
University of Akron
Akron, Ohio

Margaret P. Proctor
National Aeronautics and Space Administration
Glenn Research Center
Cleveland, Ohio

GEOMETRY

ATIGAT

a)

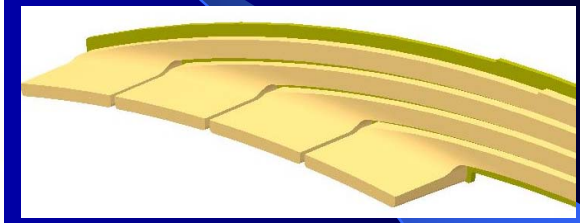

b)

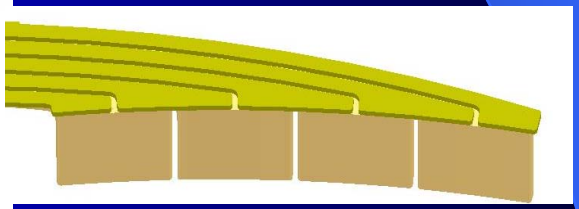

c)

HP and LP Seal Details

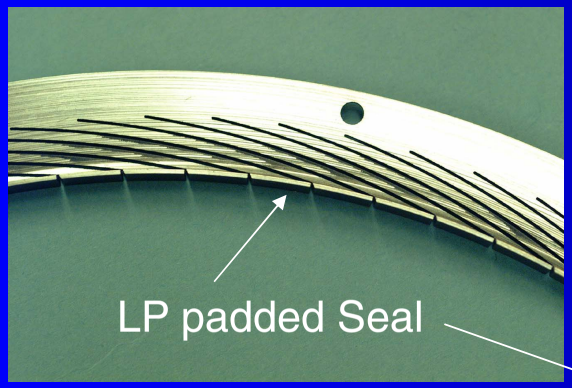

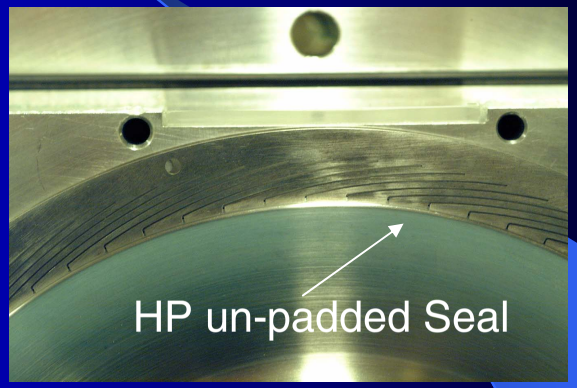

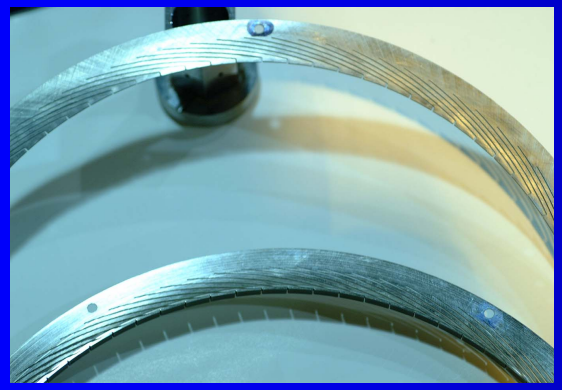

Manufactured by:
RF Cook
Stow, OH 44224

HP and LP Seal Details (cont'd)

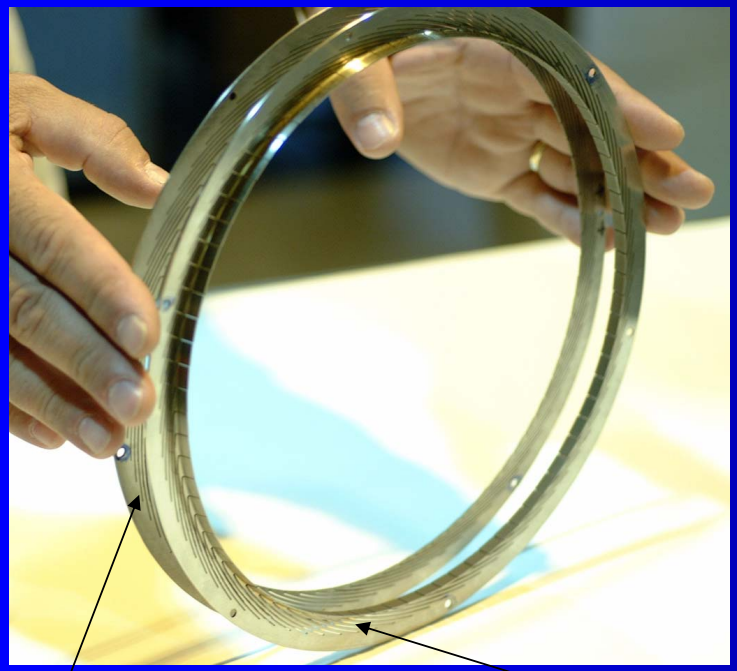

HP and LP Wafers of the Seal

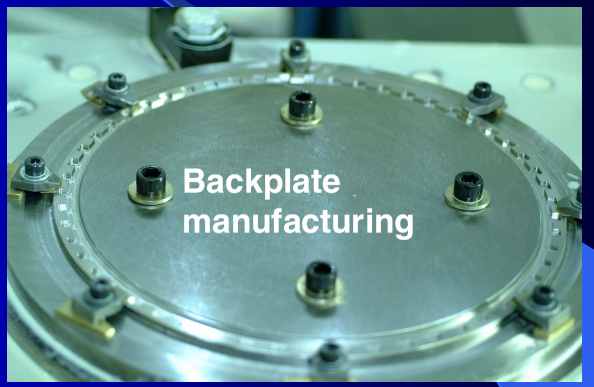

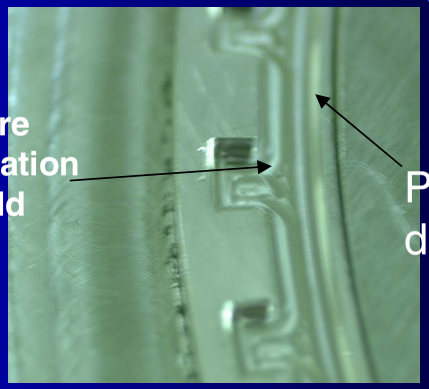

Backplate

GEOMETRY (cont'd)

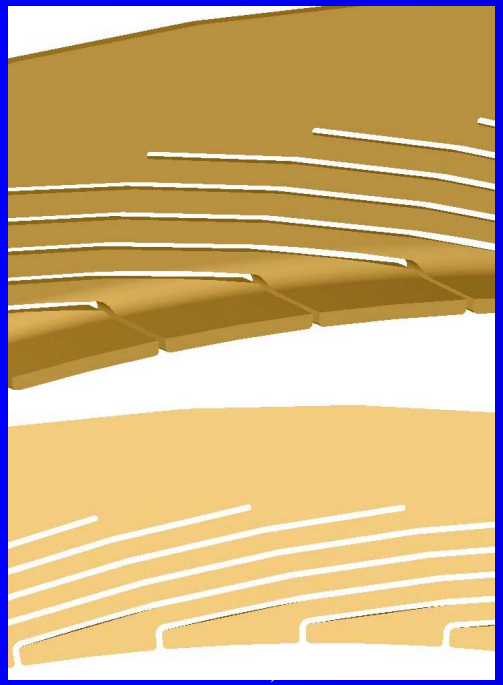

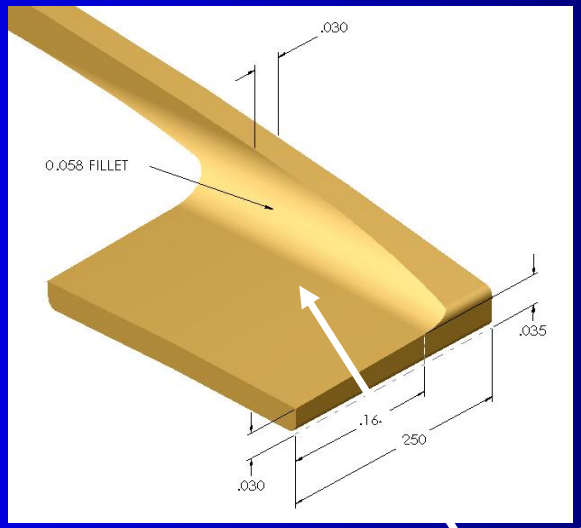

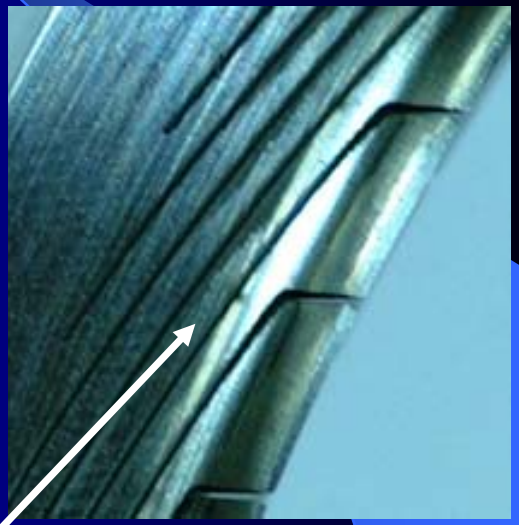

c)

Low Pressure padded seal details

THE TEST SECTION ASSEMBLY

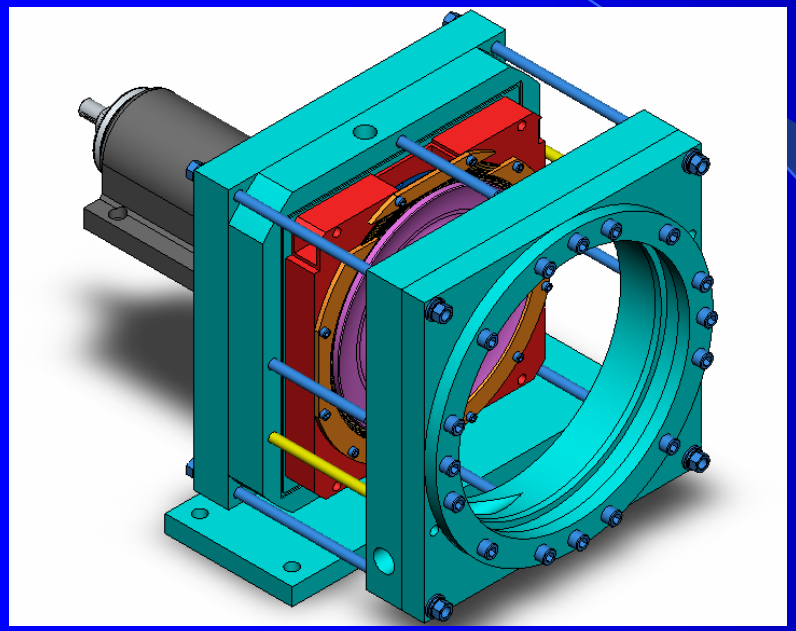

Solid model design

Actual test section

SPACER PLATE AND SEAL POSITION

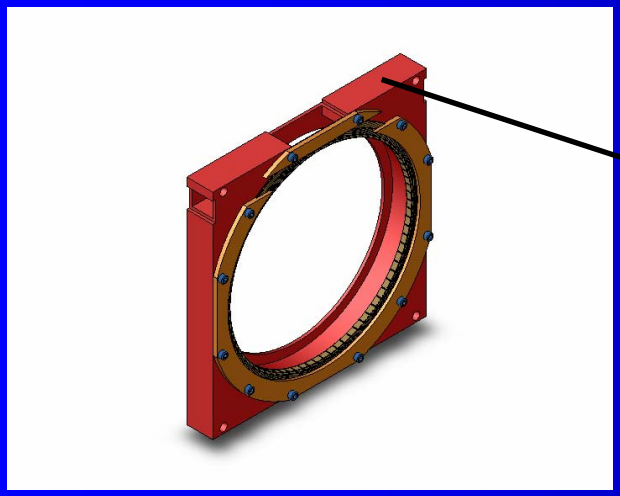

Seal holder assembly

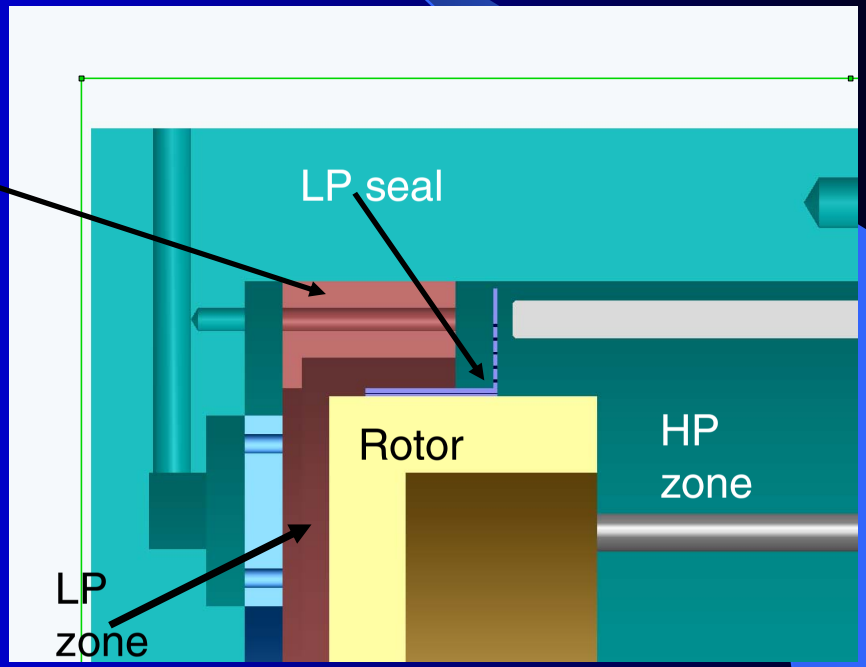

Axial Pressure=5 psi; RPM =10Krpm

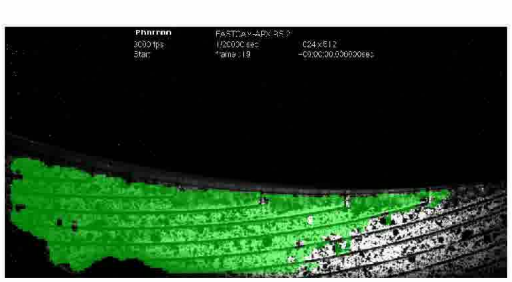

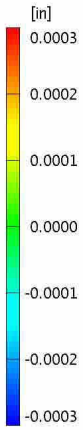

Radial Displacement

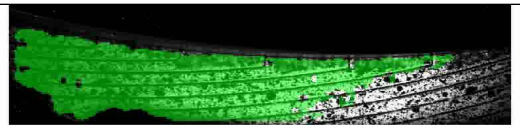

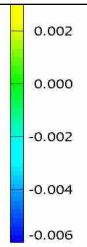

Axial Displacement

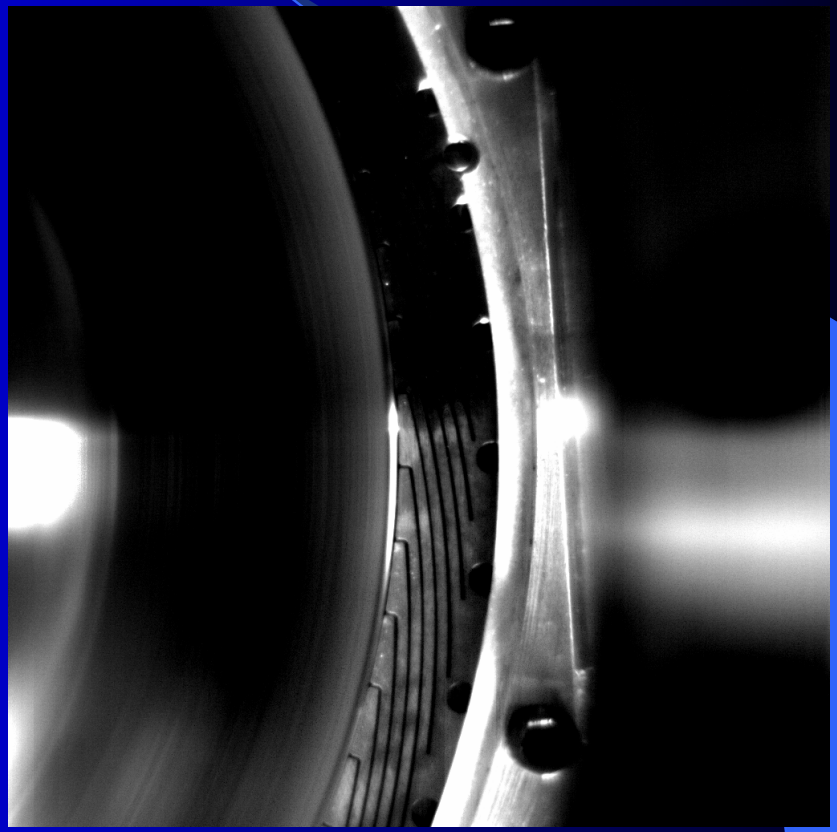

PRESSURE INDUCED FORCES

Variation with axial pressure differential, HTC and runner speed

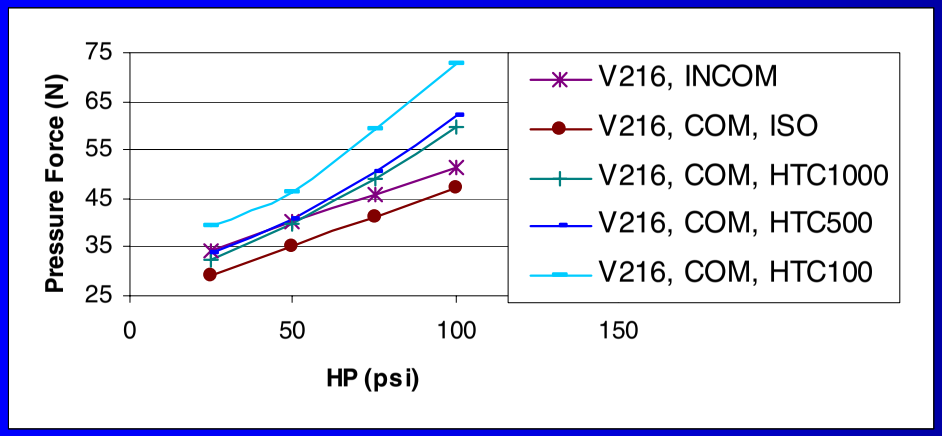

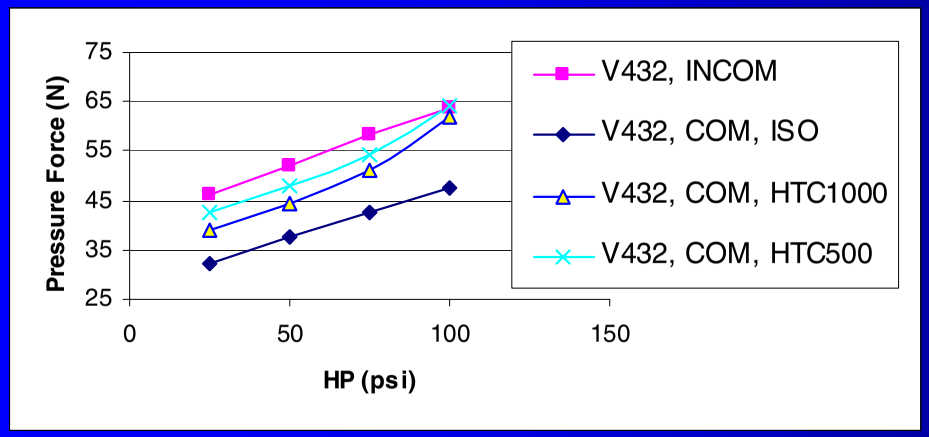

Incompresible and (compressible, isothermal): LINEAR variation

Compressible, PGL: NON-Linear

The HTC 100 vs 1000 is equivalent to the limiting cases of:

adiabatic vs. isothermal

Mass Flow as a Function of the HP side Pressure

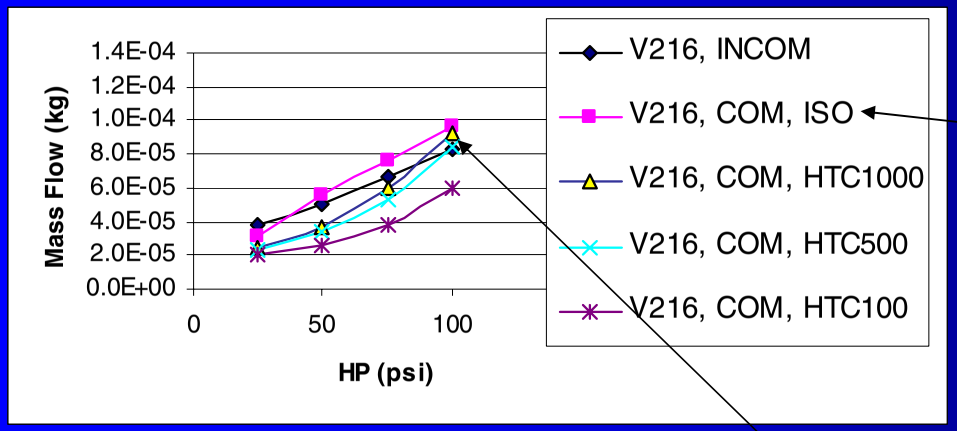

μ=const;ρ const ←PGL

As HTC goes up, T goes down, ➠ρ goes up➠mass flow goes up

At HTC=100, T goes up, ➠ρ goes down ➠Mass flow goes down

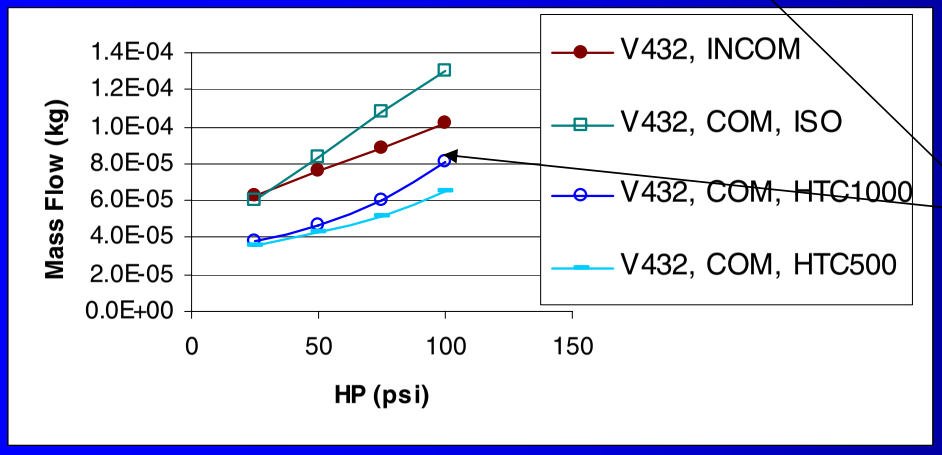

At constant HTC=1000, lower speed (216 vs 432) has lower temperatures➠ρ goes up ➠mass goes up

PARTIAL CONCLUSIONS

It was found that:

- the interplay between the rotation induced pressure generation and the axial pressure drops controlled by the HP side, is dominated by rotation at low HP side pressure, but it is then taken over by the axial pressure drop when the latter becomes larger then 173kPa at 216mps.
- the effect of allowing the dynamic viscosity to vary with temperature is to introduce strong non-linearities both in the behavior of the leakage flow and the load carrying capability.

PARTIAL CONCLUSIONS

- the numerical experiments showed that the FS behaves more like a bearing at low axial ΔPs and like a seal at high ones
- that the increase in the rotational velocity causes increased LCC, but
- the increase in the heat transfer coefficient causes more leakage and diminishes the load carrying capability.
- that the temperature maps showed that the high temperature regions shift from under the HP fingers at low ΔPs and towards the outer regions of the LP finger pad when the axial ΔPs increase


THE UNIVERSITY OF AKRON
1870
ATIGAT
DYNAMIC SIMULATION CONCEPTS AND RESULTS

FINGER SEAL EQUIVALENT MODEL FOR DYNAMIC SIMULATION—2- DOF

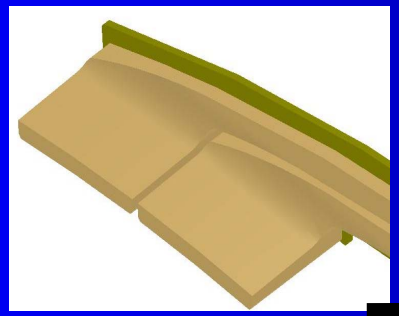

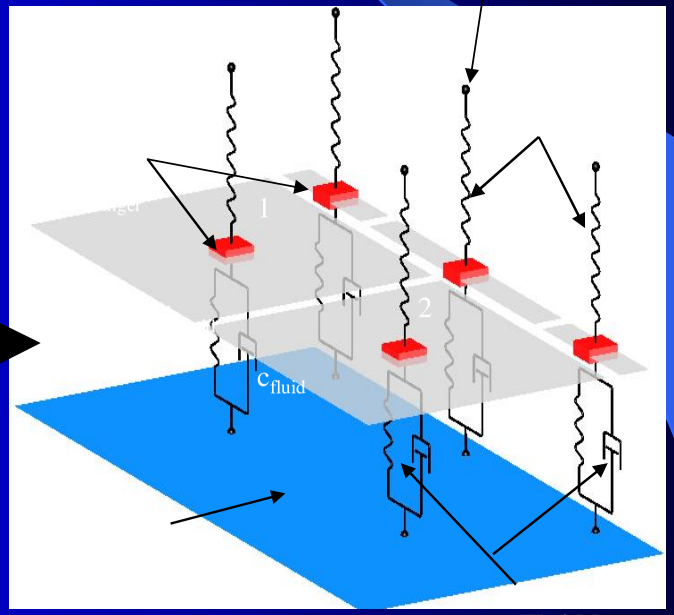

a) b)

Solid model and Equivalent Spring-Mass-Spring/Damper representation for use in the equation of motion simulation

TWO DEGREE OF FREEDOM MODEL – 2 DOF

ATIGAT

2 DOF

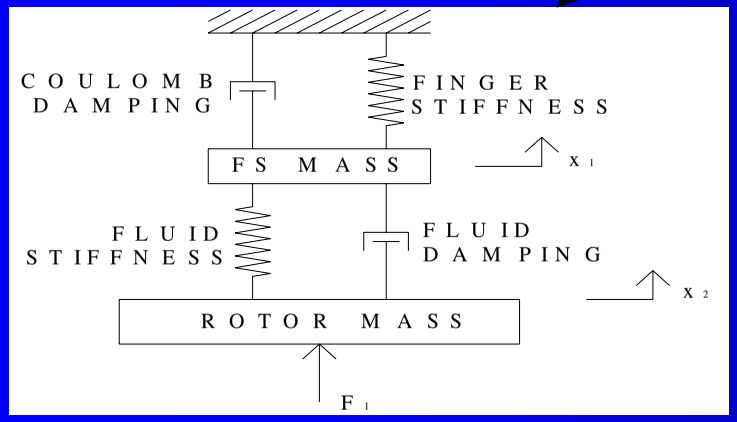

$$\begin{bmatrix} m_R & 0 \\ 0 & m_{FS} \end{bmatrix} \begin{Bmatrix} \ddot{x}_1 \\ \ddot{x}_2 \end{Bmatrix} + \begin{bmatrix} c_f & -c_f \\ -c_f & c_f + c_c \end{bmatrix} \begin{Bmatrix} \dot{x}_1 \\ \dot{x}_2 \end{Bmatrix} + \begin{bmatrix} k_f & -k_f \\ -k_f & k_f + k_s \end{bmatrix} \begin{Bmatrix} x_1 \\ x_2 \end{Bmatrix} = \begin{Bmatrix} F_1 \\ 0 \end{Bmatrix}$$

Interaction of finger and rotor mass through the fluid layer and subject to a forcing function input + Coulomb friction

1-DOF

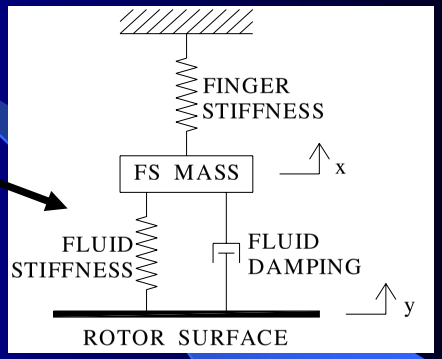

a)

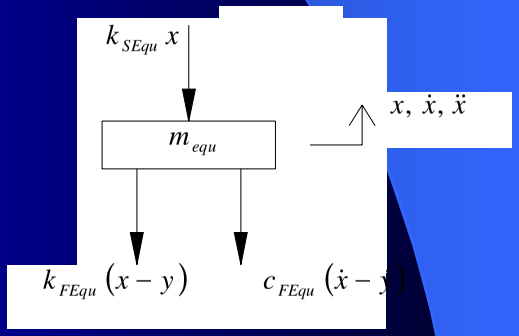

b)

$$m_{Equ}\,\ddot{x} + c_{FEqu}\,\dot{x} + (k_{FEqu} + k_{SEqu})x = c_{FEqu}\,\dot{y} + k_{FEqu}\,y$$

Finger seal mass following a displacement input

2-DOF cont'd

Now considering the input force to be harmonic,, we can assume the response of the masses to be characterized by

$$x_1(t) = X_1 e^{i\omega t}$$
$$x_2(t) = X_2 e^{i\omega t}$$

Thus

$$\dot{x}_{1,2} = i\omega X e^{i\omega t}$$
$$\ddot{x}_{1,2} = -\omega^2 X e^{i\omega t}$$

Substituting into the matrix equation above

$$\begin{bmatrix} Z_{11} & Z_{12} \\ Z_{21} & Z_{22} \end{bmatrix} \begin{Bmatrix} X_1 \\ X_2 \end{Bmatrix} = \begin{Bmatrix} F_0 e^{iwt} \\ 0 \end{Bmatrix}$$

where

$$Z_{11} = -\omega^2 m_R + i\omega c_f + k_f$$
$$Z_{12} = Z_{21} = -i\omega c_f - k_f$$
$$Z_{22} = -\omega^2 m_{FS} + i\omega(c_f + c_c) + (k_f + k_s)$$

The solution is then

$$\vec{X} = [Z(i\omega)]^{-1} \vec{F}$$

NOTE: The motion of the finger when the rotor/finger interact is represented by these equations and solution

Free vibration of the finger (2 HP- 2 LP) with an initial positive radial deflection and varying amounts of Coulomb friction.

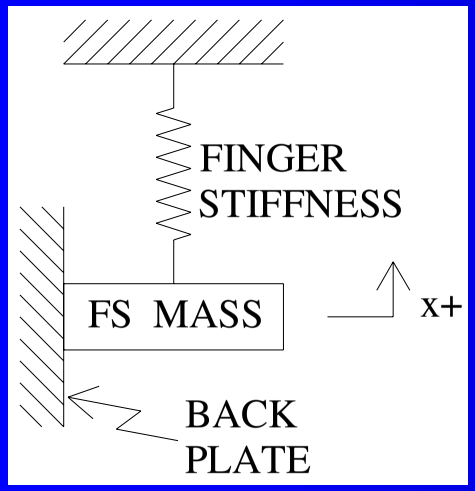

$$m\ddot{x} + kx = \pm F_f$$

The + and – signs are dependent of the direction of motion of the finger and thus orientation of the Coulomb friction

for $0 \le t \le \pi/\omega_n$

$$x(t) = \left[x_0 - \frac{F_f}{k} \right] \cos \omega_n t + \frac{F_f}{k}$$

for $\pi/\omega_n \le t \le 2\pi/\omega_n$

$$x(t) = \left[x_0 - \frac{3F_f}{k} \right] \cos \omega_n t - \frac{F_f}{k}$$

for $2\pi/\omega_n \le t \le 3\pi/\omega_n$

$$x(t) = \left[x_0 - \frac{5F_f}{k} \right] \cos \omega_n t + \frac{F_f}{k}$$

Free Finger Motion With Various Amounts Of Coulomb Friction. Finger Stiffness is Constant

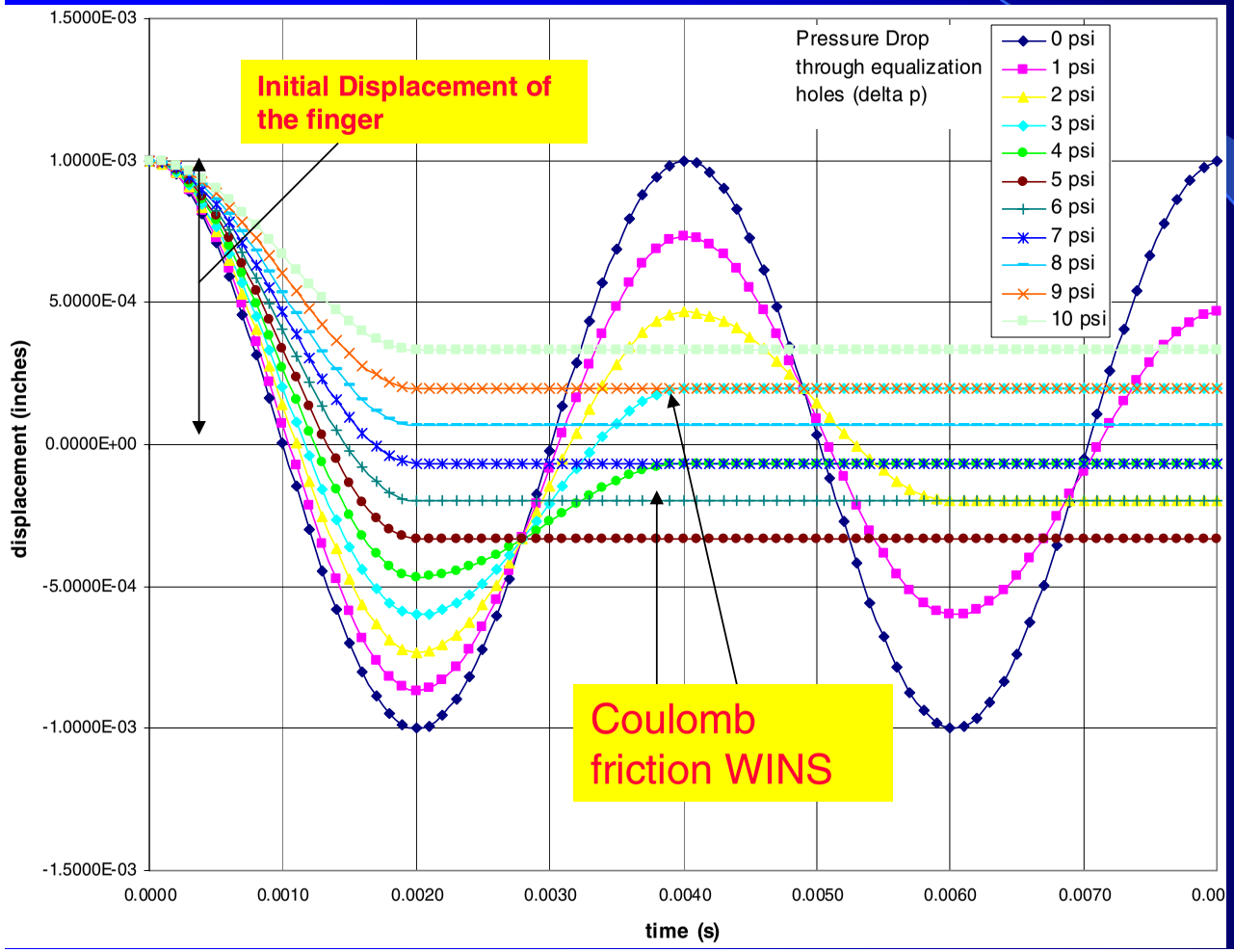

These levels do mot have enough energy left to move back to equilibrium line

These levels do mot have enough energy left to move back to equilibrium line

Free Finger Motion With Constant Coulomb Friction. Finger Stiffness is Varied.

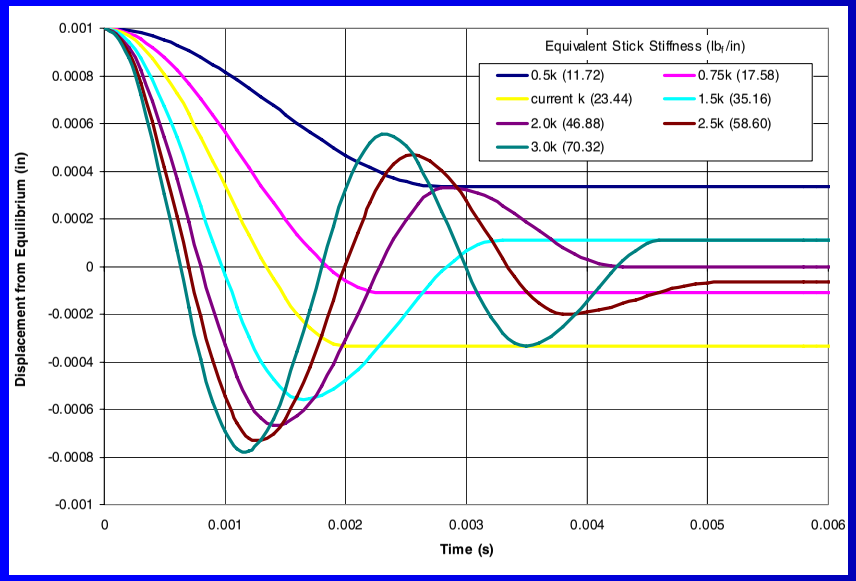

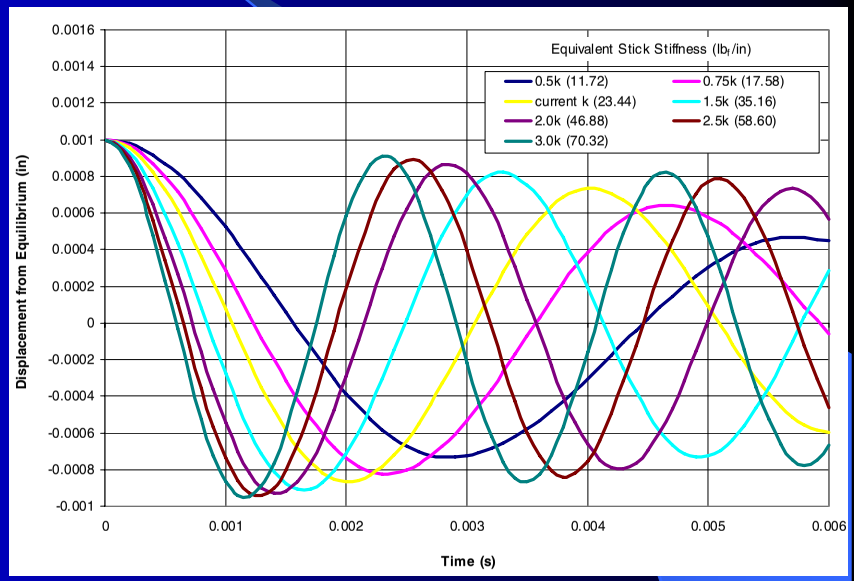

Δp=5 psi

Δp=10 psi

As the stick becomes stiffer, the Coulomb friction has less effect on damping out the free vibrations.

ROTOR AND FINGER RESPONSE TO A PERIODIC FORCING FUNCTION

ATIGAT

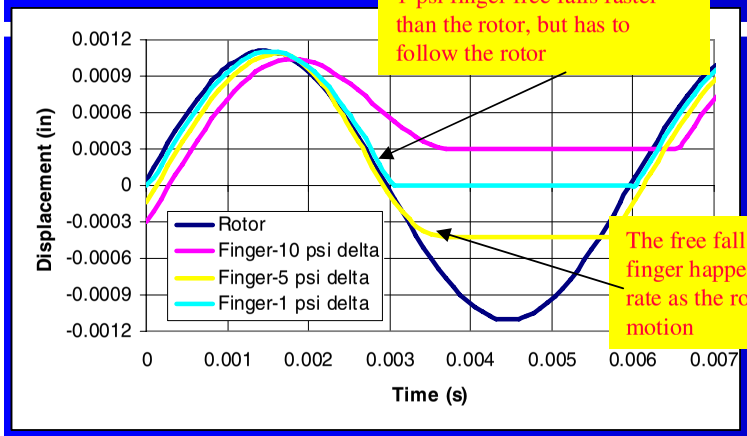

10000 rpm (1047 rad/sec)

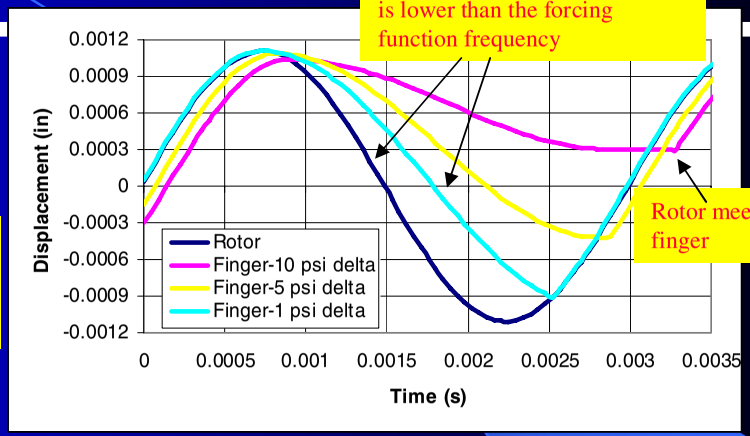

20000 rpm (2094 rad/sec)

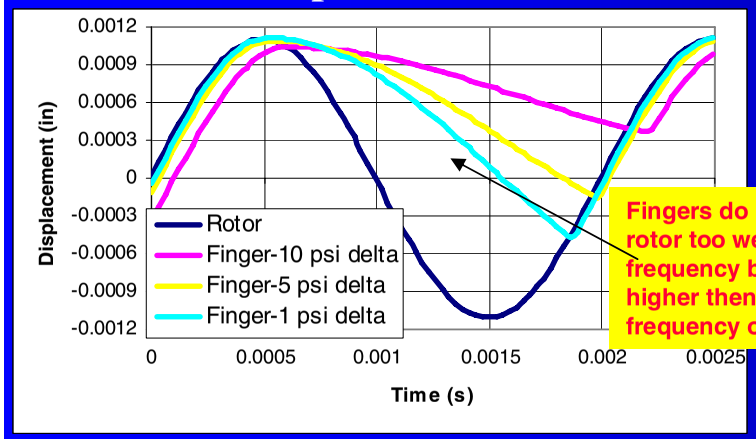

30000 rpm (3141 rad/sec)

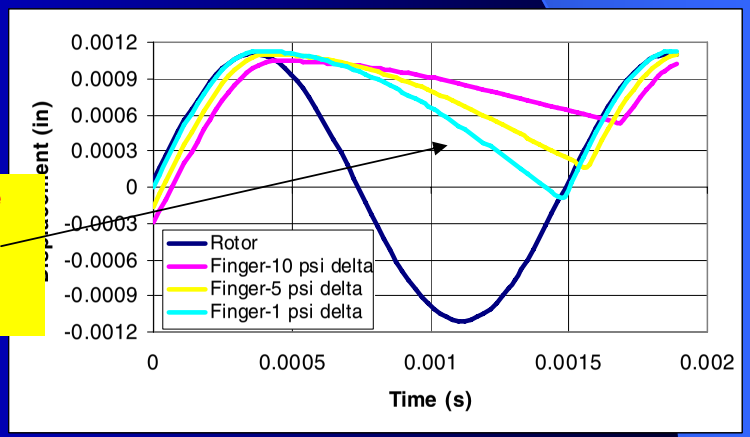

40000 rpm (4188 rad/sec)

Rotor and Finger Response to a Periodic Forcing Function with frequency of 2094 rad/s (20000 rpm) and a drop through the pressure equalization holes of 5 psi. FINGER STIFFNESS IS VARIED

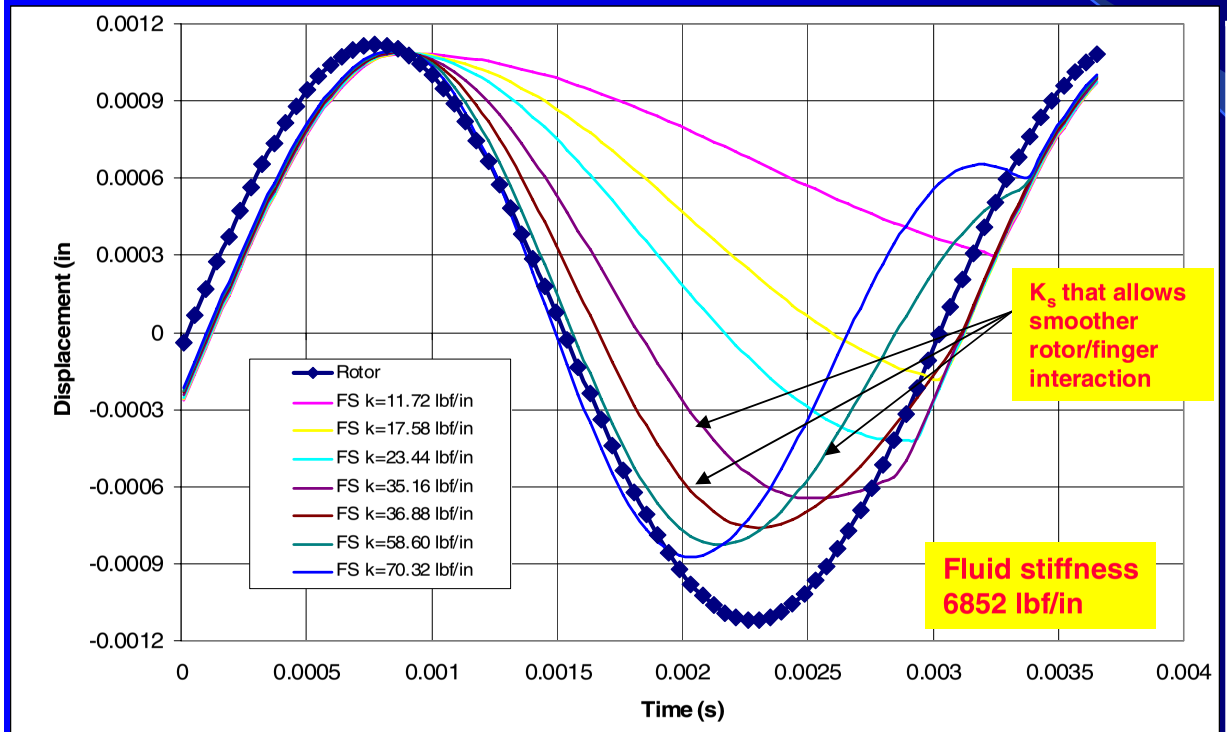

K lbf/in	LP Finger Thickness (in)	LP Finger Thickness (in)
11.72	0.015	0.015
17.58	0.030	0.015
23.44	**0.030**	**0.030**
35.16	0.045	0.045
46.88	0.060	0.060
58.60	0.075	0.075
70.32	0.090	0.090

What does this mean ????

- Fluid stiffness much larger than that of any practical finger stiffness
- The finger free fall portion is greatly influenced by small changes in equivalent finger stiffness.

$$\omega_n = \sqrt{k_s / m_{finger}}$$

- The transmissibility portion (rotor positive push) is not affected in the practical range of finger stiffness.
- A too thin of a finger will stay open (up) because it does not possess enough inner spring stiffness to overcome even a small amount of Coulomb friction
- Conversely a too thick finger could cause chatter oscillation
- For the cases studied here the best choices showing a finger picking up smoothly with the rotor are for stiffnesses between 35 and 58 lbf/in

Some notes regarding previous two slides

- In free vibration the energy of the finger gets expended eventually through Coulomb friction
- The free vibration however does not carry the day, because the finger re-encounters the rotor
- The natural frequency of the finger remains the same

CONCLUSIONS

A three dimensional Navier-Stokes based code (CFD-ACE+/FEMSTRESS) was utilized to analyze the thermofluid behavior of a modified FS[1].

• The pressure patterns, mass flows and load carrying capabilities of this structure were assessed. It was found that even at a lower linear velocity of 216mps (708 fps) the geometry proposed has good lifting capability.

.

CONCLUSIONS

- The interplay between the rotation induced pressure generation and the axial pressure drops controlled by the HP side, is dominated by rotation at low HP side pressure, but it is then taken over by the axial pressure drop when the latter becomes larger then 173kPa at 216mps.

- The pressure patterns generated by this geometry at low pressure drops prove that the seal behaves in the fashion of a mini-slider bearing.

CONCLUSIONS (cont'd)

The dynamic model introduced a simplified spring-mass-damper equivalent to the complicated structure presented by the FS.

The 1-DOF numerical experiments concentrated on the determination of the phase shift and displacement transmissibility Y .

These two parameters indicate how well and under what conditions the finger will follow the rotor.

CONCLUSIONS

- It was found that
- (i) the phase shift values increased when fluid stiffness was low and comparable to that of the stick,
- (ii) the phase shift value decreases with fluid damping increase,
- (iii) the combination of small *k*SEqu and large *k*FEqu amounts to a transmissibility Y=1,and a reversal in role leads to very small Ys,
- (iv) for damping values lower than 175 N.s/m2 (1 lbf.s/in2) damping has no effect on Y and

CONCLUSIONS

- (v) certain combinations of mass and fluid and solid stiffness lead to very large Y when the rotor speed approaches the natural frequency of the system
- (vi) in the 2-DOF model small changes in Kstick can significantly affect the rotor/stick interplay.

ROLE OF DISTRIBUTED INTER-BRISTLE FRICTION FORCE ON BRUSH SEAL HYSTERESIS

Helen Zhao and Robert Stango
Marquette University
Milwaukee, Wisconsin

MARQUETTE UNIVERSITY

Introduction and Background

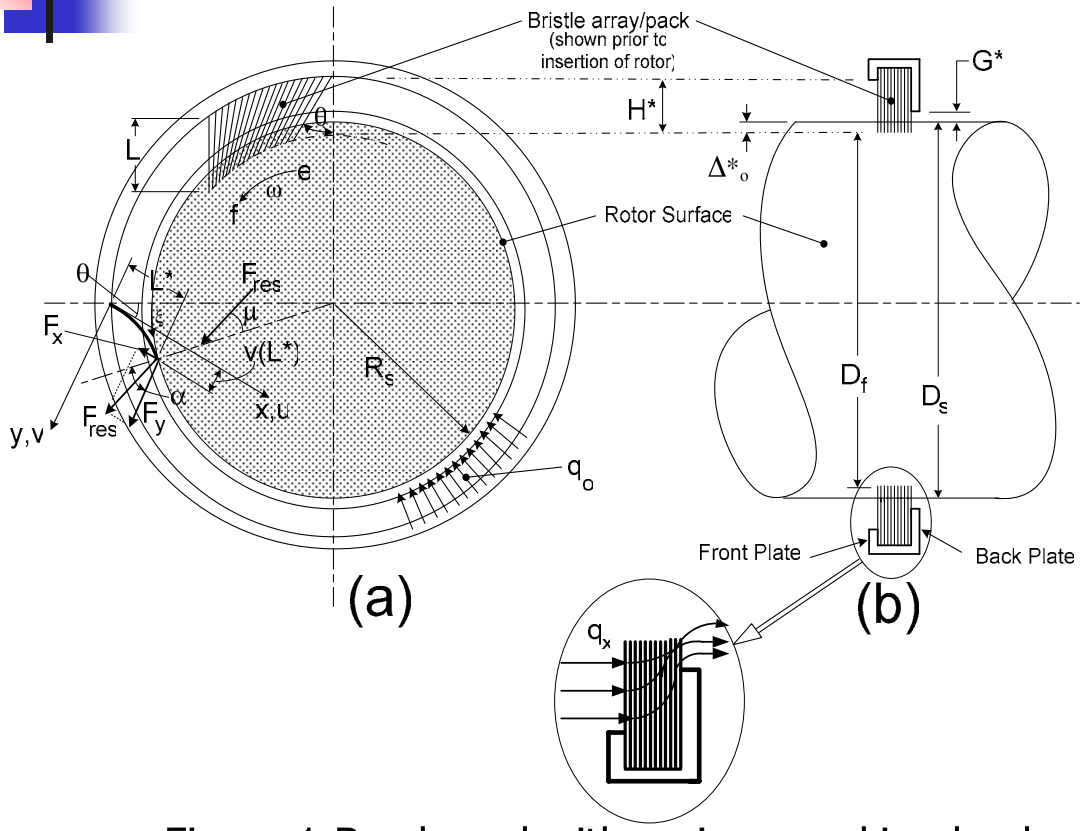

Figure 1 Brush seal with various working loads

Figure 1

- Interference parameter Δ^*_o
- Inward radial flow-induced load q_o
- Contact force F_{res} generated at interface of fiber tip and rotor
- Local oncoming flow of gas toward bristle pack q_x

Inter-bristle friction force model

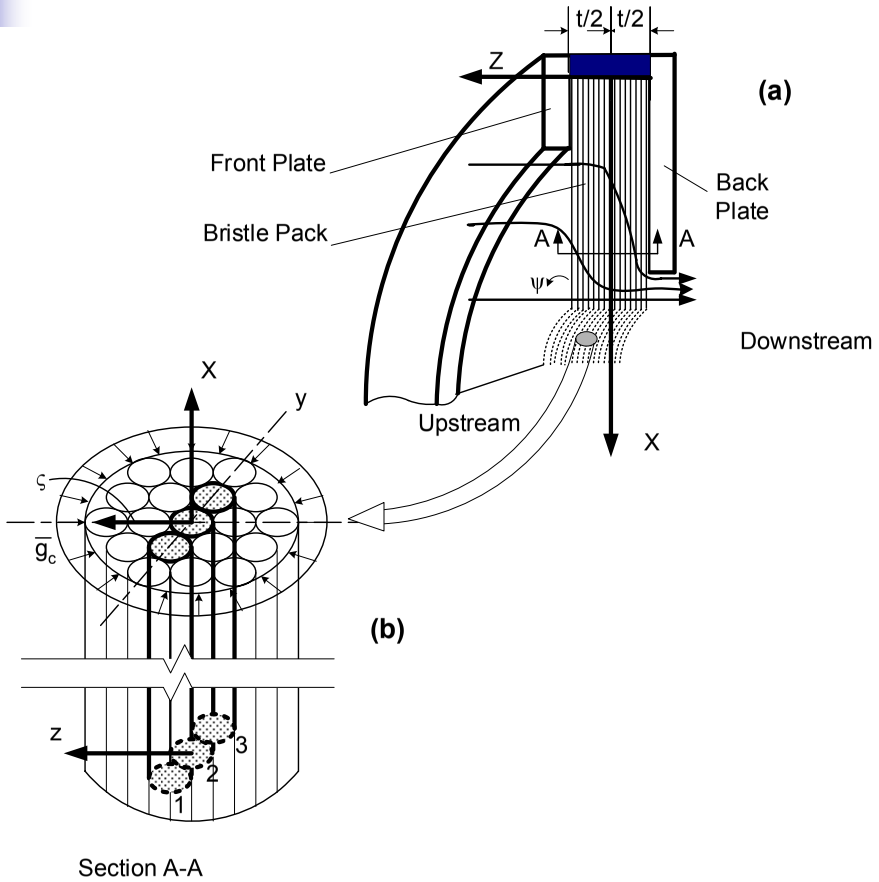

Figure 2

(a) Depiction of partial brush seal with front and back plate that constrain bristle pack

(b) Section A-A view, depicting the compactive load g_c around bristle pack. The interactive forces of three fibers (1, 2, 3) are studied for hysteresis phenomenon

Inter-bristle Friction Model (cont'd)

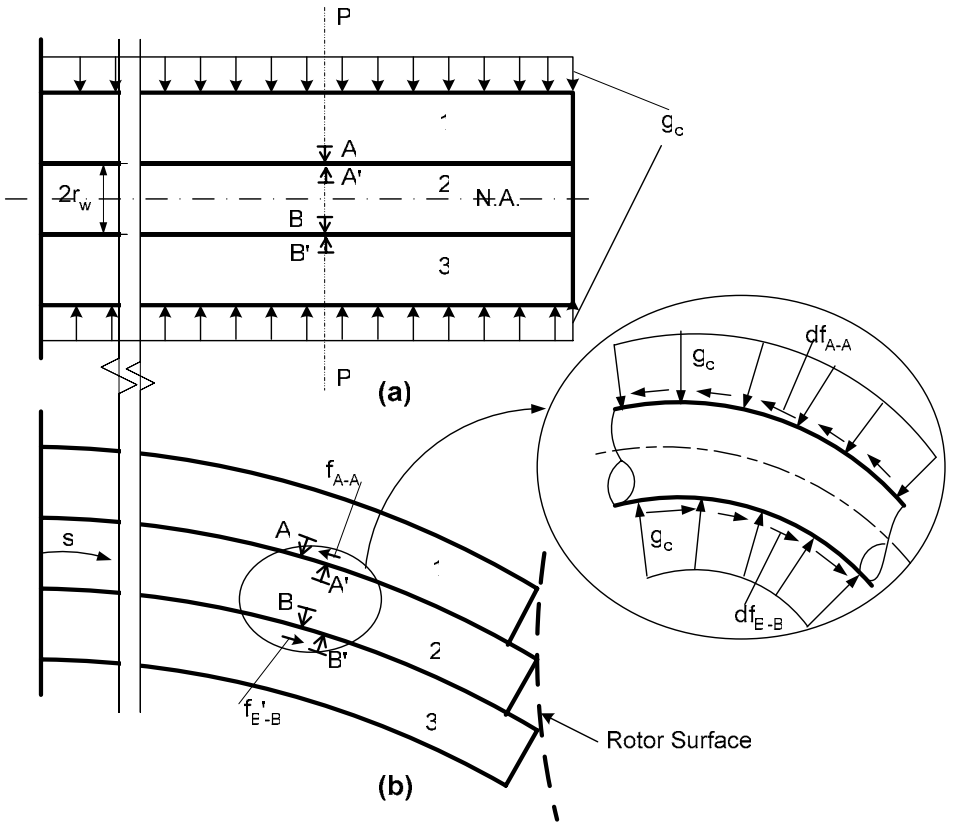

Figure 3

- Three un-deformed neighboring fibers subjected to the compactive load g_c
- Deformation of fibers under compactive load g_c.

Inter-bristle Friction Model (cont'd)

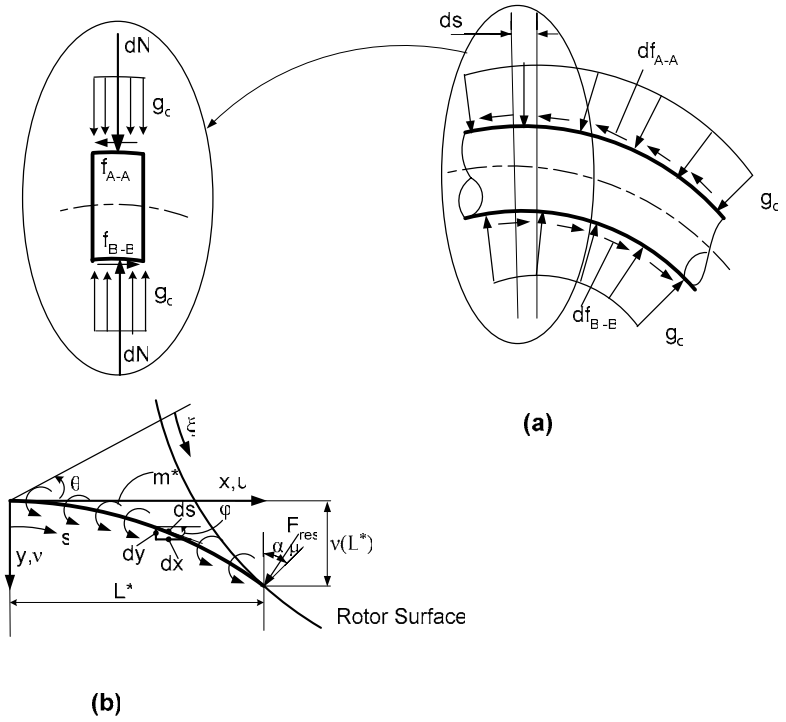

Figure 4

(a) Segment of the deformed fiber subjected to the uniform compactive load g_c and traction force $f_{A-A'}$ and $f_{B'-B}$

(b) simplified model depicting interaction between neighboring bristles as uniformly distributed moment m* along deformed fiber

Inter-bristle Friction Model---derivation of m*

MARQUETTE UNIVERSITY

Refer to Fig.3 and Fig.4:

1. Differential frictional force $df_{A\text{-}A'}$ and $df_{B'\text{-}B}$

$$\left.\begin{aligned} df_{A-A'} &= \mu dN;\ df_{B'-B} = \mu dN \\ dN &= ds \cdot g_c \end{aligned}\right\} \Rightarrow \begin{aligned} df_{A-A'} &= \mu g_c ds \\ df_{B'-B} &= \mu g_c ds \end{aligned}$$

2. Differential moment dm:

$$dm = 2\mu g_c r_w ds$$

3. Resisting bending moment m

$$m = 2\mu g_c r_w L$$

4. Distributed bending moment per unit length m

$$m^* = 2\mu g_c r_w$$

If Hexagaonal closed-pack, then $m^* = 2\mu g_c r_w (1 + 2\cos 60)$

MARQUETTE UNIVERSITY

Governing Equation

According to Euler-Bernoulli Law:

$$EI\kappa = M_{m^*} + M_{F_{res}} \qquad \text{with} \qquad \kappa = \frac{d\phi}{ds}$$

Governing Equation:

$$EI\frac{d^2\phi}{ds^2} = m^* - F_{res}\cos(\alpha - \mu - \phi)$$

Non-dimensional form of governing equation:

$$\frac{d^2\phi}{ds^{*2}} = \frac{m^* H^{*2}}{EI} - \frac{F_{res} H^{*2}}{EI}\cos(\alpha - \mu - \phi)$$

Boundary conditions and constraint conditions

MARQUETTE UNIVERSITY

Boundary conditions:

1. slope constraint at the bristle origin, i.e.

$$\Phi=0 \text{ at } s=0$$

2. Free of moment at the bristle tip, i.e.

$$d\Phi/ds=0 \text{ at } s=L$$

Constraint conditions:

$$\left|x_t - x_\xi\right| < \varepsilon; \left|y_t - y_\xi\right| < \varepsilon$$

Where,

$$x_t = \int_0^L \cos\phi ds; y_t = \int_0^L \sin\phi ds$$

$$x_\xi = (R_s + H^* - \Delta_o^*)\cos\theta - R_s\cos(\theta + \frac{\xi}{R_s})$$

$$y_\xi = R_s \sin(\theta + \frac{\xi}{R_s}) - (R_s + H^* - \Delta_o^*)\sin\theta$$

MARQUETTE UNIVERSITY

Eccentricity of Shaft

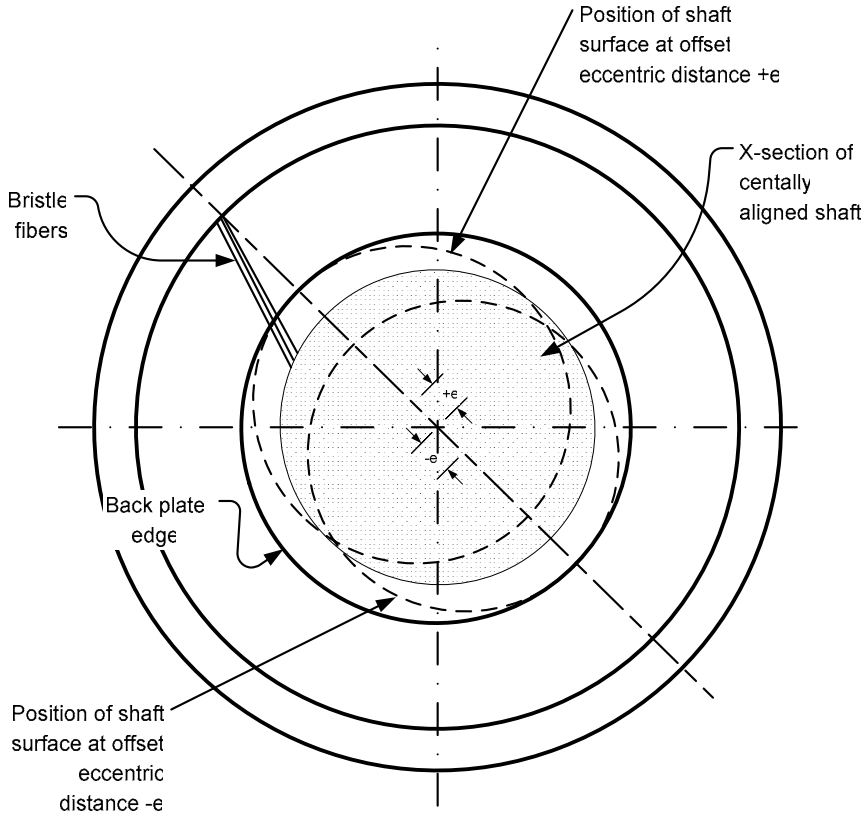

Figure 5

Eccentric movement of rotor and displacement of bristle pack

MARQUETTE UNIVERSITY

Numerical Results and Discussion

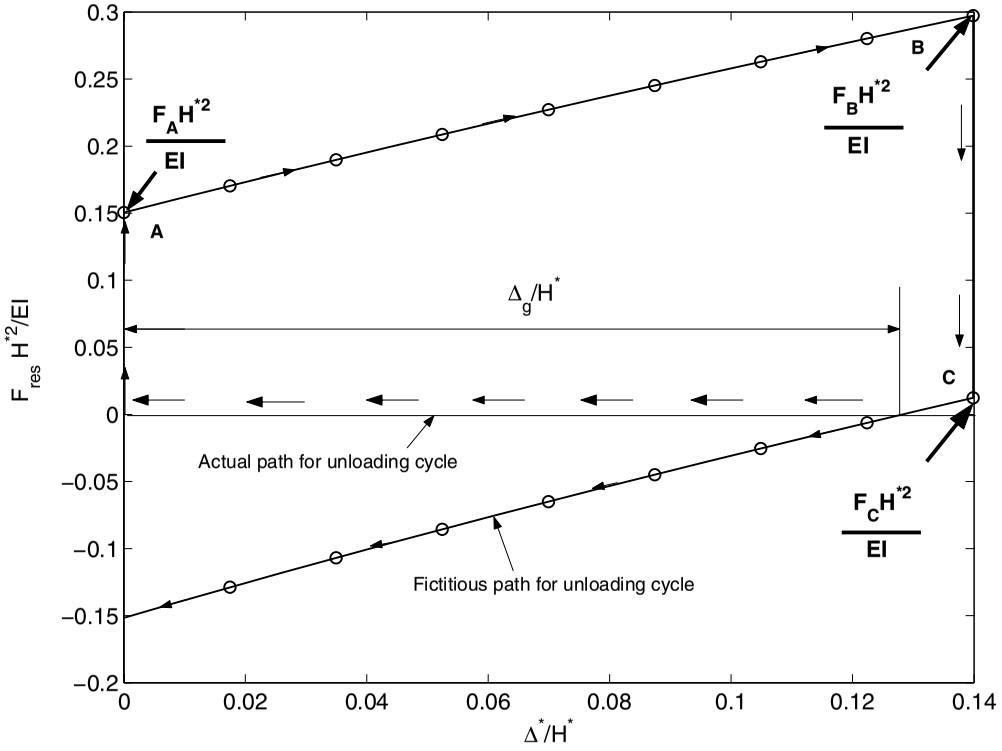

Figure 6

Relationship between $\frac{F_{res}H^{*2}}{EI}$ and $\frac{\Delta^*}{H^*}$ during loading and unloading Δ^* for a transition seal with $R_s/H^*=8.9$, $\theta=45^0$ and $\overline{m} = \frac{m^*H^{*2}}{EI}=0.135$.

Δ_g/H^* shows the position where fibers are "stuck", i.e., cannot completely recover from bending during unloading Δ^*

Numerical Results and Discussion (Cont'd)

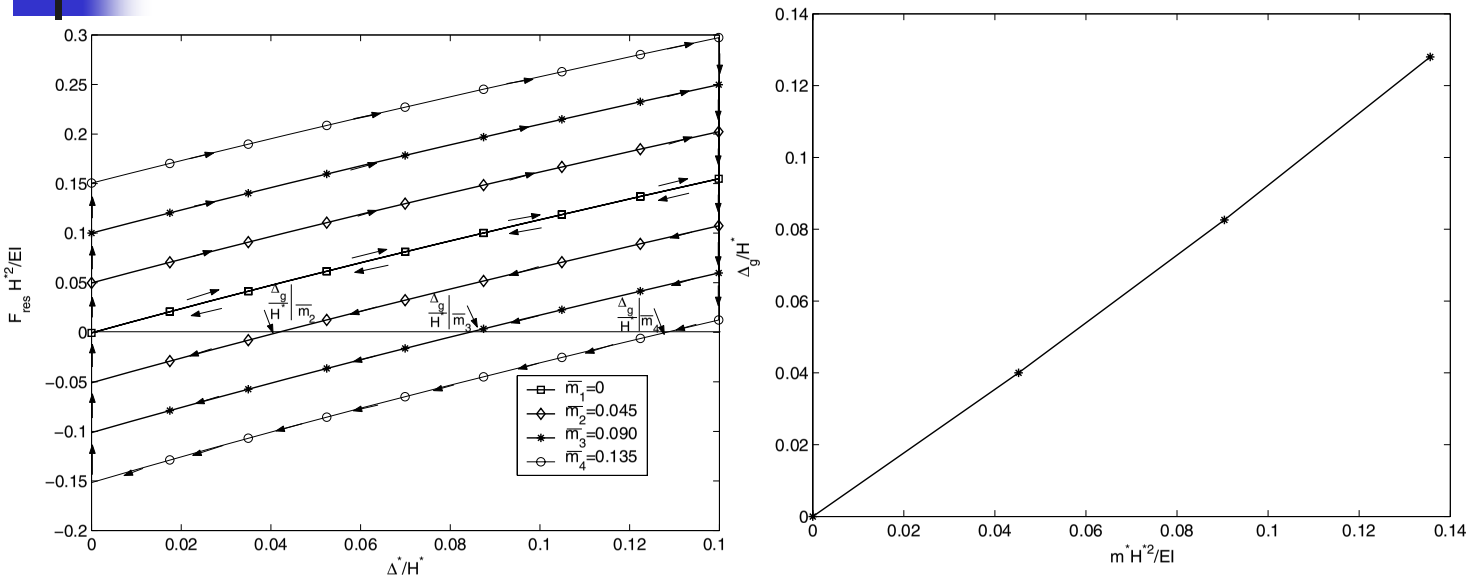

Figure 7 (a) Relationship between dimensionless contact force and dimensionless penetration depth for $\overline{m}$ =0, 0.045, 0.090, 0.135. (Results shown are for R_s/H^*=8.9, θ=45°; (b) relationship between Δ_g/H^* and non-dimensional bending moment $\overline{m}$

Numerical Results and Discussion (Cont'd)

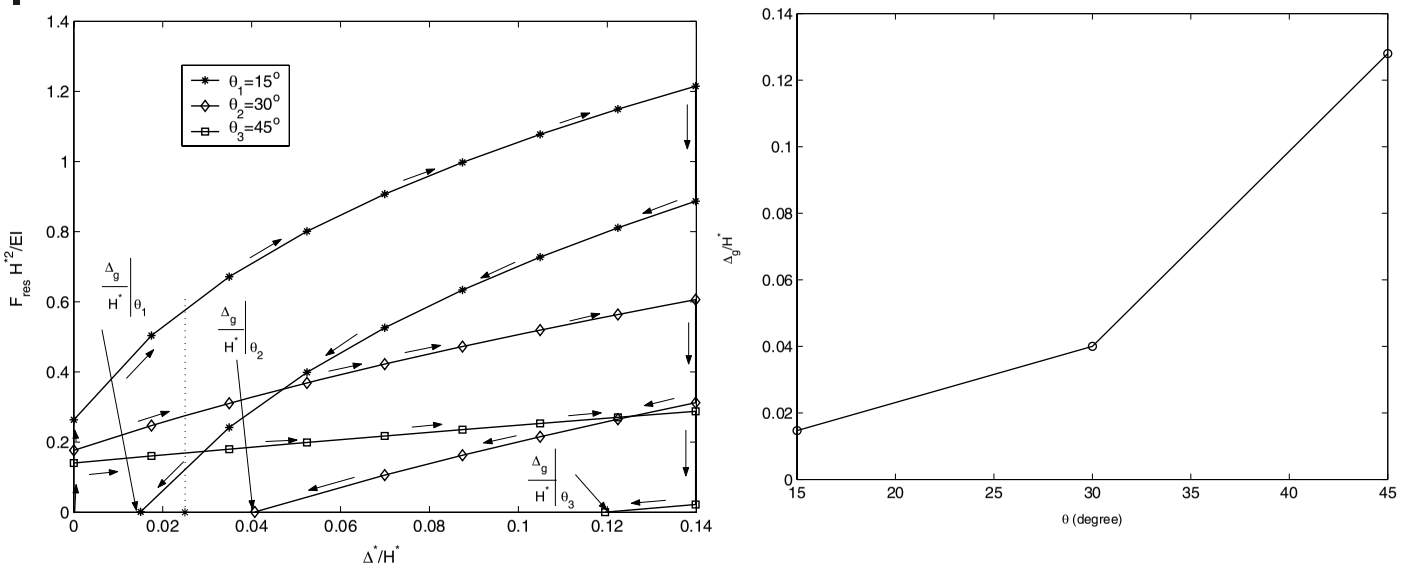

Figure 8 (a) Relationship between dimensionless contact force and dimensionless penetration depth for θ=15, 30 and 45 degrees. (Results shown are for a bristle with R_s/H^*=8.9, Δ^*_o=0, $\overline{m}$ =0.135) and (b) Relationship between Δ_g/H^* and bristle lay angle θ

MARQUETTE UNIVERSITY

Conclusions/Summary

- The micro-moment can give rise to a delayed filament displacement as the shaft undergoes transient excursion and moves radially toward bristle pack (uploading).
- However, as the shaft returns back to its concentric position (downloading), the filament CANNOT completely recover from its deformed position and remains locked in an alternate configuration.
- Consequently, an annular gap is generated between the fiber tips and shaft surface, which promotes brush seal leakage and reduces turbo-machinery performance.

Conclusions/Summary (cont'd)

MARQUETTE UNIVERSITY

- In general, for a given brush seal, the annular gap increases linearly as the micro moment m* is increased.

- The brush seal having a shallowest lay angle (15^{o}) results in the smallest annular gap, indicating that a brush seal design with shallow lay angle is least prone to hysteresis phenomenon, and can lead to improved performance.

DOE/PG&E LNG-TURBOEXPANDER SEAL AND BEARING RETROFIT

Donald E. Bently, Dean W. Mathis, and G. Richard Thomas
Bently Pressurized Bearing Company
Minden, Nevada

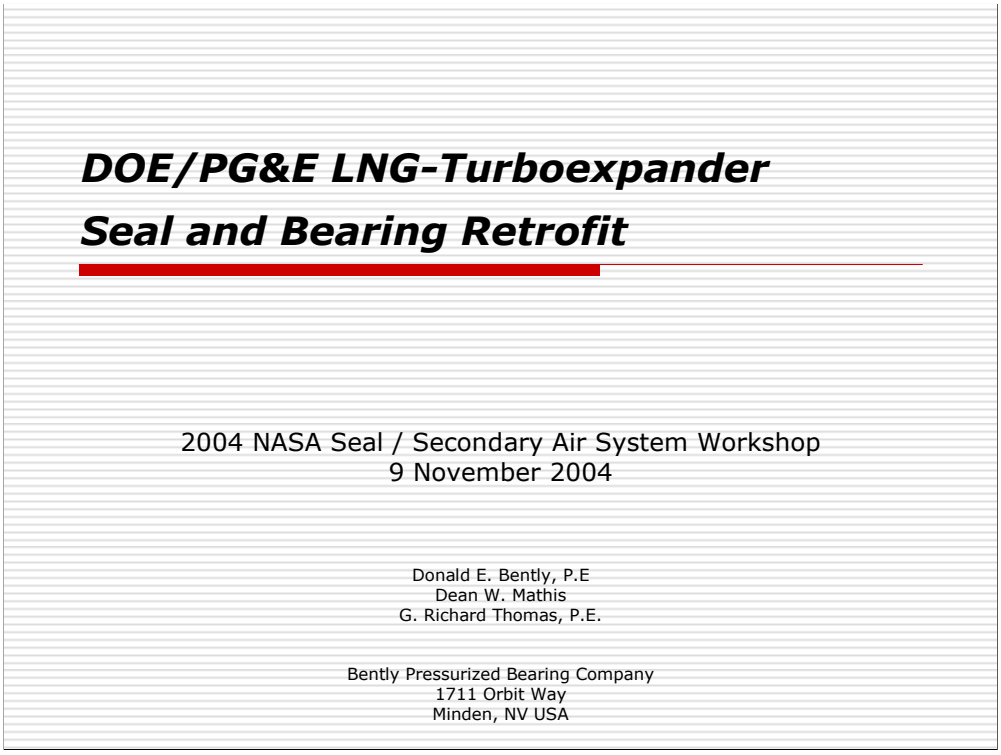

DOE/PG&E LNG-Turboexpander Seal and Bearing Retrofit

2004 NASA Seal / Secondary Air System Workshop
9 November 2004

Donald E. Bently, P.E
Dean W. Mathis
G. Richard Thomas, P.E.

Bently Pressurized Bearing Company
1711 Orbit Way
Minden, NV USA

The U.S. Department of Energy (DOE), the Idaho National Engineering and Environmental Laboratories (INEEL), and Pacific Gas & Electric (PG&E) have been involved in the development of new technologies to produce liquefied natural gas (LNG) for diverse consumer use at a PG&E facility in Sacramento, California. Their goal is to establish packaged LNG facilities at/near conventional high-pressure natural gas letdown stations where high-pressure (750 to 900 psig) pipeline gas is throttled to distribution pressures of 50 to 60 psi.

Typically, in the past, this throttling process was achieved via pressure regulation valves. The new technology utilizes a turboexpander as the pressure throttling device. The turboexpander consists of a single stage radial inflow expansion turbine wheel on end of the shaft and a centrifugal compressor wheel on the other end of the shaft, in a conventional, double overhung arrangement. The benefit of the new process is to recover the energy of expanding pipeline gas from 750 psig to 60 psig, while at the same time recompressing a portion of the pipeline gas.

Initially, the turboexpander was delivered with shaft contacting brush seals behind both wheels, 17-4 PH shaft material, and two combination radial/thrust magnetic bearings. INEEL and PG&E worked with the turboexpander OEM from early 2002 through March 2004, unsuccessfully trying to commission the turboexpander. Due to stability issues, the turboexpander could not operate above 55 to 60,000 rpm. Required design speed is 70,000 rpm.

In late March 2004, Bently Pressurized Bearing Company was asked to solve the stability issue.

This was accomplished by modifying:

- the existing shaft seal design, replacing the originally supplied brush seals with labyrinth seals (reduction in both axial loading and destabilizing tangential forces)
- the existing shaft material to a titanium alloy (12 percent gain in stability margin)
- the combination radial/thrust bearing design from magnetic bearings to pressurized gas bearings (increase in load carrying capability and stiffness with significant improvement in damping). The pressurized gas radial/thrust bearings utilizing the high pressure pipeline gas (methane) as the pressure source (425 psi) for the bearings and the gas distribution system as the low-pressure sink (60 psi) for the bearings.

This presentation documents the:

- operating characteristics of the turboexpander as originally supplied from the OEM with brush seals, 17-4 PH shaft material, and magnetic bearings,
- the design modifications made to the turboexpander,
- operating characteristics of the turboexpander with the modified labyrinth seals, titanium alloy shaft material, and pressurized radial and thrust gas(methane) bearings.

The turboexpander now successfully and continually operates at 70,000 rpm.

Project Definition

- The US Department of Energy (DOE), the Idaho National Engineering and Environmental Laboratories (INEEL), and Pacific Gas & Electric (PG&E) have developed new technologies to produce liquefied natural gas (LNG) for diverse consumer use.
- The goal is to establish packaged LNG facilities at / near conventional high-pressure natural gas letdown stations where the high-pressure (750 psig) pipeline gas is throttled to distribution pressure of 50 to 60 psi.
- The turboexpander consists of an expansion turbine stage on end of a shaft and a centrifugal compressor stage on the other end of the shaft, in a double overhung arrangement.
- The benefit of the new process is to recover the energy of expanding pipeline gas from 750 psig to 60 psig, while at the same time re-compressing a portion of the pipeline gas.

Project Definition

- Original turboexpander design:
  - Brush shaft seals - expander and compressor wheels
  - Combination radial / thrust magnetic bearings
  - 17-4 PH shaft material
  - Large Keyphasor hole / crude balancing
  - 85,000 rpm design speed
    - 667 ft/sec (455 mph) journal surface velocity
    - 450 ft/sec ≈typical maximum for most industrial turbomachinery

- Turboexpander failed to operate satisfactorily during previous two years of field testing (Jan 2002 – March 2004).
  - Unacceptable seal leakage and thrust loading
    - 300 ft/sec surface velocity
  - Lack of both radial and thrust load carrying capability of the magnetic bearings
  - Magnetic bearing control system instability
  - Inability of magnetic bearings to operate above 55-60,000 rpm

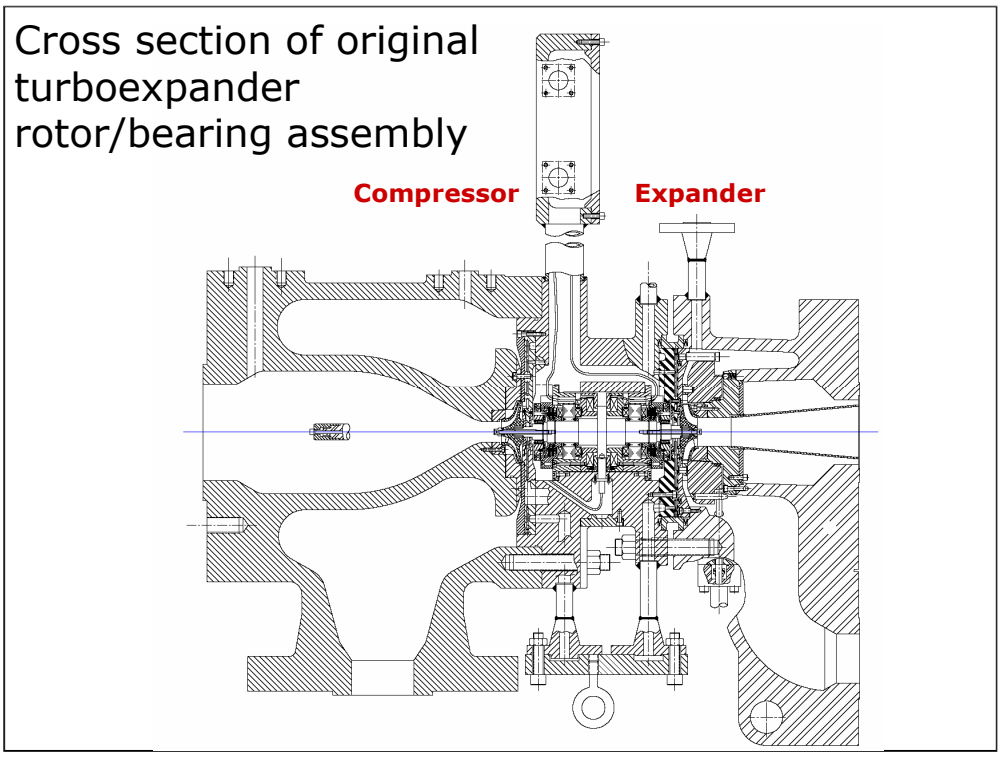

Overall cross section of turboexpander. Original configuration with magnetic radial/thrust bearings, rolling element catcher bearings, brush type shaft end seals.

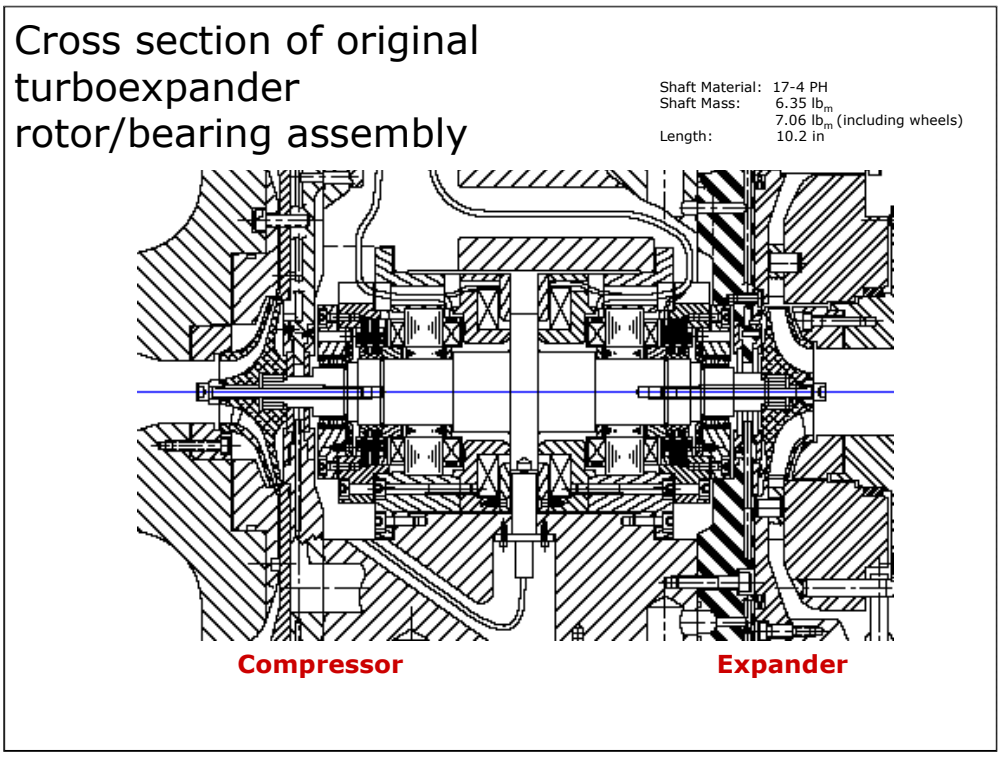

Overall cross section of turboexpander. Original configuration with magnetic radial/thrust bearings, rolling element catcher bearings, brush type shaft end seals. Note that original shaft material is 17-4 PH hardened steel.

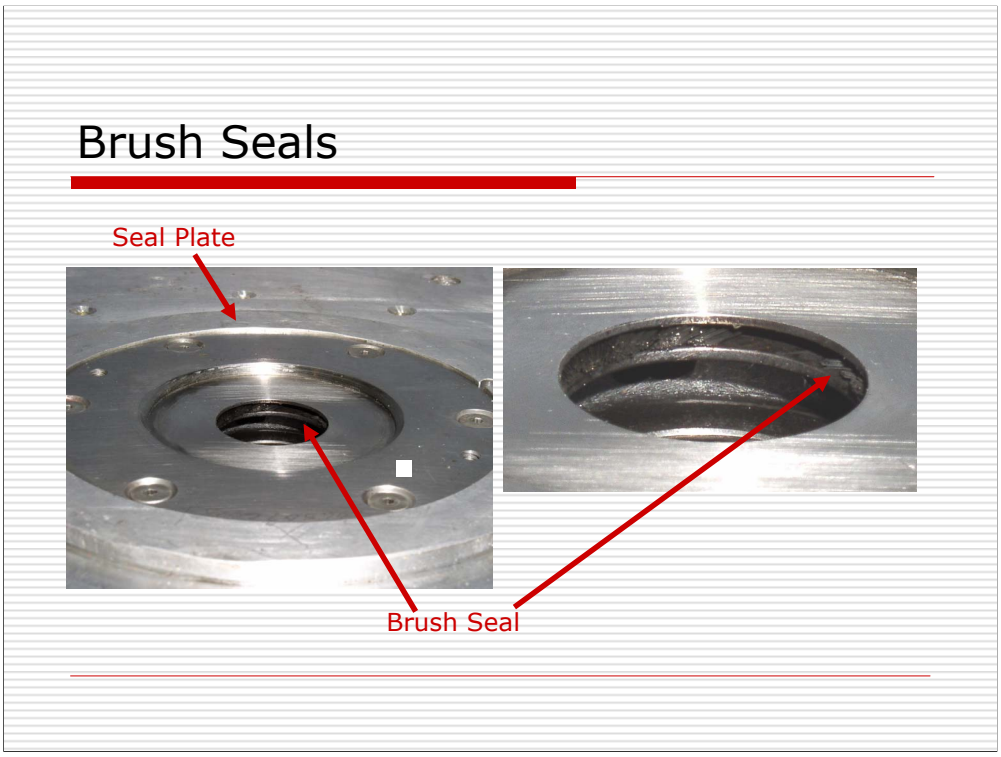

Original design shaft end seals – radial brush seal design

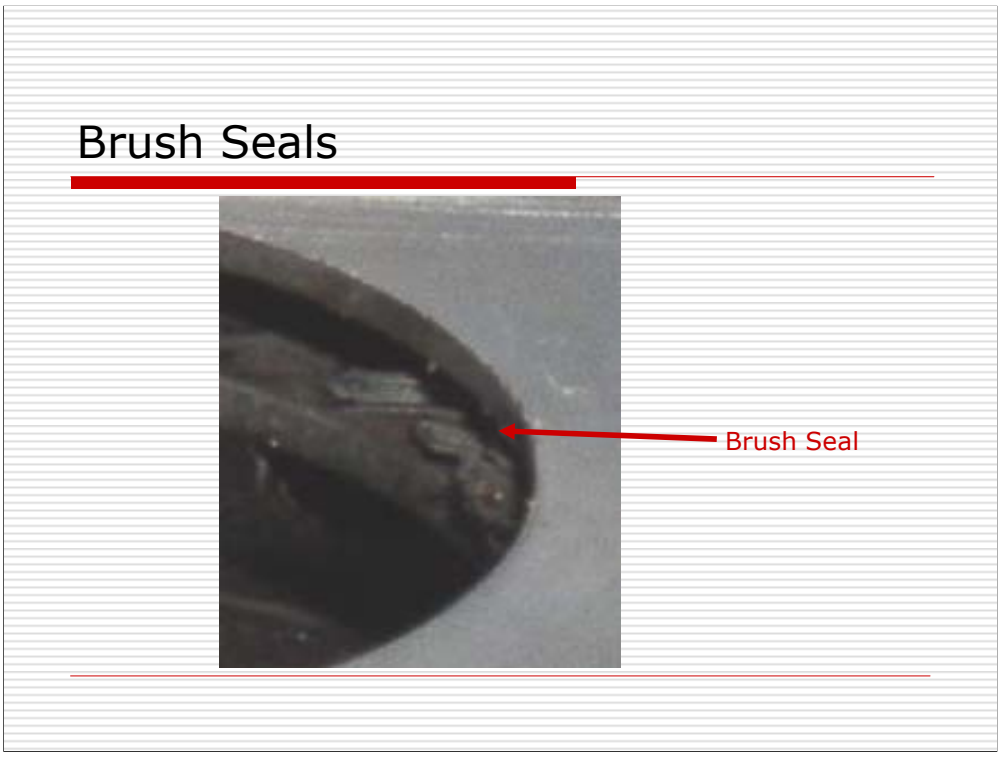

Original design shaft end seal – radial brush seal design. This particular seal is one of several that failed during operation – potentially due to surface velocities and diff pressure across the seal.

Revised turboexpander seal geometry

Original shaft end seal design replaced with multi tooth labyrinth seals. Laby seals also included axial steps or swirl brakes.

Revised turboexpander shaft geometry

Redesigned shaft: Ti Alloy, internal magnetic once per turn speed reference, WC-C PVD coating

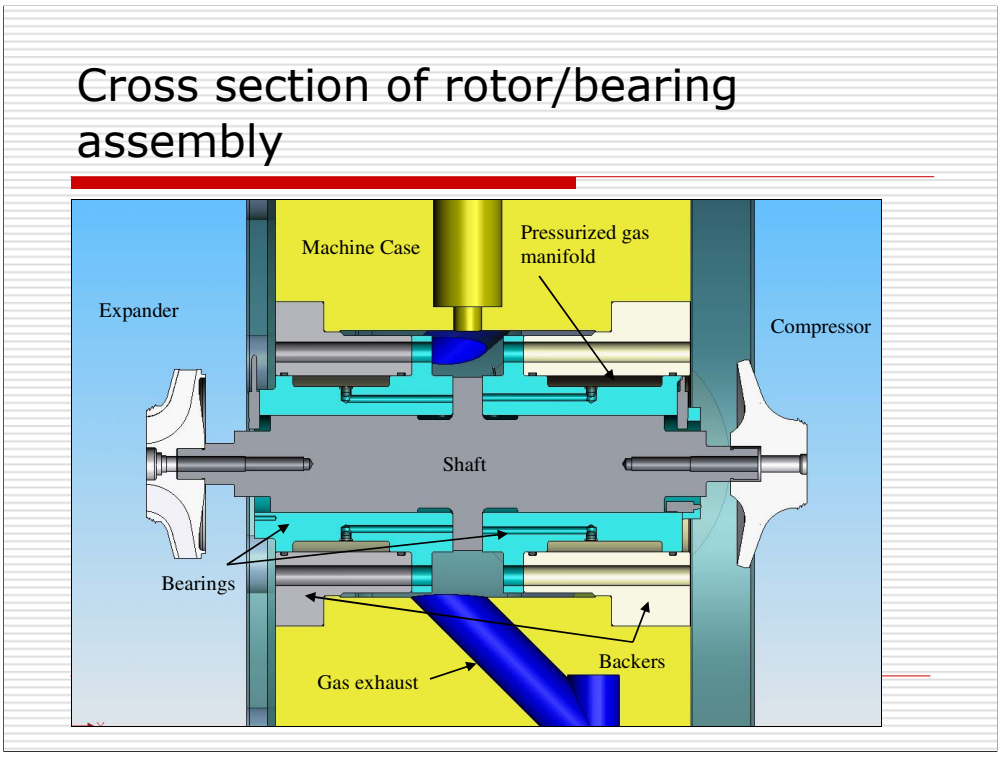

Cross section of turboexpander with replacement externally pressurized gas bearings, laby seals, and new shaft installed

Bearing Geometry and Features

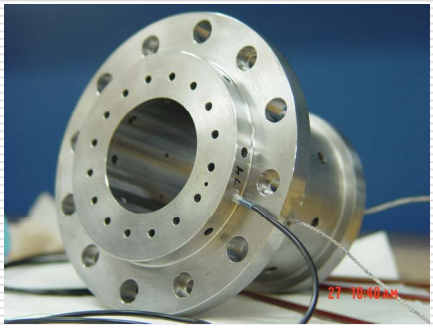

Bearing

Bearing and Backer

Left picture is the bearing itself

Right picture shows the bearing installed in the backer which was utilized to adopt the bearing geometry into the existing turboexpancer casing. Oval port w/O-Ring groove is gas inlet port. O-ring used to seal the backer to the casing.

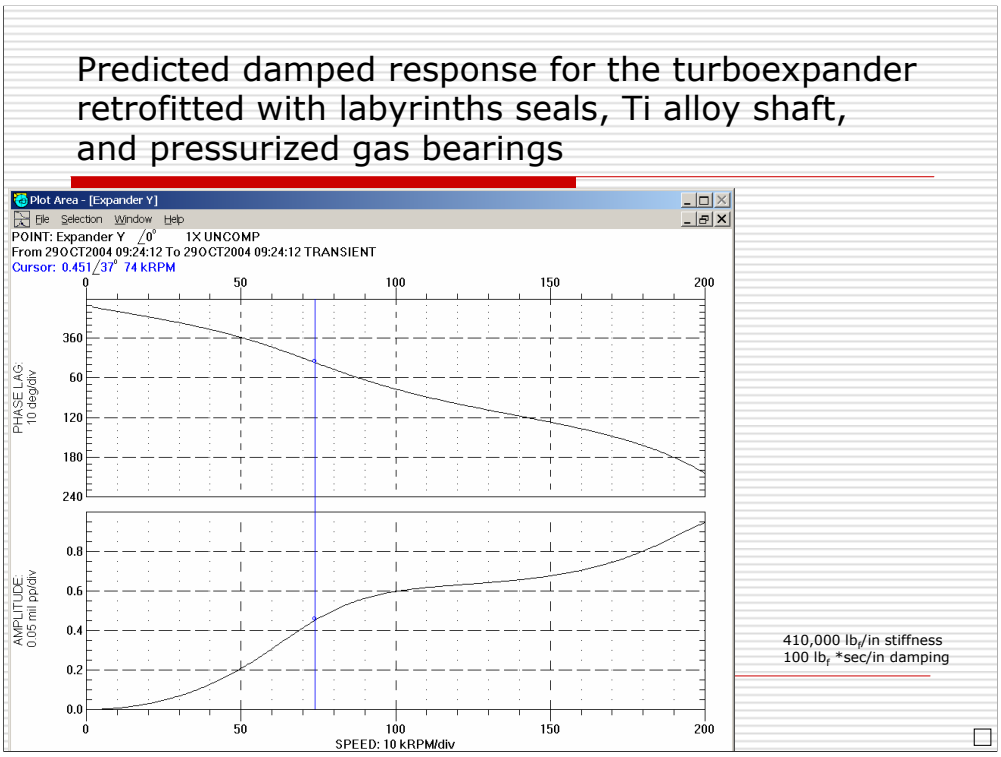

Predicted damped response, from finite element model, of the turboexpander rotor startup utilizing the new laby seals, new externally pressurized gas bearings, and redesigned Ti Alloy shaft.

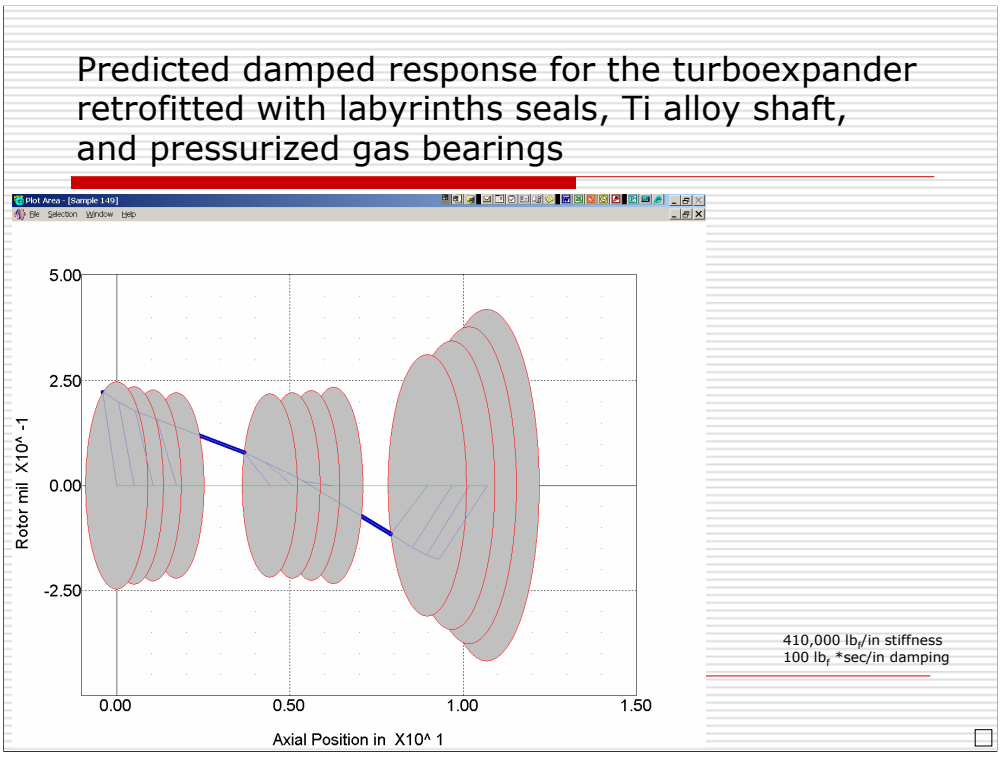

Predicted damped response, from finite element model, of the turboexpander rotor startup utilizing the new laby seals, new externally pressurized gas bearings, and redesigned Ti Alloy shaft.

Based on known residual unbalance in the impellers, vibration response was predicted to be 70-90 degrees out of phase with the expander end leading.

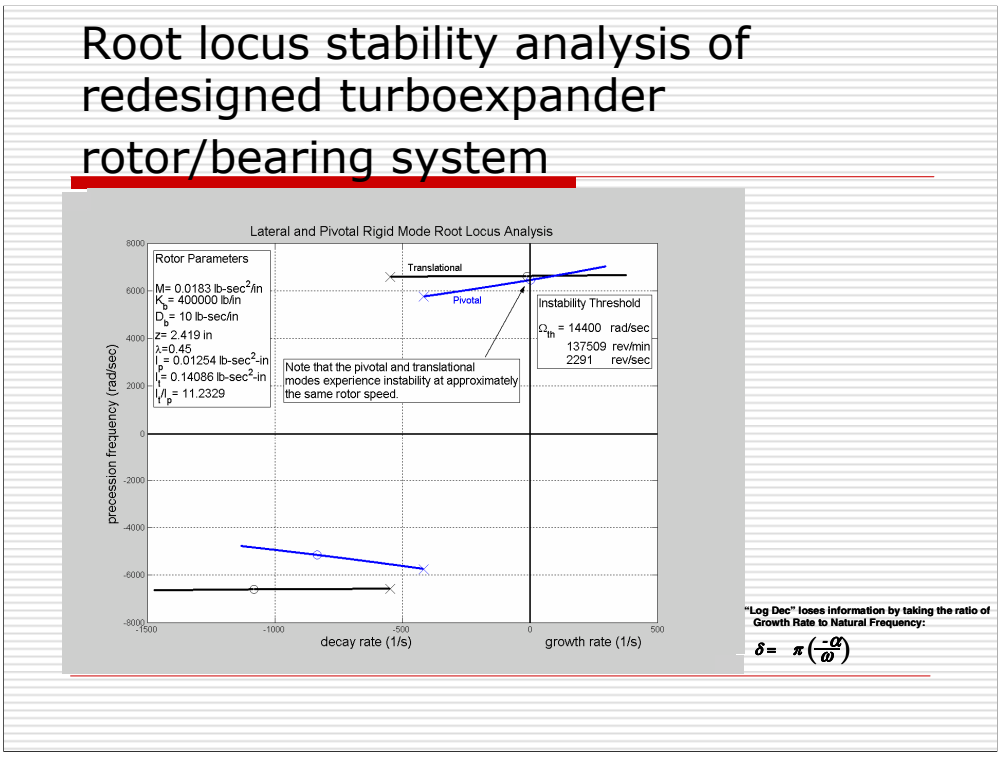

Predicted Stability analysis via Root Locus methodology – predicted stable to 137,000 rpm, discounting aerodynamic effects

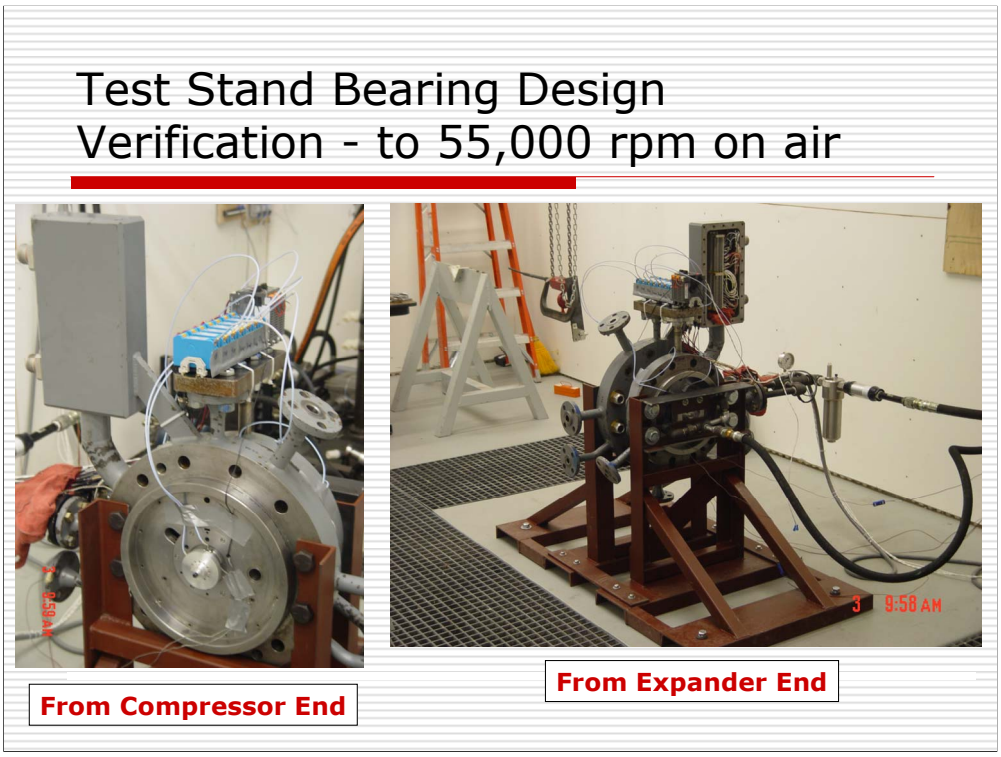

Rotor run up in externally pressurized gas (air) bearings at Bently Pressurized Bearing Company test stand – to 55,000 rpm

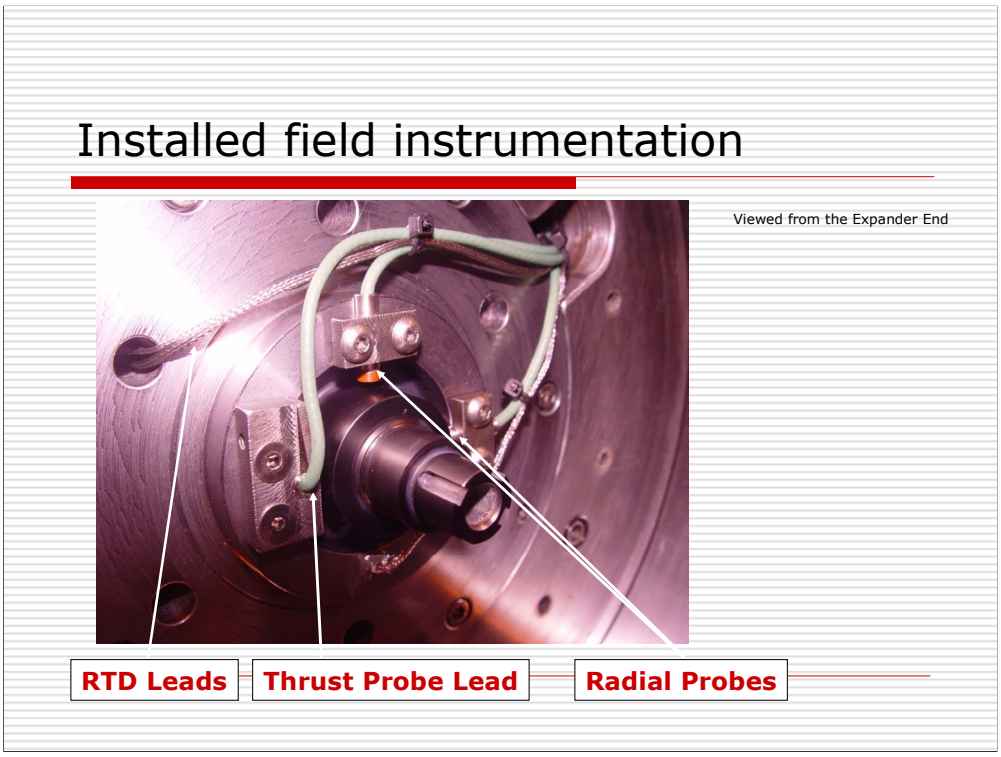

Field commissioning: expander end instrumentation

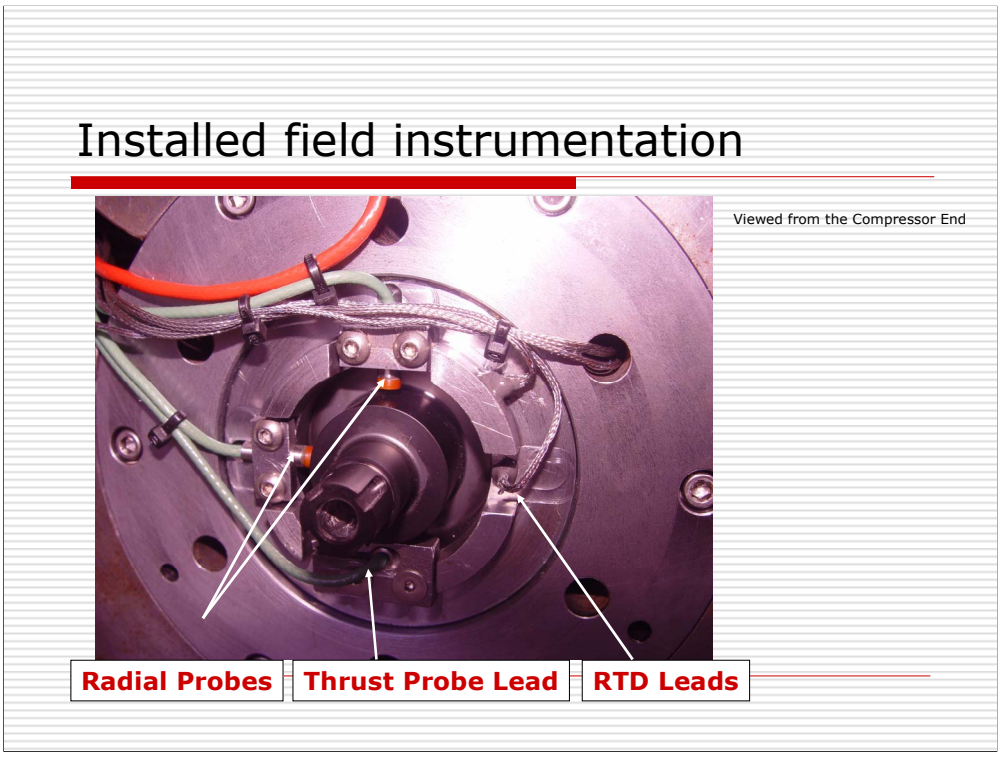

Field commissioning: compressor end instrumentation

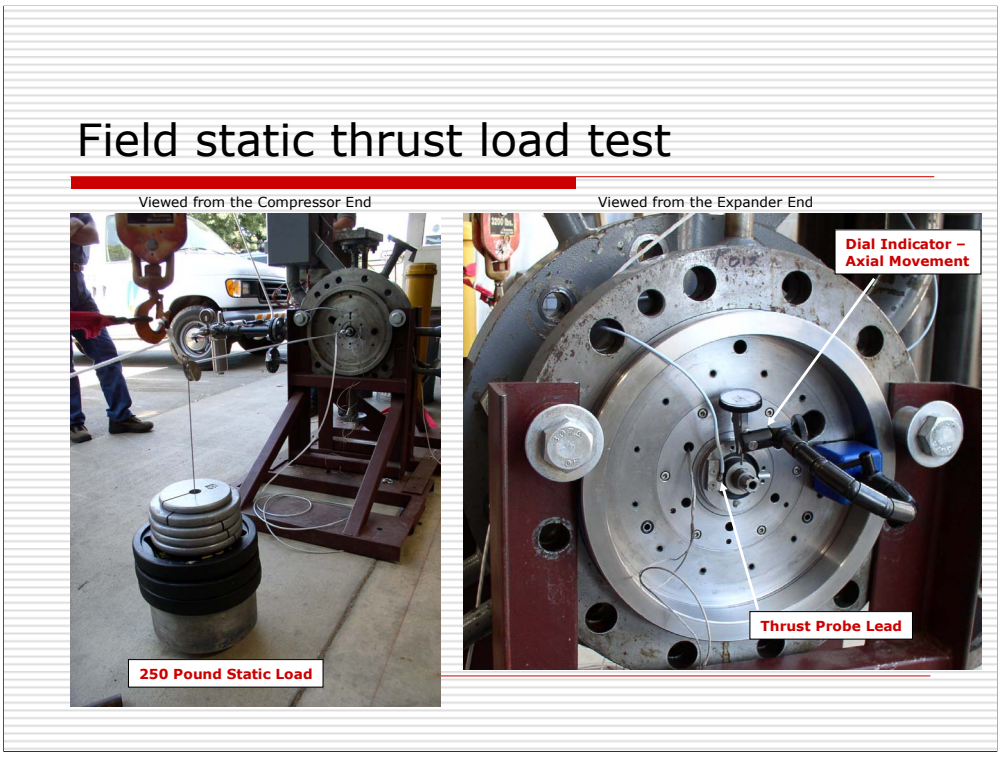

250 lb static thrust load test – radial and thrust bearings pressurized with 450 psig air

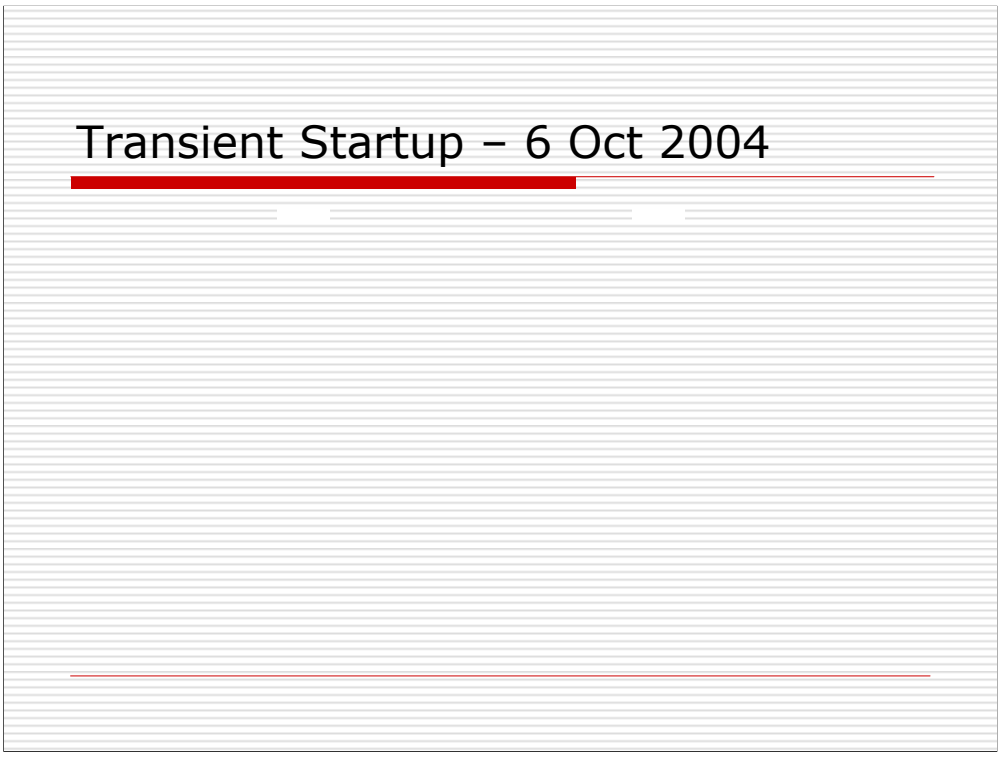
Transient Startup – 6 Oct 2004

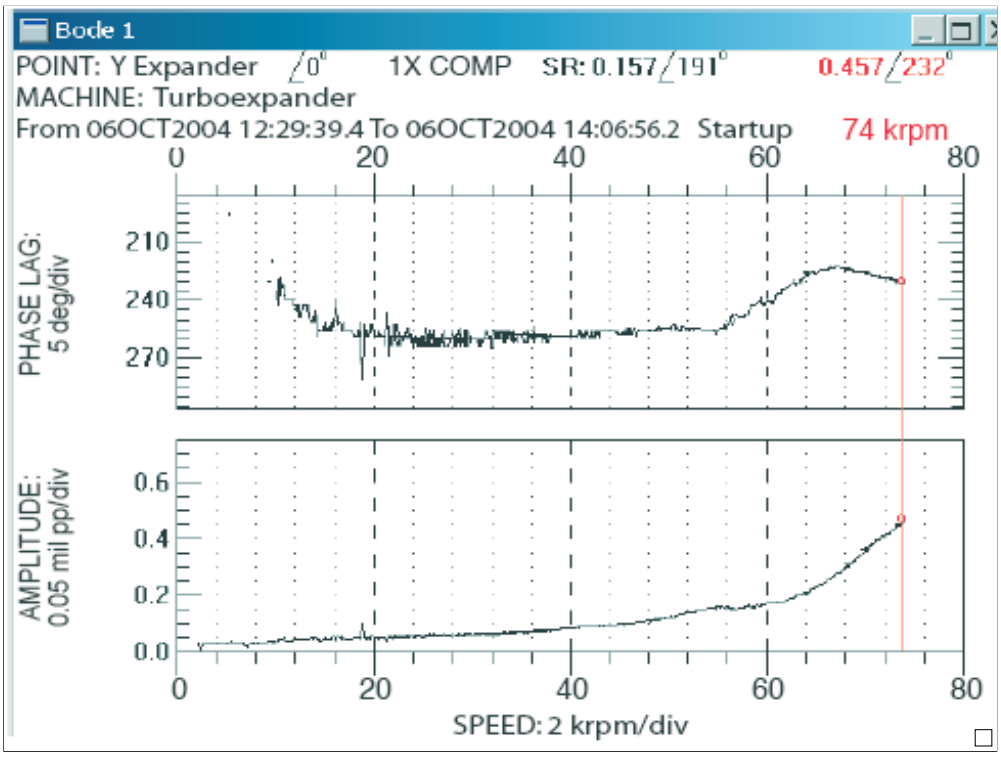

1X startup data – Bode plot

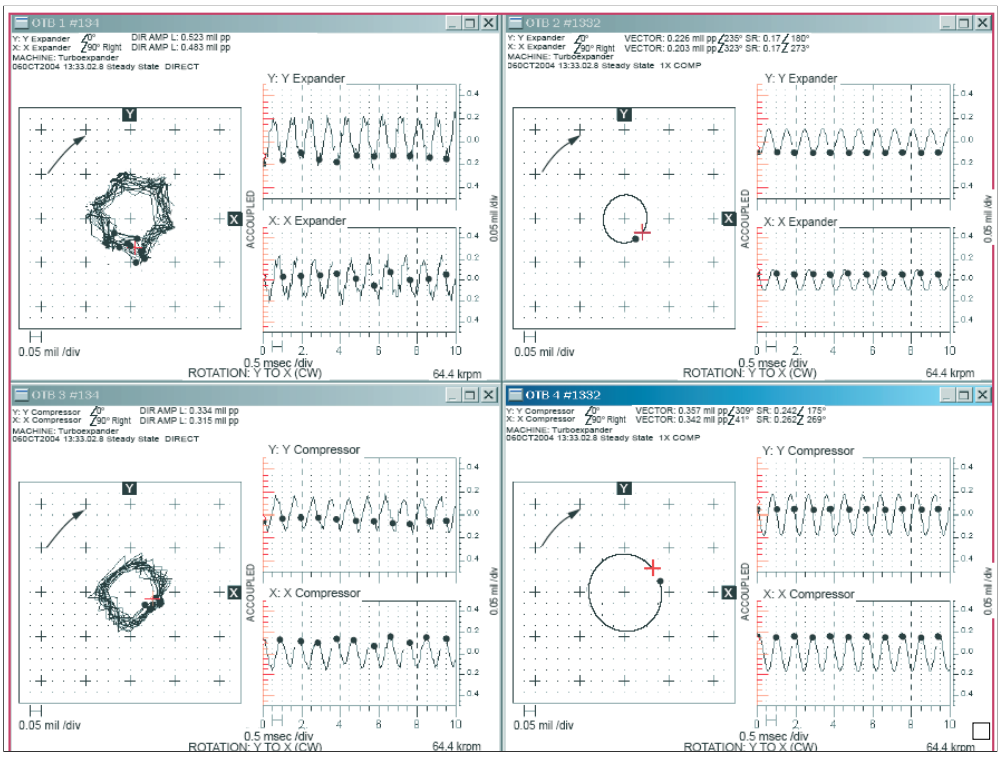

Direct and 1X shaft relative orbit plots from expander and compressor end.

Note that expander 1X phase leads compressor 1X phase by 74 deg and that compressor response is 33% larger than expander end. Refer back to predicted response on slide 13. Very good agreement between predicted and actual response.

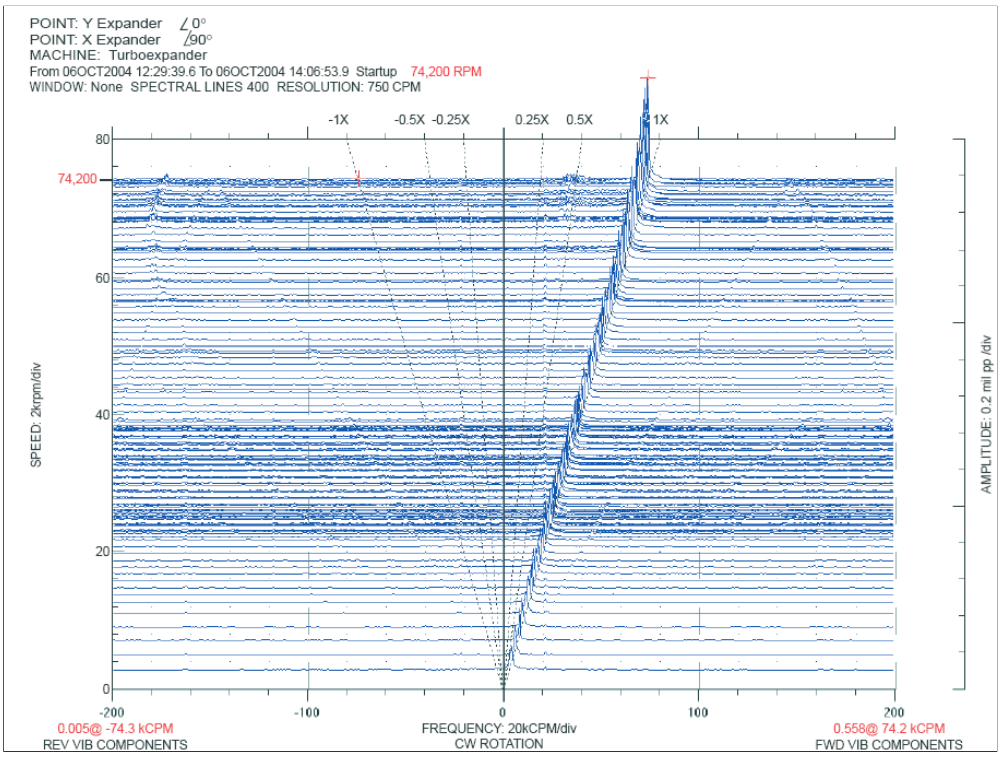

Full spectrum from expander end xy shaft relative probes, shows forward and reverse vibration frequencies up to 74,200 rpm. Response is all forward 1X, circular, symmetric response as would be expected from the externally pressurized gas bearings.

Thank You

- Questions?

ADVANCED DOCKING/BERTHING SYSTEM

Brandan Robertson
National Aeronautics and Space Administration
Johnson Space Center
Houston, Texas

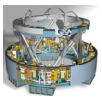

Advanced Docking/Berthing System
NASA Seal Workshop
GRC

November 9-10, 2004

Brandan Robertson, NASA-JSC/ES5 281-483-3732, Houston, TX

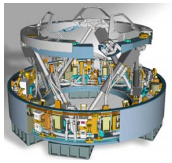

Outline

- Background
- Future Program Needs
- Existing Systems
- Status
- Advanced Docking/Berthing System (ADBS) Overview
- Key Seal Requirements
- Early Seal Development Work

Brandan Robertson, NASA-JSC/ES5 281-483-3732, Houston, TX

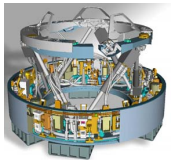

Background

Berthing refers to mating operations where an inactive module/vehicle is placed into the mating interface using a Remote Manipulator System-RMS.

Docking refers to mating operations where an active vehicle flies into the mating interface under its own power.

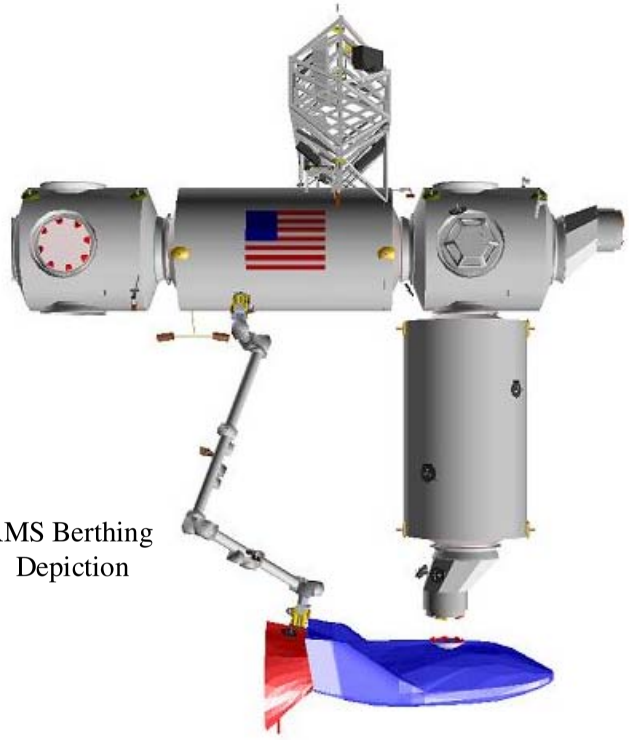

RMS Berthing Depiction

Brandan Robertson, NASA-JSC/ES5 281-483-3732, Houston, TX

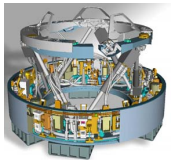

Future Needs

Future Mating System Capability Requirements:

- A system able to support a variety of missions: CTV/CEV/CRV, lunar gateway, Moon, and Mars
- Lightweight, fault tolerant system that blends well into vehicle OML (aero)
- Capable of autonomous rendezvous & docking
- Berthing capable for modular assembly and vehicle swap-out
- Software reconfigurable for a range of vehicles and operations
- Fast separation for rapid release
- Modular for maintenance and servicing
- Constellation safety & reliability goals
- Adaptable to ISS
- Crew and large cargo transfer
- Power, data, and fluid transfer
- Vehicle to vehicle mating (CRV-CTV-others) requires androgynous interface

Brandan Robertson, NASA-JSC/ES5 281-483-3732, Houston, TX

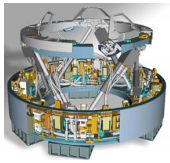

Existing Systems

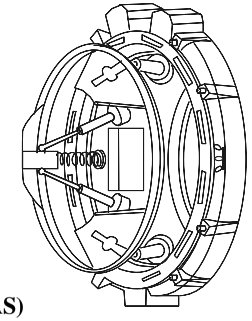

Androgynous Peripheral Docking System (APAS)
Weight: ~950 lbs (660 lbs APDA-6001 + 276 lbs avionics) (hatch not incl.)
Max OD: 69" dia
Hatch Pass Through: 31.38" dia
Source: JSC-26938, "Procurement Specification for the Androgynous Peripheral Docking System for the ISS Missions

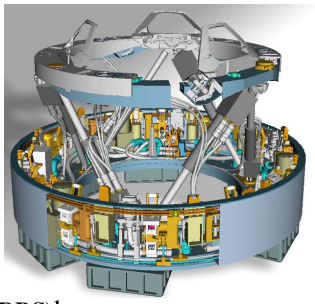

Advanced Docking/Berthing System (ADBS)[1]
Weight: est. 750 lbs (includes electronics & hatch)
Max OD: 54" dia
Hatch Pass Through: 31" dia
Source: X-38 Program Group

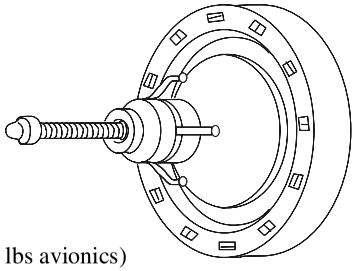

Russian Probe
Weight: 700 lbs (550 lbs cone + 150 lbs avionics)
Max OD: 61" dia
Hatch Pass Through: 31.5" dia (approximate)
Source: Energia

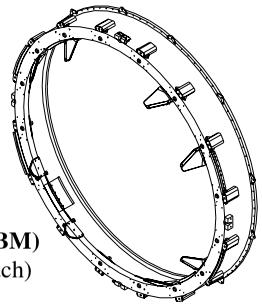

Passive Common Berthing Mechanism (PCBM)
Weight: 680 lbs[2] (440 lbs PCBM + 240 lbs hatch)
Hatch Pass Through: 50" square
Max OD: 86.3" dia
Source: SSP 41004, Part 1, "Common Berthing Mechanism to Pressurized Elements ICD" & SSP 41015, Part 1, Common Hatch & Mechanisms To Pressurized Elements ICD

[1]ADBS currently under development
[2]Bulkhead hatch ring structure not included

Brandan Robertson, NASA-JSC/ES5 281-483-3732, Houston, TX

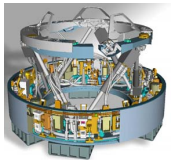

Existing Systems

Limitations of existing systems:

- Do not meet 2-fault tolerant, time-critical release requirement for crewed vehicles
  - APAS for Shuttle relies on 96 bolt EVA to meet 2nd fault tolerance
  - CBM powered bolts in nominal ops are not time critical and are single fault tolerant
- Unique active & passive halves: precludes vehicle-to-vehicle mating
- Do not support autonomous operations
  - No automatic mating of fluid, power (APAS does have a single power/data connector) and forced air umbilicals
  - CBM cannot mate to unmanned vehicles
- Standard ISS racks cannot pass through existing docking ports
- Significant velocities required to provide alignment & capture forces
- Crit-1 operations supported by intensive training & analysis
- High part count / mechanical complexity with single point failures (reliability and failure tolerance problems)
- Berthing mechanisms do not dock and docking mechanisms do not berth
- Russian systems are supplied by a foreign vendor with substantial economic concerns
  - Purchase of additional units banned by Iran Missile Proliferation Sanctions Act of 1997
  - Very limited access to engineering data
- Systems designed and/or certified for very few cycles and short exposure life

Brandan Robertson, NASA-JSC/ES5 281-483-3732, Houston, TX

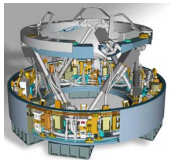

Current Status

Advanced Mating System Development Activities

- Exploration Systems Technology Maturation Program has selected advanced mating systems for continuation during the recent ICP activity.
- JSC has been developing an advanced mating system (ADBS) since 1996.
  - Originally intended for use on the X-38 project
  - Designed to support both berthing and docking operations and to provide future mission architecture flexibility (cross-cutting technology)
  - The current design baseline is a X-38-sized risk reduction unit (RRU)
    - Fully androgynous interface
    - Uses electromagnets and closed-loop force-feedback for soft-capture
    - Minimally sized for crew transfer
    - Fully integrated ground based system to show TRL 4 maturity
  - Work on Constellation scale system to begin as RRU matures
- Long-duration seal technology (seal-on-seal) has been identified as a current design gap.

Brandan Robertson, NASA-JSC/ES5 281-483-3732, Houston, TX

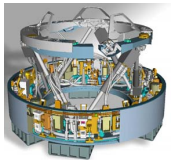

ADBS Overview

A Next-Generation Mating Mechanism

- Designed specifically to take advantage of modern electromechanical technology
- Incorporates the lessons learned and experiences from previous/current mating mechanism development and use
- Desensitizes mating mechanism operations and performance from other vehicle systems requirements
- Supports both docking and berthing operations
- Supports autonomous rendezvous & mating
- Aligned with NASA Strategic Plan

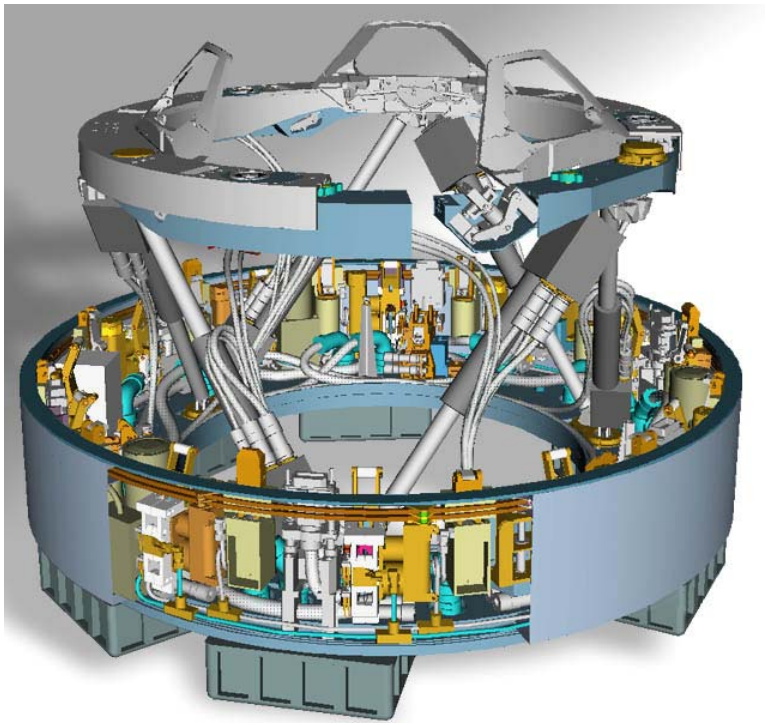

CAD Image

Interactive Overview

Brandan Robertson, NASA-JSC/ES5 281-483-3732, Houston, TX

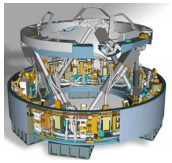

Key Seal Requirements

- Seal-on-seal interface
- Very low leak rate
- Long life
  - Long-duration exposed periods
  - Long-duration mated periods
  - Deep-space environments
  - May also be a potential for high mate/demate cycle life
- Redundancy

Brandan Robertson, NASA-JSC/ES5 281-483-3732, Houston, TX

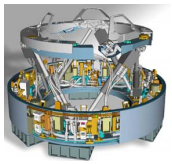

ADBS Seal Locations

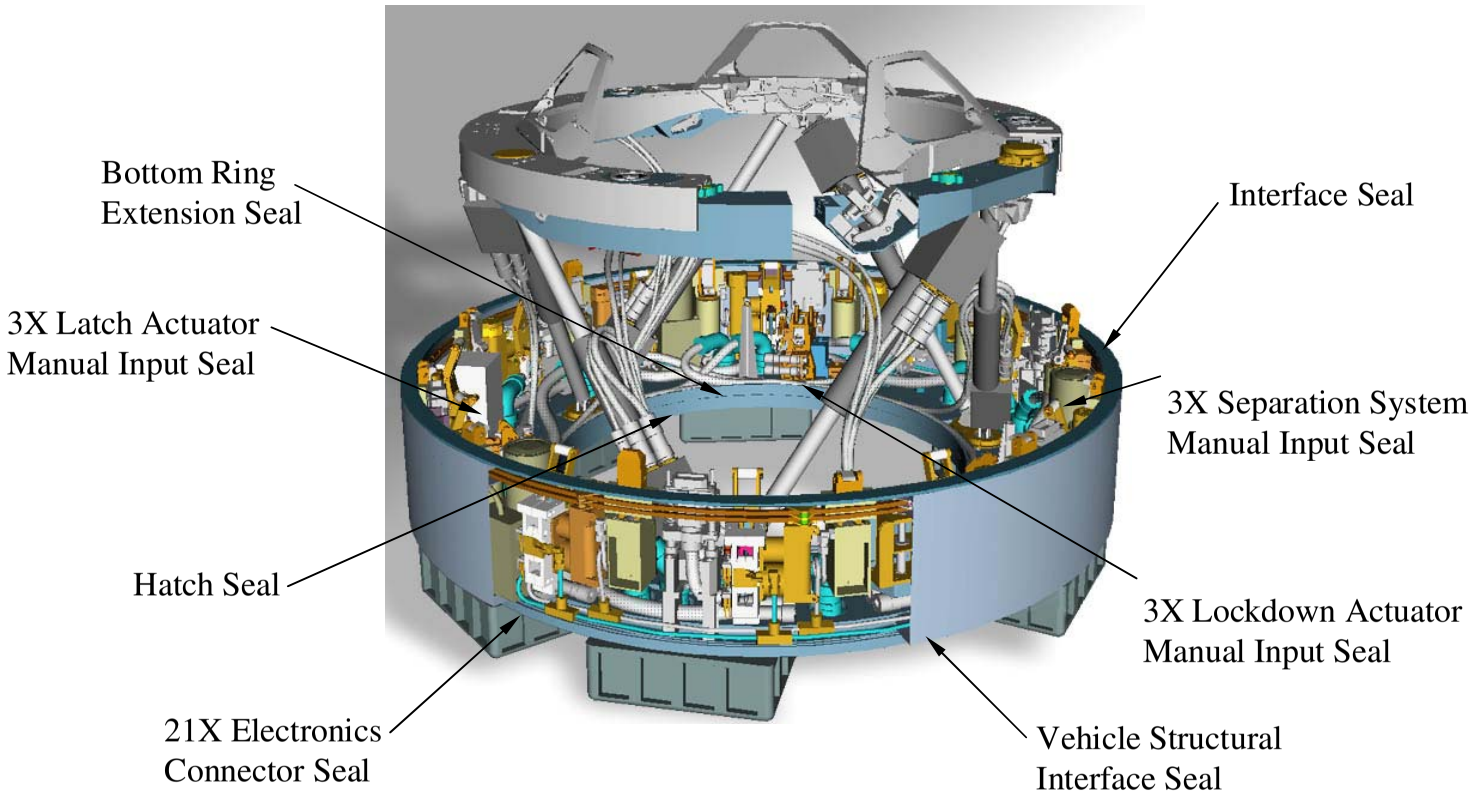

Brandan Robertson, NASA-JSC/ES5 281-483-3732, Houston, TX

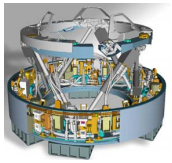

Early ADBS Seal Development

To preserve the fully androgynous design concept the seal design approach baselined was a seal-on-seal implementation similar to the Apollo Soyuz (ASTP) seals.

Subscale seal-on-seal elastomeric development with Parker Inc.

- Quick development and testing to evaluate seal-on-seal potential
- 2 cross-sections (flat top and elliptical) and 2 different durometer silicon materials
- Helium leak testing and seal load force testing completed in July 2001
- Adhesion testing is ongoing

Test results

- Leak rates comparable to ISS CBM seals with offset of 0.050 inches and no gapping (~20 configurations tested)
- Compression force testing showed that “flat top” slightly higher than “elliptical” for the 70 durometer at (96 & 87 lb/in) and for the 50 durometer at (46 & 42 lb/in). Results indicated that seal-on-seal in the “acceptable” range for use.
- Adhesion test results pending; series of “buttons” molded from each material are currently mated and compressed for eventual separation and inspection at TBD regular intervals of time.

Brandan Robertson, NASA-JSC/ES5 281-483-3732, Houston, TX

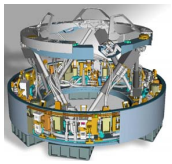

RRU Interface Seal Concept

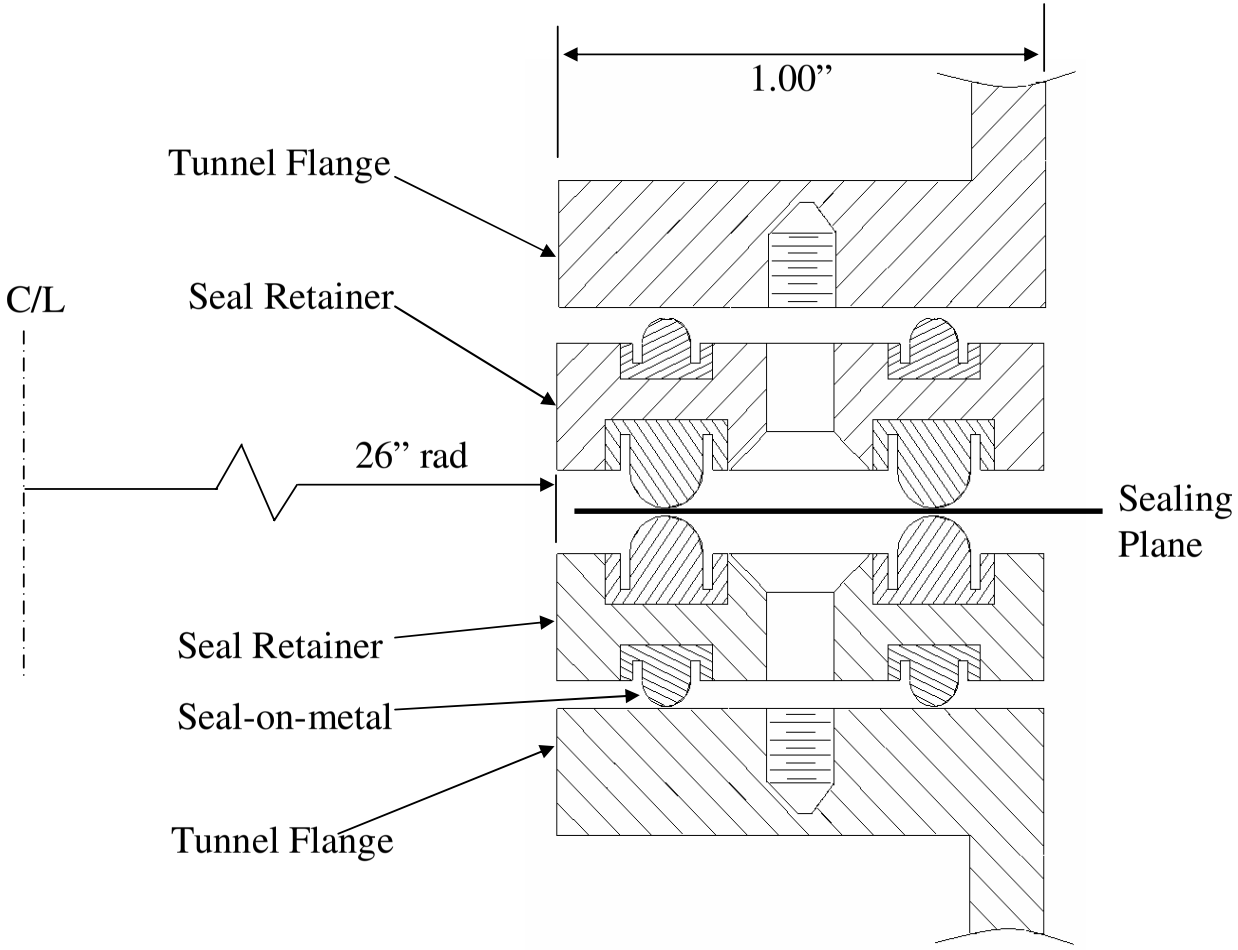

Brandan Robertson, NASA-JSC/ES5 281-483-3732, Houston, TX

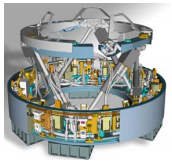

Early ADBS Seal Development

Conclusions

- No elastomeric seal-on-seal show stoppers yet

Forward work

- As soon as funding picture clears up, move forward with a full development seal purchase for the RRU
- Need to establish “the” baseline seal cross-section
  - Optimize seal to guarantee optimal sealing: percent of fill, squeeze, crown profile and height, if elastomeric
  - Establish total potential seal mismatch: misalignment, thermal expansion, flange deflection
  - Establish acceptable seal force and leak rate
- Determine if a single piece ~54” seal/retainer construction possible. Parker has indicated they do this now in a newly acquired facility.
- Evaluate concepts and results for full-scale Constellation implementation
  - Evaluate RRU design upward scaling
  - Are metallic seals a better solution?

Brandan Robertson, NASA-JSC/ES5 281-483-3732, Houston, TX

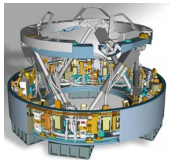

Backup Slides

Brandan Robertson, NASA-JSC/ES5 281-483-3732, Houston, TX

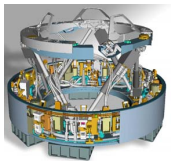

Existing System Seals

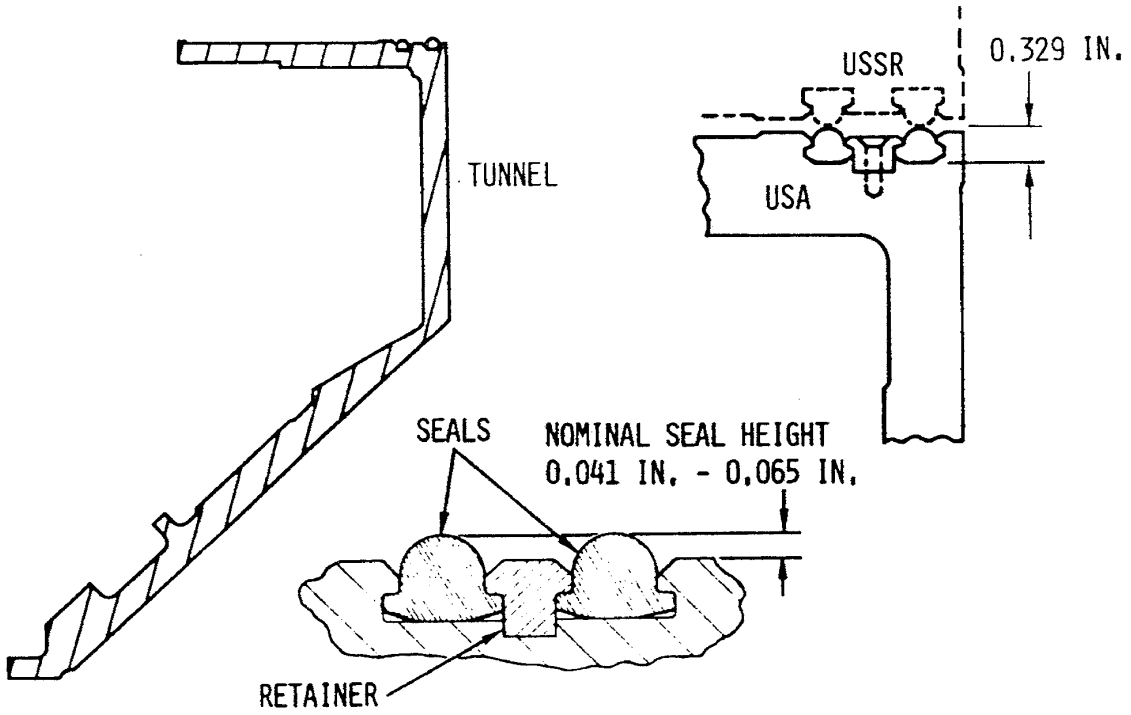

Apollo Soyuz Test Program
Docking System Interface Seal Diagram

Brandan Robertson, NASA-JSC/ES5 281-483-3732, Houston, TX

Page intentionally left blank

EVALUATION OF CERAMIC WAFER SEALS FOR FUTURE SPACE VEHICLE APPLICATIONS

Patrick H. Dunlap, Jr., and Bruce M. Steinetz
National Aeronautics and Space Administration
Glenn Research Center
Cleveland, Ohio

Jeffrey J. DeMange
University of Toledo
Toledo, Ohio

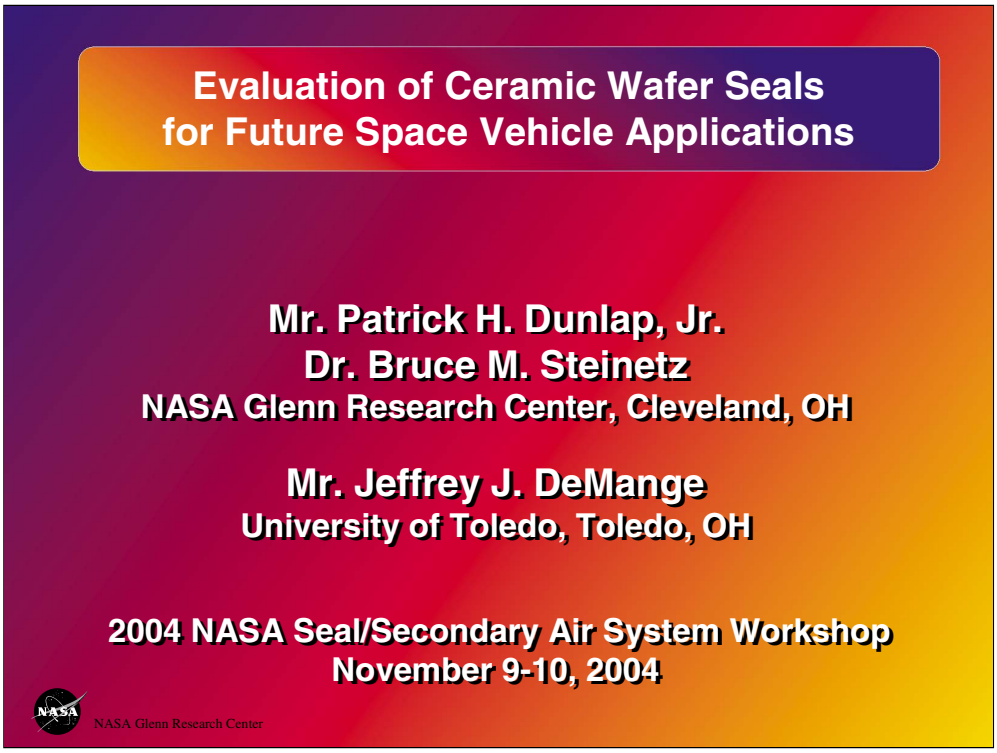

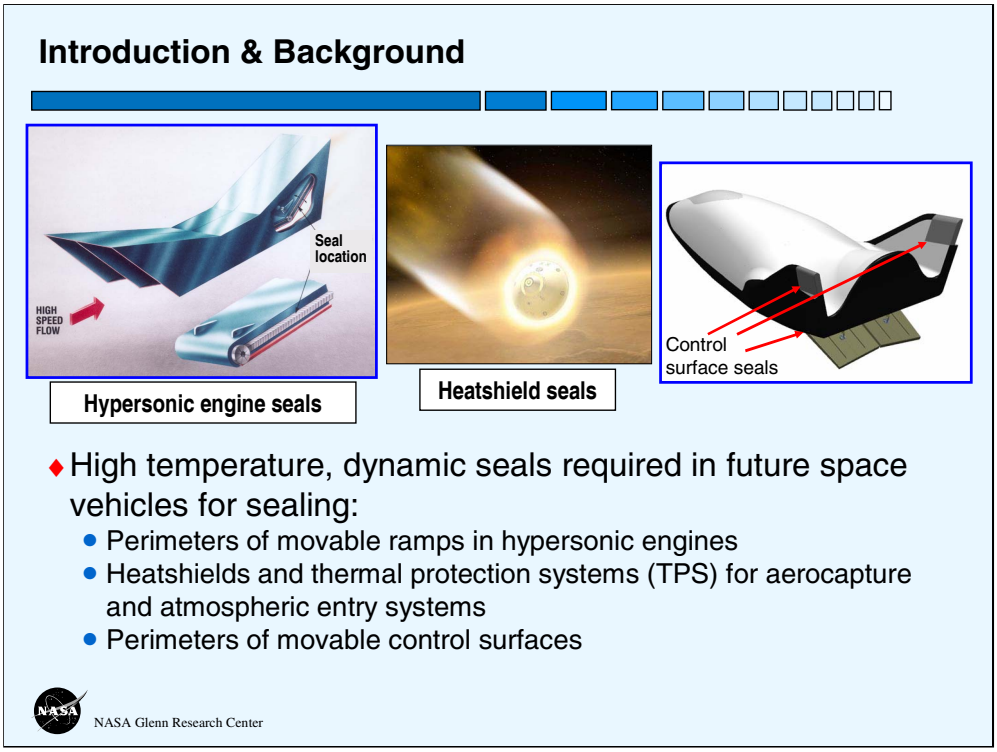

High temperature, dynamic structural seals are required in many different locations on future space vehicles. Seals are required in advanced hypersonic engines to seal the perimeters of movable engine ramps for efficient, safe operation in high heat flux environments at temperatures from 2000 to 2500 °F. High temperature seals are also required around heatshields and within thermal protection systems for aerocapture and atmospheric entry systems. If a winged vehicle is used as an entry system, seals would also be required around the perimeters of movable control surfaces on the vehicle.

Seal Challenges & Design Requirements

- Design requirements are demanding:
  - Restrict flow of hot gases at extreme temperatures
    - Propulsion system applications: Up to 2500 °F with high heat fluxes
    - Airframe applications:
      - 2100 °F for tile-based TPS
      - 2600+ °F for CMC systems
  - Seal against distorted/curved surfaces
  - Limit loads against sealing surfaces
  - Stay resilient for multiple load/heating cycles
  - Resist scrubbing damage
- Existing seals do not meet requirements

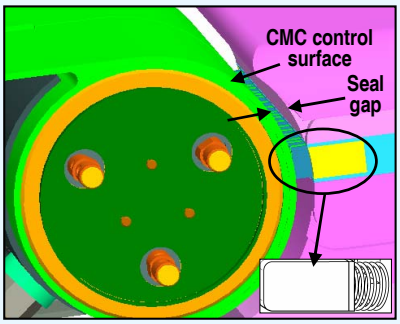

Goal: Develop sealing systems that meet these requirements and demonstrate performance in relevant environments

NASA Glenn Research Center

The design requirements for these seal applications are very demanding. The seals must restrict the flow of hot gases and survive at very extreme temperatures. For propulsion system applications, temperatures can reach 2500 °F in the presence of very high heat fluxes. For airframe applications, such as TPS and control surface seals, peak temperatures depend on the type of materials used in the structures surrounding the seals. If insulating tiles are used around the seals, temperatures can reach about 2100 °F. However, if hot structure ceramic matrix composite (CMC) materials are used, seal temperatures can reach 2600 °F or even hotter.

In addition to surviving at extreme temperatures, the seals must seal against distorted, curved surfaces while not applying excessive loads to those surfaces. The seals must remain resilient for multiple load cycles and heating cycles in order to stay in contact with the opposing sealing surface. These seals are used in dynamic applications in which the sealing surfaces move during each mission. Because these surfaces are often rough, the seals must be able to survive scrubbing against them without a large change in leakage performance.

Existing seals do not meet these challenging requirements, so the Seal Team at NASA GRC is developing sealing systems that do meet these requirements and demonstrating their performance in relevant environments.

Seal Specimens

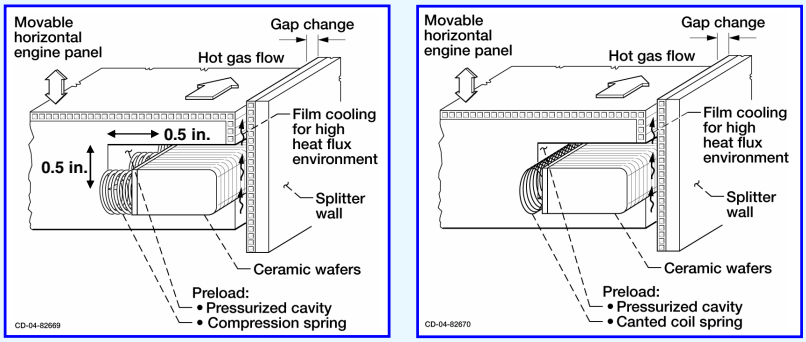

- Ceramic wafer seals originally developed during NASP program
- Preload device behind wafers maintains contact with sealing surface
- Current design:
  - Material: monolithic silicon nitride (Honeywell AS800)
  - Size: 0.5 in. wide x 0.92 in. long x 0.125 in. thick

NASA Glenn Research Center

The seals examined in this study were ceramic wafer seals that were originally developed during the NASP program. They are composed of a series of thin ceramic wafers installed in a channel in a movable panel and preloaded from behind to keep them in contact with the opposing sealing surface. Preload devices that have been considered for this application include helical compression springs and canted coil springs.

Materials that were evaluated for the wafer seals during the NASP program included a cold-pressed and sintered aluminum oxide, a sintered alpha-phase silicon carbide, a hot-isostatically-pressed silicon nitride, and a cold-pressed and sintered silicon nitride. A detailed analytical comparison of all the materials that were considered ranked the advanced silicon nitride ceramics as the most promising material for future consideration. Given that those tests were performed in the late 1980's, considerable improvements have been made since then to produce stronger and tougher ceramic materials. Because of these improvements and the high ranking of silicon nitride as a candidate wafer seal material, GRC selected silicon nitride as the best candidate for these seals. The wafers tested in the current study were made of monolithic silicon nitride (Honeywell AS800) and were 0.5-in. wide, 0.92-in. tall, and 0.125 in. thick. They had corner radii of 0.050 in.

Seal Preload Device Designs

- Goal: Provide ~0.1-in. stroke to keep seal in contact with sealing surface
- Silicon nitride compression springs
  - Commercially available
  - Potential for high temperature use (2000+°F)
  - Evaluated 2 designs:
    - Standard: 0.815 in. high x 0.520 in. diam.
    - Modified: 0.694 in. high x. 0.435 in. diam.
- Canted coil springs
  - Unique load vs. displacement curve provides nearly constant force over large range
  - Spring modeling and development to be discussed in other presentations

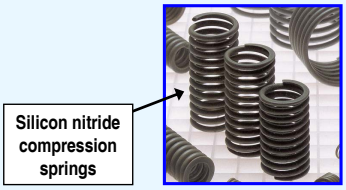

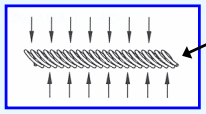

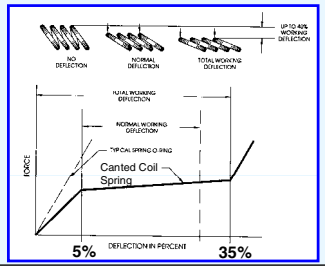

Large working deflection of canted coil spring

NASA Glenn Research Center

The high temperature seal preload devices that are being developed and evaluated would be installed behind the seals to ensure sealing contact with the opposing sealing surfaces. The requirements for these devices are also quite challenging as they must operate in the same environment and temperature as the seals. For the sealing applications being considered, the goal is to have the preload devices provide a stroke of about 0.1 in. to keep the seals in contact with their opposing sealing surfaces for multiple load and heating cycles.

Two types of preload devices have been focused on for these applications. The first type of device was a silicon nitride compression spring produced commercially by NHK Spring Co., Ltd. Because they are made of silicon nitride, these springs have the potential to be used as high temperature (2000+ °F) seal preloading devices. Two different designs were tested for the current study: a standard spring and a modified design. The main physical difference between these designs was that the standard design was larger than the modified design.

Canted coil springs have also been evaluated as part of this effort because of their unique load versus displacement curve that provides a nearly constant force over a relatively large deflection range. The Seal Team's efforts to develop and model these types of springs will be discussed in other presentations that follow this one.

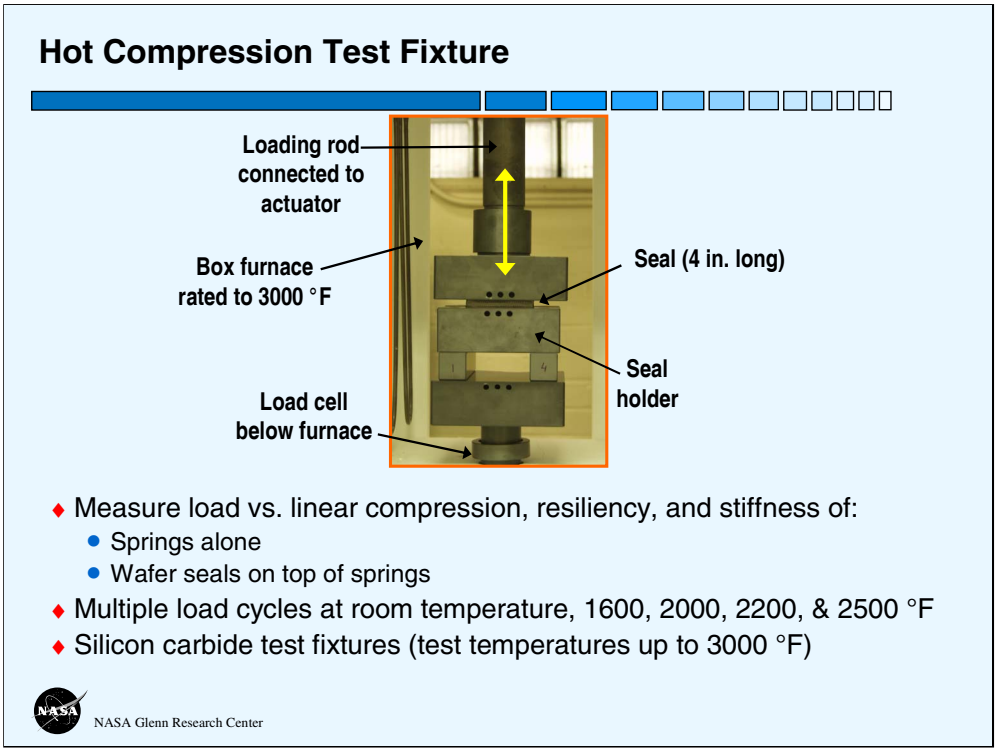

A series of hot compression tests were performed on the wafer seals and silicon nitride compression springs using GRC's hot compression test rig. Compression tests were performed inside a box furnace capable of 3000 °F using the test setup shown here. These tests were performed to determine the resiliency and stiffness of the springs by themselves and for the wafers on top of the springs. Load versus displacement (i.e., linear compression) data was also generated by these tests. Test specimens were installed into a holder that rested on a stationary base. A movable platen attached to the actuator was translated up and down to load and unload the test specimens. Test specimens were loaded for multiple load cycles at a variety of test temperatures including room temperature, 1600 °F, 2000 °F, 2200 °F, and 2500 °F.

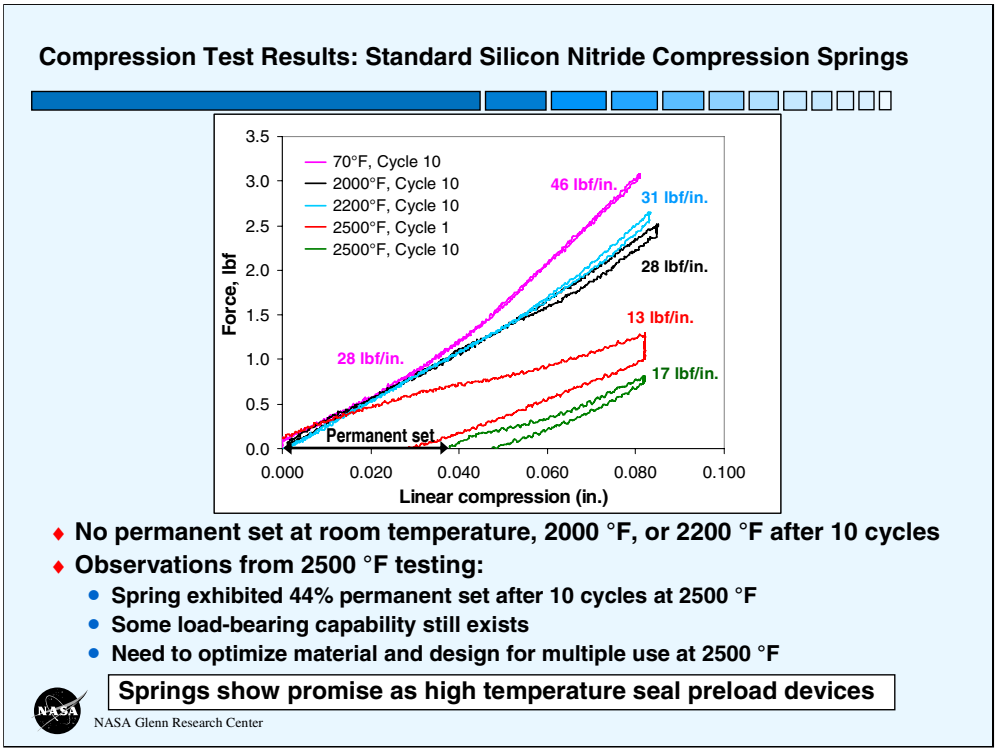

This figure shows the results for the compression tests performed on the standard silicon nitride compression spring design. For the tests performed at room temperature, 2000 °F, and 2200 °F, there was no permanent set or relaxation observed after 10 load cycles. For clarity, the figure only shows the curves for cycle 10 of these tests because they were almost identical to the curves for all other load cycles.

The test at 2500 °F produced somewhat different results than the tests performed at lower temperatures. The figure shows load cycles 1 and 10 for this test. For both of these load cycles, the peak loads were lower than those for the other tests. After 10 load cycles at 2500 °F the spring exhibited 44% permanent set but still had some load-bearing capability.

The results of these tests indicate that the silicon nitride compression springs show promise as high temperature seal preload devices, but some work needs to be done to optimize this material and spring design for use at 2500 °F.

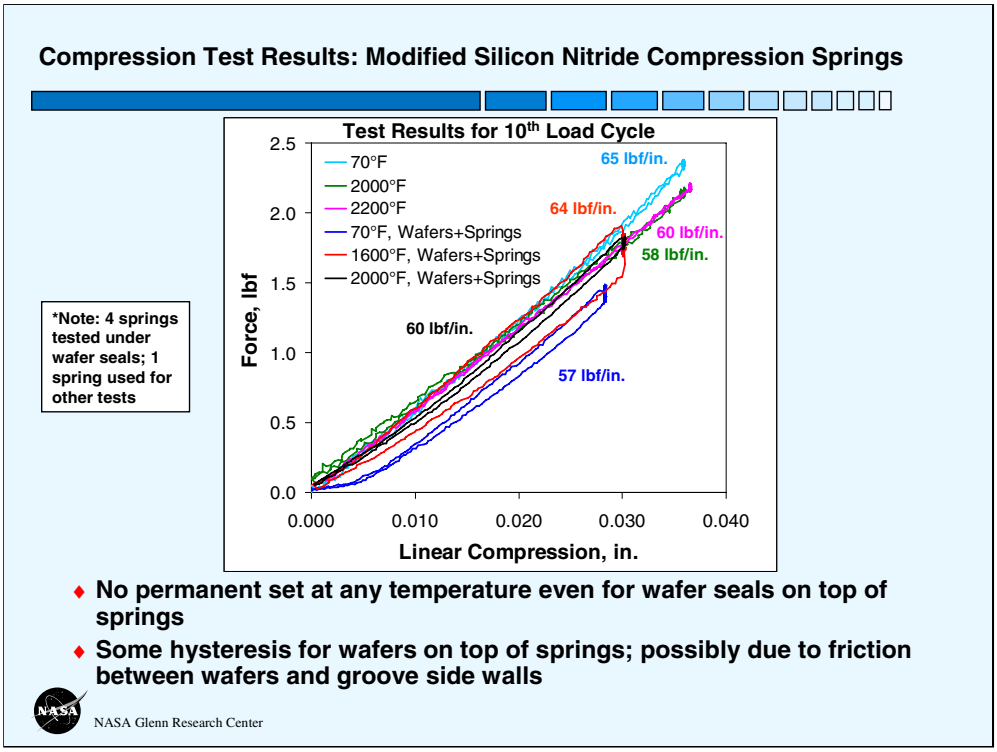

This figure shows the results for the compression tests performed on the modified silicon nitride compression spring design. The modified springs were smaller than the standard springs, allowing them to be installed in a groove behind the wafer seals so that compression tests could be performed on the sealing system as a whole. In all of these tests there was no permanent set or relaxation observed after 10 load cycles at room temperature, 1600 °F, 2000 °F, or 2200 °F. For clarity, the figure only shows the curves for cycle 10 of each test because they were almost identical to the curves for all other load cycles. For all of the tests performed on the silicon nitride springs by themselves, there was very little hysteresis in their load vs. linear compression data. For the tests performed with seals on top of the springs, there was virtually no hysteresis for the room temperature tests but a small amount for the tests at 1600 °F and 2000 °F. It is possible that during the high temperature tests, there was some small amount of friction between the wafers and the side walls of the seal groove that caused this hysteresis as the wafers and springs were unloaded during each load cycle.

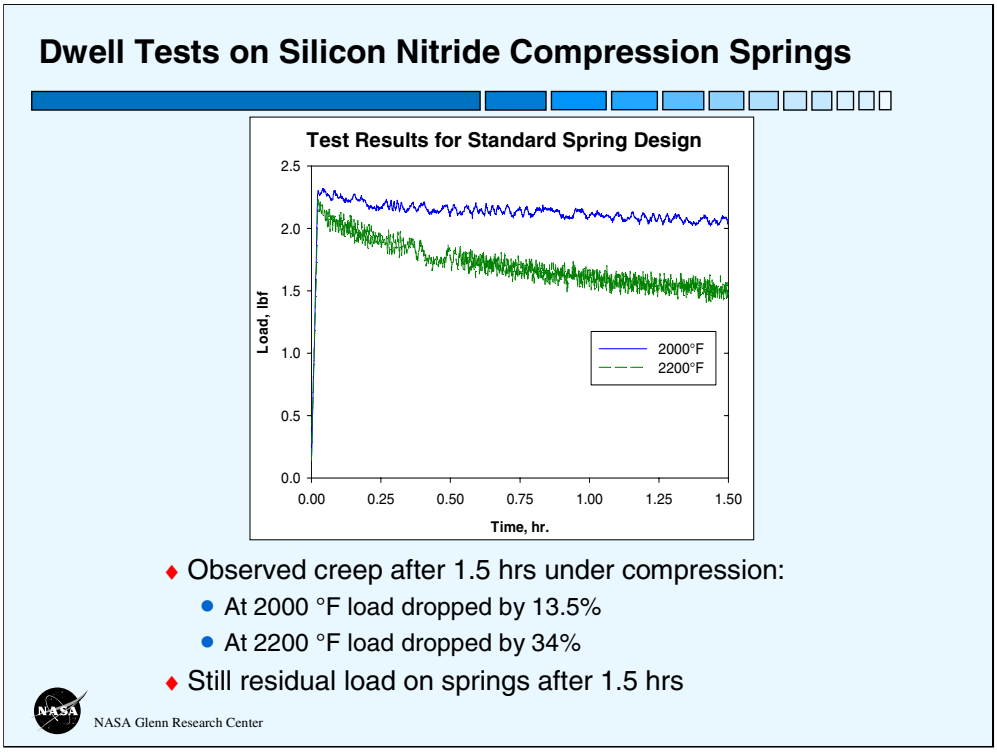

Dwell tests were also performed on the standard silicon nitride compression springs in which the springs were held under load for an extended period of time. After an hour and a half under compression at 2000 °F the load dropped off by 13.5%. At 2200 °F the load dropped by 34% after an hour and a half. Although the loads dropped, the springs were still able to bear a good amount of load in both cases after an hour and a half of loading at high temperatures. If these springs are used as preload devices in future seal applications, this drop in load will have to be accounted for.

Hot Scrub Test Fixture

- Measure seal frictional loads and wear rates
- Test parameters:
  - Tests at room temperature and 1600 °F
    - Inconel 625 rub surfaces
    - Rub surface roughness before testing = 6 μin
  - Test performed at 2000 °F
    - Silicon carbide rub surfaces
    - Rub surface roughness before testing = 29 μin
  - Two sets of 32 wafers preloaded by silicon nitride compression springs
  - Seal gap size = 0.125-0.135 in.
  - 1000 scrub cycles; 2000 in. of scrubbing

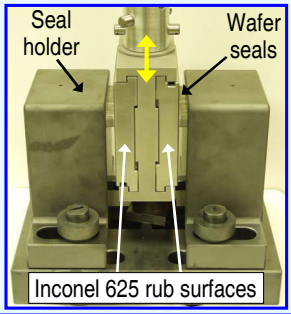

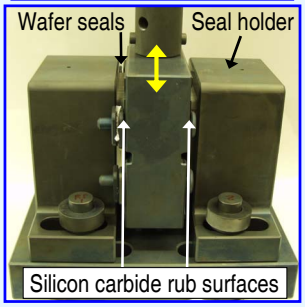

NASA Glenn Research Center

The main test rig that was used for the compression tests was also used to perform scrub tests on the seals using the set of test fixtures shown here. Tests were performed at room temperature, 1600 °F, and 2000 °F to evaluate seal wear rates and frictional loads as the seals were scrubbed against Inconel 625 and silicon carbide rub surfaces. The seals were installed in grooves in two stationary seal holders on either side of a pair of movable rub surfaces. The rub surfaces were assembled in a holder that was connected through the upper load train to the actuator.

Inconel 625 rub surfaces were used for the tests performed at room temperature and 1600 °F, while silicon carbide rub surfaces were used for the test performed at 2000 °F. The Inconel 625 rub surfaces had an average surface roughness before testing of about 6 μin. The roughness of the silicon carbide rub surfaces before testing was 29 μin. The gaps between the rub surfaces and the seals were set by spacer shims in front of and behind the seal holders. Gap sizes of 0.125-0.135 in. were used for these tests.

Four silicon nitride compression springs (modified spring design) were installed in the bottom of each seal groove to keep the wafer seals preloaded against both rub surfaces. A load transfer element was placed on top of the springs to support the wafers and distribute the load from the springs. Thirty two wafers were installed into each seal holder to fill the 4-in.-long seal grooves. The amount of compression on the seals and springs (0.030 in.) was set through an interference fit between the seals and the rub surfaces resulting in a preload of about 2 lb per inch of seal.

During these tests, the seals were held in place in the holders while the rub surfaces were scrubbed up and down against them. The seals were subjected to 1000 scrub cycles at 1 Hz for a total scrub length of 2000 in. for each test. Frictional loads were measured by the load cell under the furnace below the test fixture base. Seal wear rates were determined by examining the condition of the seals before and after each test and by measuring seal weight changes and changes in flow rates.

Scrub Test Results

- Room temperature test against Inconel 625
  - Frictional loads peaked at 15.5 lb
  - Friction coefficient reached ~1
  - Rub surfaces became rougher (43 µin)
- 1600 °F test against Inconel 625
  - Loads reached 23.5 lb
  - Max friction coefficient = 1.5
  - Final rub surface roughness = 34 µin
- 2000 °F test against silicon carbide
  - Loads peaked at 12.8 lb
  - Friction coefficient ~1 by end of test; surface roughness stayed ~28-29 µin
  - No load spike at start of test; seals did not stick to surface during furnace heatup

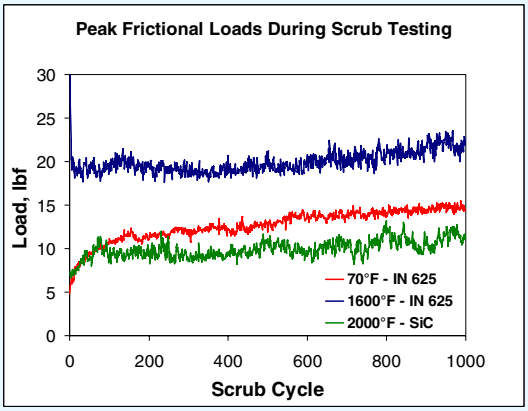

NASA Glenn Research Center

Peak frictional loads for each of the scrub tests are presented in this figure. For the test performed at room temperature against Inconel 625 rub surfaces, the frictional loads started around 6 lbf at the beginning of the test and gradually rose as the test proceeded until they reached about 15.5 lbf by the end of the test. Based on these loads, the friction coefficient at the end of the test was about 1.0. Before this scrub test, the average surface roughness of the rub surfaces was about 6 µin. After the test, the surface roughness had risen to about 43 µin. This increase in surface roughness during testing likely contributed to the increase in frictional forces as the test proceeded.

For the test performed at 1600 °F against Inconel 625 rub surfaces, the load peaked initially before quickly dropping and then slowly rising again to about 23.5 lbf by the end of the test. The friction coefficient reached 1.5 by the end of this test, corresponding well with an increased surface roughness of 34 µin.

For the test at 2000 °F using silicon carbide rub surfaces, lower loads were recorded than for the tests performed at lower temperatures against Inconel 625 rub surfaces. There was no load spike at the start of the test, indicating that the seals did not stick to the silicon carbide rub surfaces during furnace heatup. By the end of the test, the load peaked at about 12.8 lbf. The friction coefficient for this test reached about 1.0, and the surface roughness of the silicon carbide rub surfaces remained at about 28-29 µin, the same roughness as at the start of the test.

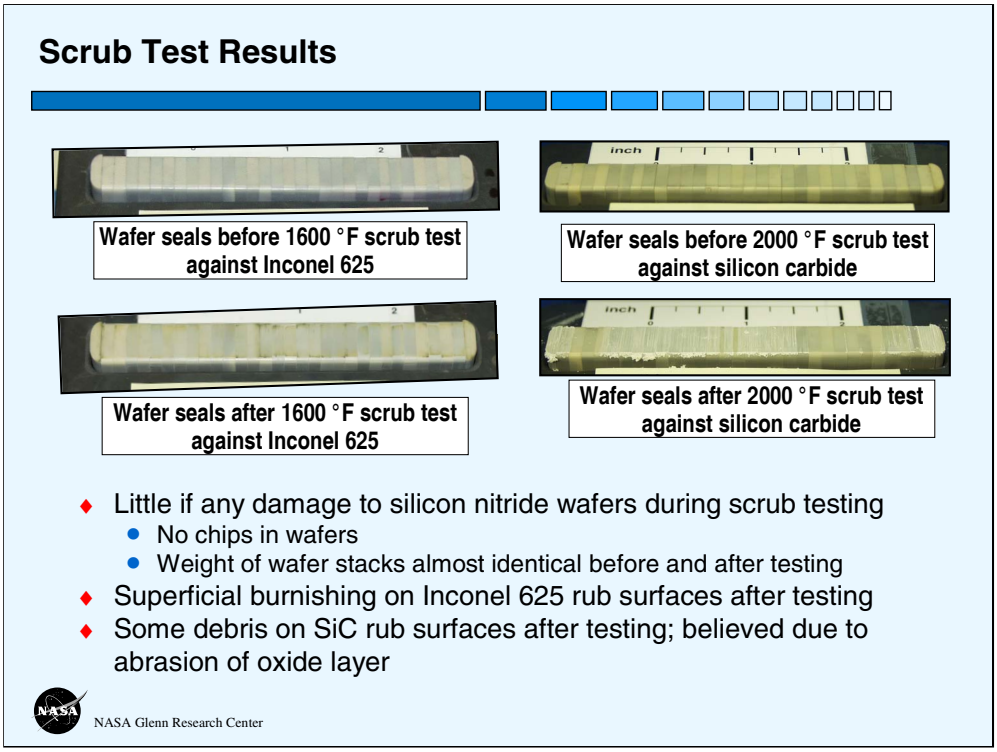

After the scrub tests were completed, the seals and rub surfaces were inspected for signs of damage. These figures show what the seals looked like before and after scrubbing at 1600 °F against Inconel and before and after scrubbing at 2000 °F against silicon carbide. The seals showed little if any damage after testing. None of the wafers were chipped or broken during testing, and the total weight of the wafers before and after testing was almost identical. Superficial burnishing was observed on the Inconel rub surfaces after testing, but this was not deemed to be significant. A small amount of debris was observed on the silicon carbide rub surfaces after testing (also visible in the photo of the wafers after this test). It is believed that this debris is due to abrasion of the oxide layer that forms on the silicon carbide rub surfaces at high temperatures.

Flow Test Results

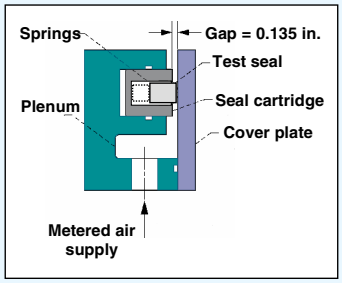

Flow fixture

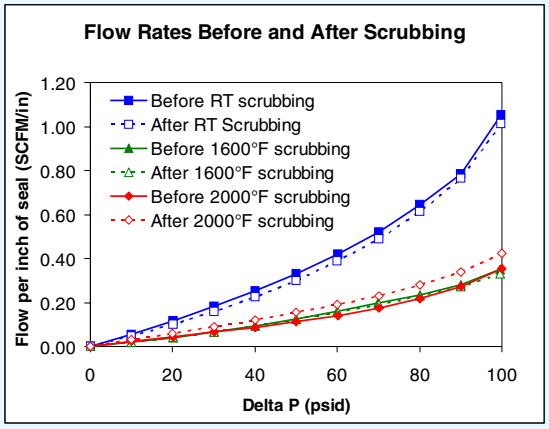

- No change in flow rates after scrubbing at room temp., 1600°F, or 2000°F
- Flow rates were ~32 times lower than those for best braided rope seals
- Flow rates lower for wafers tested at 1600°F and 2000°F due to tighter wafer height tolerance (0.0005 in. vs. 0.001 in. for RT test)

NASA Glenn Research Center

Flow test results for the wafer seals before and after each scrub test are presented here for a gap size of 0.135 in. These tests were performed with four silicon nitride springs installed behind the wafers to keep them preloaded against the cover plate. Flow rates for the wafers before and after scrubbing were almost identical in each case. This is consistent with the observation that the wafers were not damaged during the scrub test. These results are encouraging because they show that the seals are still effective at blocking flow even after 1000 scrub cycles at room temperature. Additionally, flow rates for the wafer seals were up to 32 times better than those for the best braided rope seals.

Flow rates for the wafers tested at 1600°F and 2000°F were lower than those for the test performed at room temperature. This was because a tighter wafer height tolerance was used for the high temperature tests (0.0005 in.) than what was used for the room temperature test (0.001 in.).

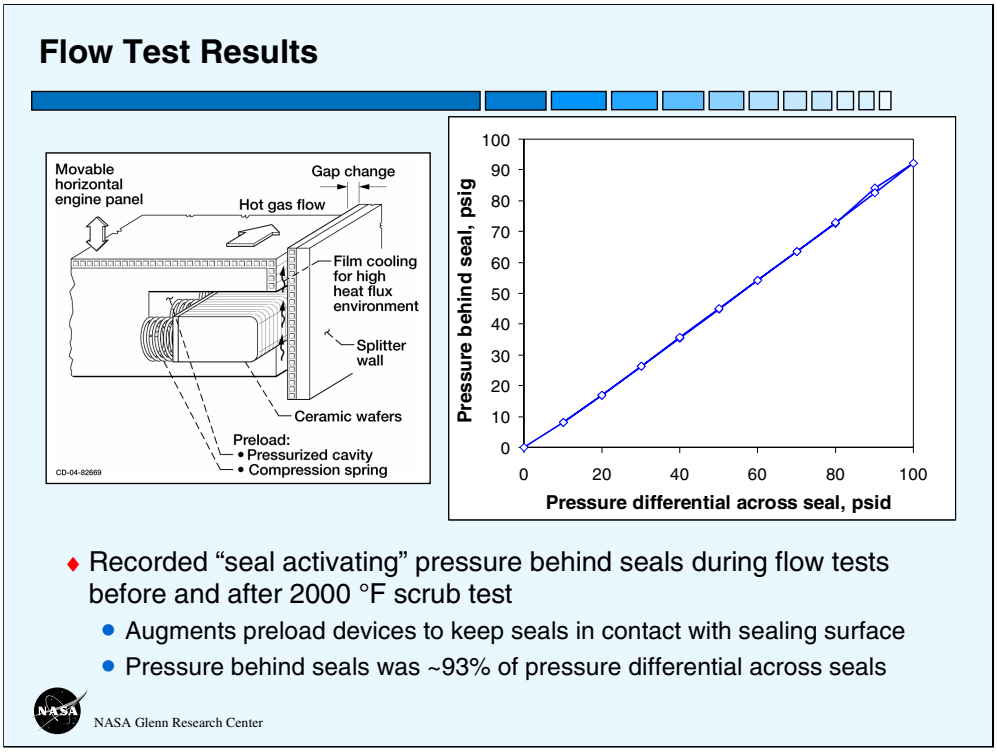

For the flow tests that were performed on the wafers before and after the 2000 °F scrub test, a new pressure measurement was made that was not recorded in the previous flow tests. This pressure measurement allowed the pressure behind the wafers to be recorded as a function of the differential pressure across the seals. The figure on the right presents pressure data behind the wafer seals versus the pressure differential across the seals for the flow test performed on the wafers that were scrub tested at 2000 °F. This plot shows a linear relationship between these pressures such that the pressure behind the seals was equal to about 93% of the pressure differential across the seals. The pressure behind the seals serves as a “seal activating” pressure that augments the preload devices to further preload the seals against the sealing surface and keep them in contact with it. This seal activating pressure phenomenon for wafer seals was observed previously for wafer seals tested during the NASP program.

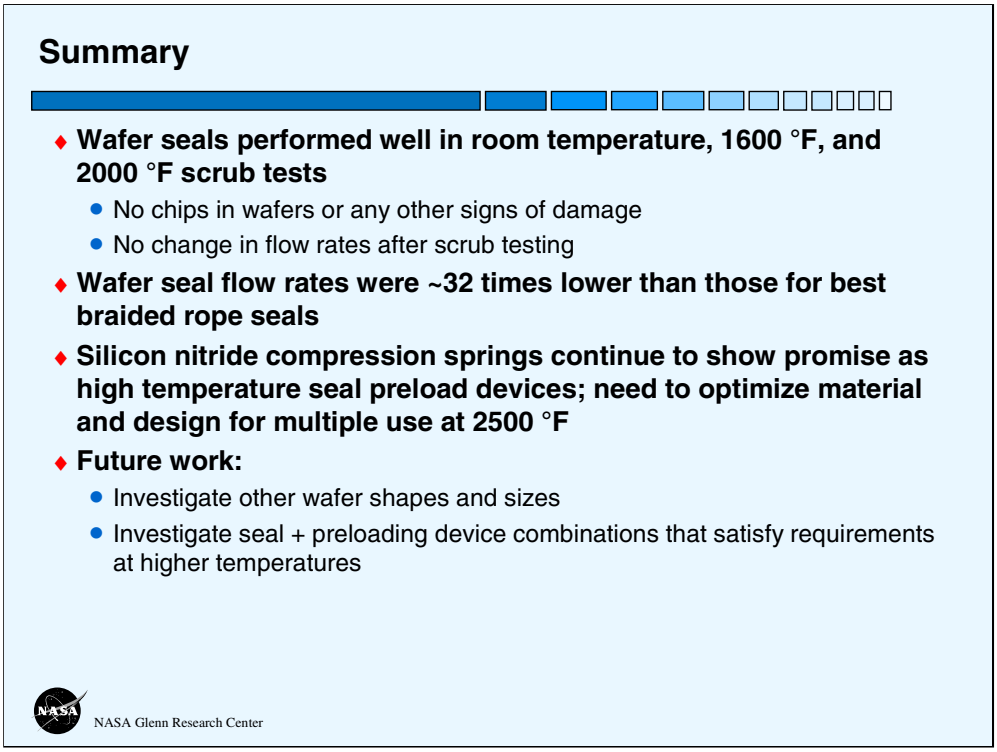

Based on the results of these tests, the following conclusions were made:

1. The silicon nitride wafer seals performed very well in scrub tests performed at room temperature, 1600 °F, and 2000 °F. No chips or any other signs of damage were observed on the wafers after testing, and there was no change in flow rates past the seals after scrub testing.
2. Flow rates for the wafer seals were up to 32 times better than those for the best braided rope seals.
3. Commercially available silicon nitride compression springs continue to show promise as high temperature seal preload devices, but the material and design for these springs needs to be optimized for multiple uses at 2500 °F.

More work needs to be done to investigate seal and preloading device combinations that ultimately satisfy all of the seal requirements. The authors plan to investigate other wafer shapes and sizes to see if those changes affect seal durability, frictional forces, and flow rates. Longer scrub tests will also be performed at higher temperatures to examine seal durability.

ON THE DEVELOPMENT OF A UNIQUE ARC JET TEST APPARATUS FOR CONTROL SURFACE SEAL EVALUATIONS

Joshua R. Finkbeiner, Patrick H. Dunlap, and Bruce M. Steinetz
National Aeronautics and Space Administration
Glenn Research Center
Cleveland, Ohio

Malcolm Robbie, Gus Baker, Arthur Erker, and Joe Assion
Analex Corporation
Cleveland, Ohio

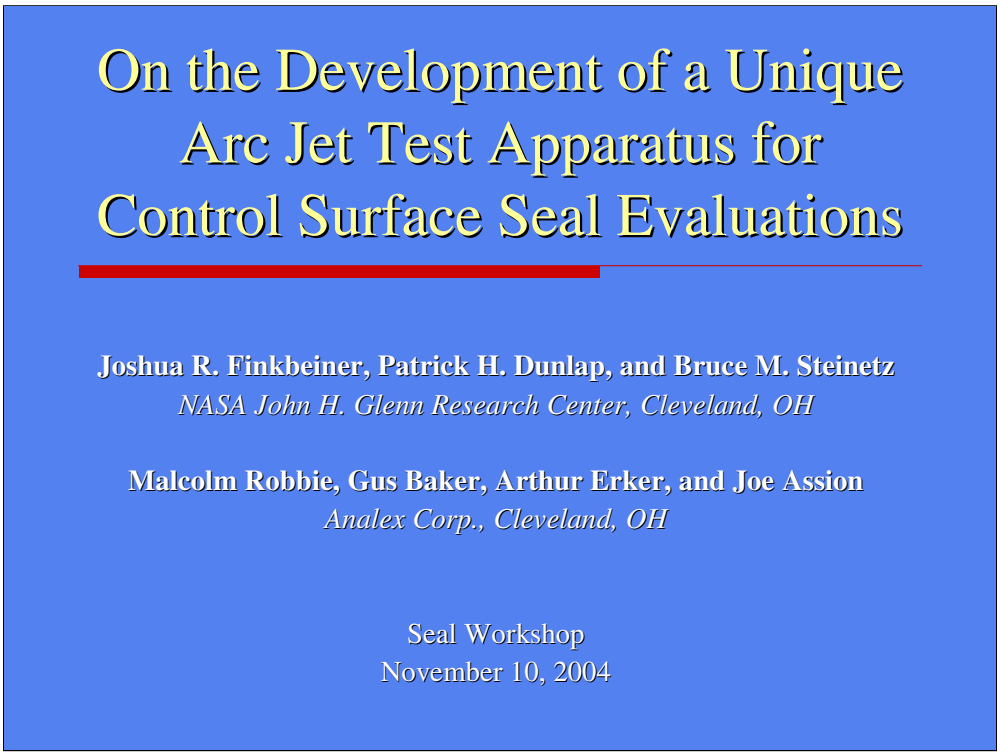

Outline

- Future seal requirements
- Test fixture design objectives
- Simulation of reentry environment
- Test fixture design and capabilities
  - Modular seal cartridge
  - Modular flap
  - Metal-to-ceramic flap transmission system
  - Instrumentation
  - Angular positioning

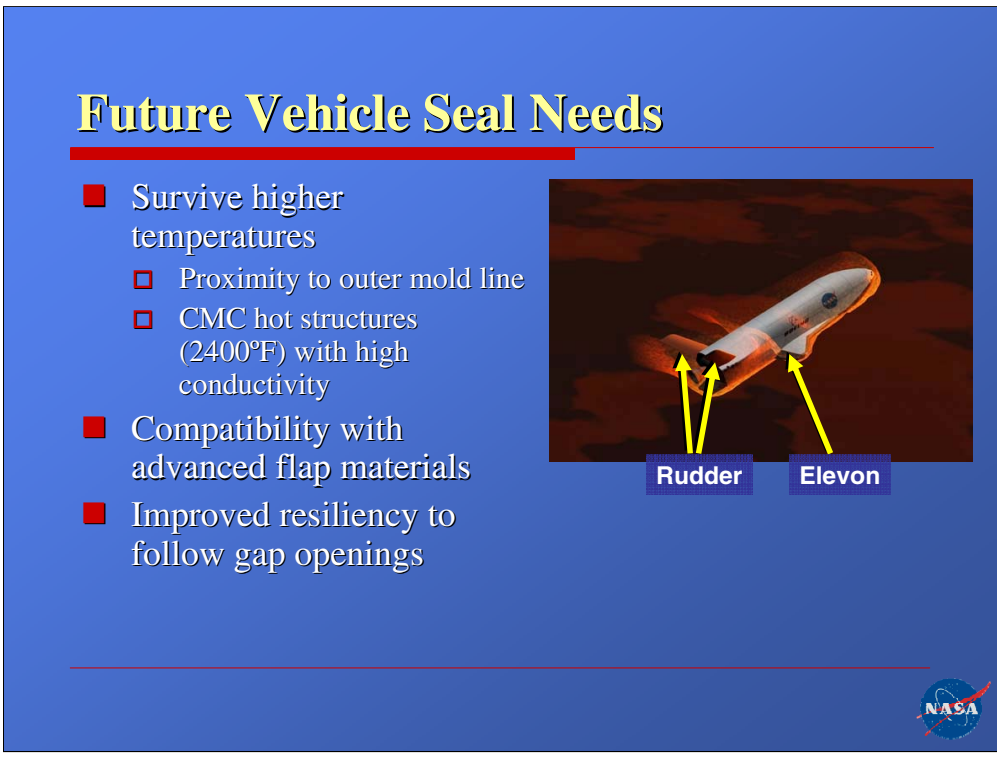

Future reentry vehicles will require more advanced seals than the current generation of vehicles (i.e. Shuttle). The seals must be capable of surviving higher temperatures for two primary reasons. Next-generation vehicles will be smaller in size than the Shuttle, and as a consequence, the seals will be closer to the outer mold line of the vehicle. Additionally, the next generation vehicles will employ CMC hot structures in place of the tile-insulated aluminum control surfaces currently used in Shuttle. These materials will be exposed directly to temperatures of (anticipated) 2400 ºF. Combined with the high thermal conductivity of these materials, new seal designs will be exposed to more severe thermal environments.

The use of CMC materials also introduces a second challenge in the design of new control surface seals. The seal materials must be chosen with care to ensure that the seal does not stick to the control surface material.

Finally, the seal must be able to maintain resiliency at the elevated temperatures. The seal gap size can change due to thermal expansion and movement of the control surface during flight. The seal must be capable of responding to gap size changes in these conditions.

Seal Test Requirements

- Require environment representative of reentry
- NASA JSC Arcjet simulates reentry environment
  - Heat Flux
  - Seal temp 1800-2400ºF
  - Pressure drop 56-100 psf
  - Exposure time ~15 min

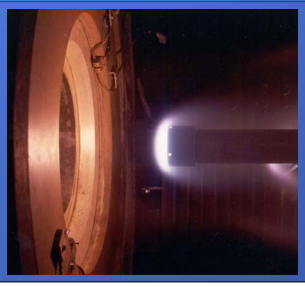

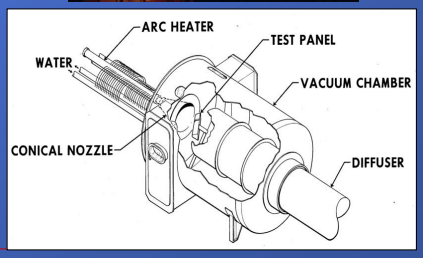

A simulated reentry environment is ideal for testing next-generation reentry vehicle control surface seals. This includes a combination of the heat flux, temperature, pressure drop, and exposure time encountered during hypersonic flight.

The arcjet facility at NASA Johnson Space Center will provide the simulated reentry heat. Depending on the nozzle used in the facility, the arcjet will expose the seal to temperatures of 1800-2200 ºF with a pressure drop of 56-100 psf. The facility is actively cooled, allowing it to simulate the reentry environment for 15 minutes, a typical reentry time for Shuttle.

Seal Test Fixture Objectives

- Test control surface seals in JSC arcjet tunnel
  - Expose seals to reentry conditions
  - Survive arcjet environment
- Movement of control surface during hot test
- Variability of test parameters
  - Seal shapes, sizes, and materials
  - Fixture position (angular, spacial)

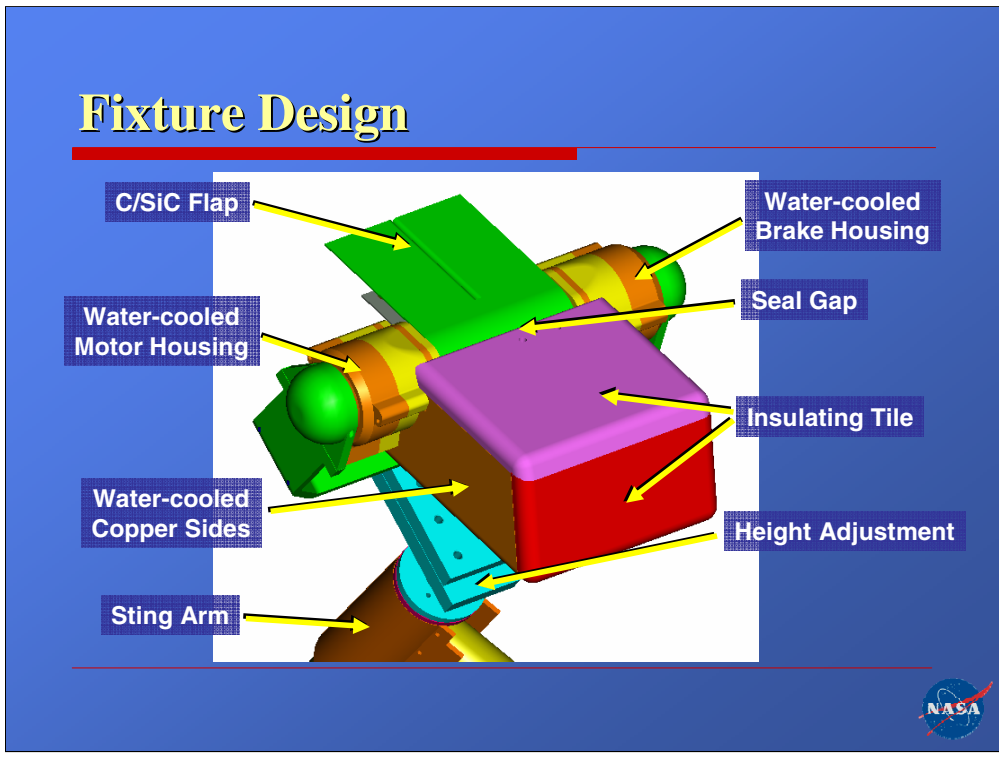

The design of the advanced seal arcjet test fixture provides flexibility for testing diverse seal designs at the same time as it is capable of surviving the harsh arcjet environment. The leading edge of the fixture contains the seal specimen, instrumentation, and provides the primary structure of the test fixture. The underlying structure of the leading edge is formed from water-cooled oxygen-free high-conductivity (OFHC) copper and is covered with insulating tile panels designed to minimize heat transfer to the structure. The tiles are coated with a high emissivity coating to further reduce the heat loading on the interior structure.

The leading edge is mounted against a C/SiC flap. The leading edge and flap are connected via a set of motor and brake systems housed inside water-cooled OFHC copper enclosures. The motor and brake systems allow the flap to move while the arcjet test is active. This simulates loading on the seal during reentry conditions, including the effects of scrubbing a rough surface against the seal at high temperature.

The sting arm supports the test fixture in the arcjet facility and holds the fixture in the arcjet flow. The sting arm allows movement of the fixture in the direction of the arcjet flow, while a high adjustment mechanism allows adjustment of the position of the fixture perpendicular to the flow stream.

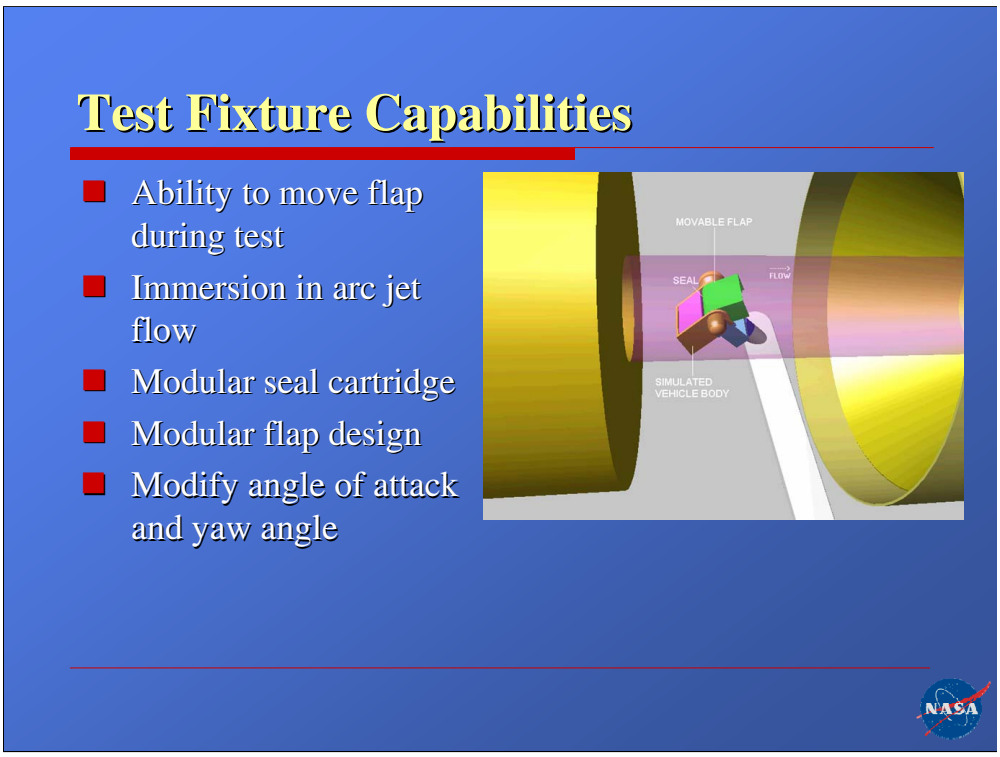

The flap can be moved while the arcjet is active while a test is in progress. This allows recording of dynamic changes in the seal environment and permits recording the seal response to these dynamic changes.

The seal specimen is mounted in a modular cartridge. This cartridge allows diverse seal shapes and materials to be tested in the fixture while minimizing changes to the fixture. New seal designs can be incorporated into the fixture by manufacturing a new low-cost cartridge instead of requiring expensive design changes to the entire fixture.

The flap is also modular, allowing not only the standard C/SiC flap, but also other designs (such as a tile-insulated aluminum flap). The attachment mechanism of other flap designs need only conform to the interface transmission system of the fixture.

The fixture also permits changes to the angle of attack of the leading edge and the yaw angle.

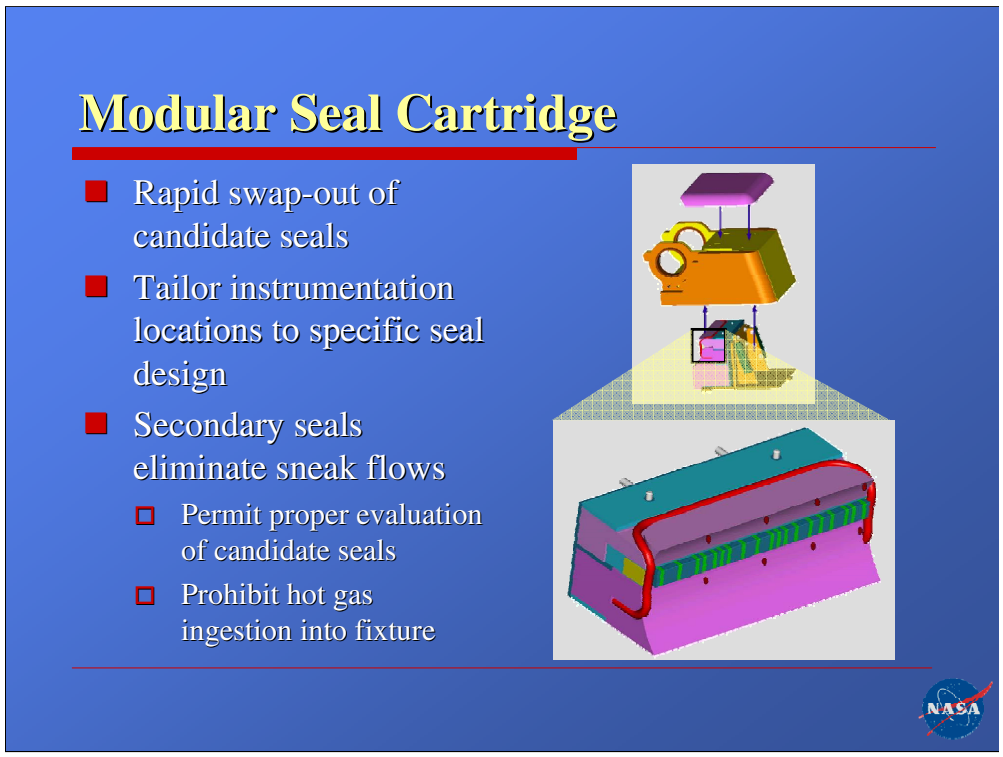

The modular seal cartridge allows inexpensive testing of diverse seal shapes, sizes, and materials as well as fast turn-around time to incorporate new seal designs. The cartridge is formed from a series of insulating tile blocks mounted to a metal backing plate. The seal (in this case, a stack of ceramic wafers) fits between the two blocks. A secondary rope seal fits around the cartridge, sealing the edges of the test seal and preventing sneak flows into the internals of the leading edge. Each test seal has its own seal cartridge, providing a low-cost solution to expanding the capabilities of the test fixture. Furthermore, the instrumentation locations can be altered for different seal designs by altering the instrument locations in the tile blocks.

The seal cartridge attaches to a removable instrumentation tray which slides in and out of the bottom of the fixture along a series of guiding rails. These rails constrain the instrumentation tray such that the seal is compressed uniformly against the flap.

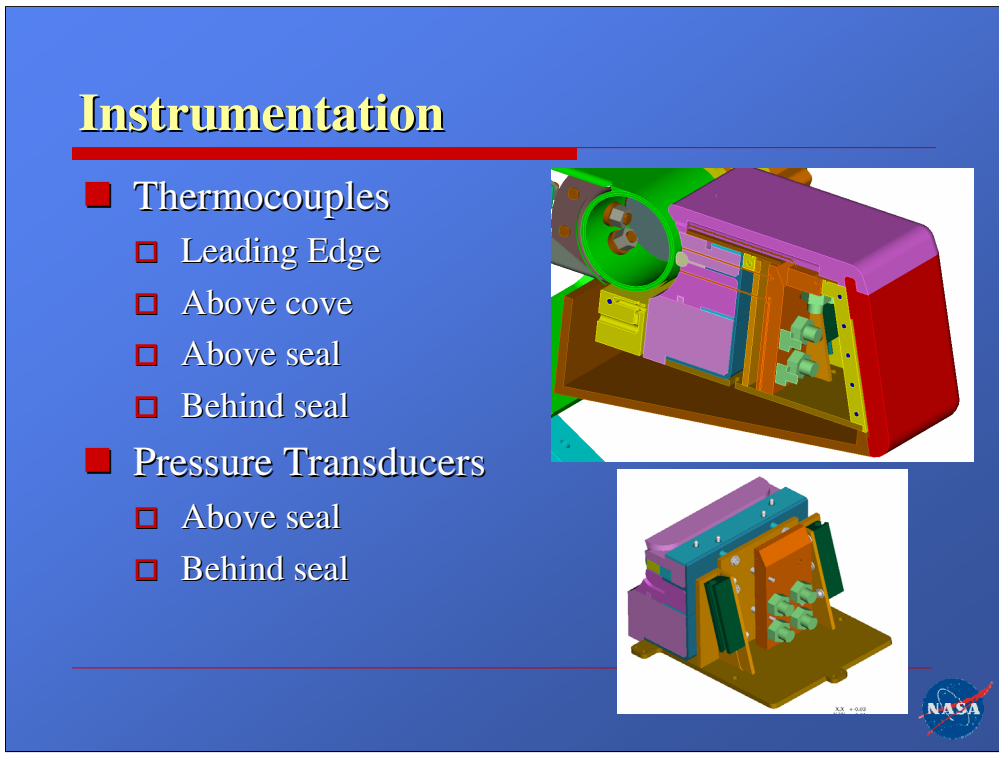

Seal performance measurements include both pressures and temperatures.

Thermocouple passages are machined into the top tile cover and seal cartridge and provide temperature measurements above the seal cove, inside the seal cove both immediately above and below the seal, and downstream of the seal cove, all at several locations along the width of the fixture. Additionally, temperatures are monitored in sensitive locations inside the test fixture (e.g. the pressure transducers, motor and brake, etc.) to ensure that electronic components are not exposed to temperatures above their design specifications.

Pressure taps are also embedded in the top insulating tile and in the seal cartridge. These lines pass through the tile material and connect to one of two manifold blocks. Each manifold block contains machined passages leading from the pressure taps to threaded connectors. Small pressure transducers thread into these connectors. This system allows fast-response pressure measurements while at the same time protecting the pressure transducers from the harsh arcjet environment. The manifold block permits the pressure transducers to fit into the small space provided in the leading edge.

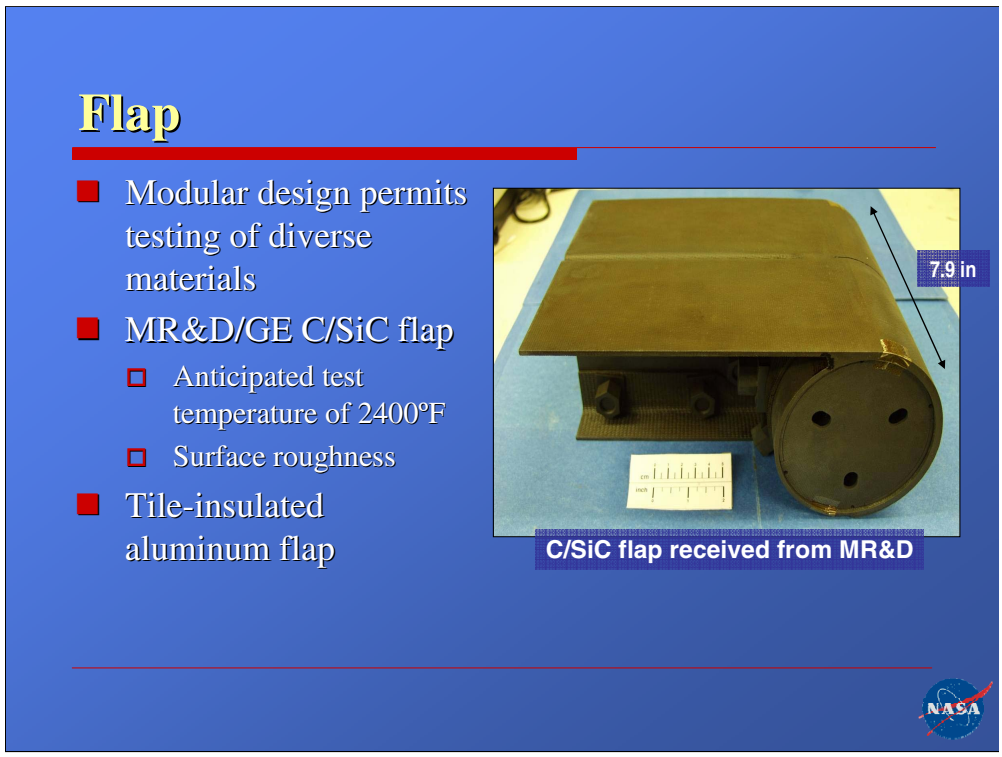

The flap is a modular design, permitting diverse flap materials to be tested in the advanced seal arcjet test fixture. As with the modular approach to seal designs, the modularized flap permits testing of various flap materials and finishes with candidate seal designs.

The flap shown here is a C/SiC flap provided by MR&D and GE Power Systems. The flap is expected to be exposed to temperatures as high as 2400 ºF. The C/SiC material represents future sealing challenges in an environment including a combination of high heat loading, high temperature, rough sealing surface, and scrubbing conditions.

The modular design of the flap permits the use of other flap designs such as a tile-insulated aluminum flap characteristic of Shuttle.

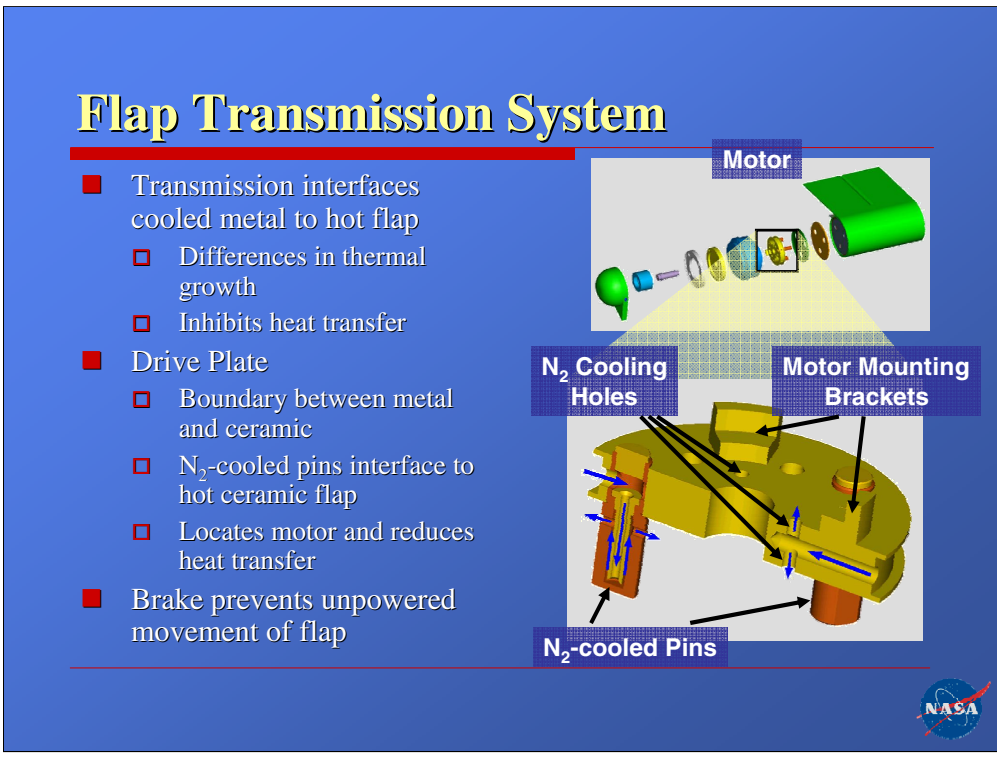

The flap transmission system is capable of altering the flap angle while the fixture is in the arcjet flow stream. At the same time, the transmission system holds the flap despite the differences in thermal expansion between the hot C/SiC flap and the cooled metallic components. Furthermore, the transmission system inhibits heat transfer from the flap to the motor and brake, keeping the temperatures of these critical components below their design temperature limits. The transmission system also permits manual adjustment of the angle of attack of the leading edge.

The key to the transmission system is the nitrogen-cooled drive plate. Nitrogen is fed into the plate through a channel around the outer diameter of the disk. Three pairs of cooling holes blow nitrogen onto the motor/brake face and onto the inboard labyrinth seal. These holes can be orificed or plugged completely in order to supply more nitrogen to three Inconel drive pins. Each pin has an internal Inconel tube which supplies nitrogen directly to the internal tip of the pin. The nitrogen flows along the inside surface of the hot pin and exits through holes near the plate. The flow of nitrogen maintains the pin tips below 1500 ºF, even though the flap temperature is approximately 2400 ºF. After exiting the pin, the nitrogen maintains a positive purge pressure in the motor/brake housings, preventing the ingestion of hot arcjet gases. This effect is boosted by the inboard labyrinth seal.

Heat transfer from the flap to the inboard labyrinth seal is inhibited by a silicon nitride insulating disk.

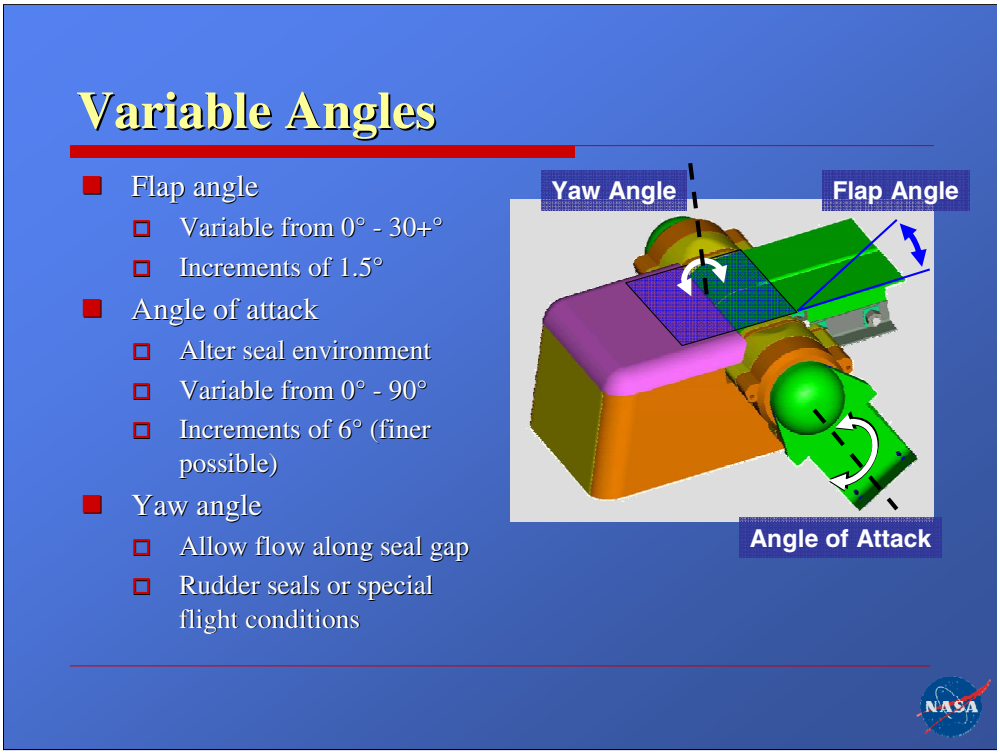

Three test fixture angles are capable of being independently adjusted.

The flap angle can be adjusted while the test fixture is exposed to the arcjet flow stream. The angle can be adjusted between 0º and 30º, with small negative angles possible. The brake constrains the flap angle to increments of 1.5º.

The angle of attack of the leading edge can be manually adjusted between tests. This permits alteration of the seal environment by manipulating the shock structure near the seal cove. The angle of attack can be easily adjusted between 0º and 90º in increments of 6º. Finer angular increments can be obtained with some disassembly and reassembly of the fixture.

The fixture yaw angle can also be manually adjusted. This adjustment permits some of the arcjet flow to move along the seal gap, exposing the seal to higher heat fluxes. This simulates control surface environments such as rudders as well as special flight conditions where flow moves along seal gaps.

Summary

- Future reentry vehicles pose greater sealing challenges than shuttle
  - Seal proximity to outer mold line
  - Hot (2400°F) CMC control surfaces
- Control surface seal test fixture permits seal tests:
  - Under reentry-like conditions (arc jet)
  - With variable position/geometry
  - Using several diverse seal concepts
  - Against various flap materials and shapes

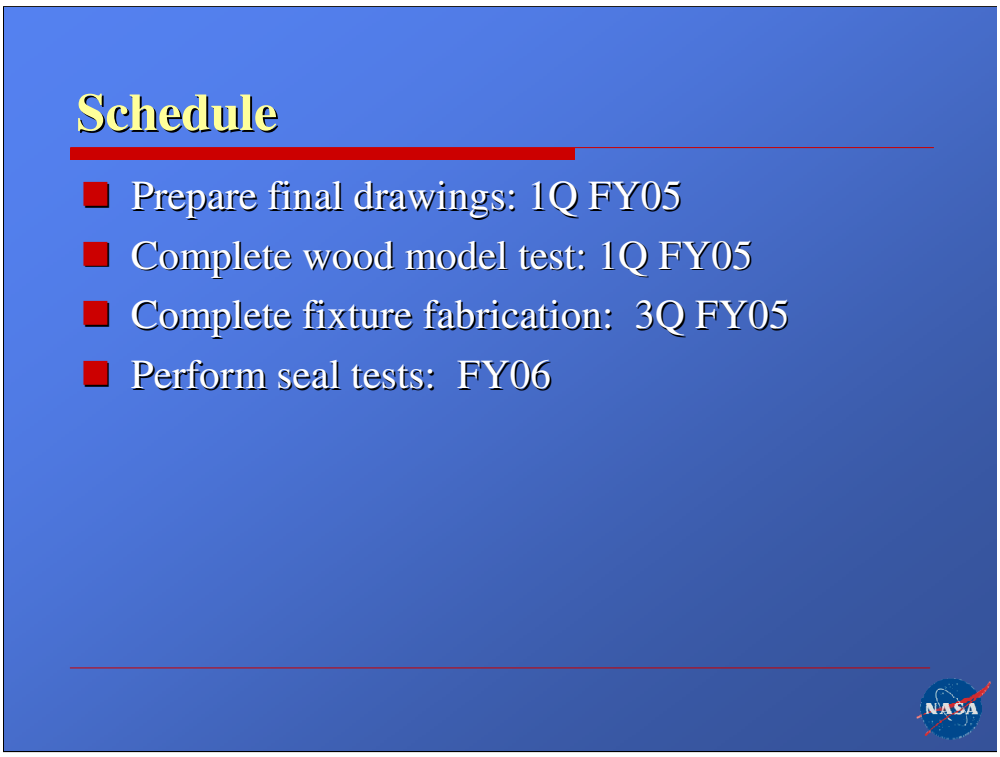

Checkout tests may be conducted in late FY05

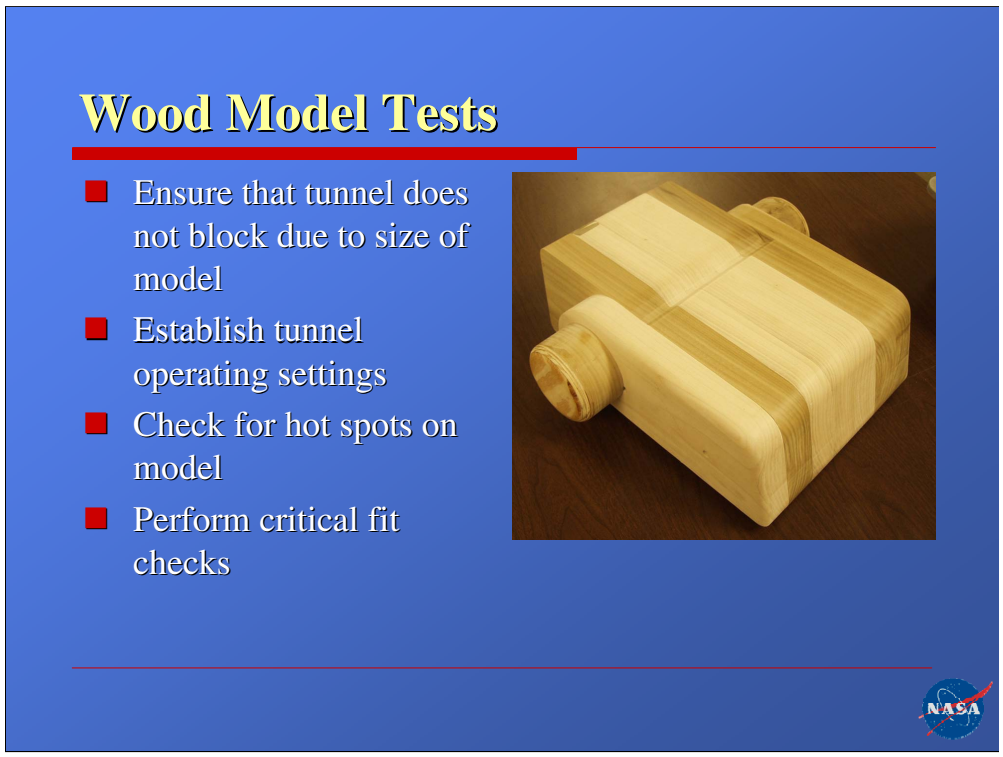

The advanced seal arcjet test fixture is anticipated to be one of the largest objects tested in JSC's Arcjet facility. The large size of the fixture has introduced the possibility that the fixture could block the JSC Arcjet tunnel. In this situation, the fixture deflects flow into the arcjet vacuum chamber, increasing the chamber pressure. The higher chamber pressure prevents the arcjet stream from expanding, resulting in a high enthalpy gas stream tightly focused on a small area of the fixture. This situation would result in the destruction of the fixture. Fortunately, this situation is avoided by an automatic tunnel shutdown sequence.

To permit the successful completion of seal tests, the test fixture must not block the arcjet tunnel. The use of a larger tunnel nozzle can prevent the fixture from blocking the tunnel, although this comes with the trade-off of lower seal temperature and heat flux. To determine the correct nozzle, a wood model of the test fixture was constructed and shipped to JSC.

The wood model will be placed in the arcjet stream for a few seconds. The short time increment will be enough to determine whether the fixture size is too large for a particular nozzle. Additionally, the wood model will reveal hotspots. If these hotspots occur in places not forseen, the fixture cooling system can be modified to account for the higher heat transfer in these locations.

Test Fixture Analysis

- Temperature profile
  - Within limits for OFHC copper
  - Below annealing temperature
- Heating rates are conservative
  - Stagnation heating over front face, housings
  - Side wall heating rates

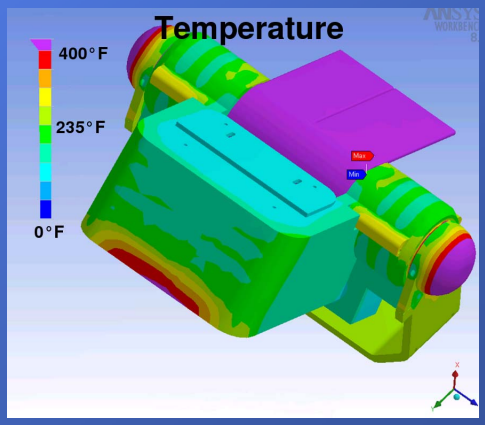

This is the temperature profile of the fixture before an insulating tile panel was added to the front face of the fixture.

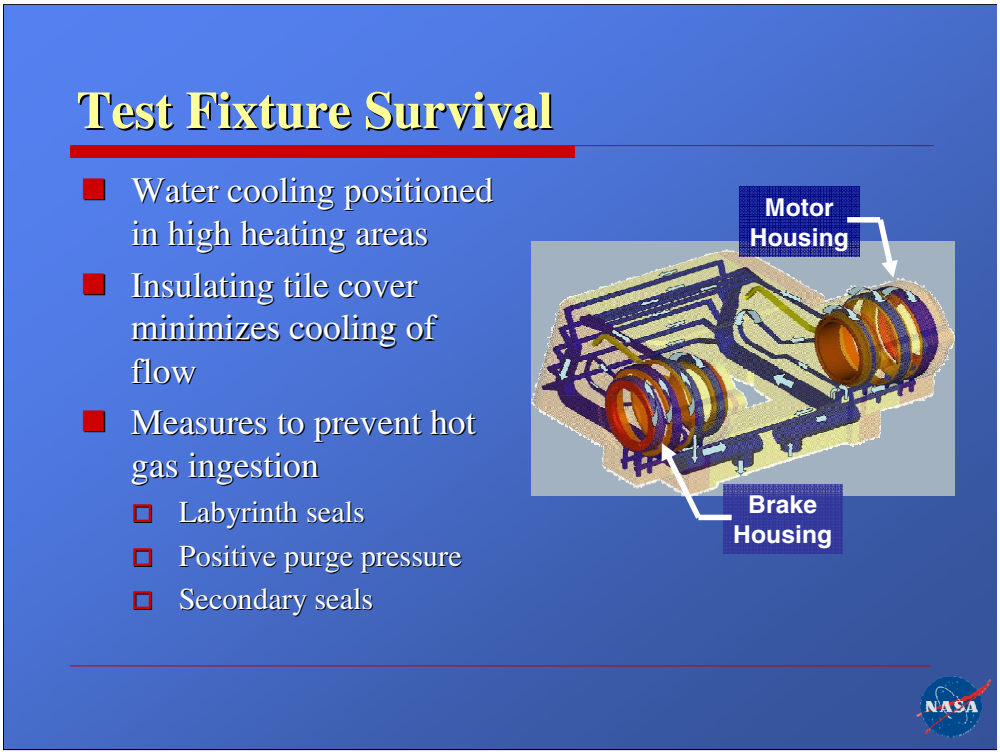

The cooling system for the leading edge and motor/brake housings. This shows the water passages before an insulating tile was added to the front face of the leading edge.

Brazing Trials for Main Housing

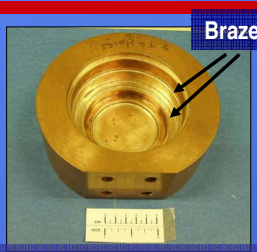

Test specimen for motor and brake housings

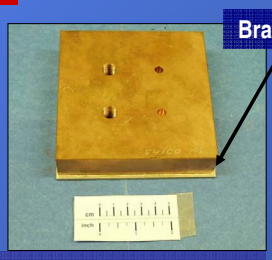

Test specimen for side walls

- Brazing trials on OFHC copper test specimens
  - Motor and brake housings
  - Sidewalls
- Passed hydrotest at 750 psi for 10 min.

INVESTIGATIONS OF HIGH-TEMPERATURE KNITTED SPRING TUBES FOR STRUCTURAL SEAL APPLICATIONS

Shawn C. Taylor
Case Western Reserve University
Cleveland, Ohio

Jeffrey J. DeMange
University of Toledo
Toledo, Ohio

Patrick H. Dunlap, Jr., and Bruce M. Steinetz
National Aeronautics and Space Administration
Glenn Research Center
Cleveland, Ohio

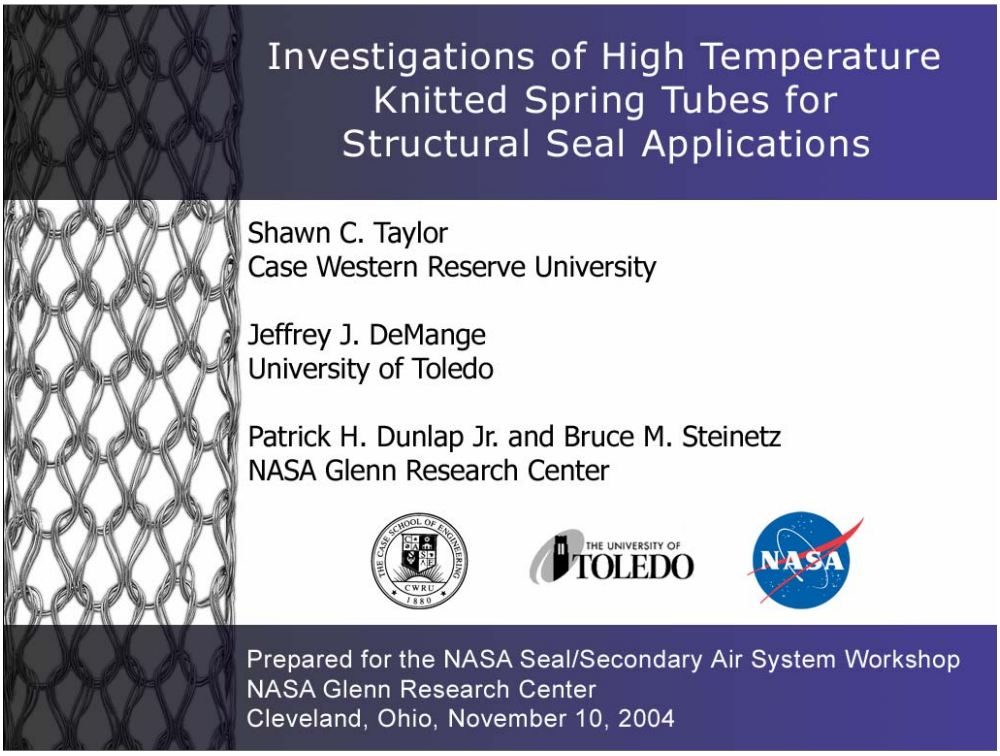

Control Surface Seal Design Challenges

- Prevent hot gas ingestion around actuated structures during atmospheric reentry
- Protect underlying temperature-intolerant structures
- Survive high temperature exposure (1800 – 2200°F)
- Maintain resiliency through multiple load/heating cycles
- Limit loads against sealing surfaces
- Resist abrasion damage

Control surface seals are used to fill the gap at the interface of static panels and actuated control surfaces such as rudders and elevons. These seals protect underlying temperature-intolerant structures such as mechanical actuators from the hot gases encountered during atmospheric reentry. The seals are typically installed in a compressed state that is 80% of the nominal seal diameter (20% compression). This allows the seal to accommodate expansions and contractions of the gap as panels shift relative to one another during flight.

To be effective, control surface seals must maintain enough resiliency to survive multiple compressive cycles at temperatures ranging from 1800-2200°F and remain in contact with both sealing surfaces. Since control surface seals often experience scrubbing across the sealing surfaces as the control surfaces are actuated they must also be capable of resisting abrasion damage. In addition, these seals must also limit the force that they apply to contacted surfaces, as some surface materials (e.g., Shuttle tiles) are easily damaged if compressive loads are excessive.

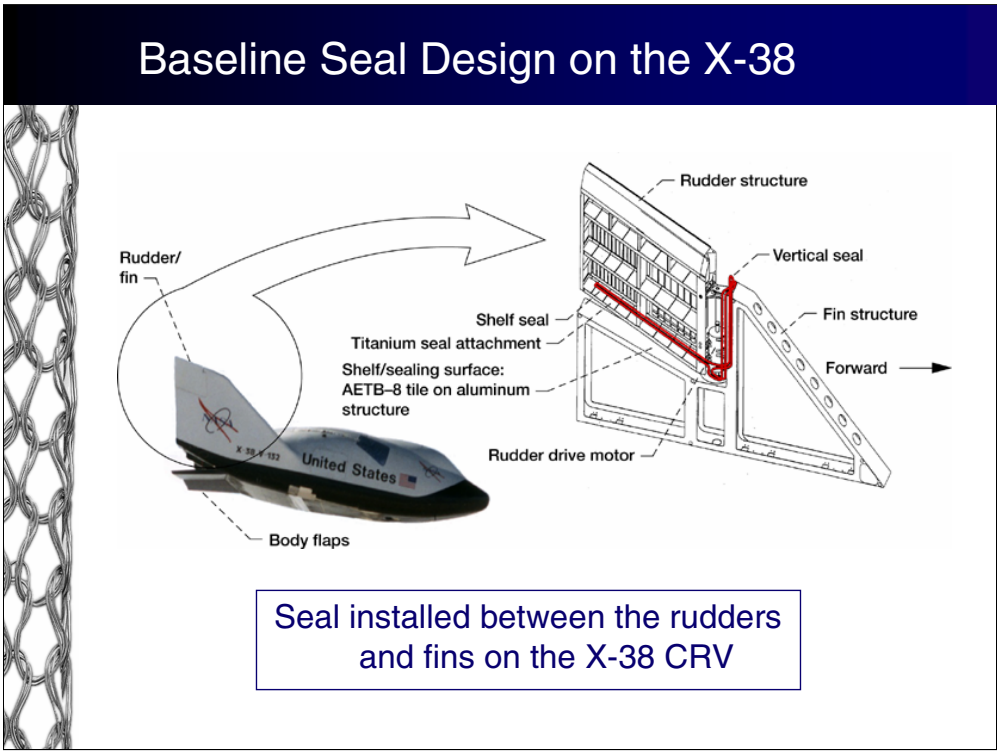

Control surface seals are typically installed in locations like the rudder/fin section shown above on the X-38 Crew Return Vehicle (CRV). The baseline control surface seal to be discussed in this presentation was selected as the primary seal installed in this location to protect the CRV's rudder drive motors from hot gas ingestion during atmospheric reentry.

Different sized versions of the baseline control surface seal are used as thermal barriers on the Space Shuttle. Seals are located around the landing gear doors, the payload bay door vents, and the orbiter external tank umbilical door.

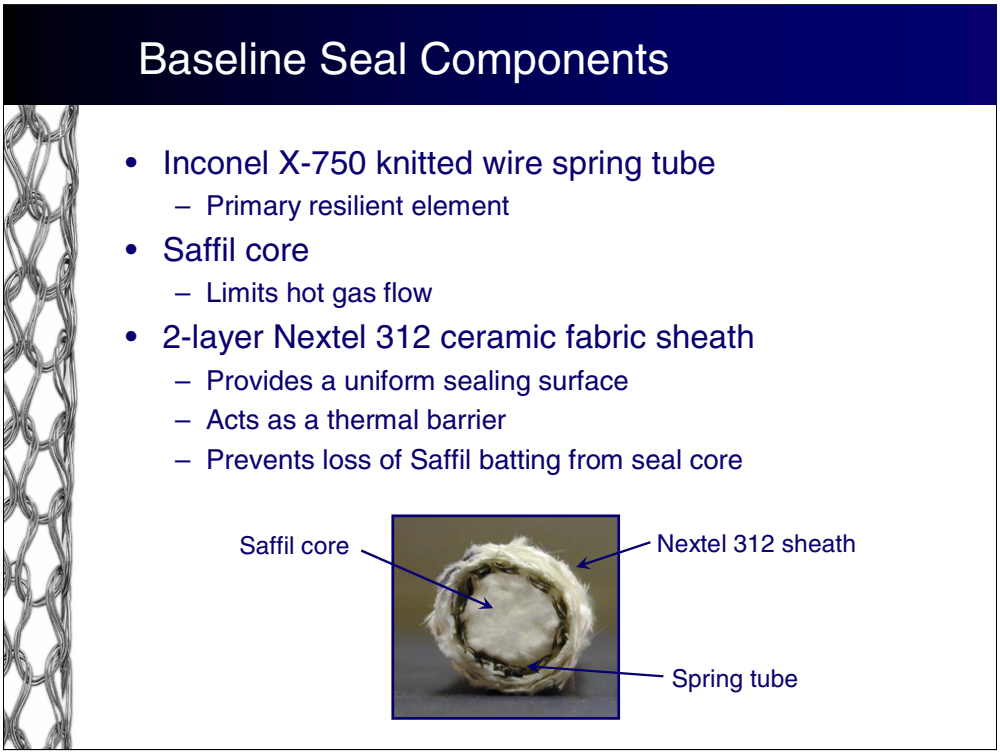

The baseline control surface seal is comprised of three parts:

1. A knitted Inconel X-750 spring tube which is the primary resilient element of the seal
2. A Saffil core that limits the flow of hot gases through the seal
3. A 2-layer Nextel 312 ceramic fabric sheath which provides a uniform sealing surface, acts as a thermal barrier, and prevents the loss of Saffil from the core of the seal through the walls of the knitted spring tube

Addressing Seal Inadequacies

- Permanent set and loss of seal resiliency occur above 1200°F
- Poor performance due to creep and low yield strength of Inconel X-750
- Potential Resiliency Improvements
  - Material substitution
  - Knit geometry modifications

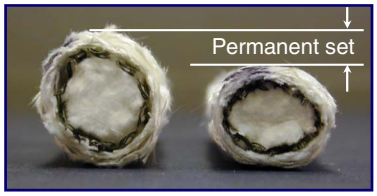

Baseline Seal

Goal: Enhance seal resiliency through spring tube design improvements

The baseline control surface seal has shown significant levels of permanent set in previous compression tests at elevated temperatures. The image above presents a comparison between an untested seal and a seal that has been compressed and heated to 1900°F in a tube furnace. The loss of resiliency in the tested seal is attributed to a decrease in strength of the Inconel alloy at the elevated test temperature. Further testing has shown that resiliency loss becomes evident at test temperatures as low as 1200°F. This temperature is noticeably close to the temperature at which the yield strength of the Inconel X-750 alloy begins to sharply decrease. Based on these observations, efforts to enhance seal resiliency by improving the performance of the spring tube have become the primary focus. To enhance spring tube resiliency, material substitutions and knit geometry modifications are being investigated.

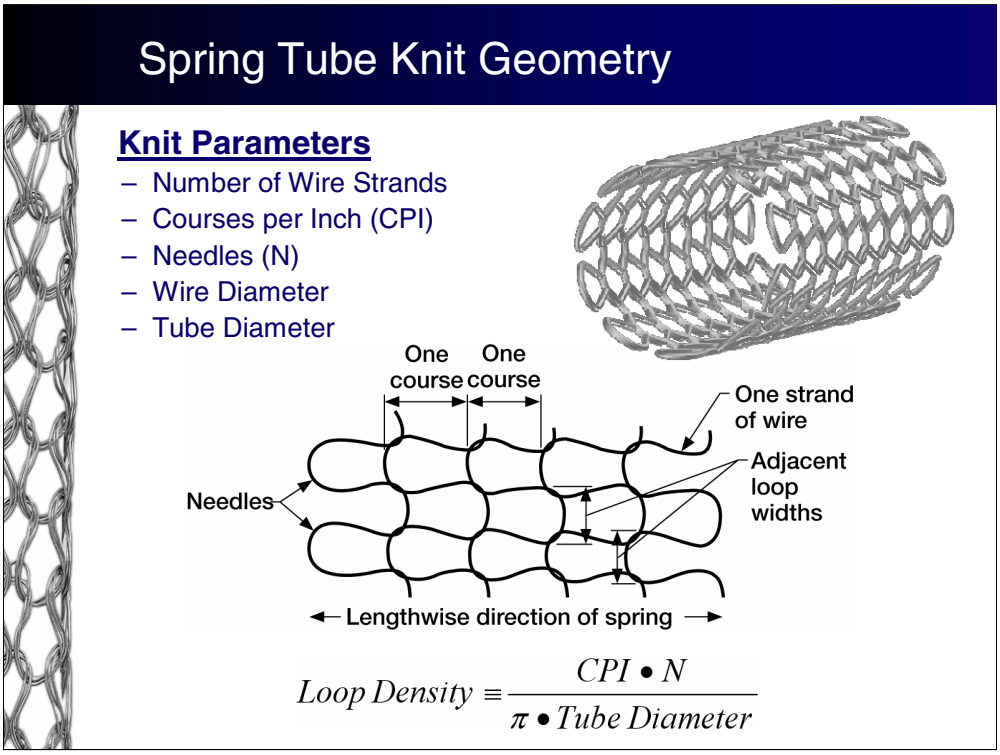

The schematic above shows a representative geometry of a spring tube. A defined set of knit parameters is used describe the spring tube geometry as follows:

•Number of Wire Strands: The number of individual wires that are knitted in a parallel fashion to form the spring tube. The baseline design has three wire strands, where the illustration above shows only a single strand.

•Courses per Inch (CPI): The number of individual courses (loops) counted per inch along the length of a spring tube. The baseline design has 4.9 CPI.

•Needles (N): The number of individual loops counted in a single rotation around the spring tube circumference. The baseline spring tube has 10 needles.

•Wire Diameter: The diameter of the individual wires that are knitted to make the spring tube. The baseline wire diameter is 0.009".

•Tube Diameter: The outer diameter of the spring tube. The baseline tube diameter is 0.560".

Spring tube loop density (LD) was defined to facilitate an equivalent comparison of modified spring tube geometries. This value combines both CPI and needles into a single parameter which represents the number of loops per square inch.

Spring Tube Material Selection

- Inconel X-750 baseline material
- Material substitution requirements
  - High temperature yield strength
  - Resistance to creep deformation at elevated temperatures
  - Available in wire form
- Rene 41 chosen as X-750 replacement
  - Improved high temperature yield strength
  - Better resistance to creep deformation

The spring tube in the baseline control surface seal is fabricated from Inconel X-750 wire. Inconel X-750 is a precipitation hardenable nickel based superalloy. To improve high temperature spring tube performance, material substitutions were investigated. Replacement materials were screened on the basis of availability of wire form, high temperature yield strength, and resistance to creep deformation at elevated temperatures. Based on these criteria, Rene 41, another precipitation hardenable nickel based superalloy, was selected as a potential near term replacement for the baseline material. Rene 41 is commercially available in wire form, and it has high temperature creep and yield strength properties superior to those of Inconel X-750. Oxide dispersion strengthened (ODS) alloys including PM 2000 and Inconel MA754 have high temperature creep properties better than Rene 41 above approximately 1550°F; however, these materials are difficult to obtain in wire form.

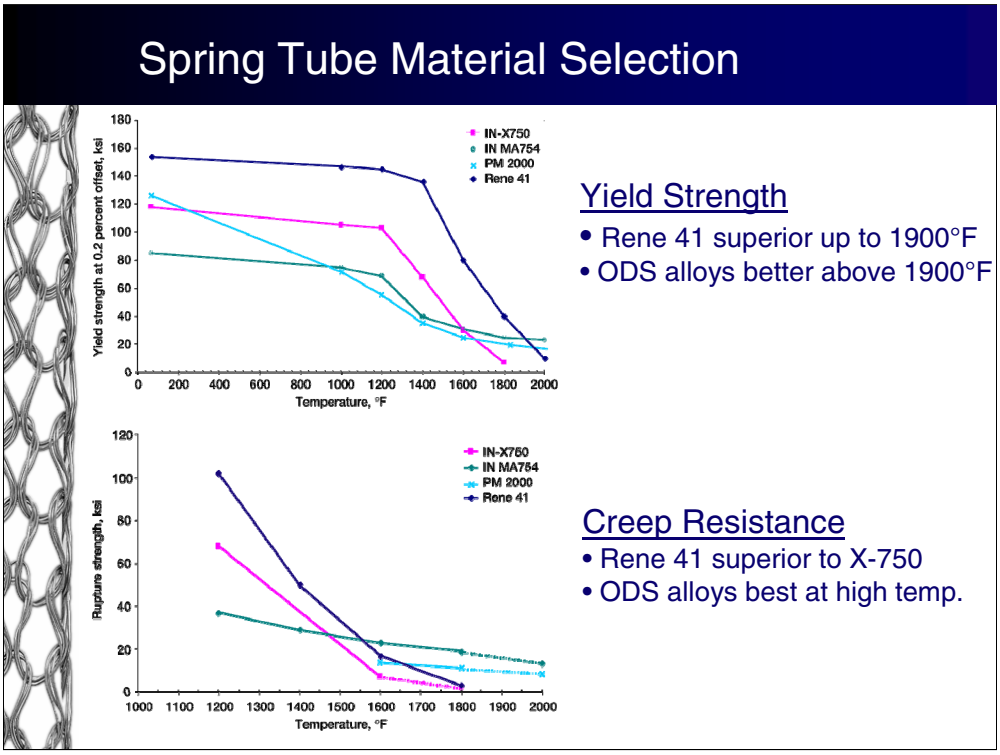

The plots above present yield and creep rupture strength values at multiple temperatures for candidate materials. On the plot of yield strength vs. temperature, it can be seen that Rene 41 is superior to the other alloys up to approximately 1900°F. After that temperature, the ODS alloys maintain higher yield strengths. The plot of rupture strength vs. temperature shows a similar trend. Up to approximately 1550°F Rene 41 has the highest rupture strength, but once that temperature is exceeded, the ODS alloys have better strength. It is notable that Rene 41 has better strength properties than the baseline Inconel X-750 material at all temperatures. These figures also suggest that if the ODS alloys were obtainable in wire form for knitting, they could hold promise for improved spring tube performance at temperatures near 2000°F.

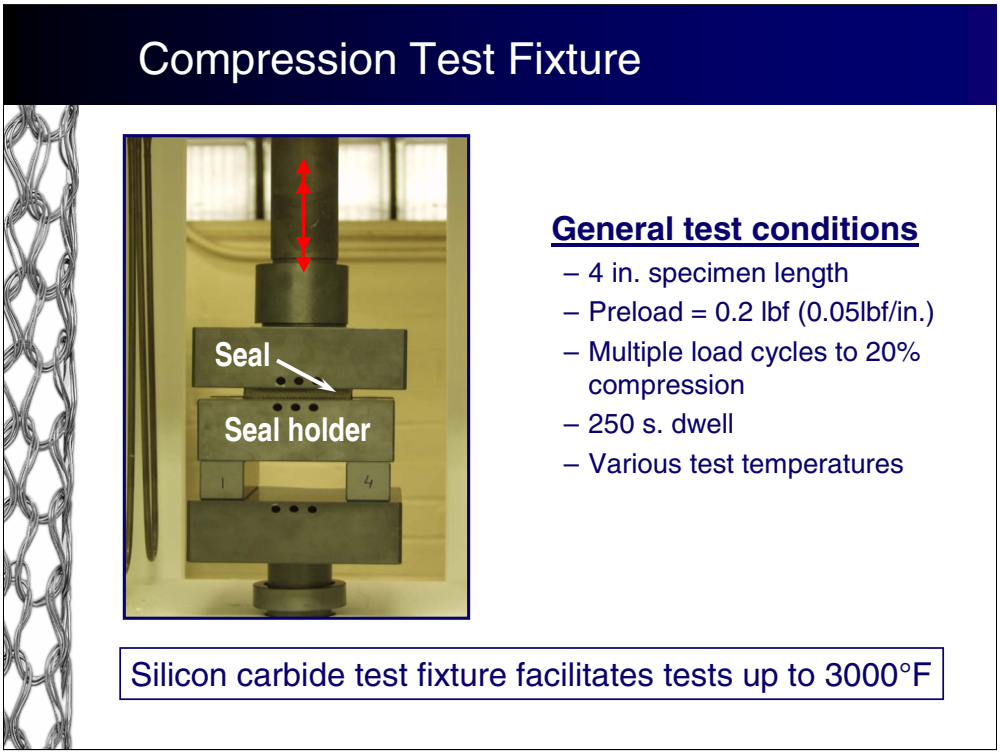

To evaluate the performance of spring tubes and seals, samples were tested using a state-of-the-art test rig at NASA Glenn Research Center. This rig facilitates high temperature compression testing at temperatures up to 3000°F. This is made possible by the SiC test fixture shown above that can withstand the elevated test temperatures. Spring tubes were tested in 4" lengths. A preload 0.2 lbf was used in the testing to define uniform contact between the spring tube and the loading platen. This was necessary because the samples are not visible during high temperature testing, as the furnace doors are closed. The spring tubes were subjected to multiple load cycles to a nominal 20% compression. At maximum deflection, a dwell period of 250 seconds was used to simulate the predicted time of maximum heating during atmospheric reentry. Multiple test temperatures were used to evaluate the performance of the spring tube samples.

Knit Geometry Screening Tests

- Test matrix
  - Inconel X-750 spring tube specimens
    - Baseline, 3 strand, 28 loop density
    - Modified, 1 strand, 34 loop density
    - Modified, 1 strand, 64 loop density
  - Heat treated and non-heat treated samples
  - Single tests (no replicates)
- Additional test conditions
  - Room temperature and 1500°F
  - Flat platen spring tube support
  - 10 compression cycles

A preliminary set of tests was conducted to evaluate the impact of knit geometry modifications on spring tube resiliency and load generation. The investigated geometry parameters included the number of wire strands and spring tube loop density. Single strand designs having loop densities of 34 and 64 loops per in.^{2} were compared to the three strand 28 LD baseline design. Both heat treated and non-heat treated samples were tested. Only single tests were run during the screening stage due to scheduling limitations and sample availability. These tests were conducted at both room temperature and 1500°F, and consisted of 10 loading cycles. Spring tubes were supported with a flat platen to simplify contact conditions allowing test results to be used in support of numerical modeling efforts.

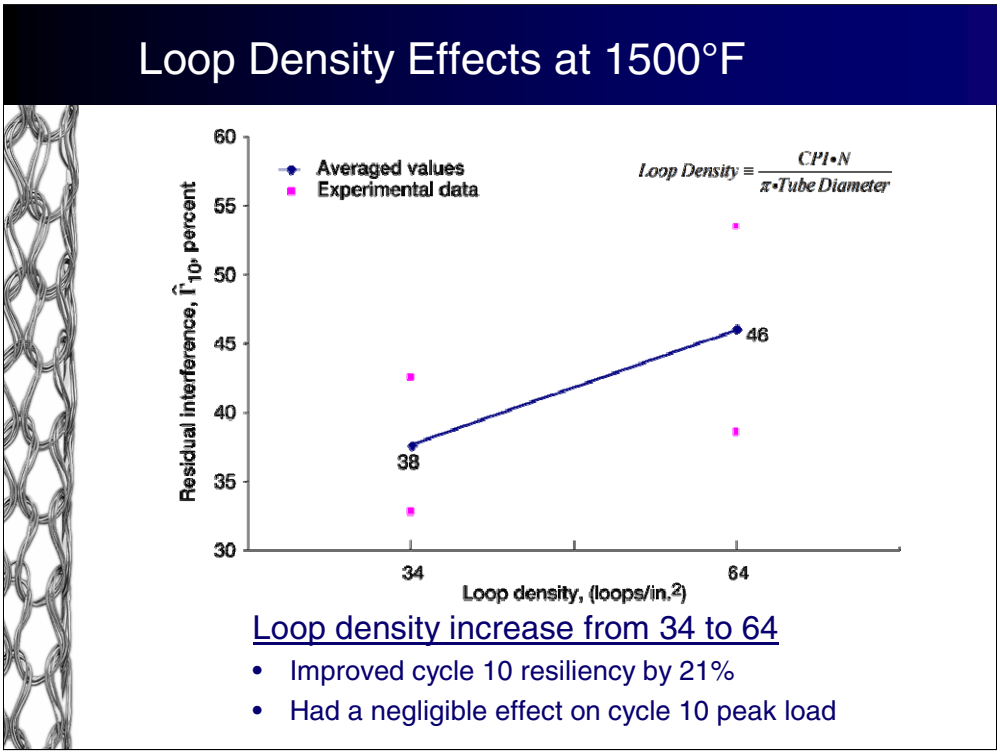

Effects plots were used to highlight trends in the collected data. In the effects plot above, residual interference (seal spring-back) at the start of compression cycle 10 is plotted against loop density. A greater line slope suggests a more dominant influence of the factor on the response variable, which in this case is residual interference. A zero slope would indicate that the factor had no influence on the response. As shown above, increasing spring tube loop density from 34 to 64 improved post deflection spring back by approximately 21%. The effect of loop density on cycle 10 load was determined to be negligible.

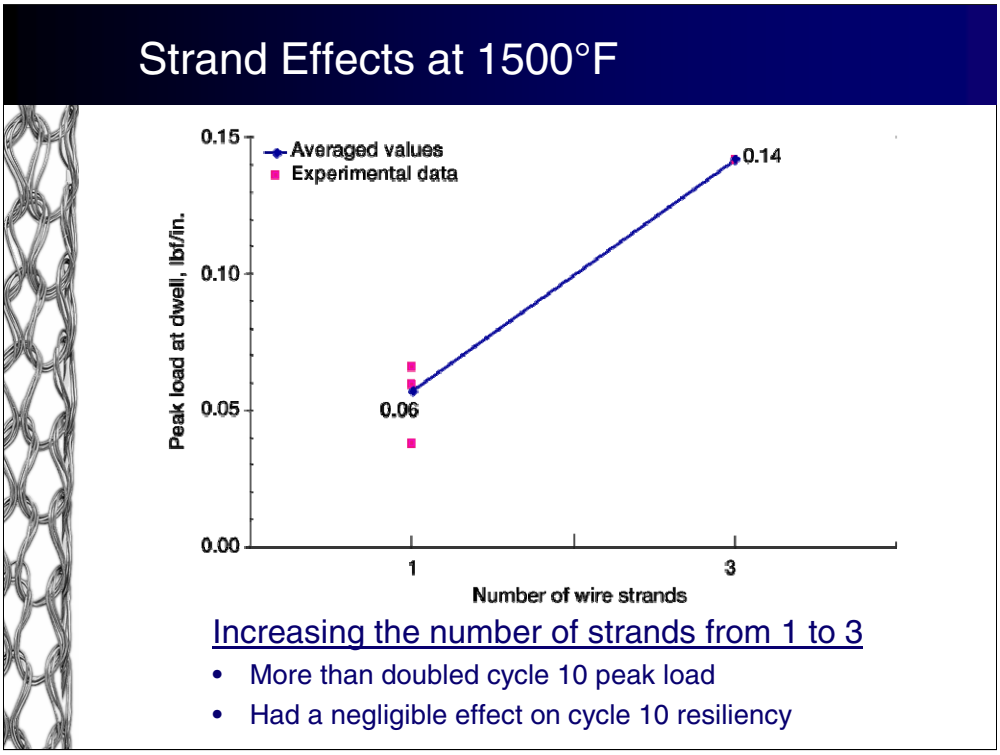

In the effects plot above, the influence of the number of wire strands on the peak load generated by the spring tube at maximum deflection is highlighted for testing at 1500°F. Increasing the number of strands from 1 to 3 more than doubled the cycle 10 peak load. The change in the number of wire strands had a negligible effect on the resiliency.

Material Selection Tests

- Test matrix
  - Inconel X-750 and Rene 41 spring tube specimens
    - Baseline knit geometry
    - Heat treated and non-heat treated samples
  - Rene 41 tests were repeated once
  - Inconel X-750 tests were not replicated
- Additional test conditions
  - Room temperature, 1200°F, 1500°F, 1750°F, and 2000°F
  - Grooved seal holder spring tube support
  - 20 compression cycles

To evaluate the impact of material selection on spring tube performance, baseline geometry spring tubes fabricated from Inconel X-750 and Rene 41 were tested at room temperature, 1200°F, 1500°F, 1750°F, and 2000°F. Spring tubes of both materials were tested in the as-knitted (non-heat treated) and heat treated state. Material selection tests used a grooved seal holder to support the samples and were extended to 20 compression cycles instead of 10. These procedural changes were used to create a test that was more representative of typical re-entry conditions. Other test variables such as dwell time and compression level remained the same as in previous tests. Tests on Rene 41 samples were repeated once, whereas tests on the Inconel X-750 samples were not.

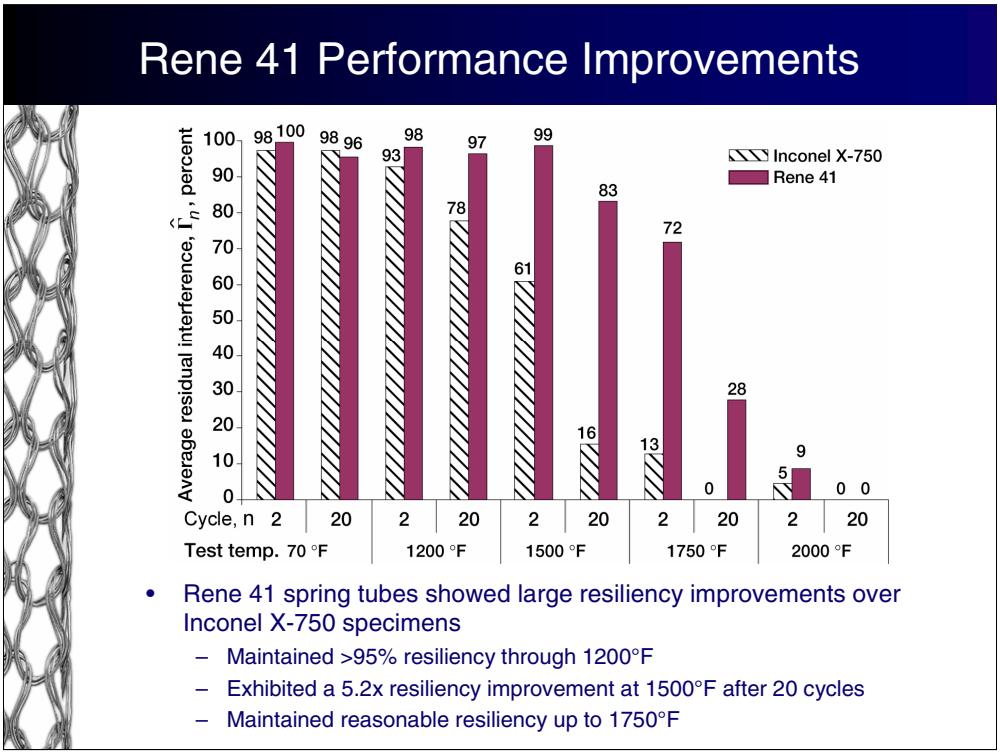

The impact of material substitution (Rene 41 for Inconel X-750) is highlighted in the bar chart above, where average residual interference (spring back) at the start of cycles 2 and 20 is plotted against test temperature. Unlike the baseline Inconel X-750 spring tubes, Rene 41 samples maintained greater than 95% resiliency through 1200°F for all 20 compression cycles. At 1500°F, Rene 41 spring tubes showed a 5.2x improvement during cycle 20 over the baseline design. At 1750°F, Rene 41 spring tubes maintained a 28% cycle 20 residual interference when all resiliency was lost in the Inconel specimens. Despite the performance improvements achieved by the interim material substitution, further material substitutions will be necessary in order to satisfy the 1800°-2200°F design requirements, as all resiliency was lost by cycle 20 in both spring tubes at 2000°F.

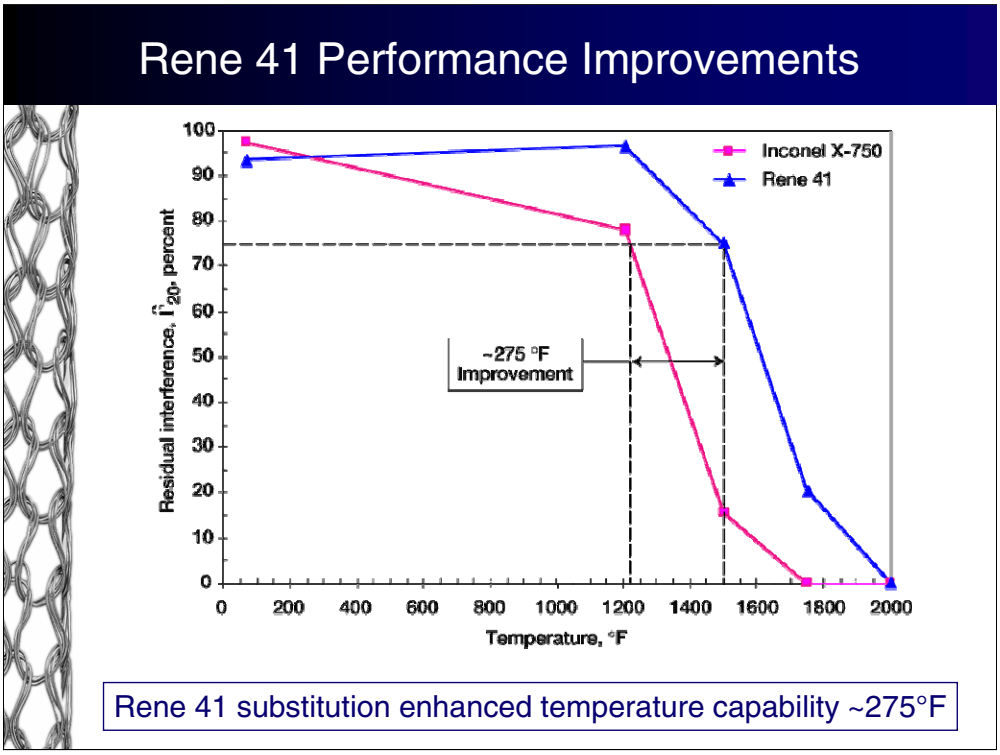

The chart above plots cycle 20 residual interference vs. temperature for both spring tube materials to highlight the improvement in temperature capability attained through material selection only. For an arbitrary 75% spring back, the substitution of Rene 41 for Inconel X-750 showed a temperature improvement of ~275°F.

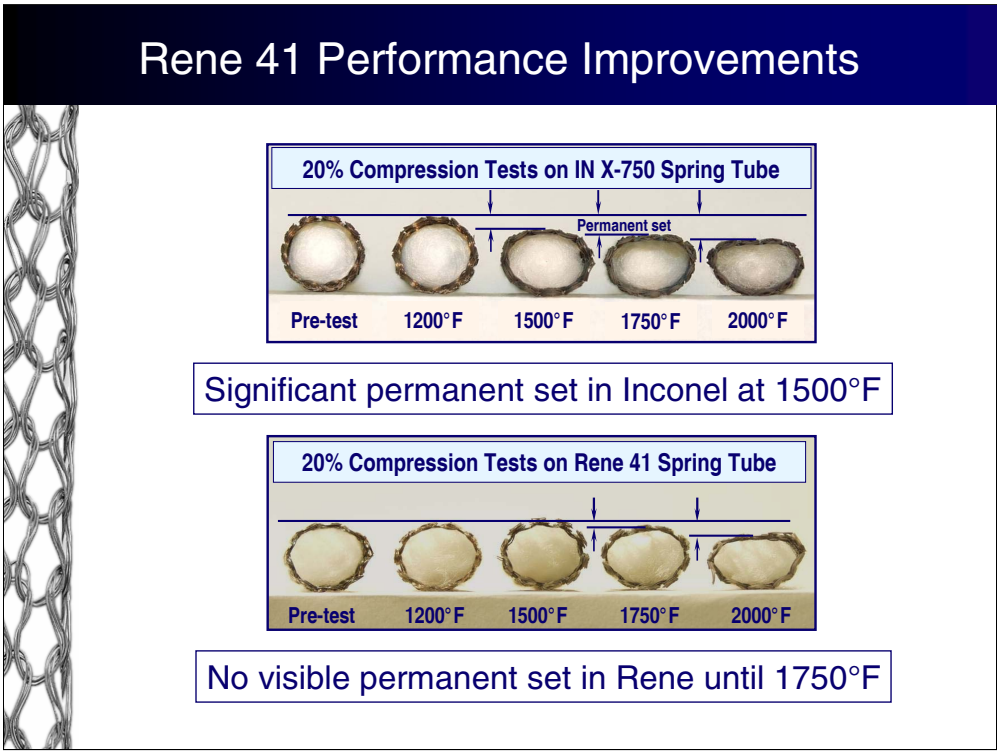

Calculated resiliency improvements resulting from material substitution were visually confirmed during post test inspection of the spring tube samples. As shown above, permanent set in the Inconel X-750 specimens was clearly evident at 1500°F. In the Rene 41 samples, however, resiliency loss was not visually distinguishable until 1750°F.

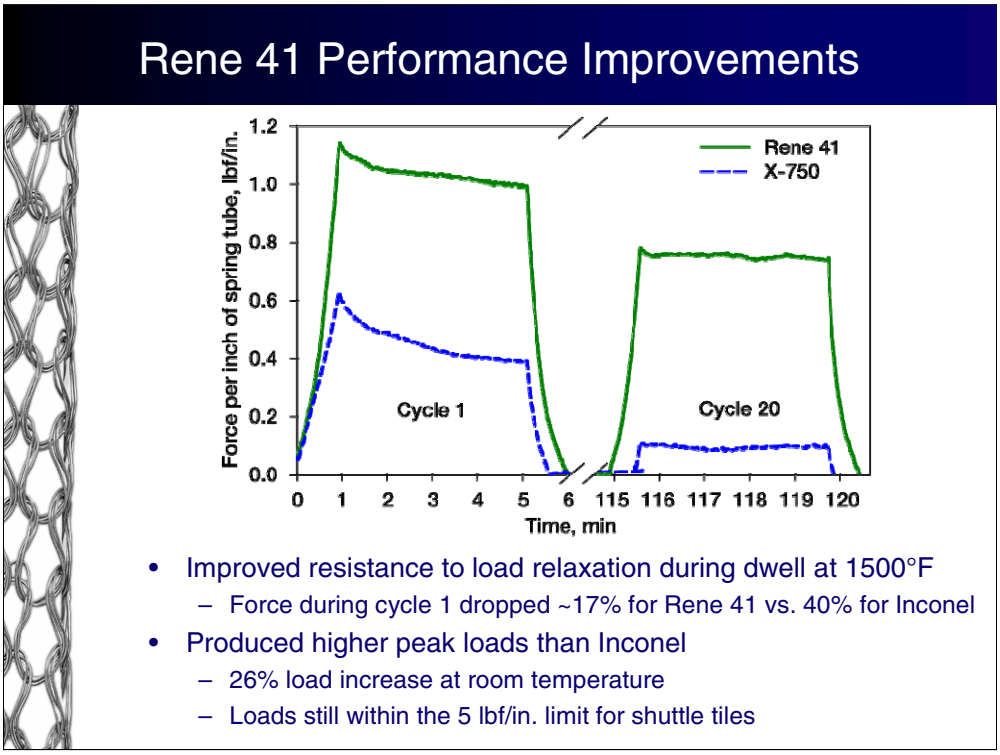

Rene 41 spring tubes knitted using the baseline knit geometry produced higher peak loads throughout all test cycles at 1500°F and resisted load relaxation during dwell better than the baseline Inconel X-750 spring tube samples. The plot of load vs. time above shows that during compression cycle 1, the load generated by the Inconel X-750 spring tube decreased approximately 40%, whereas the Rene 41 spring tube suffered only a 17% load relaxation. Even though the Rene 41 spring tube generated room temperature peak loads that were approximately 26% higher than those produced by the Inconel X-750 spring tube, contact forces were still well below the 5 lbf/in. load limit for Space Shuttle tiles.

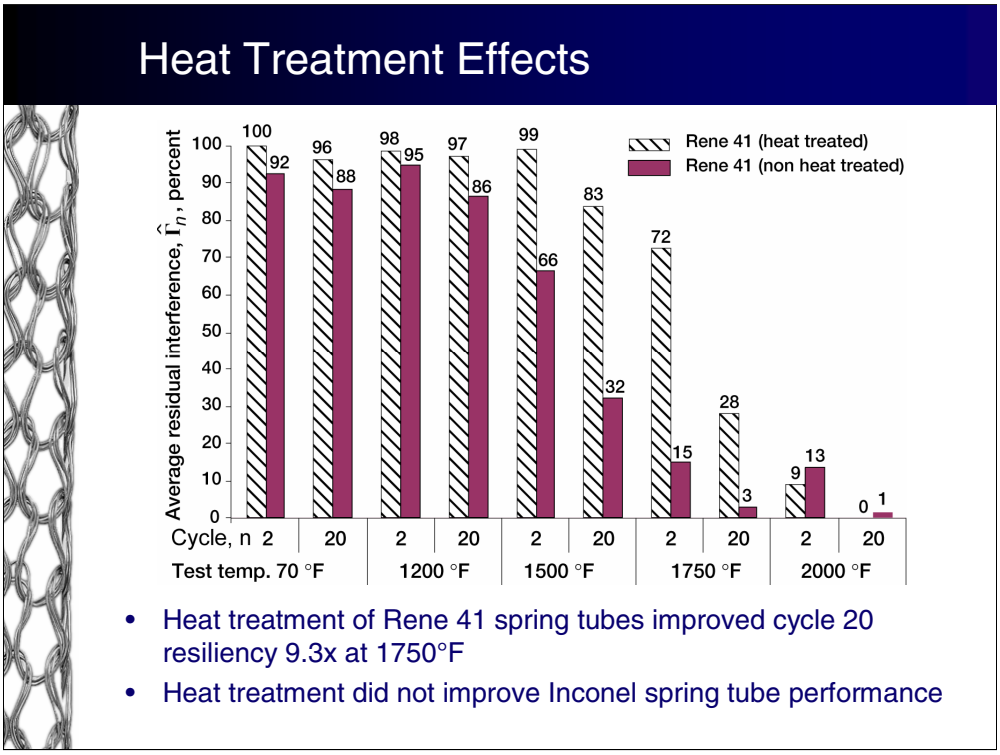

A comparison was also made during screening tests to determine the effects of heat treatment on the performance of the individual materials. As illustrated above, heat treated Rene 41 maintained much better high temperature resiliency than the non-heat treated samples. At the start of cycle 20 at 1750°F, heat treated Rene 41 spring tubes showed a 9.3x higher residual interference than the non-heat treated specimens. This behavior was not observed in tests of the baseline Inconel X-750 spring tubes.

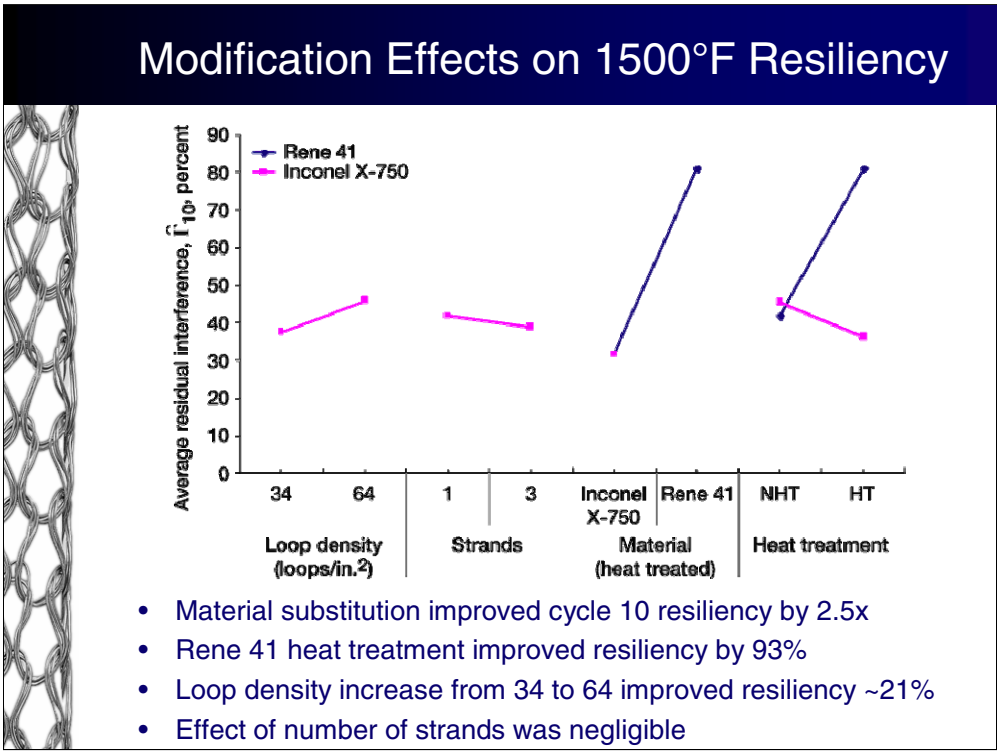

The effects plot above summarizes the relative influence of each of the evaluated spring tube factors on average residual interference at the start of cycle 10 for tests ran at 1500°F. As shown, the most significant factors were material selection and heat treatment of the Rene 41 spring tube. Material substitution of heat treated Rene 41 improved cycle 10 resiliency by approximately 2.5x when compared to the baseline Inconel X-750 spring tube. Heat treatment of the Rene 41 spring tube increased resiliency by 93% over the non-heat treated sample. Geometry effects were determined to be less significant; however, results did show that moderate performance improvements through knit geometry modification were feasible. Increasing the loop density in single stranded Inconel X-750 spring tubes from 34 to 64 improved residual interference by approximately 21%. Resiliency changes due to increasing the number of wire strands from 1 to 3 were determined to be negligible.

Further Improvements

- Rene 41 material substitution for Inconel X-750 yielded ~275°F temperature improvement
- Further improvements needed to reach design goal of 2200°F
  - Material selection
  - Heat treatment
  - Geometry
- Determination of dominant deformation mechanism
  - Identify creep or time-independent plastic flow as primary cause of resiliency loss
    - Eliminated test dwell periods and increased load rates to minimize 'time effects'
    - Tested heat treated Rene 41 spring tubes (standard geometry) at 1750°F

Screening tests showed that a material substitution of heat treated Rene 41 for the baseline Inconel X-750 alloy could increase temperature capabilities of the baseline knit geometry spring tube by ~275°F for an arbitrary residual interference of 75%. Preliminary geometry modifications also showed potential for enhancing spring tube performance. However, to reach the operating temperature design goal of 2200°F, further spring tube improvements will be needed. Utilizing data collected through the effects screening tests, material selection, heat treatment, and knit geometry will be revisited as opportunities for additional spring tube performance enhancement.

Previous tests showed a correlation between the temperature at which resiliency loss was detected and the temperature at which the alloys being tested were known to suffer significant decreases in yield strength. Permanent deformation in the spring tubes was suspected to be the result of both creep deformation and non time dependent plastic flow, but the dominant deformation mechanism was unknown. To distinguish between the two mechanisms, standard test conditions were modified to minimize the 'time effects' influencing the experimental results. Dwell periods were eliminated, and load rates were increased to limit the amount of creep deformation occurring during the tests. These tests were conducted at 1750°F using heat treated Rene 41 spring tubes with standard geometries and a 20% compression level.

Deformation Mechanism Identification

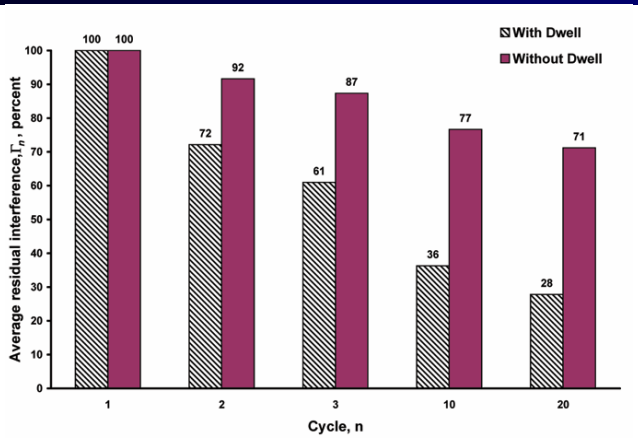

Eliminating dwell and increasing load rates at 1750°F

- Showed higher resiliency: 2.1x at cycle 10 and 2.5x at cycle 20
- Identified creep as dominant mechanism causing permanent set

The bar chart above plots average residual interference vs. compression cycle to illustrate the effect of eliminating the dwell periods and increasing load rate of the standard spring tube compression tests. Calculated resiliencies for spring tubes tested without dwell periods at maximum deflection were 2.1x higher at the start of cycle 10 and 2.5x higher at the start of cycle 20 when compared to the corresponding resiliencies calculated from standard compression tests with dwell periods. These results provided a strong indication that creep deformation was the dominant mechanism that will need to be addressed in order to further improve spring tube performance.

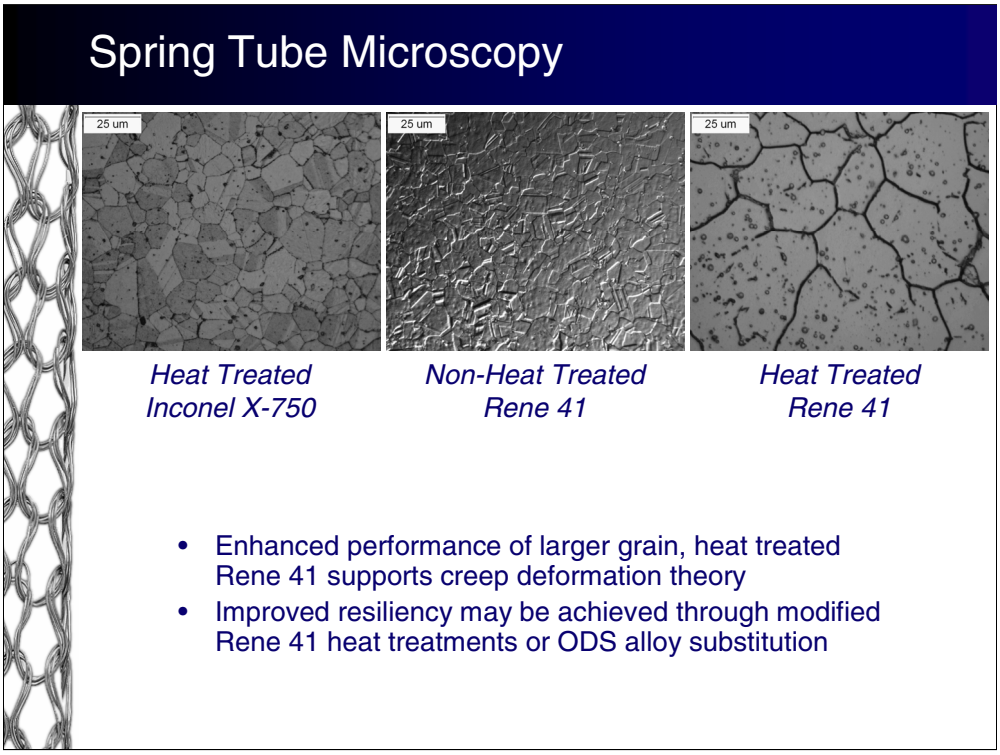

To support the theory identifying creep as the dominant deformation mechanism leading to permanent set in tested spring tubes, a microstructure evaluation was conducted. Untested samples of heat treated Inconel X-750, non-heat treated Rene 41, and heat treated Rene 41 spring tubes were mounted in epoxy, sectioned, and examined using an optical microscope. As shown above, heat treated Inconel X-750 and non-heat treated Rene 41 samples had comparable grain sizes. These two spring tubes performed similarly during high temperature compression testing, taking on significant permanent set, whereas larger grain, heat treated Rene 41 spring tubes showed significant resiliency improvement. These findings support the theory of creep dominance, as large grain metals are classically better for resisting creep deformation than fine grain alloys. Based on this, improved resiliency may be achieved through modified Rene 41 heat treatments or ODS (oxide dispersion strengthened) alloy substitution that would provide an enhanced resistance to creep deformation.

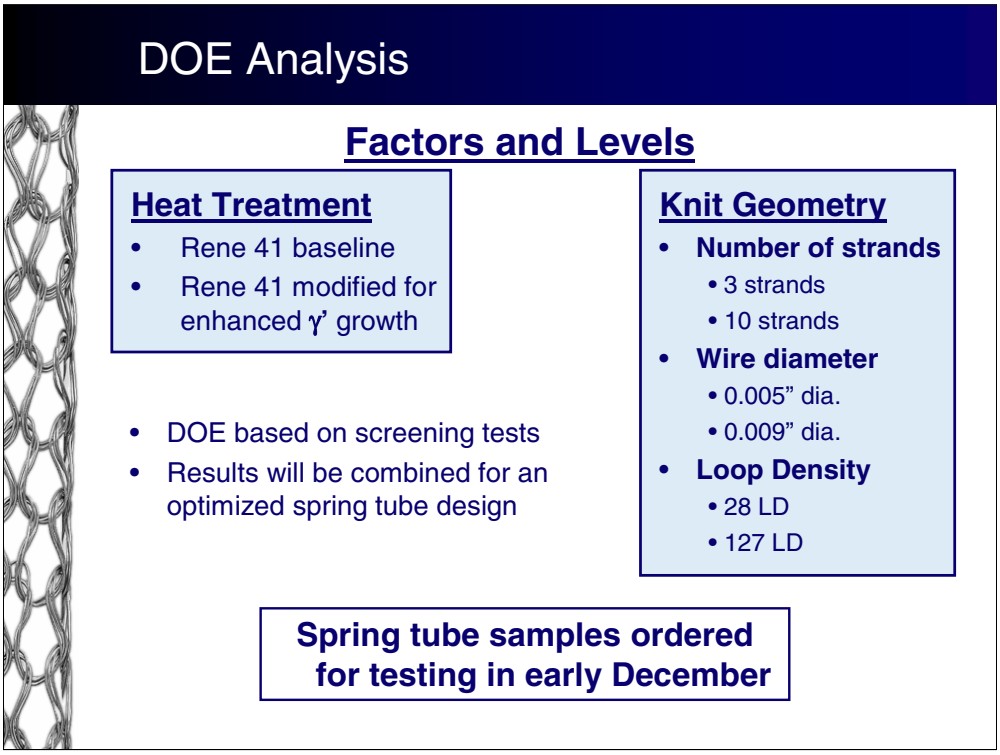

In order to apply and test the concepts for improving spring tube performance generated through preliminary testing, a formalized design of experiments (DOE) study will be conducted. The factors to be tested include heat treatment, number of strands, wire diameter, and loop density. The levels for these factors are presented above. Spring tubes will be fabricated from Rene 41 and tested using previously defined test parameters, including a 20% nominal compression, 1750°F test temperature, and a 250 second dwell period at maximum deflection during each of the 20 compression cycles. Results from these tests will be used to produce an 'optimized' spring tube design which will then be incorporated into a control surface seal for evaluation.

Conclusions

- Current baseline control surface seal is inadequate for future space vehicles
- Heat treated Rene 41 material substitution for Inconel X-750 yielded ~275°F temperature improvement
- Material substitution showed resiliency improvements as high as 5.2x at cycle 20, 1500°F
- Preliminary geometry modification showed resiliency improvements as high as 21% at cycle 10, 1500°F
- Creep deformation identified as dominant mechanism leading to resiliency loss
- DOE analysis will be used to optimize Rene 41 spring tube design
- Further material substitution may be needed to reach 2200°F design goal

MODELING OF CANTED COIL SPRINGS AND KNITTED SPRING TUBES AS HIGH-TEMPERATURE SEAL PRELOAD DEVICES

Jay J. Oswald and Robert L. Mullen
Case Western Reserve University
Cleveland, Ohio

Patrick H. Dunlap, Jr., and Bruce M. Steinetz
National Aeronautics and Space Administration
Glenn Research Center
Cleveland, Ohio

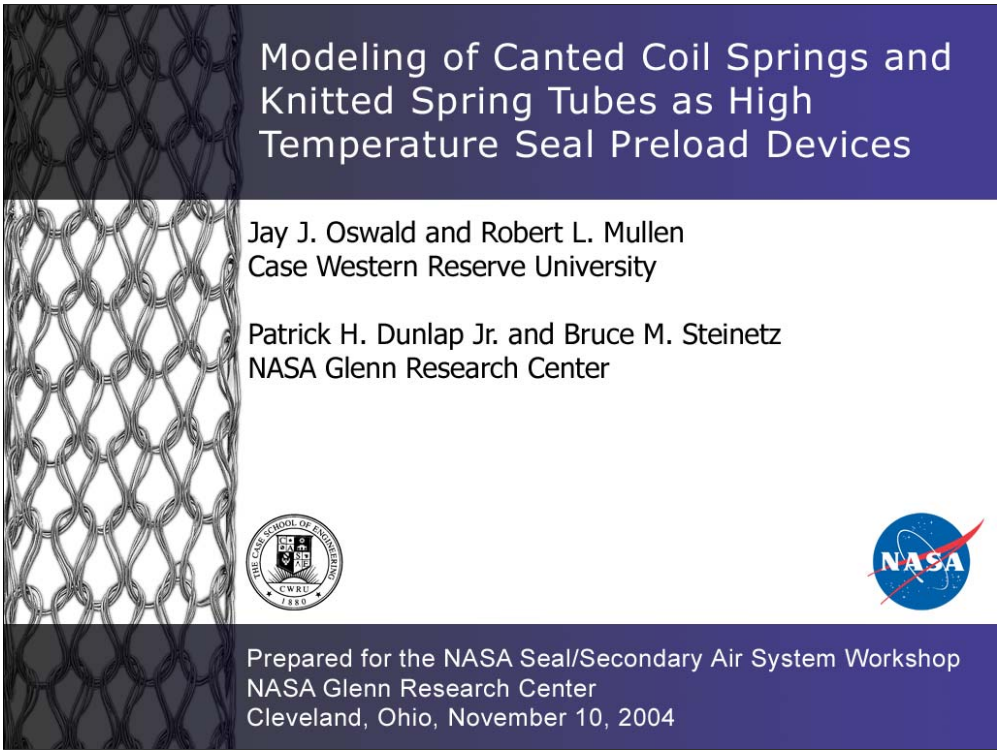

Seal Preloaders - Applications

Canted Coil Springs

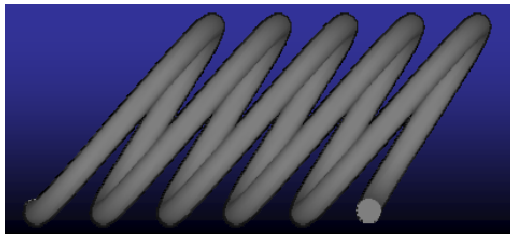

Canted coil spring installed behind wafer seals

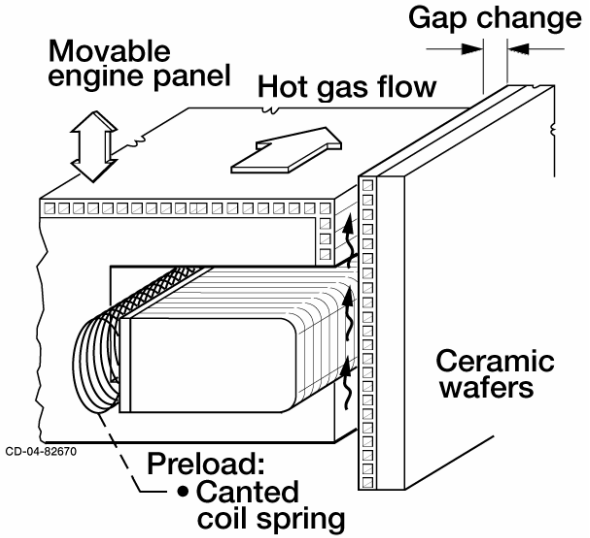

Knitted Spring Tubes

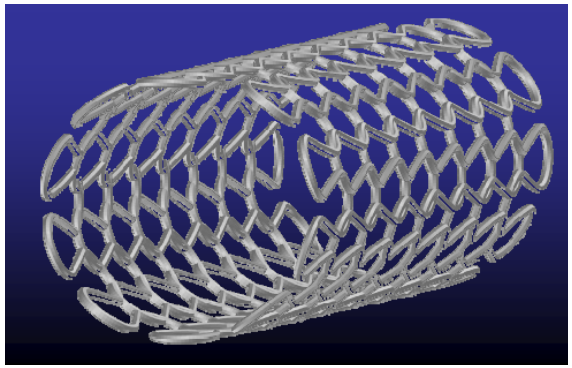

Spring tube in rope seal

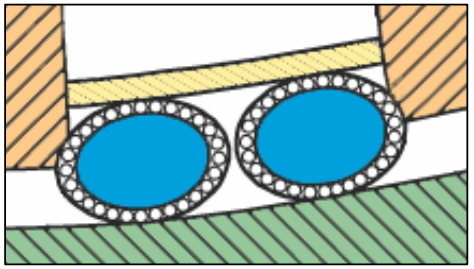

Rope seals installed in groove

Canted Coil Springs

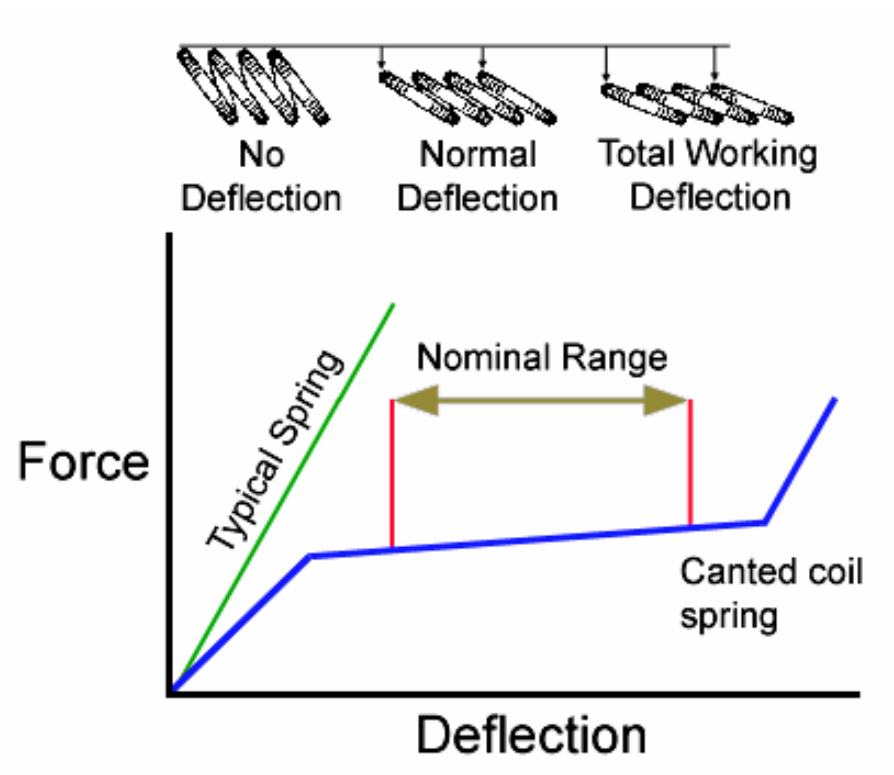

Canted coil springs offer a nearly constant force over a wide displacement range

Wire Mesh

- 20 node solid elements
- Mesh density refined by increasing:
  - Elements per face
  - Faces per unit length
- Evaluated low and high mesh densities

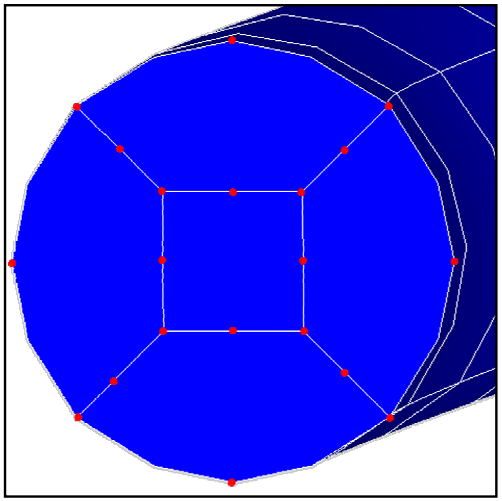

5 elements per face

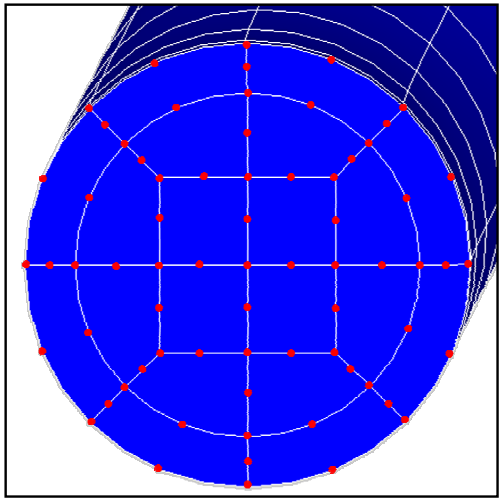

20 elements per face

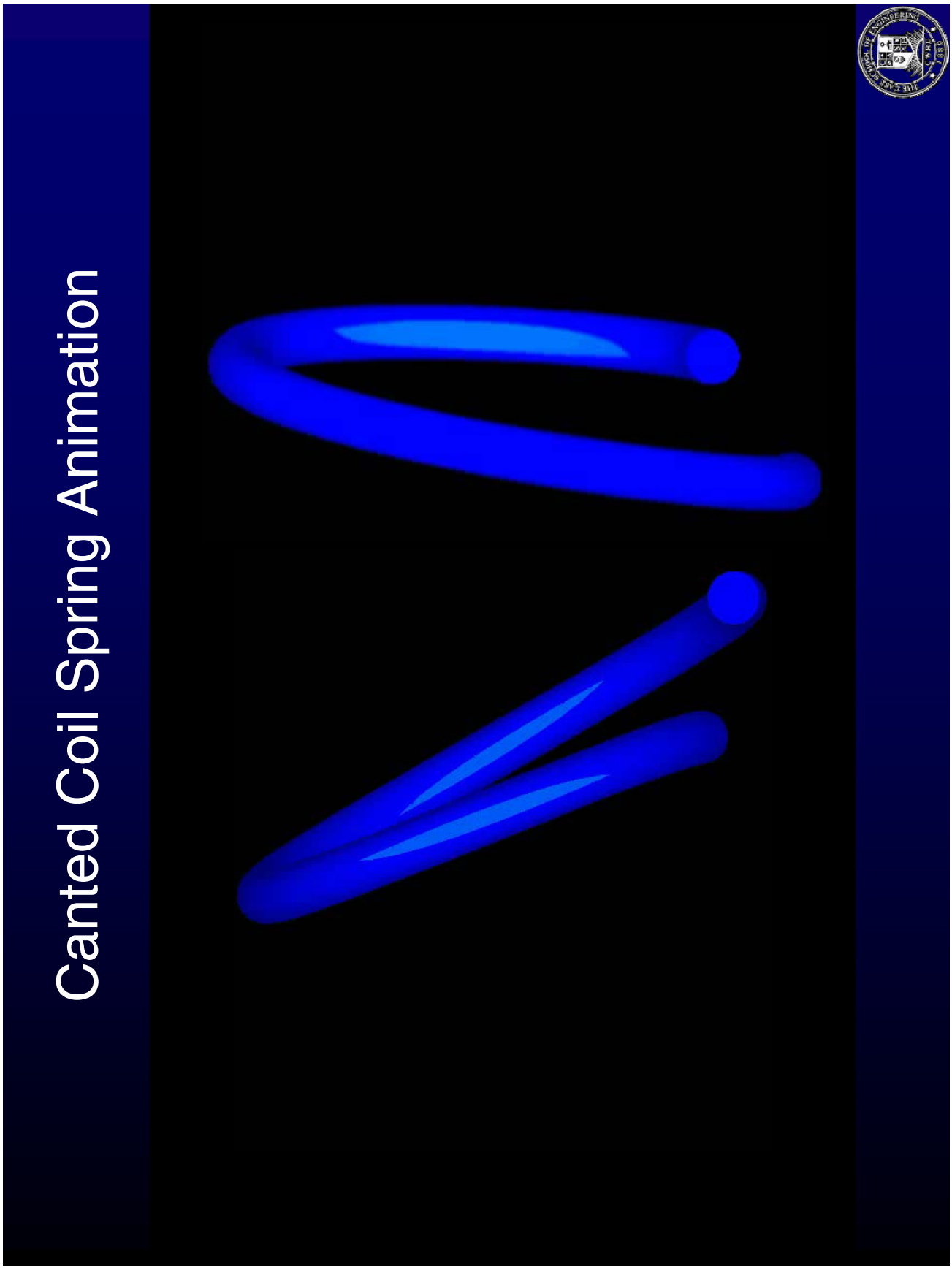
Canted Coil Spring Animation

Canted Coil Spring Behavior

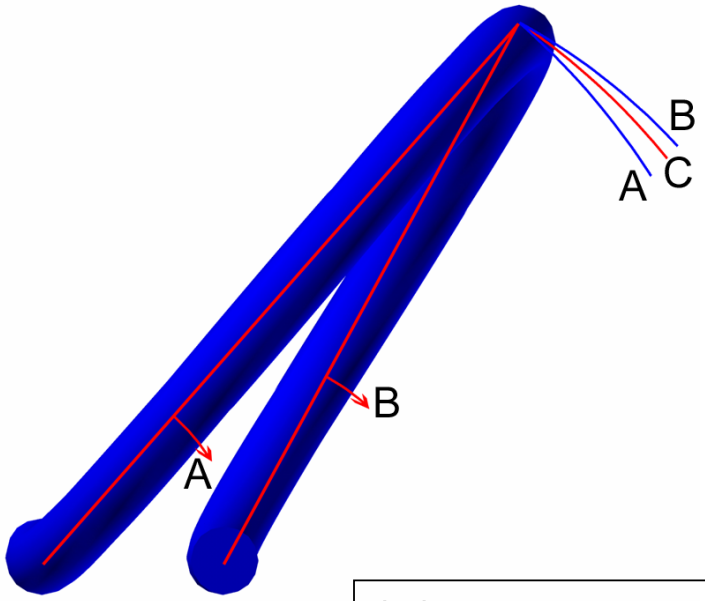

(A) and (B) rotate about the bottom of each coil.

Each arc must follow path (C)

(A) is stretched

(B) is compressed

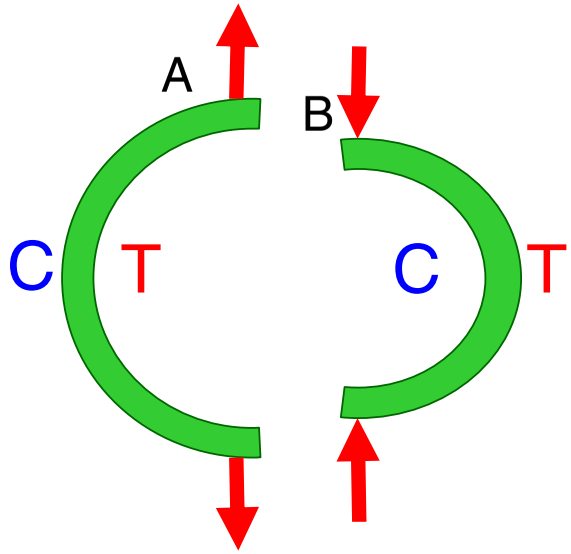

Verification of Spring Behavior Model

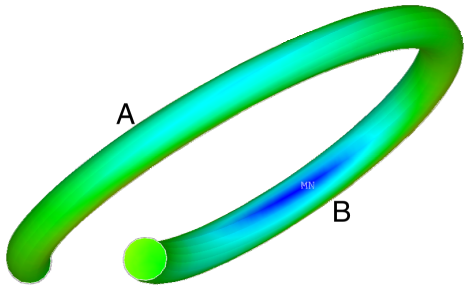

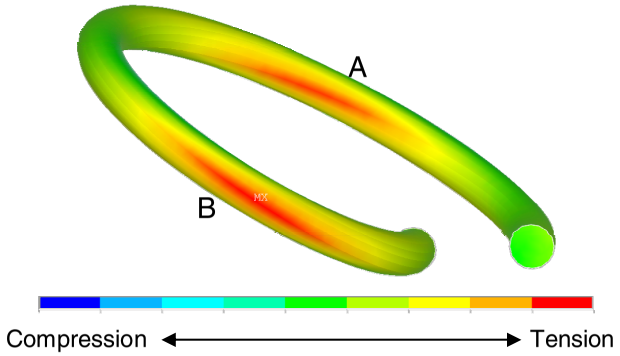

FEA results show compression and tension as predicted in behavior model

Canted coil springs store energy in bending rather than torsion

Comparison of Experimental and Analytical Results

Observations

- Good agreement in behavior and magnitude
- Model accuracy decreases with higher stiffness springs
- Model initially underestimates spring stiffness

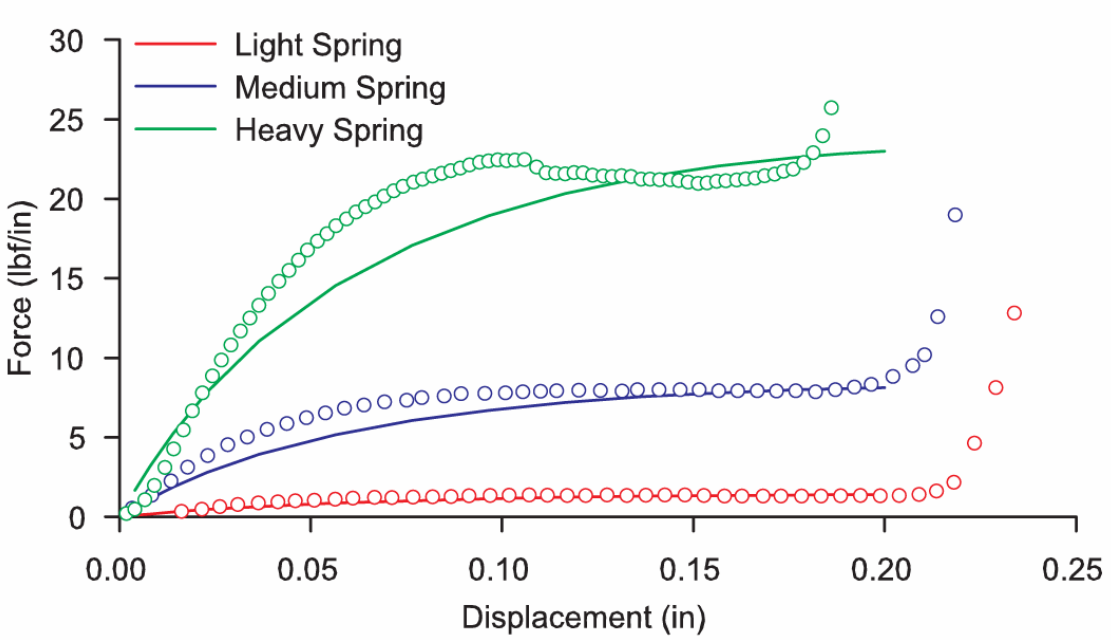

Effect of Spring Length

- Spring stiffness depends on length
  - Shorter segments are softer, more non-linear
  - Shorter springs compress axially under transverse loading

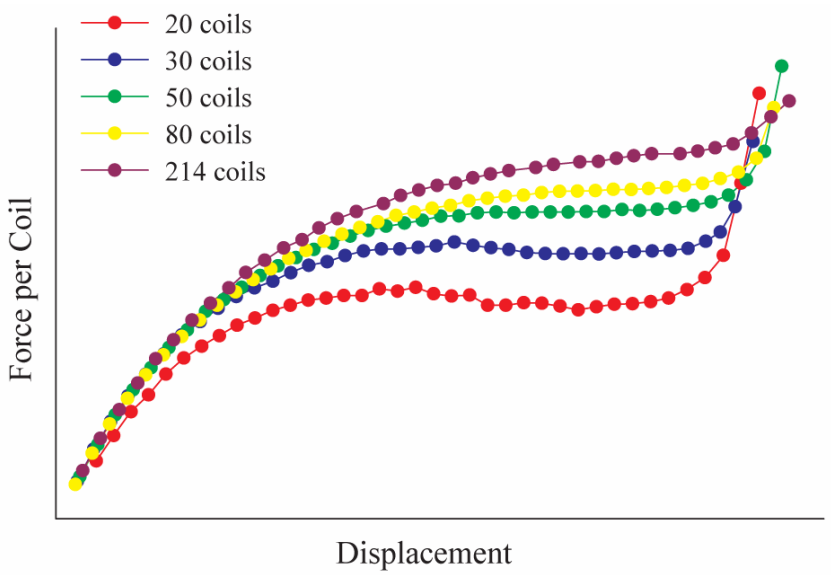

Effect of Friction on Canted Coil Springs

- Friction is modeled with a Coulomb approximation
  (F = μN)
- Increasing friction increases the stiffness of the spring

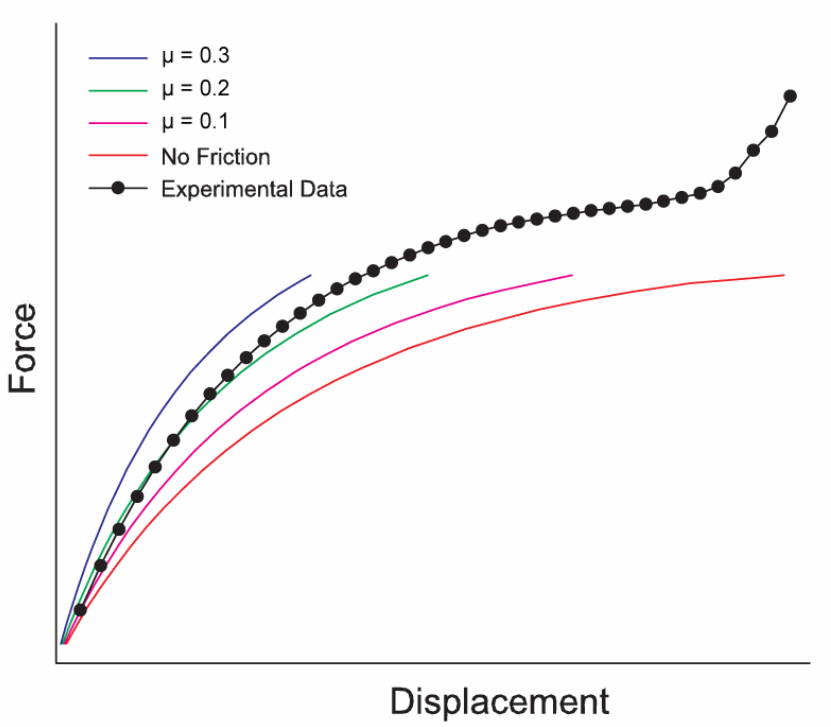

Summary of a Canted Coil Spring Parameter Study

Parameter study

- width
- eccentricity
- coils per inch
- wire diameter
- cant amplitude

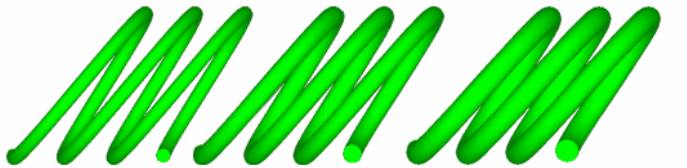

Increasing wire diameter

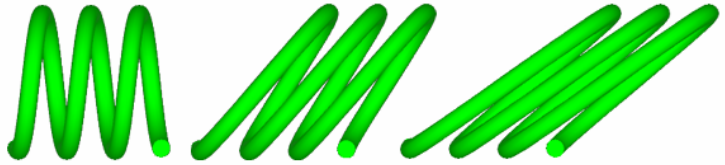

Increasing cant amplitude

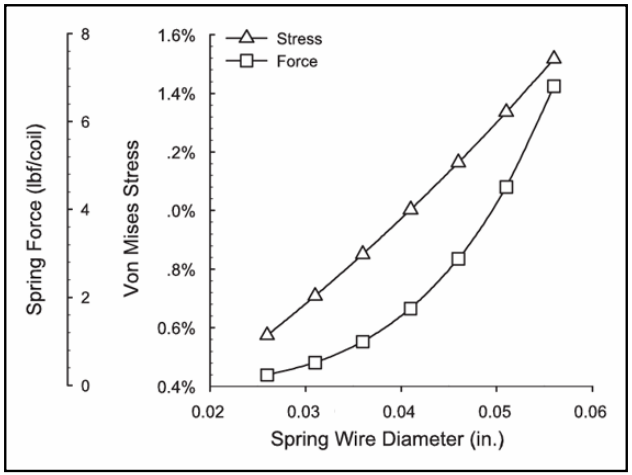

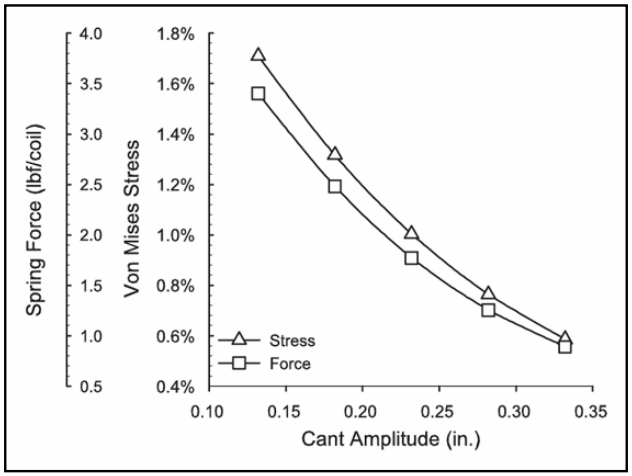

Spring Tube Construction

Base shape:
- Line
- Circle segment

→ Mirror base shape 2x → "Wrap" base shape pattern around helix → Stack helix pattern to create tube

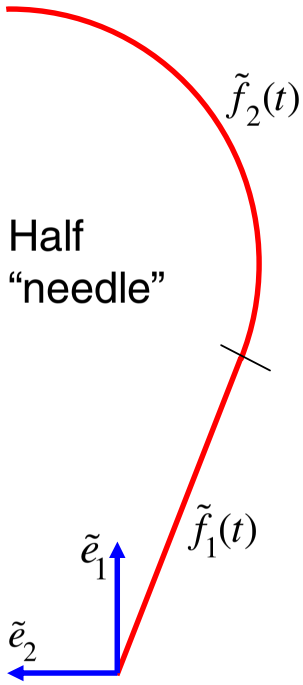

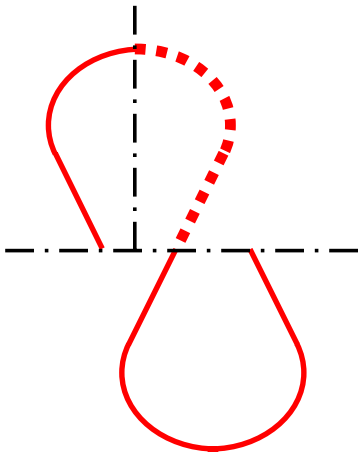

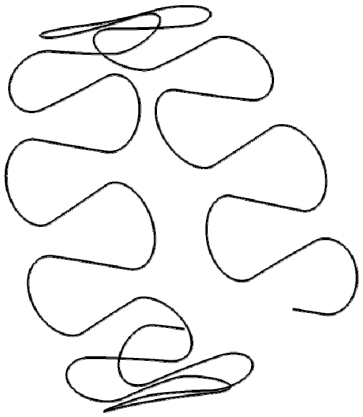

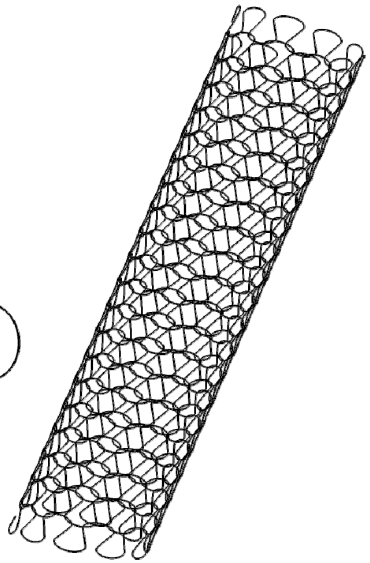

Symmetry/Node Coupling

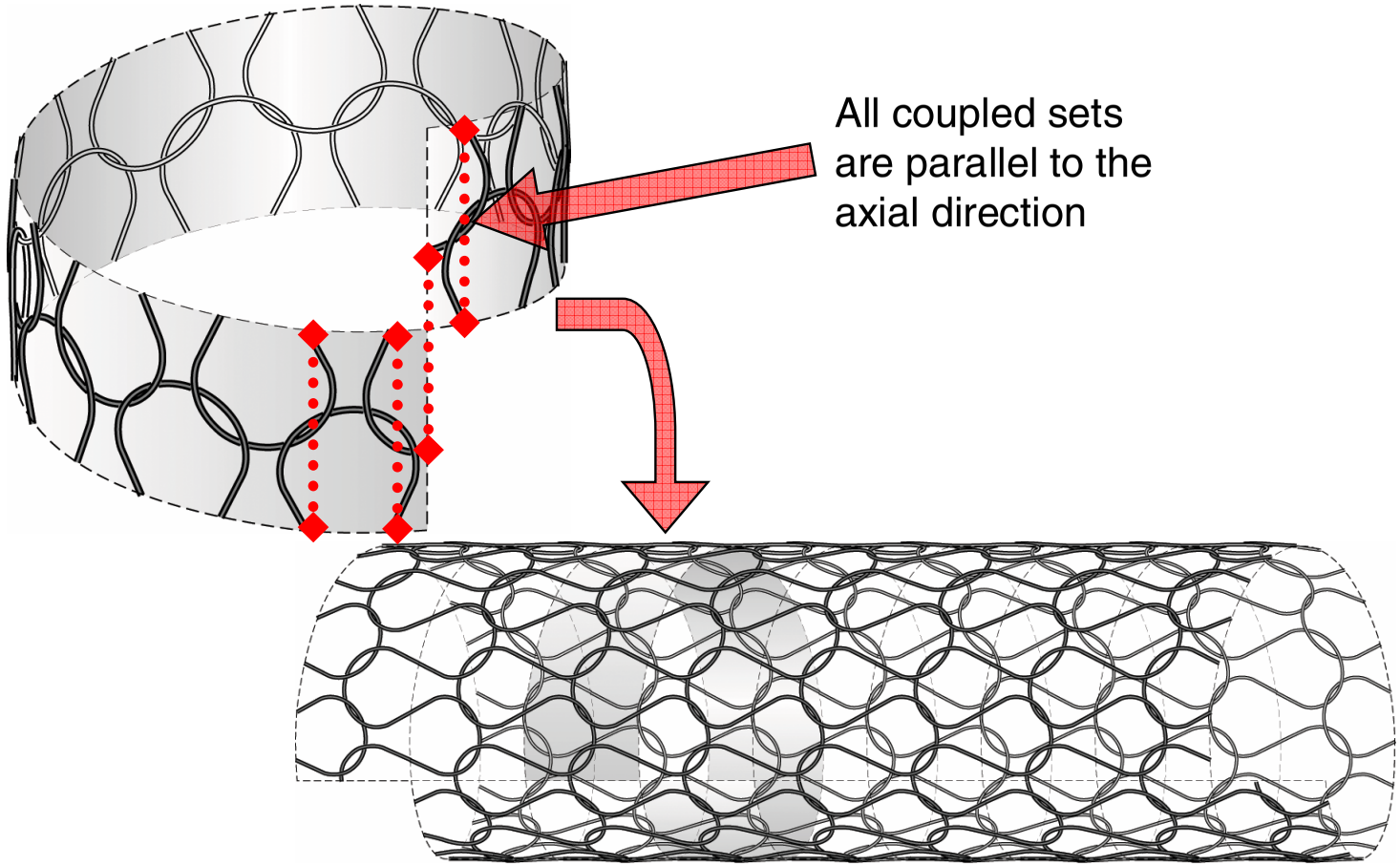

Needle Interaction Models

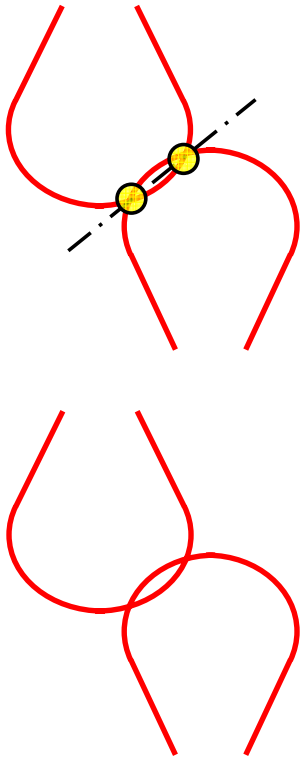

Linked: Needles are "hinged" with adjacent needles

Free: Adjacent needles have no influence on allowed motion

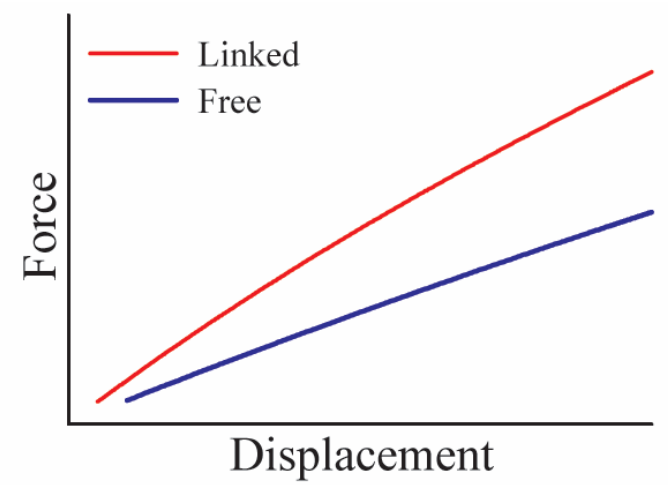

Linked needles assume more needle interaction and increase the stiffness of the model.

Spring Tube Animation

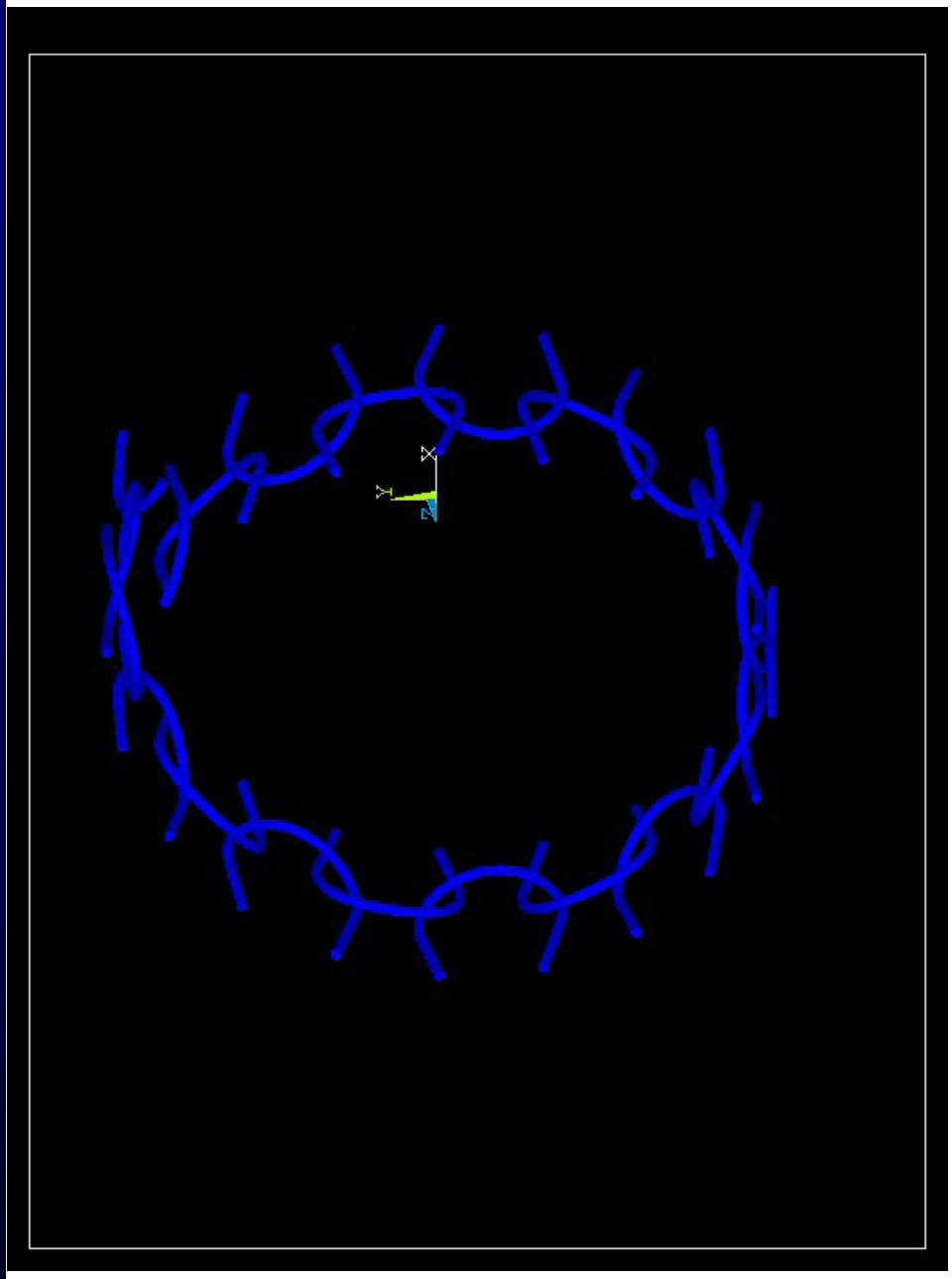

Single Strand Results

Single strand
6 courses per inch
10 needles per turn

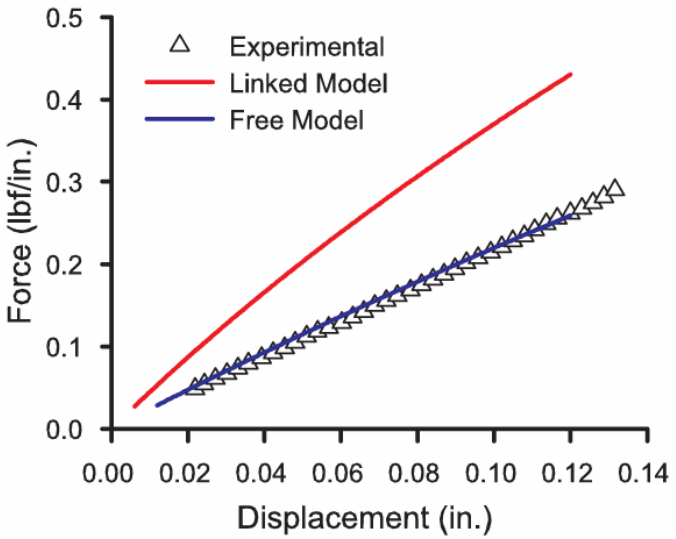

Single Strand
7 courses per inch
16 needles per turn

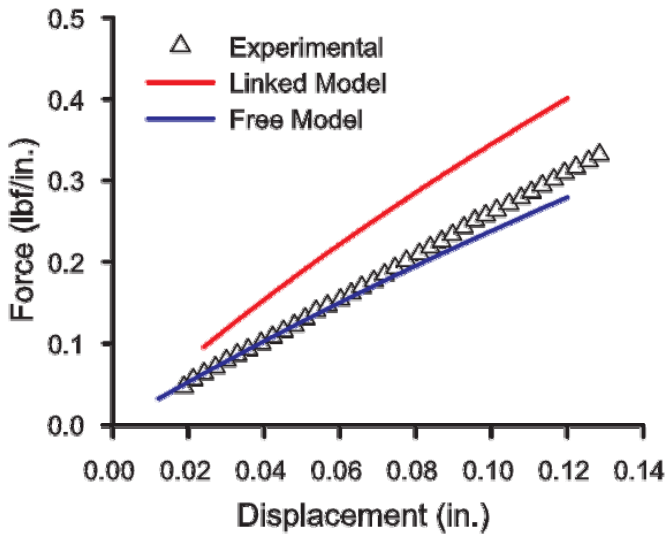

Both single strand cases are best approximated with free (unlinked) needles

Triple Strand Results

- Experimental data shows 2 regions
  - Small compression – less interaction
  - High compression – more interaction
- Line slopes
  - Linked model: 0.007 lbf/in.
  - High compression 0.007 lbf/in.
  - Unlinked model: 0.004 lbf/in.
  - Low compression 0.005 lbf/in.

Triple strand
4.9 courses per inch
10 needles per turn

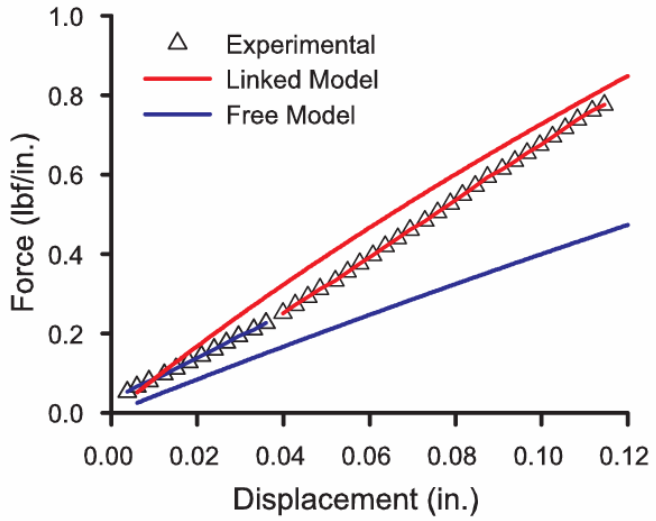

Higher wire density spring tubes exhibit more needle interaction

Summary of Preload Device Analyses

- Both models verified with experimental data
- Canted Coil Spring
  - Energy storage is in bending
  - Including a friction model and comparing with a longer test spring improves accuracy
- Spring tube
  - Linear behavior predicted
  - “Free” needles model is better for less dense tubes
  - Combination of “free” and linked models yields best prediction for more dense spring tubes
- Both models guide and optimize design of high temperature seal preload devices

HIGH-TEMPERATURE METALLIC SEAL DEVELOPMENT FOR AERO PROPULSION AND GAS TURBINE APPLICATIONS

Greg More
Advanced Products
North Haven, Connecticut

Amit Datta
Advanced Components and Materials
East Greenwich, Rhode Island

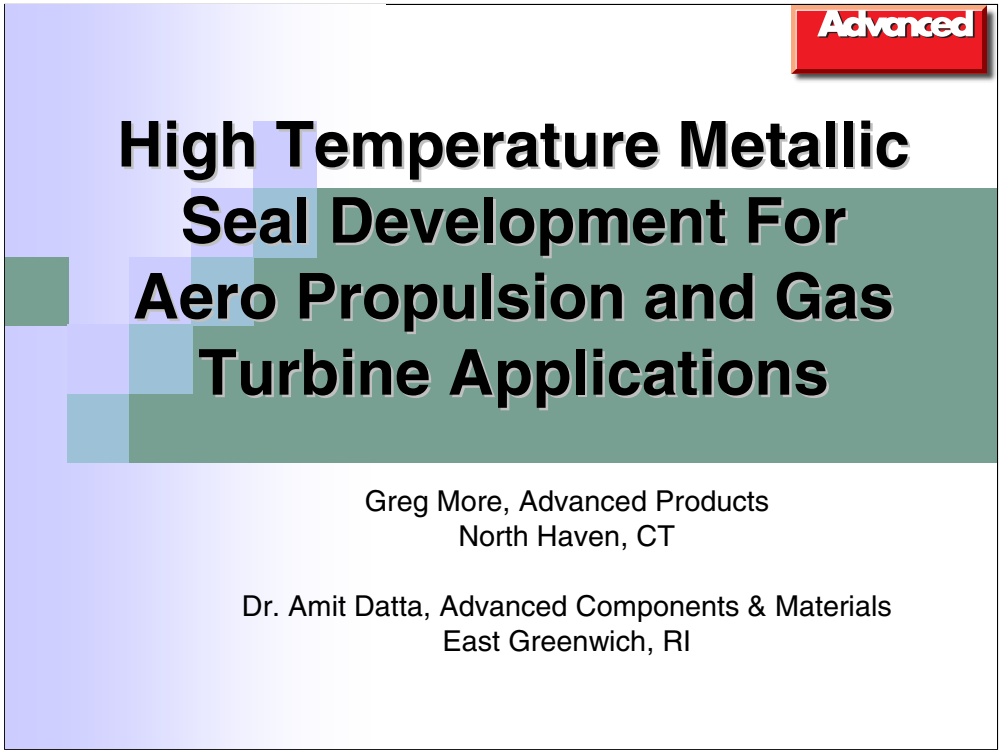

Outline

- Background
- Innovative seal design with turbine blade alloy spring and its performance
- New concept with single crystal blade alloy springs
- Conclusions

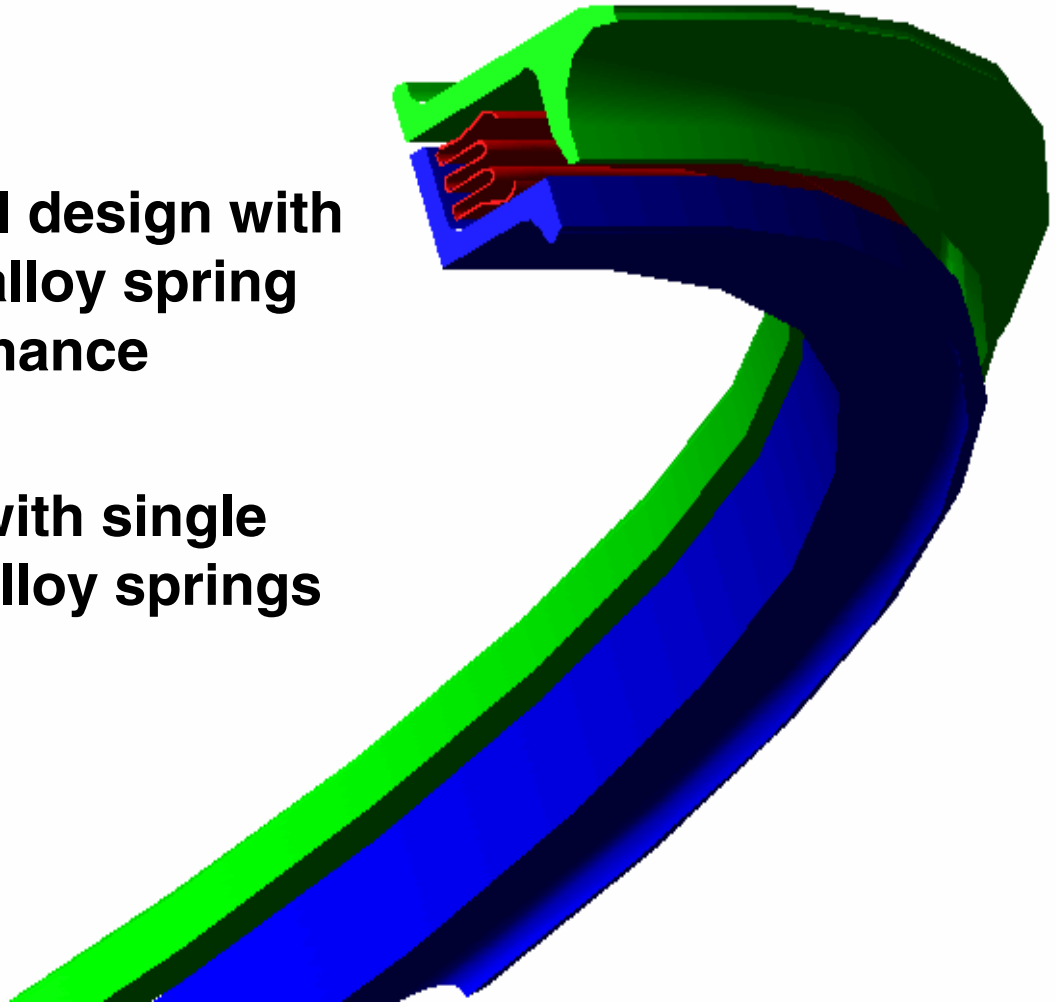

Advanced

Background: Stress relaxation of current cold formable seals

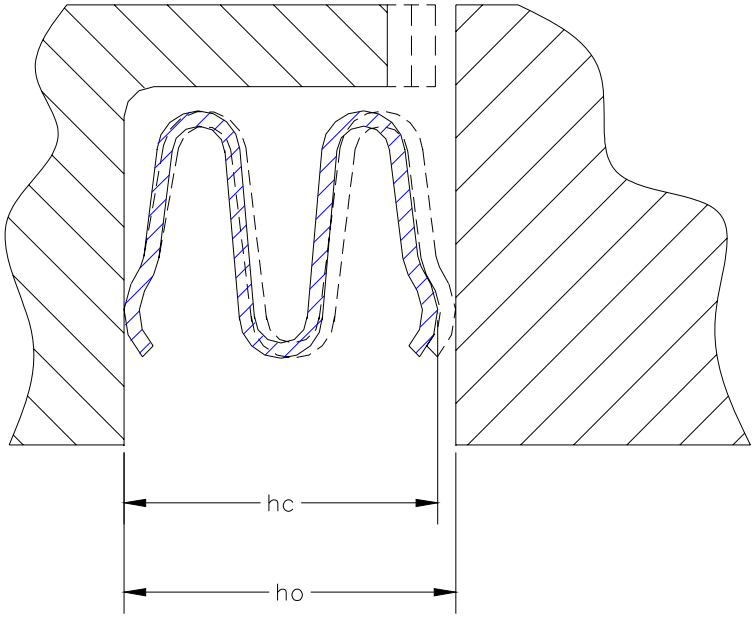

Seal gap is created resulting from stress relaxation at elevated temperatures. The original seal height ho is reduced to hc creating a gap when the flange moves away from the compressed condition.

Advanced

Background: Inefficiency associated with current seals

- Expensive bleed air is needed for cooling current seals if used above 1300ºF. Less compressed air is available to generate power!
- Seals are protected from high temperature environments with complex structures, increasing weight and cost

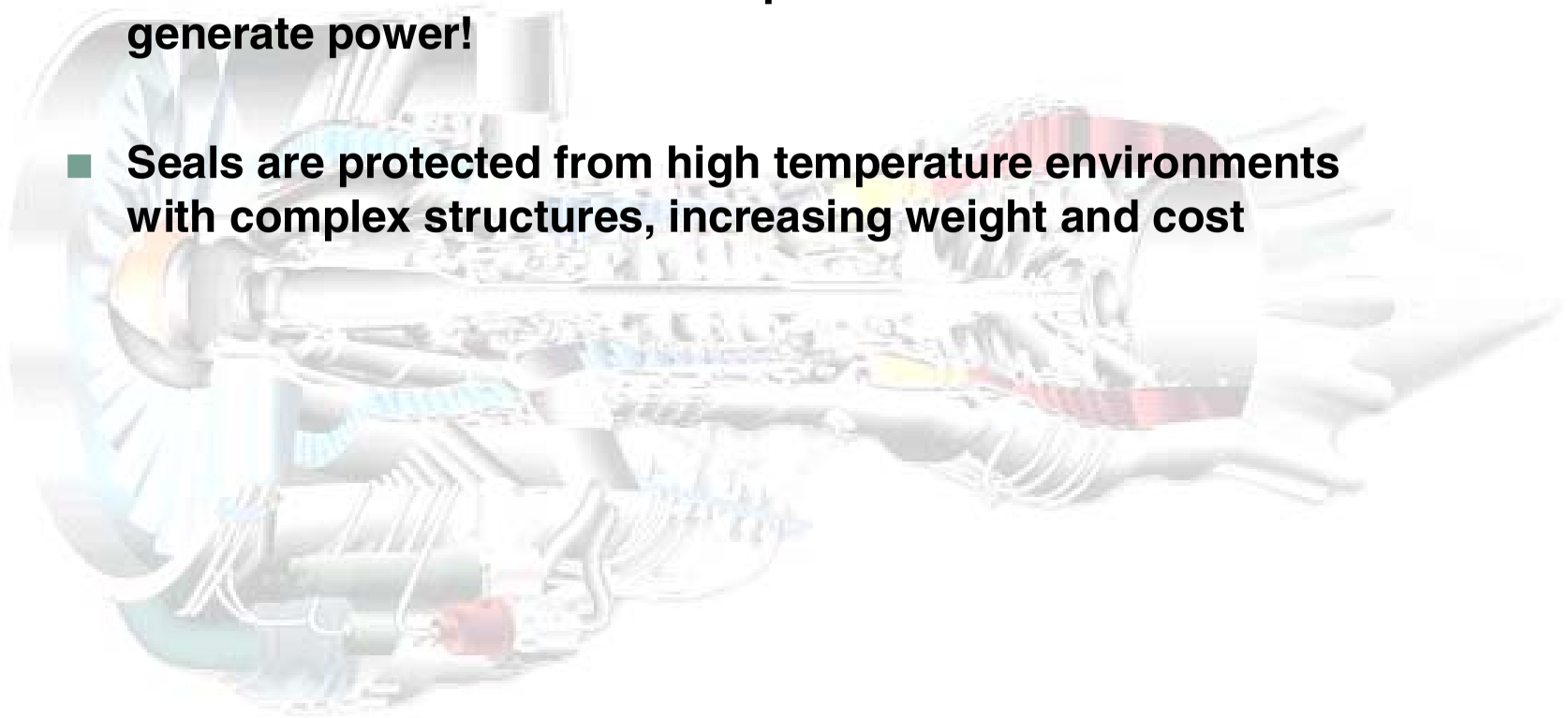

Advanced

Background: Market Needs for High Temperature(1500 - 1800ºF)Seals or Springs

- Reduce cooling air and simplify seal cavity structure in current gas turbine engines.
- Gas Turbine Combustor applications to hold the CMC liner.
- Spring loading device for extremely high(>2000ºF) temperature ceramic sliding seals.
- Seals for engine heat exchanger panels and back-up structures for future hypersonic engines.

Innovative Seal with Blade Alloy Spring

Thin cold formable alloy jacket providing a continuous sealing surface

Cast blade alloy spring energizer for operation up to 1800 °F

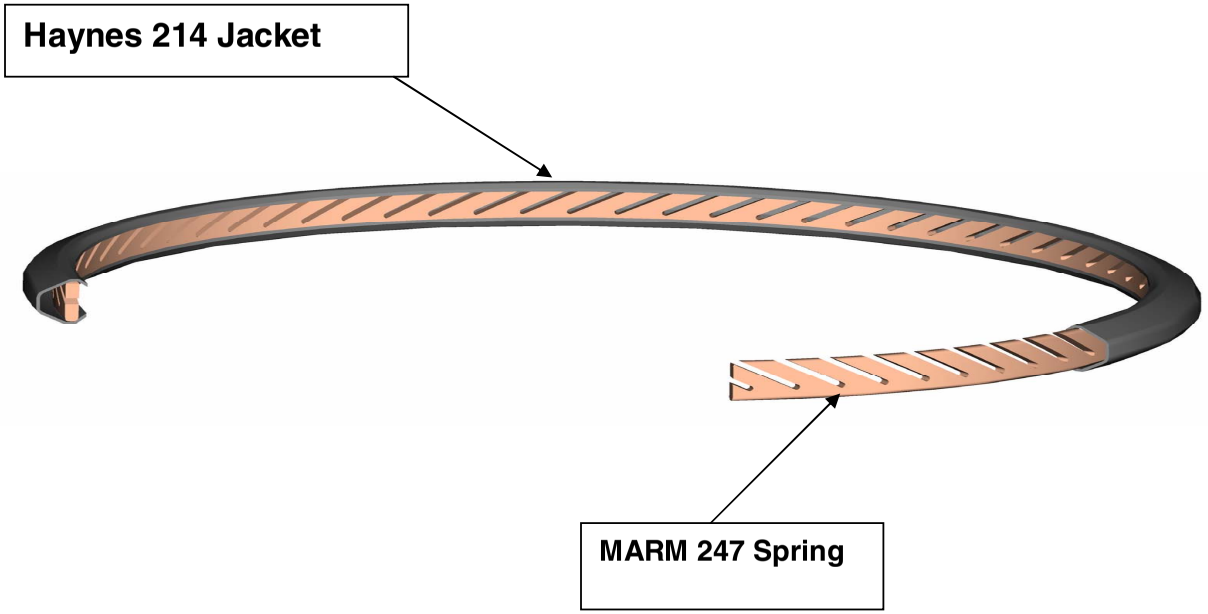

Advanced

Innovative Seal with Blade Alloy Spring

Cast Blade alloys have extremely high strength

Alloy	Temperature,º F	Yield Strength,ksi	Elongation,%
MARM 247, poly crystal	1400	130	12
CMSX4, Single crystal	1600	114	18
INCO 718,poly crystal	1472	100	10
Waspaloy,poly crystal	1600	75	35

Blade alloys also have superior creep and stress rupture strength compared to cold formable superalloys. Hence, blade alloys have higher resistance to stress relaxation.

Blade alloys are available only in the cast condition (poly or single crystal)

Advanced

Innovative Seal with Blade Alloy Spring

Comparison of high temperature sealing design

Standard E-Seal produced from high temperature Waspaloy alloy

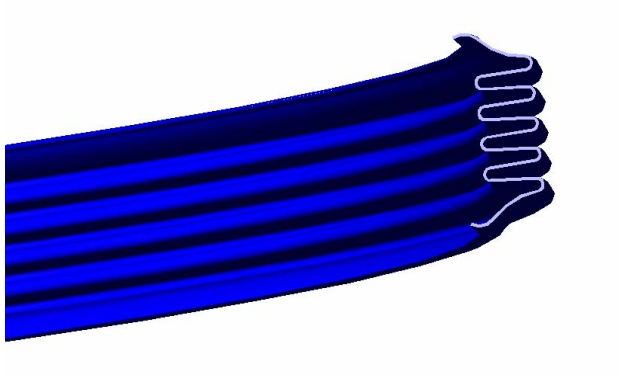

Cross section

Standard E-Seal with blade alloy spring

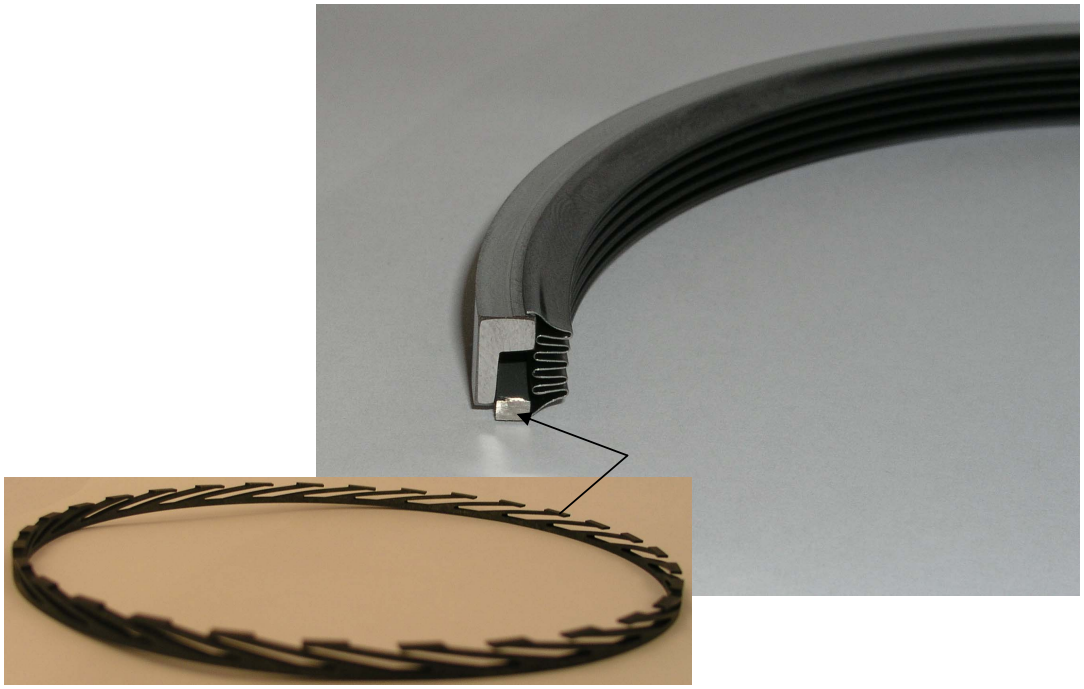

Cross section

Innovative Seal with Blade Alloy Spring

Experimental procedure:

- Seals were compressed 20% between flanges and heated to 1600 °F for various time periods
- After each exposure, seals were cooled to room temperature to measure change in seal free height
- Seals were leak tested to evaluate high temperature exposure on sealing performance
- Both free height change and seal leakage were plotted as a function of exposure time at 1600 °F

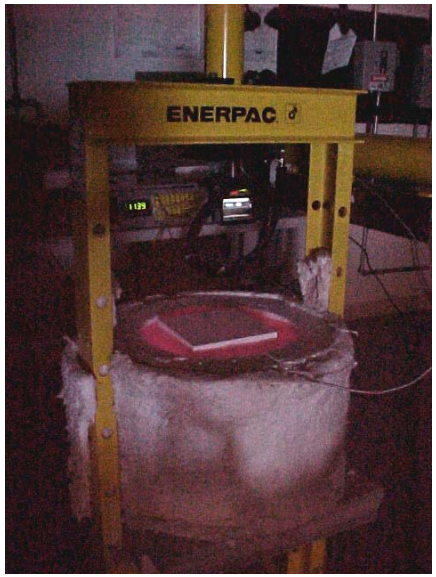

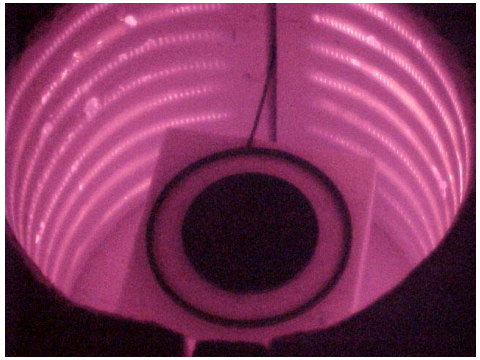

Advanced

Innovative Seal with Blade Alloy Spring

Comparison of seal free height change vs. exposure time at 1600F

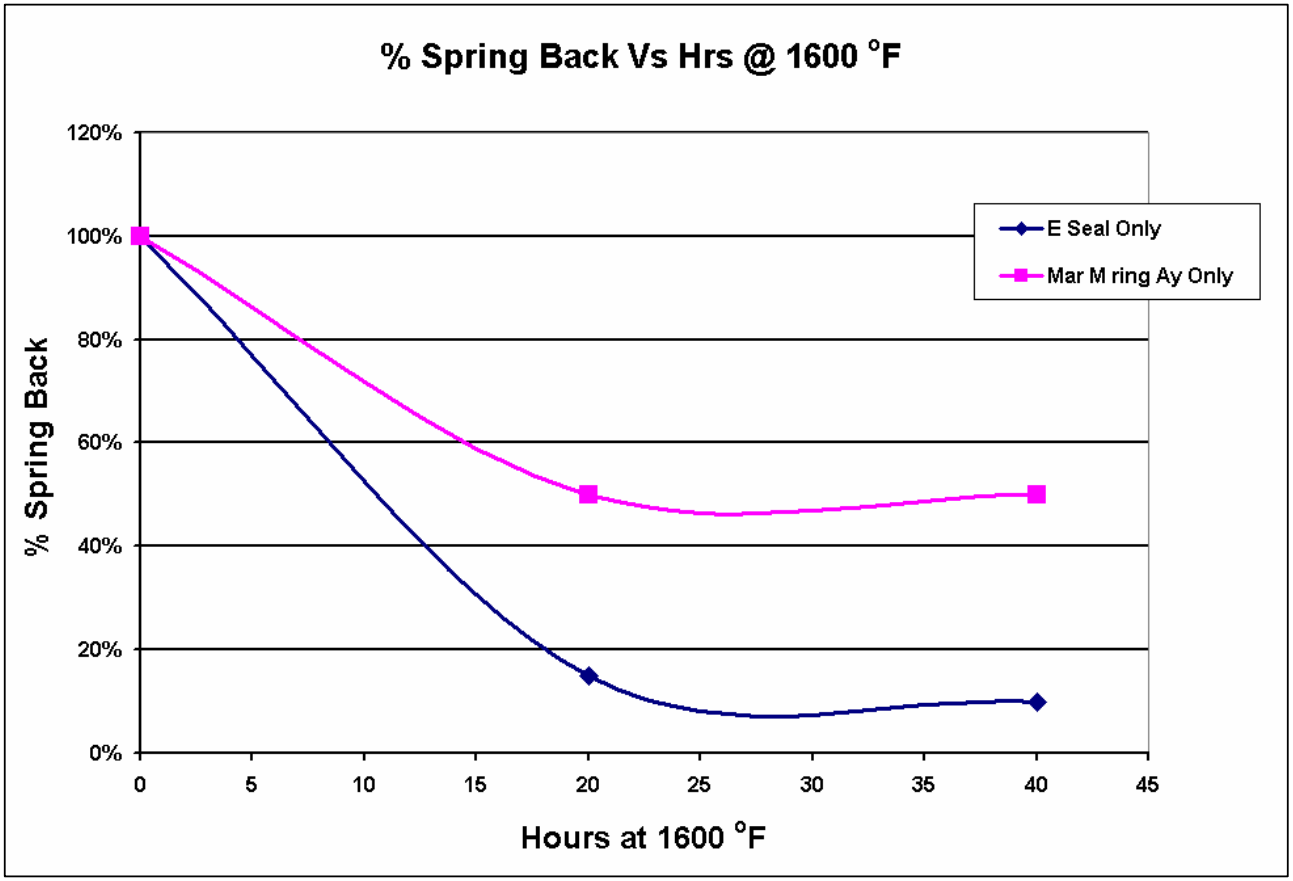

Advanced

Innovative Seal with Blade Alloy Spring

Comparison of seal leakage vs. exposure time at 1600F

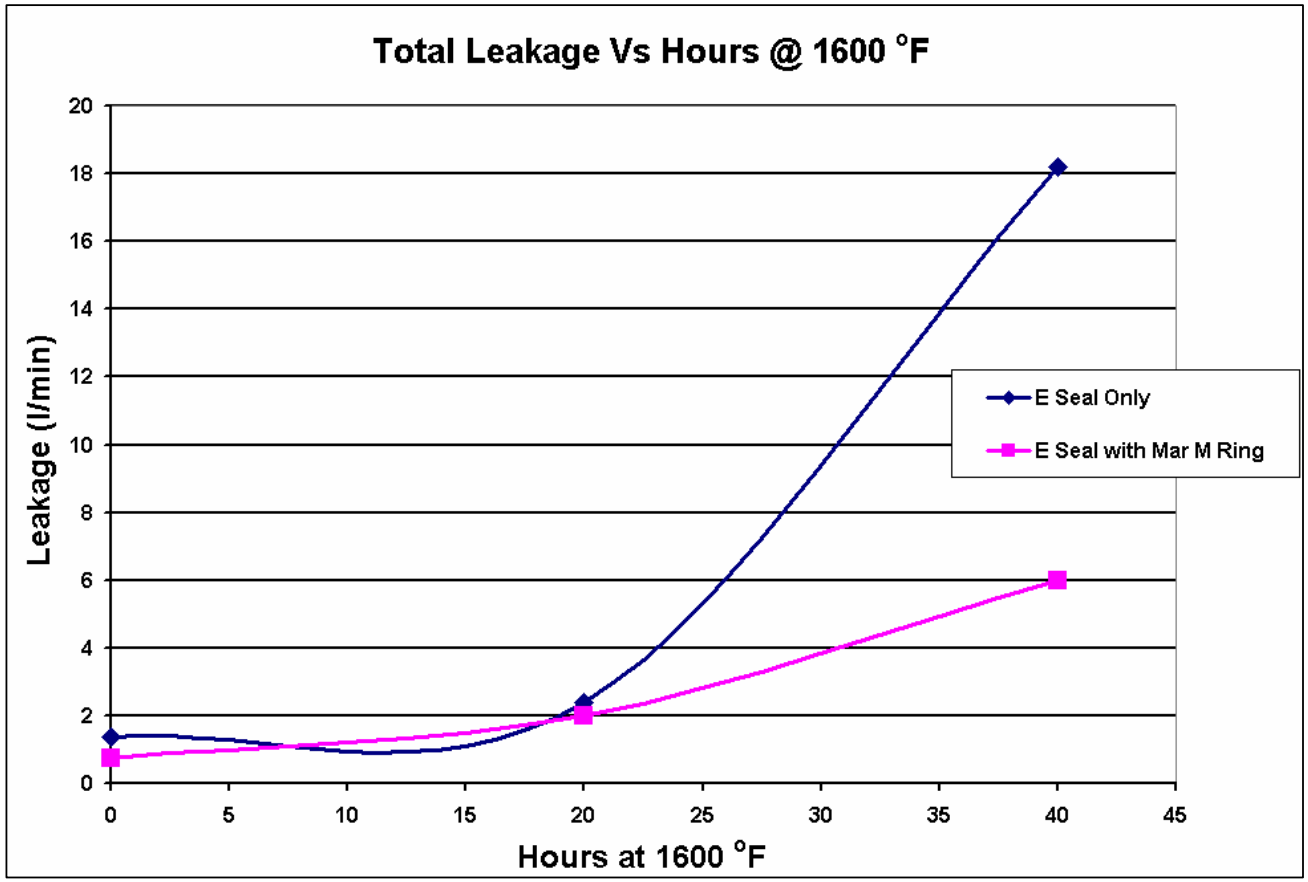

New Design with single crystal spring

- Cast polycrystalline MARM247 ring was machined using EDM --- prohibitively expensive!
- By controlling finger design(angle, thickness, width, #of fingers/linear inch…) spring rate or sealing load could be adjusted
- Single crystals are more resistant to creep and stress relaxation because of the elimination of grain boundaries
- Single crystal fingers can be cast to near–net shape and attached to easily machinable and cheaper superalloy ring

Advanced

New Design with single crystal spring

Cost effective design with cast single crystal blade alloy springs attached to lower cost machined ring

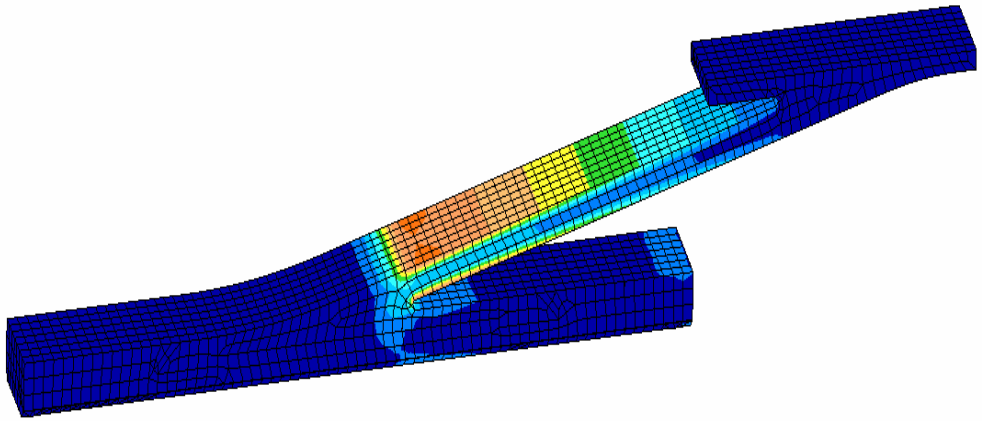

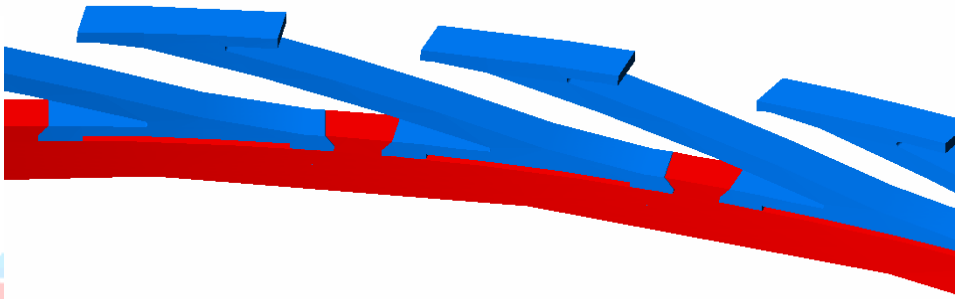

Advanced

New Design with single crystal spring

- Highest stress components(fingers) are made from the most creep resistant single crystals, cost effectively cast to net shape
- Individual fingers are attached to a lower cost superalloy ring which are easily fabricated. Stresses in the ring are significantly lower
- Device spring rate can be easily changed by selecting the # finger/linear inch and the finger design

New Design with single crystal spring

- By selecting “soft” crystallographic axis, <100>, along the spring axis, the elastic range of deflection can be maximized
- For Ni, $E_{111}/ E_{100} = 2.2$
- Elastic range of seal height change or seal deflection can be more than doubled by selecting crystal orientation
- FEA optimization has yielded designs with elastic ranges more than 30% of seal height at 1600-1800ºF

Advanced

Influence of Crystallographic Direction on Seal Deflection Capabilities

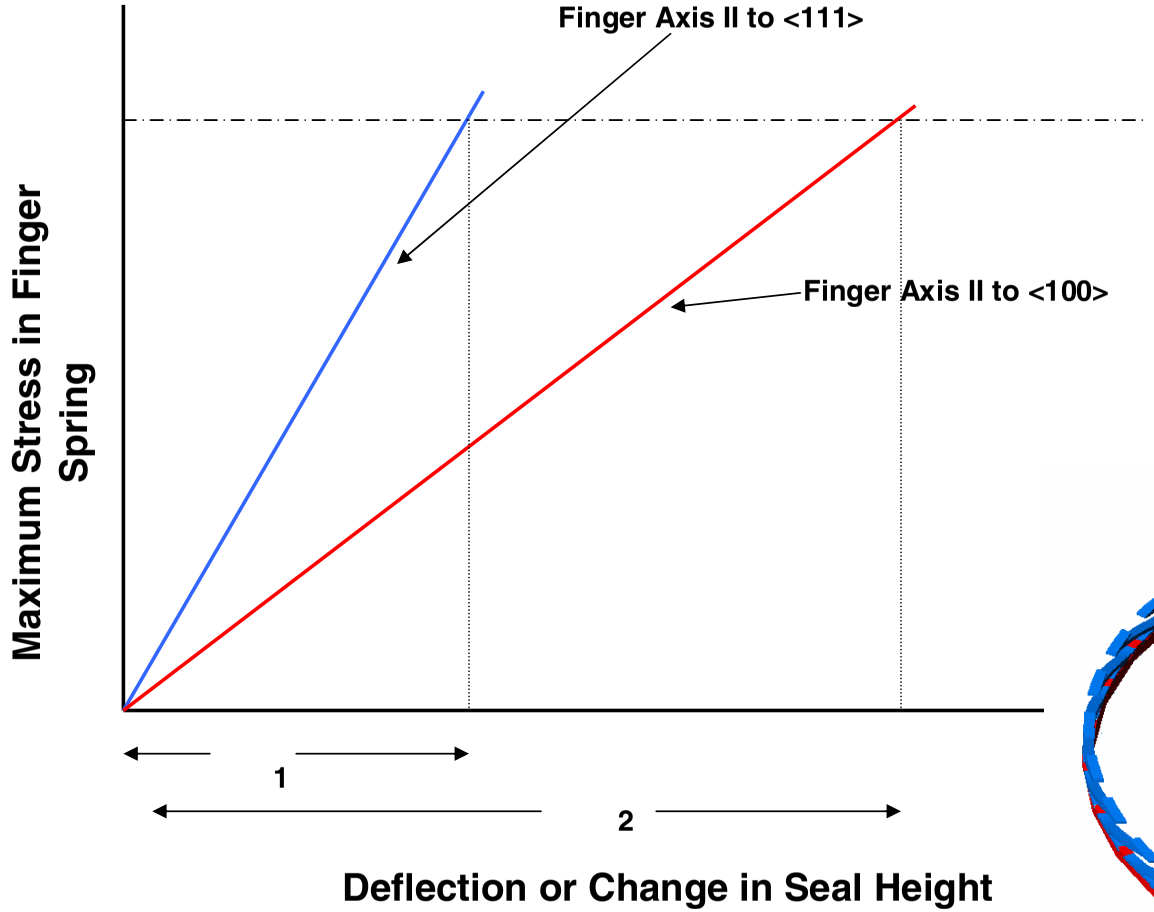

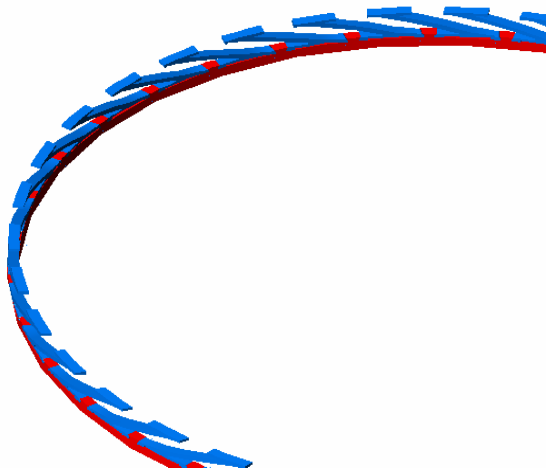

Advanced

New Design with single crystal spring

Applications other than seals

Transition fastener between metal and ceramic components with a large α-mismatch

Combustor CMC liner– low load, large deflection spring at 1800F

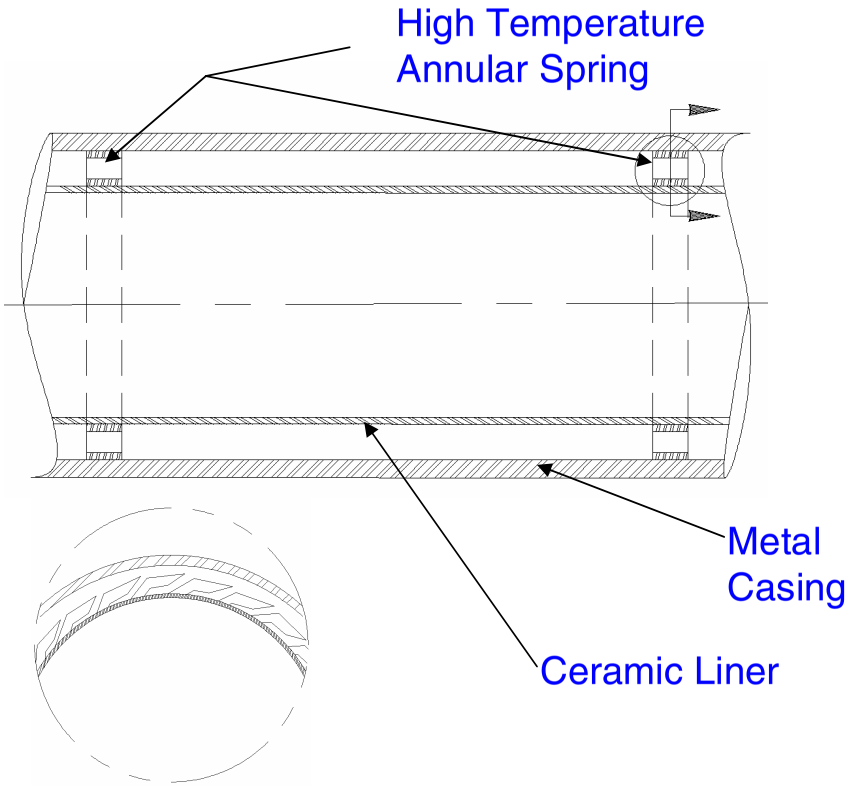

Low-load/ high deflection spring energizer for extremely high temperature (>2000F) ceramic sliding seal

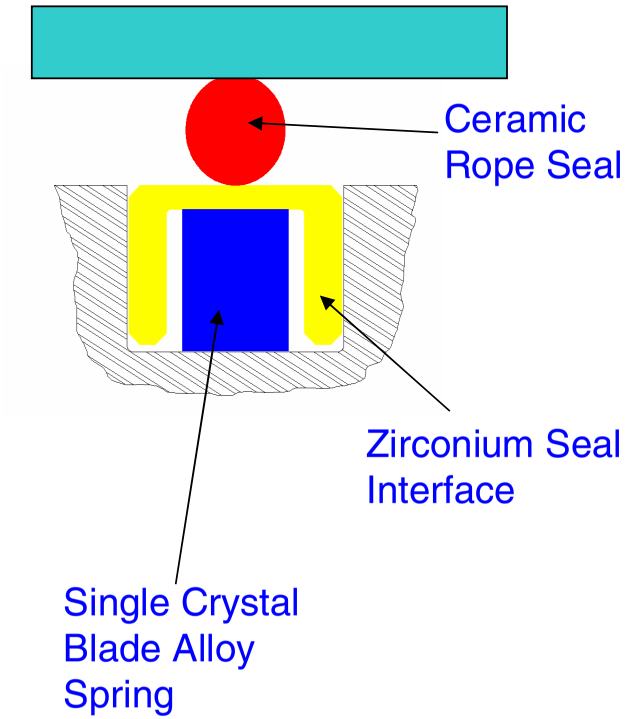

Conclusions

Advanced

- An innovative seal consisting of a blade alloy spring energizer and cold formable superalloy jacket can be designed for applications above 1500 °F
- The seal is expected to minimize cooling air and leakage thereby enhancing engine efficiency
- The design can be further improved with cast net shape single crystal springs attached to an easily machinable superalloy ring
- The single crystal spring structure can also be used where low load/ high deflection device is required for extremely high temperature applications

OXIDATION OF HIGH-TEMPERATURE ALLOY WIRES FOR HYBRID SEAL APPLICATIONS

Elizabeth J. Opila
National Aeronautics and Space Administration
Glenn Research Center
Cleveland, Ohio

Jonathan A. Lorincz
CON/SPAN
Dayton, Ohio

Marissa M. Reigel
Colorado School of Mines
Golden, Colorado

Jeffrey J. Demange
University of Toledo
Toledo, Ohio

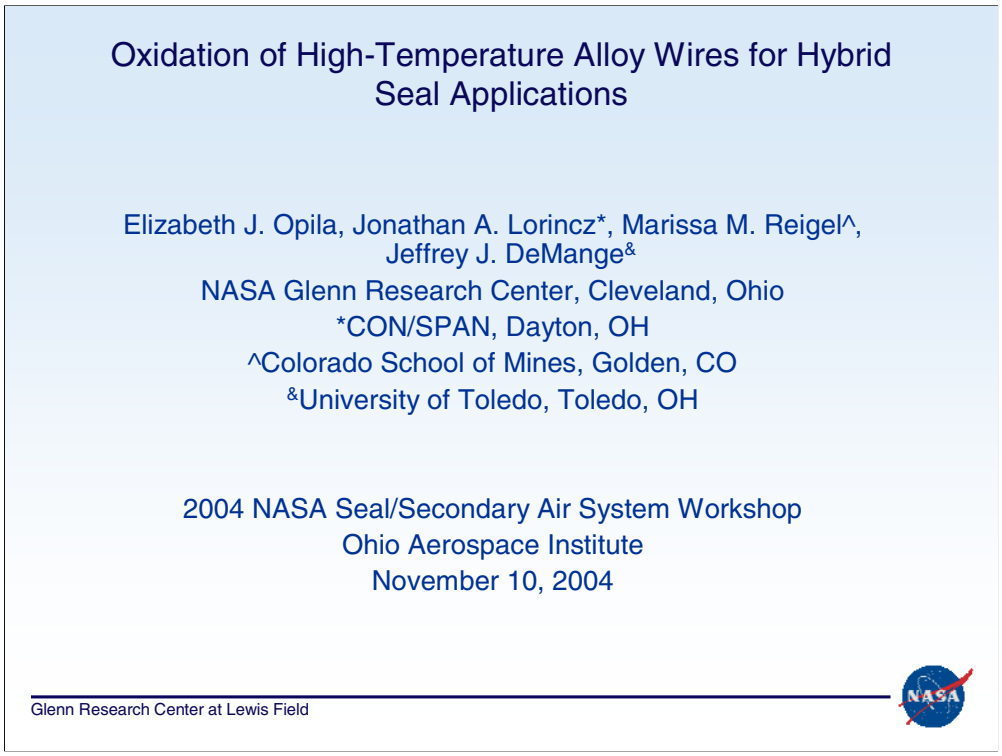

Small diameter wires (150 to 250 μm) of the high-temperature alloys Haynes 188, Haynes 230, Haynes 214, Kanthal A1 and PM2000 were oxidized at 1204 °C in dry oxygen or 50 percent H_2O/50 percent O_2 for 70 hours. The oxidation kinetics were monitored using a thermogravimetric technique. Additional cyclic oxidation exposures were conducted in air for one hour cycles at 1204 °C for times up to 70 hours. Oxide phase composition and morphology of the oxidized wires were determined by x-ray diffraction, field emission scanning electron microscopy, and energy dispersive spectroscopy. The alumina-forming alloys, Kanthal A1 and PM2000, out-performed the chromia-forming alloys under these test conditions. Correlations between oxidation lifetime and wire diameter were considered. PM2000 was recommended as the most promising candidate for advanced hybrid seal applications for space reentry control surface seals or hypersonic propulsion system seals.

Why study oxidation of wires?

Understanding of wire oxidation needed for development of advanced high-temperature seals for future hypersonic and reentry vehicles.

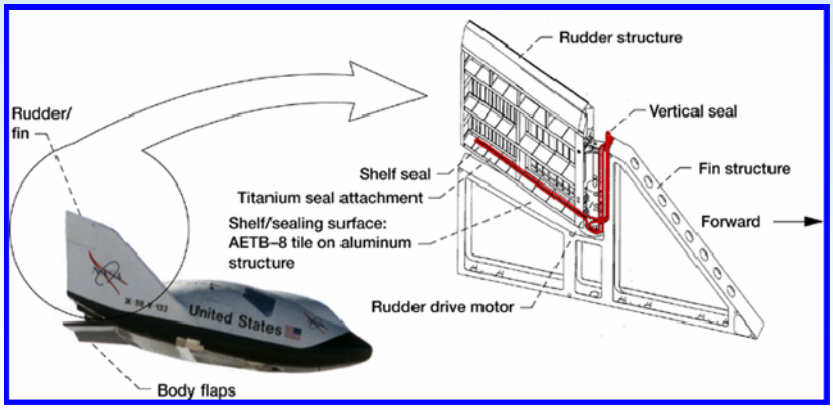

•Structural seal restricts hot gas leakage to underlying low-temperature control actuators

• Wire overwrap needed for wear resistance

State of the art hybrid seals

- T_{max}=800°C
- Ceramic batting or fiber core (alumina or aluminosilicate)
- Haynes 188 or 230 overwrap/overbraid, 40-125 micron diameter wire

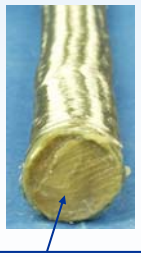

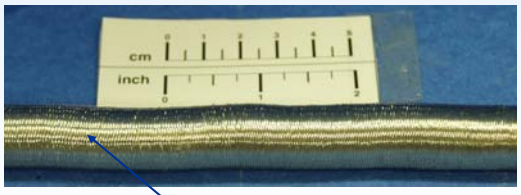

Haynes 230 overbraid

Nextel 312 fibers

Glenn Research Center at Lewis Field

Requirements for advanced hybrid seals

- Withstand temperatures up to 1400°C
- Operate without active cooling
- Flexible, resilient, wear resistant
- Airframe control surface seals
  - Reentry environment: reduced pressure air, plasma
  - Reusability of 10 to 100 cycles of 30 minutes each
- Hypersonic propulsion system seals
  - Propulsion environment: high pressure water vapor
  - Reusability of 1000 cycles of 250 sec/cycle (70 hours)

Objectives of this study

- Characterize isothermal and cyclic oxidation resistance of high-temperature alloy wires
- Guide selection of higher temperature alloys for hybrid seal applications

Glenn Research Center at Lewis Field

Alloy wires

Alloy	Composition, wt%	Diameter, μm
Haynes 188	Co base, 22 Cr, 22 Ni, 14 W, Fe< 3, Mn <1.25, 0.5 Si, 0.12 La, trace: C, B	250
Haynes 230	Ni base, 22 Cr, 14 W, Co<5, Fe<3, 2 Mo, 0.5 Mn, 0.4 Si, 0.3 Al, trace: C, La, B	250
Haynes 214	Ni base, 16 Cr, 4.5 Al, 3 Fe, 0.2 Si, trace: Mn, Zr, C, B, Y	250
Kanthal A1	Fe base, 22 Cr, 5.8 Al, Si<0.7, Mn<0.4	250
PM 2000	Fe base, 20 Cr, 5.5 Al, 0.5 Ti, 0.5 Y_2O_3	150

Glenn Research Center at Lewis Field

Haynes 188, and 230 are chromia forming alloys. Haynew 214 is a marginal alumina forming alloy. Kanthal A1 and PM2000 are alumina forming alloys. PM2000 contains the reactive element Y_2O_3 which improves oxide adherence.

Note smaller diameter wire for PM2000.

Experimental Procedure

- Coil 60 cm length of wire
- Oxidation of wires
  - 1204°C (2200°F)
  - 1 atm
  - 70h
  - Three exposure environments
    - Isothermal: O_2 (0.4 cm/sec)
    - Isothermal: 50% H_2O/50% O_2 (4.4 cm/sec)
    - Cyclic: stagnant air, 1h hot, 20 min. cool, 70 cycles
- Weight change of wires
- X-ray diffraction (XRD) analysis
- Field Emission-Scanning Electron Microscopy/Energy Dispersive Spectroscopy (FE-SEM/EDS)

Glenn Research Center at Lewis Field

Weight gain indicates oxide formation. Weight loss indicates loss of oxide by spallation or volatilization.

Thermogravimetric Analysis

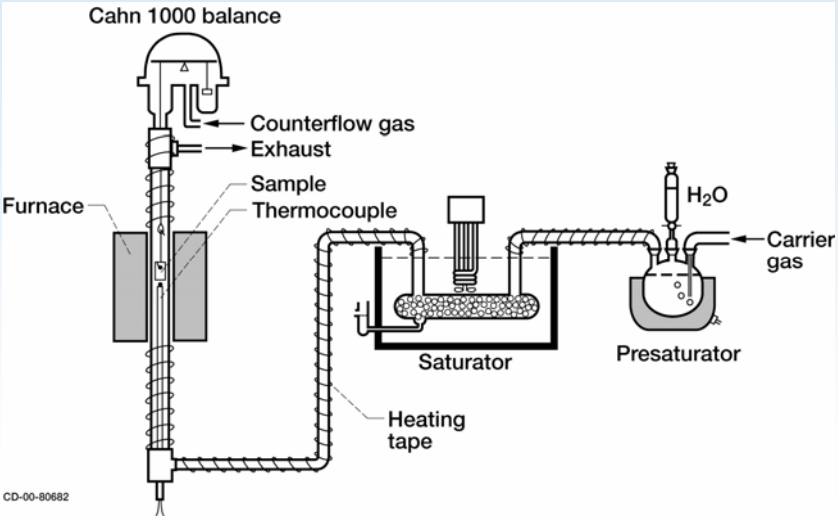

Cyclic Oxidation

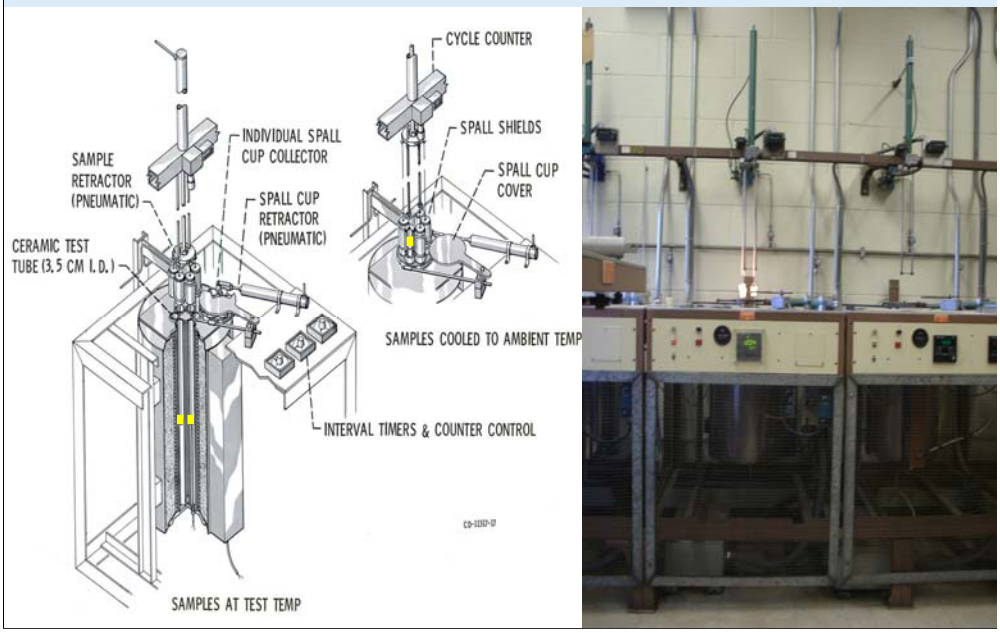

One cycle = 1 hour hot, 20 minute cool..

Results for wire oxidation in dry O_2

Glenn Research Center at Lewis Field

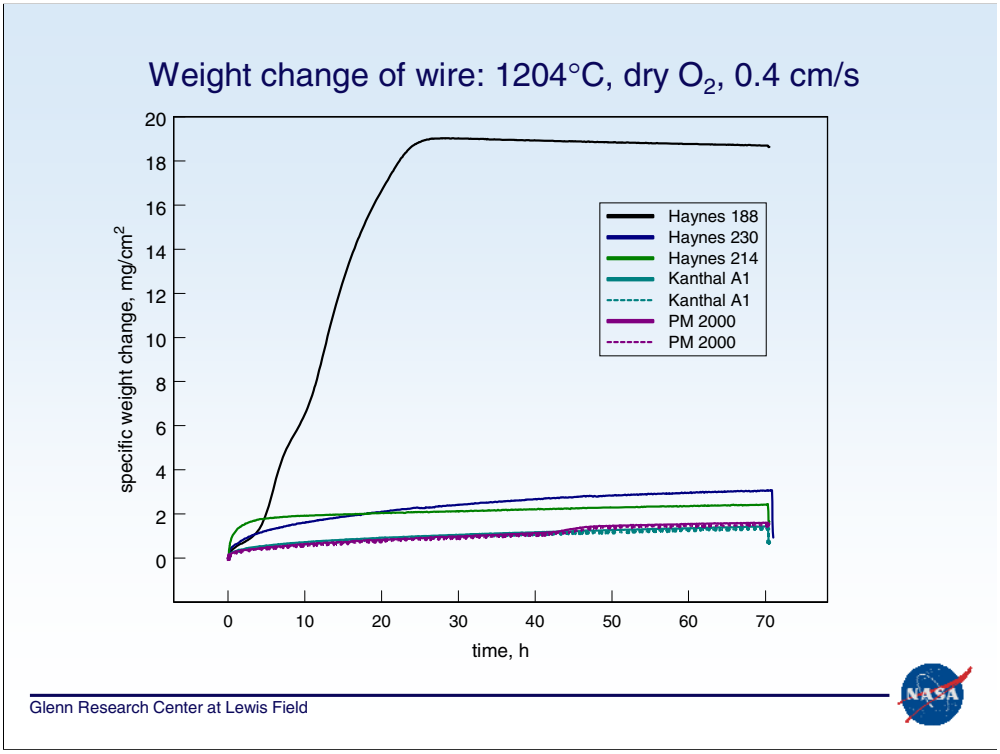

Haynes 188 completely oxidized after about 20 hours.

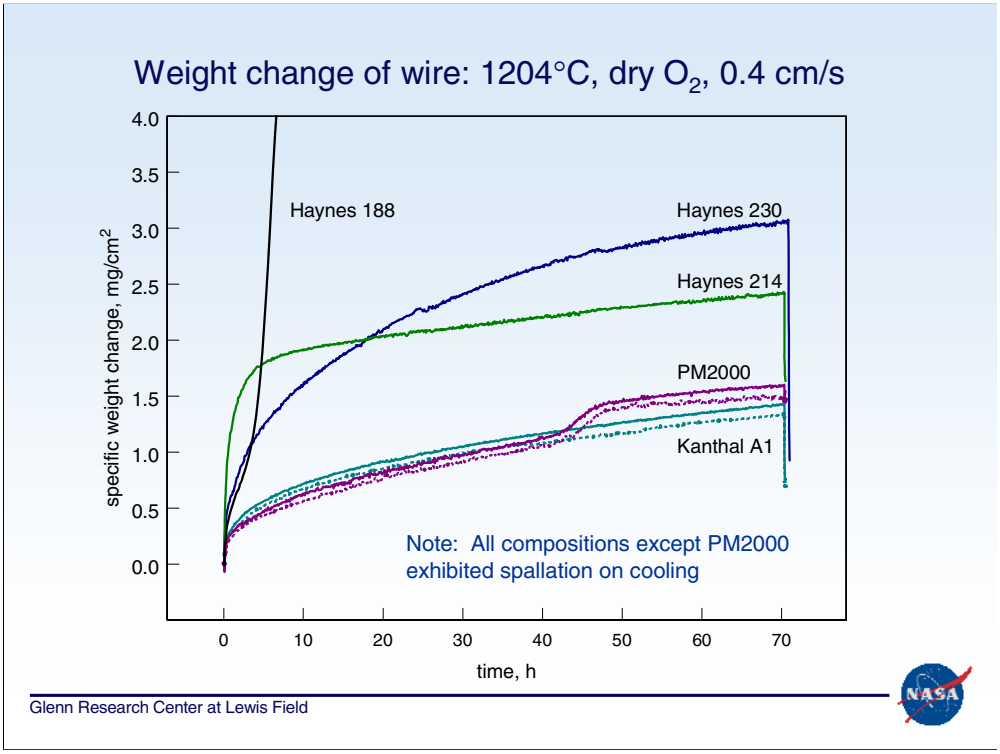

Haynes 230, PM2000, Kanthal A1 show desired parabolic oxidation kinetics.

Haynes 214 shows protective oxidation after initial transient of fast oxidation.

Bump in PM2000 kinetics at 45h may be due to depletion of alumina and beginning of chromia scale formation.

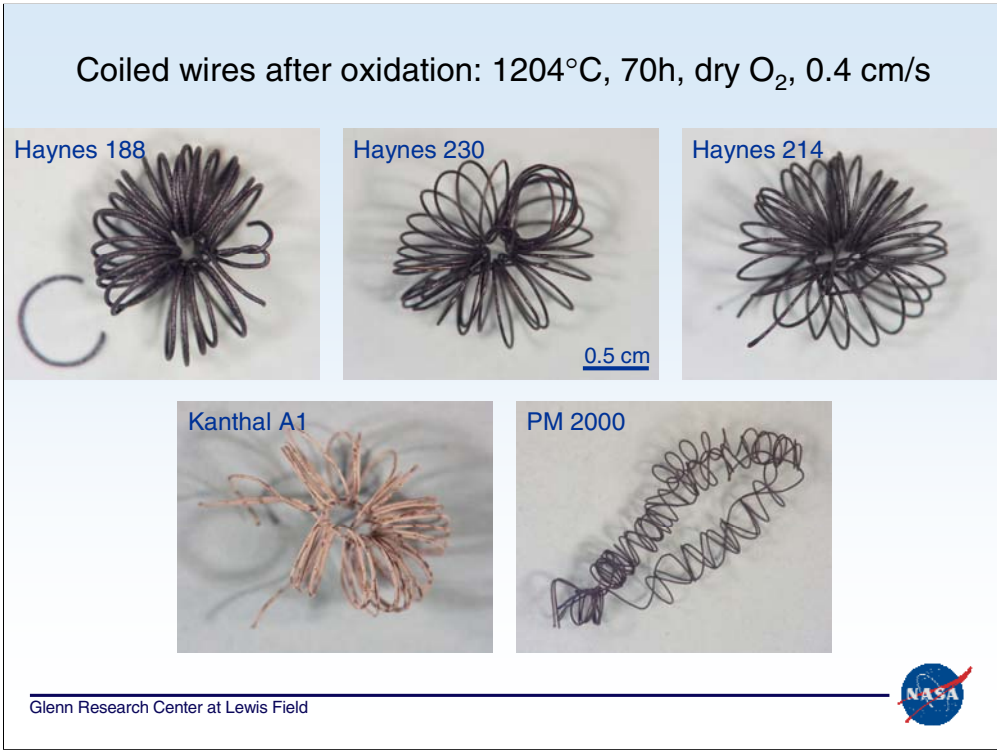

Haynes 188 brittle. Haynes 230, 214, Kanthal A1 show spallation to bare metal.

X-ray diffraction results for wires: 1204°C, 70h, dry O_2, 0.4 cm/s

Alloy	Major components of alloy, wt%	Oxidation products
Haynes 188	Co base, 22 Cr, 22 Ni, 14 W	$NiWO_4$ $NiCr_2O_4$ NiO
Haynes 230	Ni base, 22 Cr, 14 W	Cr_2O_3 $NiCr_2O_4$ NiO
Haynes 214	Ni base, 16 Cr, 4.5 Al	$NiCr_2O_4/NiAl_2O_4$ NiO
Kanthal A1	Fe base, 22 Cr, 5.8 Al	α Al_2O_3
PM 2000	Fe base, 20 Cr, 5.5 Al, 0.5 Y_2O_3	α Al_2O_3

Glenn Research Center at Lewis Field

Chromia formation not observed for Haynes 188 after 70h. Note presence of $NiWO_4$ oxide phase.

First three alloys show spinel (AB_2O_4) formation. This is not a protective oxide.

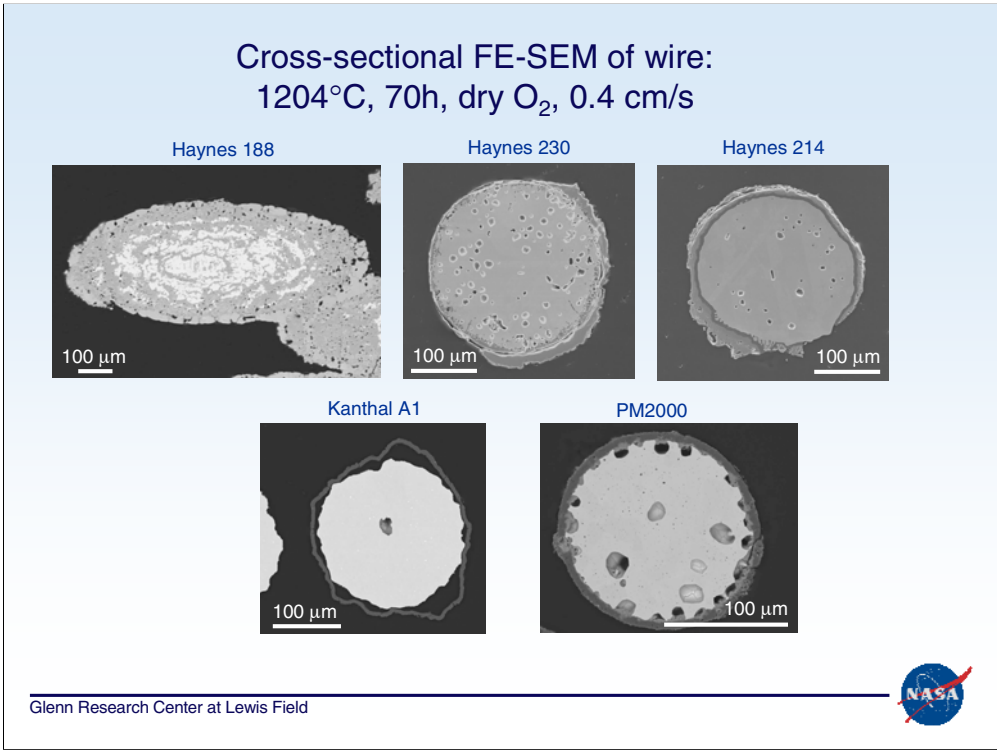

Haynes 188: (Co,Ni)O, CoCr2O4, CoWO4-bright phase. Wire completely consumed.

Haynes 230: Cr2O3

Haynes 214: Al2O3 inner layer, spinel outer layer, NiO blocks on surface

Kanthal A1: Oxide scale completely nonadherent.

Summary of results:
Wire oxidation 1204°C, 70h, dry O_2, 0.4 cm/s

- Haynes 188 completely oxidized
- Haynes 230 formed chromia scale, spalled on cool down
- Haynes 214 formed inner alumina scale, external spinel, NiO, spalled on cool down
- Kanthal A1 formed alumina scale, completely nonadherent after cool down
- PM2000 smaller diameter wire formed an adherent alumina scale, aluminum completely depleted from wire, inner discontinuous layer of chromia, internal void formation

Results for wire oxidation in 50% H_2O/50% O_2

Glenn Research Center at Lewis Field

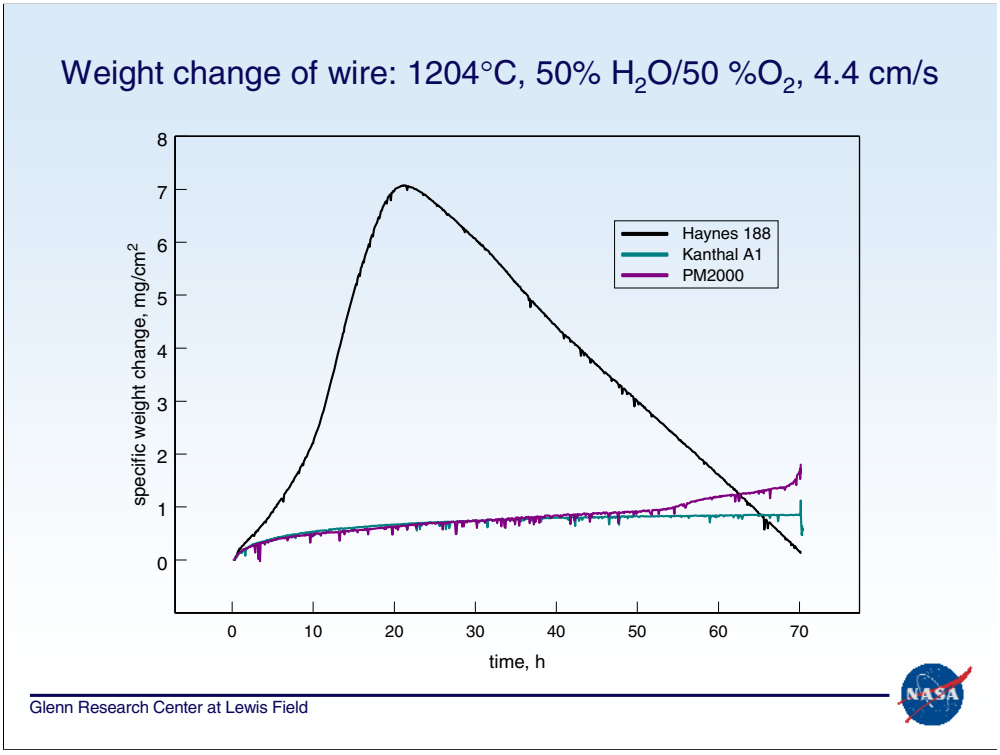

Different weight change behavior for Haynes 188 explained on next slide.

Weight change of Haynes 188 wire: 1204°C

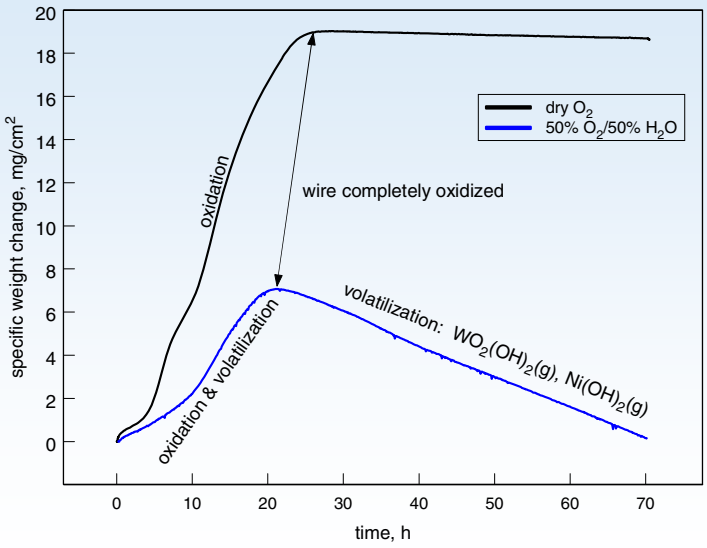

Glenn Research Center at Lewis Field

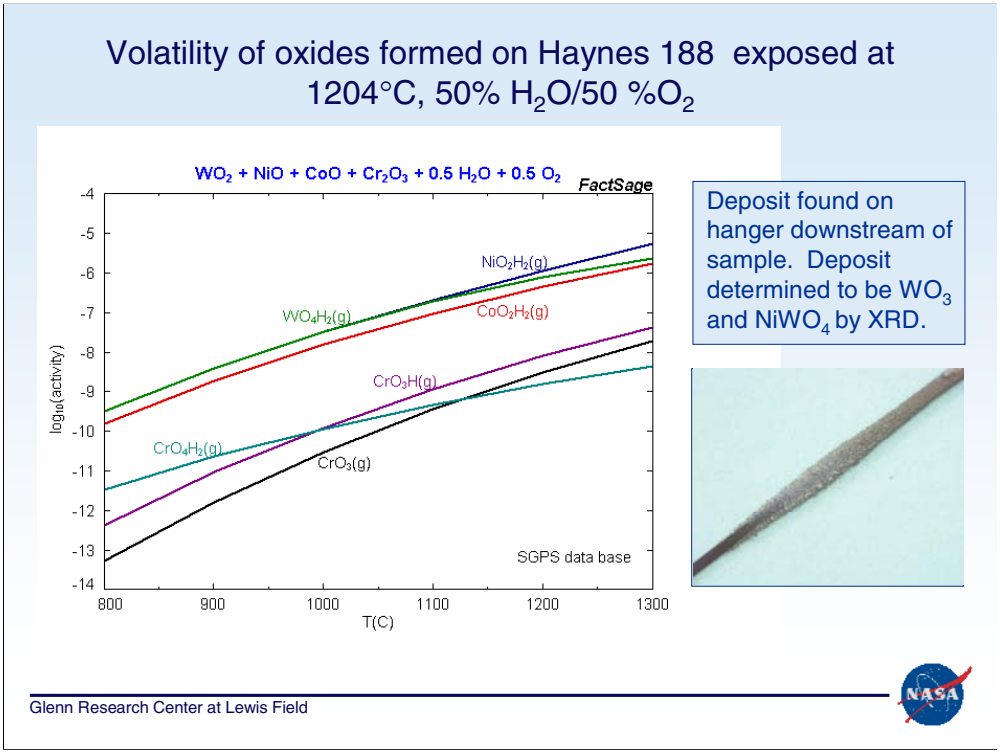

Calculated gas species formed from oxides in water vapor. W is very volatile.

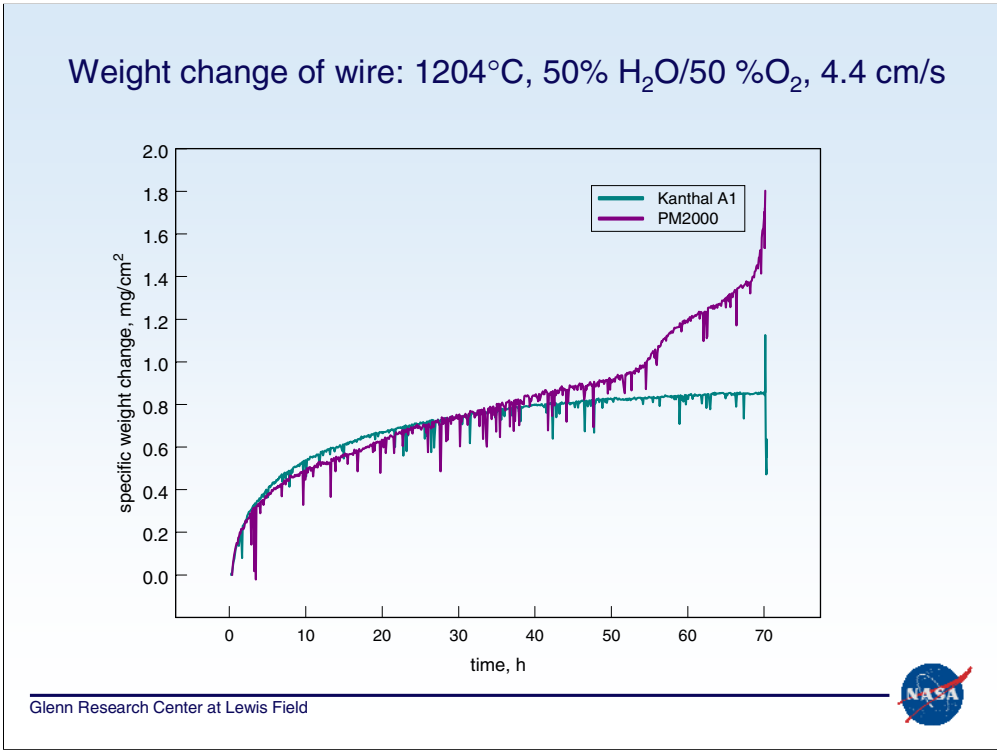

Breakaway oxidation for PM2000 at 68 h.

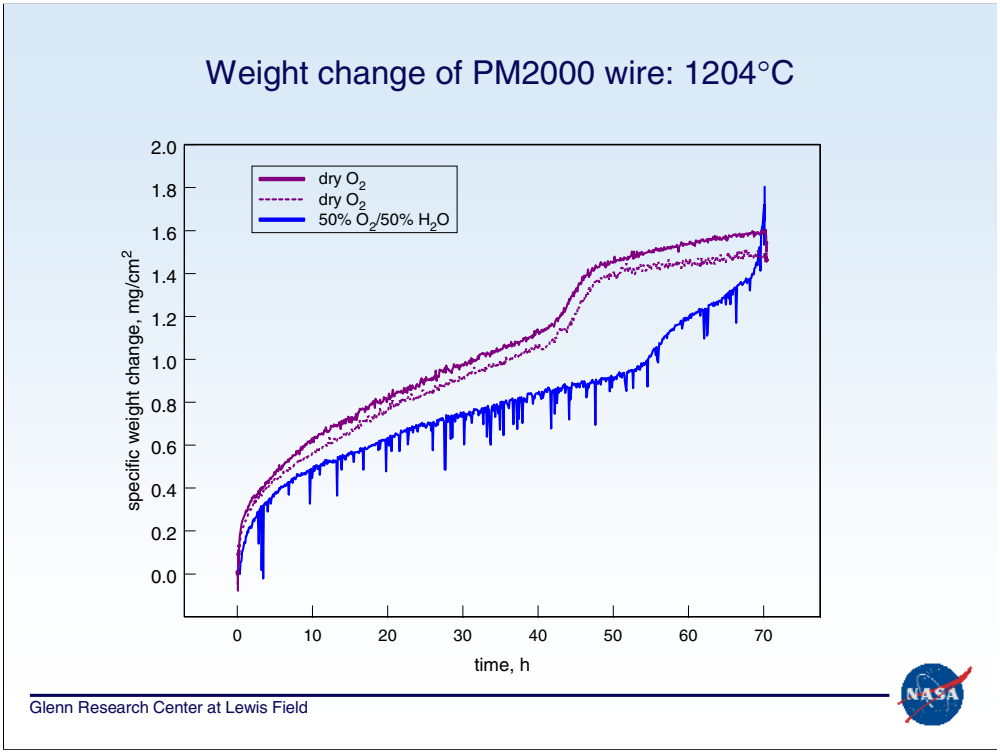
Weight change of PM2000 wire: 1204°C
dry O_2
dry O_2
50% O_2/50% H_2O
specific weight change, mg/cm^2
2.0
1.8
1.6
1.4
1.2
1.0
0.8
0.6
0.4
0.2
0.0
0
10
20
30
40
50
60
70
time, h
Glenn Research Center at Lewis Field
NASA

Correlation between breakaway oxidation and wire diameter

- Breakaway oxidation occurs when aluminum is depleted to low level: protective oxide scale formation no longer possible
- Aluminum depletion depends on ratio of wire volume to surface area.
  - Extrapolating time to breakaway for PM2000 at 1204°C in 50% H_2O for other wire diameters.

$$W_m \propto \frac{V}{A} = r \quad W_m \propto \sqrt{t}$$

$$\frac{t_a}{t_b} = \frac{r_a^2}{r_b^2}$$

W_m = weight of metal consumed during oxidation, V = wire volume, A = wire surface area, r = wire radius, t = oxidation time

  - Experimentally determined time to breakaway for 150 μm dia wire is 68h.
  - Predict time to breakaway for 250 μm dia wire is 189h for comparison to other alloy wires of 250 μm dia.
  - Predict time to breakaway for 40 μm dia wire at 5h for finest diameter wire proposed for use in seal applications.

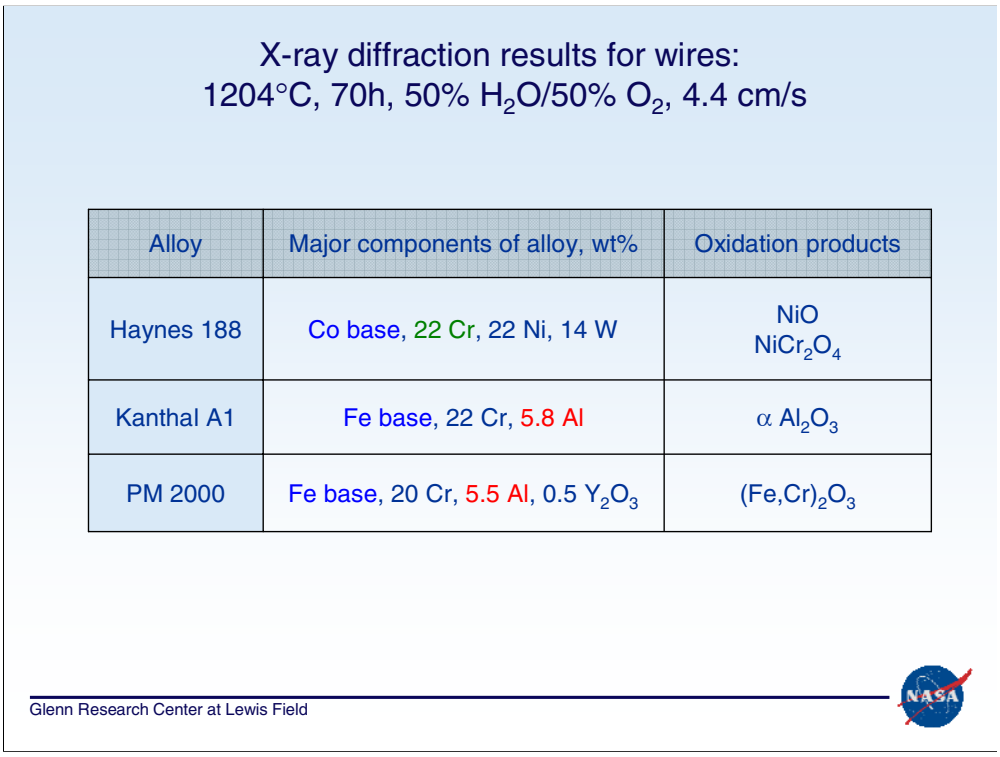

No W containing phase found on Haynes 188. W is completely volatilized.

Al2O3 not found on PM2000 after 70h in this environment in contrast to results in dry O2.

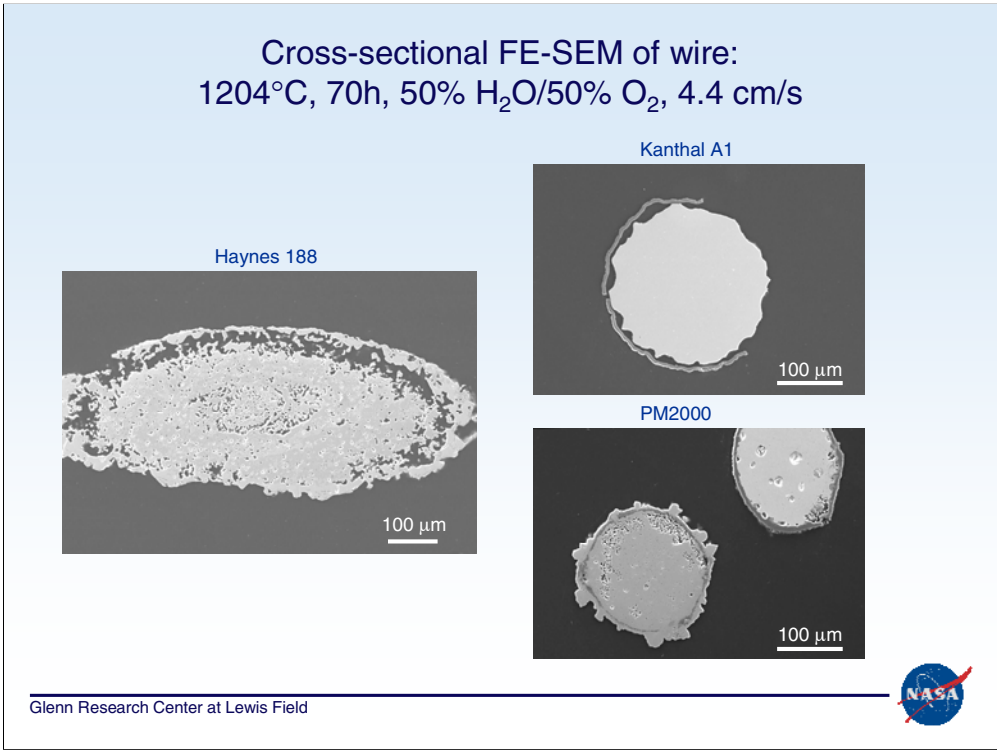

Porosity in Haynes 188 where $NiWO_4$ found after exposure in dry O2.

Oxide scale not adherent on Kanthal A1.

Adjacent cross-sections of PM2000 show one completely oxidized, the other metallic with nearly protective scale still intact.

Summary of results: Wire oxidation, 1204°C, 70h, 50% H_2O/50% O_2, 4.4 cm/s

- Haynes 188 completely oxidized, all W volatilized leaving porosity.
- Kanthal A1 formed alumina scale, completely nonadherent, much of scale spalled.
- PM2000 smaller diameter wire experienced breakaway oxidation. Portions of wire completely oxidized, show remainder of alumina scale. Portions of wire show protective alumina scale.
- Time to breakaway oxidation expected to vary with the square of the wire diameter.

Cyclic Oxidation Results

Glenn Research Center at Lewis Field

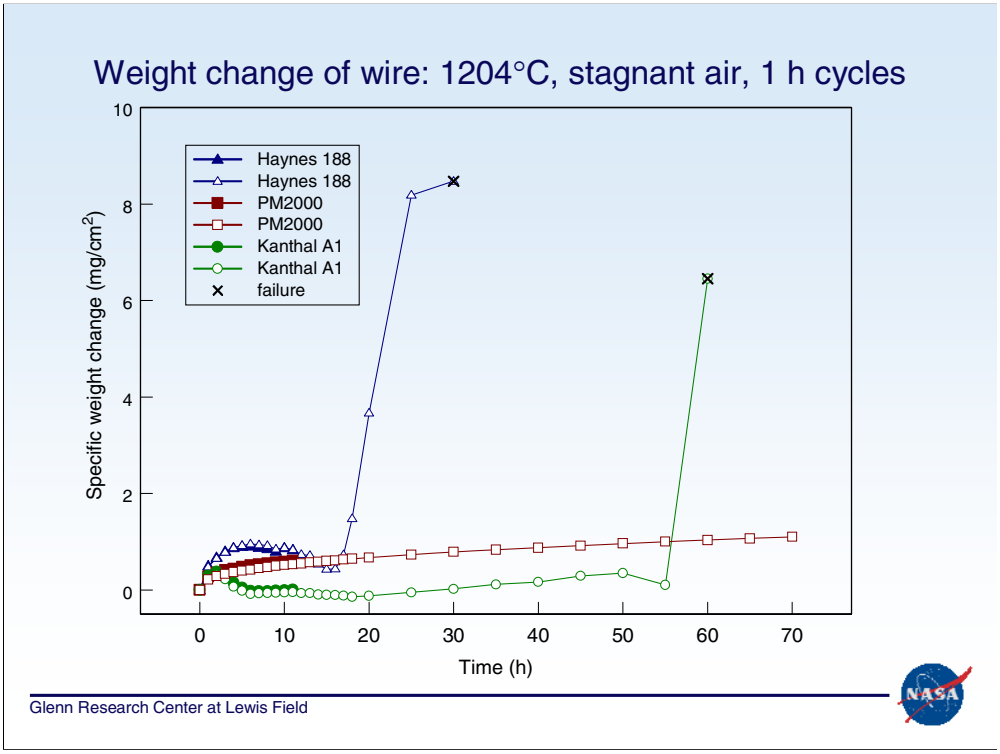

Haynes 188 weight change similar to isothermal exposures in that oxidation is about complete at 20h.

PM2000 showing parabolic oxidation to 60+ hours.

Kanthal A1 shows weight loss and spallation after third cycle. Breakaway oxidation at 55h.

X-ray diffraction results for wires: 1204°C, 1h cycles, stagnant air

Alloy	Major components of alloy, wt%	Time to failure, h	Oxidation products
Haynes 188	Co base, 22 Cr, 22 Ni, 14 W	30	(Ni,Co)O $(Ni,Co)Cr_2O_4$
Kanthal A1	Fe base, 22 Cr, 5.8 Al	60	Fe_2O_3
PM 2000	Fe base, 20 Cr, 5.5 Al, 0.5 Y_2O_3	>70	tbd

Glenn Research Center at Lewis Field

Non protective Fe2O3 found for Kanthal A1.

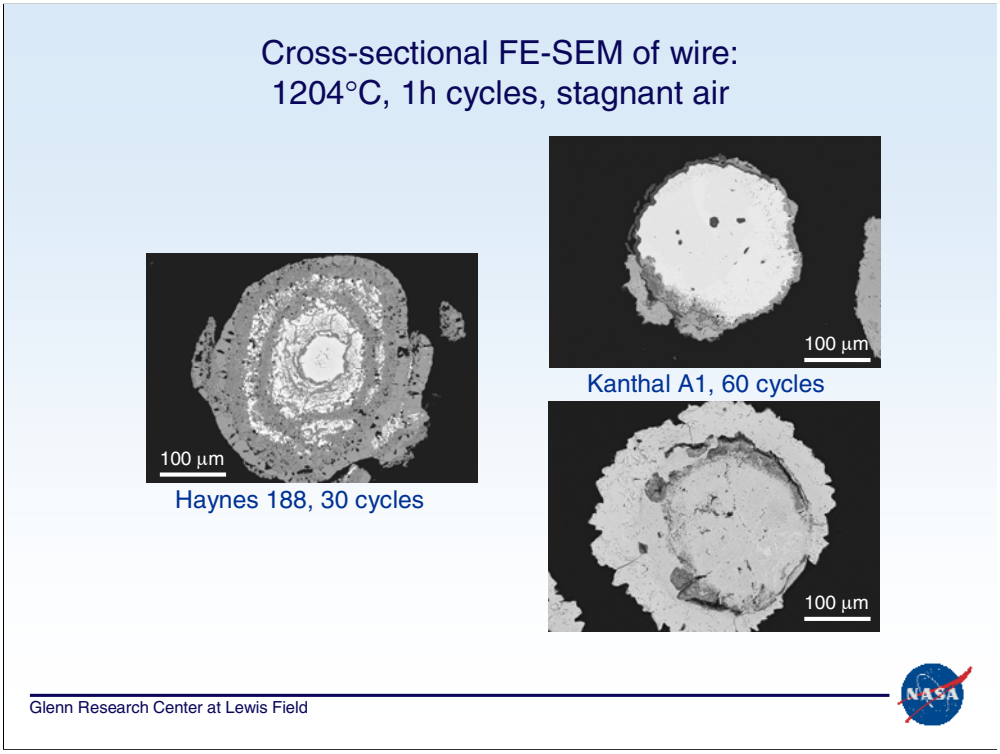

Haynes 188 shows core of wire still present after 30 cycles.

Kanthal A1 has some cross-sections just beginning non-protective oxide formation (top) and others completely oxidized (bottom). The original wire diameter of Kanthal A1 is marked by darker phases (alumina and chromia) in lower right micrograph.

Summary of results: Wire oxidation, 1204°C, 1h cycles, stagnant air

- Haynes 188 had similar failure time as in isothermal testing.
- Kanthal A1 failed earlier in cyclic oxidation testing. Weight loss and oxide spallation detected as early as third temperature cycle. Breakaway oxidation occurred after 55 cycles.
- PM2000 showed parabolic oxidation kinetics throughout 70h cyclic test. No evidence of spallation.

Conclusions

- Alumina-forming alloys with reactive element additions perform best at 1204°C under all test conditions: O_2, H_2O, temperature cycling
  - Slow growing oxide
  - Alumina is the most stable protective oxide scale in water vapor
  - Adherent scales
- Small diameter wires have limited oxidation lifetimes.
  - Limited reservoir of aluminum for protective scale formation
  - Smaller diameter wires more prone to spallation: increased stress in oxide due to larger radius of curvature
- Oxidation lifetimes can be predicted based on the wire diameter and rate of aluminum loss.
- From these results PM2000 is recommended as the best candidate for further development in advanced hybrid seal applications.

Acknowledgments

Jim Smialek, many helpful discussions
Ralph Garlick, X-ray diffraction
Patrick Dunlap, Bruce Steinetz, program support

This work was funded by the Next Generation
Launch Technology Program

Glenn Research Center at Lewis Field

2004 NASA Seal/Secondary Air System Workshop
Attendees

Last	First	Company	City	State	Zip	Phone	Email
Albers	Robert J.	General Electric	Cincinnati	OH	45215	513.243.7039	bob.albers@ae.ge.com
Assion	Joe	Analex Corp.	Cleveland	OH	44135	216.433.6712	jassion@grc.nasa.gov
Bauman	Steve	NASA Glenn Research Center	Cleveland	OH	44135	216.433.3826	steve.bauman@nasa.gov
Bill	Robert	NASA Glenn Research Center	Cleveland	OH	44135	216.433.3694	robert.c.bill@grc.nasa.gov
Bond	Bruce	Jackson Bond Enterprises, LLC	Rochester	NH	03867	603.335.7913	brucebond@earthlink.net
Bown	Charles	ATK Thiokol	Brigham City	UT	84302	435.279.6259	Charley.Bown@ATK.com
Boyle	Marcia	GE Aircraft Engines	Cincinnati	OH	45215	513.243.5315	Marcia.Boyle@ae.ge.com
Braun	Minel (Jack)	University of Akron	Akron	OH	44325	330.972.7734	mjbraun@uakron.edu
Breen	Dan	NASA Glenn Research Center	Cleveland	OH	44135	216.433.2660	daniel.p.breen@grc.nasa.gov
Cash	Carol	GE Aircraft Engines	North Olmsted	OH	44070	440.777.9545	carol.cash@ae.ge.com
Chen	Victor	The Boeing Company	Huntington Beach	CA	92647	714.896.4989	victor.chen@boeing.com
Christiansen	Richard	NASA Glenn Research Center	Cleveland	OH	44135	216.433.5308	Richard.Christiansen@nasa.gov
Chupp	Ray	GE Global Research	Niskayuna	NY	12302	518.387.7550	raymond.chupp@crd.ge.com
Cikanek	Harry	NASA Glenn Research Center	Cleveland	OH	44135	216.433.6196	harry.cikanek@nasa.gov
Clark	Stephen	Boeing	Seattle	WA	98124	425.237.1224	stephen.f.clark@boeing.com
Clarke	Dana	Applied Innovation Alliance, LLC	West Bloomfield	MI	48323	248.682.3368	dclarke@aia-consulting.com
Compton	Tom	GE Transportation	Evandale	OH	45215	513.243.2422	tom.compton@ae.ge.com
Daniels	Chris	NASA Glenn Research Center	Cleveland	OH	44135	216.433.6714	christopher.c.daniels@grc.nasa.gov
Datta	Amit	Advanced Components & Materials Inc.	E. Greenwich	RI	02818	401.885.5064	ADatta@worldnet.att.net
DeCastro	Jonathan	NASA Glenn Research Center	Cleveland	OH	44135	216.433.3946	jonathan.decastro@grc.nasa.gov
Delgado	Irebert	NASA Glenn Research Center	Cleveland	OH	44135	216.433.3935	irebert.r.delgado@nasa.gov
DeMange	Jeffrey J.	NASA Glenn Research Center	Cleveland	OH	44135	216.433.3568	Jeffrey.Demange@nasa.gov
DiCarlo	James	NASA Glenn Research Center	Cleveland	OH	44135	216.433.5514	james.a.dicarlo@nasa.gov
Dietzel	Bill	Flowserve FSD	Kalamazoo	MI	49001	269.226.3493	wdietzel@flowserve.com
Dimofte	Florin	Universary of Toledo	Cleveland	OH	44135	216.433.7468	florin.dimofte@nasa.gov
Dobek	Louis J.	Pratt and Whitney	East Hartford	CT	06108	860.565.3034	dobeklj@pweh.com
Dunlap	Pat	NASA Glenn Research Center	Cleveland	OH	44135	216.433.3017	patrick.h.dunlap@nasa.gov
Eberly	Eric	NASA Marshall Space Flight Center	MSFC	AL	35812	256.544.2092	eric.a.eberly@nasa.gov
Eppehimer	John	Stein Seal Company	Kulpsville	PA	19443	215.256.0201	JohnEppehimer@steinseal.com
Erker	Art	NASA Glenn Research Center	Cleveland	OH	44135	216.433.2911	arthur.erker@analex.com
Finkbeiner	Joshua	NASA Glenn Research Center	Cleveland	OH	44135	216.433.6080	joshua.finkbeiner@nasa.gov
Flaherty	Andrew	Flowserve Corp.	Temecula	CA	92590	951.719.4412	Aflaherty@Flowserve.com
Garrett	William	Powdermet Inc.	Euclid	OH	44117	216.404.0053x118	wrgarrett@powdermetinc.com
Garrison	Glenn	Stein Seal Company	Kulpsville	PA	19443	215.256.0607	glenngarrison@steinseal.com
Geisheimer	Jon	Radatec, Inc.	Atlanta	GA	30308	404.526.6037	jong@radatec.com
Ginty	Carol	NASA Glenn Research Center	Cleveland	OH	44135	216.433.3335	Carol.Ginty@nasa.gov
Giriunas	Julius	NASA Glenn Research Center	Cleveland	OH	44135	216.433.3794	julius.giriunas@nasa.gov
Giron	Mark	PerkinElmer Fluid Sciences	Beltsville	MD	20705	301.902.3648	mark.giron@perkinelmer.com
Goshorn	David	GE Aircraft Engines	Cincinnati	OH	45215	513.243.8164	david.goshorn@ae.ge.com
Gravereaux	Stephen J.	Advanced Products Company, Inc	North Haven	CT	06473	860.658.6200	sgravereaux@advpro.com
Grondahl	Clayton	CMG Tech, LLC	Rexford	NY	12148	518.371.5050	cmgtech@earthlink.net
Harmon	Crystal	Pratt & Whitney	North Olmsted	OH	44070	440.734.3990	crystal.harmon@pw.utc.com
Hendricks	Robert C.	NASA Glenn Research Center	Cleveland	OH	44135	216.977.7507	robert.c.hendricks@nasa.gov
Herron	William L.	General Electric	Cincinnati	OH	45215	513.243.7445	william.herron@ae.ge.com
Higgins	Mark	PerkinElmer Fluid Sciences	Beltsville	MD	20705	301.902.3645	mark.higgins@perkinelmer.com
Jackson	Hank	Jackson Bond Enterprises, LLC	Rochester	NH	03867	603.335.7913	
Justak	John F.	Advanced Technologies Group	Stuart	FL	34994	772.283.0253	jjustak@advancedtg.com
Keith	Theo G.	NASA Glenn Research Center	Cleveland	OH	44135	216.433.3944	theo.g.keith@nasa.gov

2004 NASA Seal/Secondary Air System Workshop
Attendees

Last	First	Company	City	State	Zip	Phone	Email
Kiser	J. Douglas	NASA Glenn Research Center	Cleveland	OH	44135	216.433.3247	James.D.Kiser@nasa.gov
Klamar	Joseph	JGK TechnoSystems	Hudson	OH	44236	330.656.3274	jgklamar@yahoo.com
Kraft	Thomas	NASA Glenn Research Center	Cleveland	OH	44135	216.433.2936	thomas.g.kraft@nasa.gov
Kroha	Michael	Flowserve	Kalamazoo	MI	49001	269.226.3428	mkroha@flowserve.com
Krumpelt	Michael	Argonne National Laboratory	Argonne	IL	60439	630.252.8520	krumpelt@cmt.anl.gov
Lattime	Scott	OAI - NASA Glenn Research Center	Cleveland	OH	44135	216.433.5953	scott.lattime@nasa.gov
Loewenthal	Robert	Advanced Components & Materials Inc.	Jamestown	RI	02835	401.423.1957	bobloew@cox.net
Makhobey	Mark	Car-Graph, Inc.	Tempe	AZ	85281	480.894.1356	mmakhobey@car-graph.com
McCall	Ryan	Garlock Helicoflex	Columbia	SC	29209	803.783.1880	ryan.mccall@garlock.com
Melis	Matthew	NASA Glenn Research Center	Cleveland	OH	44135	216.433.3322	Matthew.Melis@grc.nasa.gov
More	D. Greg	Advanced Products Company	North Haven	CT	06473	203.985.3141	gmore@advpro.com
Munson	John	Rolls Royce Corp.	Indianapolis	IN	46260	317.230.6409	John.H.Munson@Rolls-Royce.com
Nagpal	Vinod	N&R Engineering and Mangagment Services	Parma Hts.	OH	44130	440.845.7020	vnagpal@nrengineering.com
Opila	Elizabeth	NASA Glenn Research Center	Cleveland	OH	44135	216.433.8904	Elizabeth.Opila@nasa.gov
Oswald	Jay	Case Western Reserve U.	Cleveland	OH	44106	216.754.1808	jxo26@po.cwru.edu
Paolillo	Roger	Pratt & Whitney	East Hartford	CT	06108	860.557.1460	paolilre@pweh.com
Paquette	Ted	Refractory Composites, Inc.	Glen Burnie	MD	21060	410.768.2490	tedpaquette@rciusa.com
Parrish	Tom	Eaton Aeroquip	Jackson	MI	49202	517.789.4171	TomAParrish@eaton.com
Pendleton	Edmund	Air Force Research Lab/VASD	Wright Patterson AFB	OH	45433	937.255.7387	Edmund.Pendleton@wpafb.af.mil
Pickett	Paul	Solar Turbines, Inc.	San Diego	CA	92186	619.544.5420	pickett_paul_e@solarturbines.com
Pierson	Hazel M.	University of Akron	Akron	OH	44325	330.941.3017	hmpierson@ysu.edu
Proctor	Margaret	NASA Glenn Research Center	Cleveland	OH	44135	216.977.7526	margaret.p.proctor@nasa.gov
Rawlings	Christopher	Florida Turbine Technologies, Inc.	Jupiter	FL	33477	561.746.3317	crawlings@fttinc.com
Robbie	Malcolm	NASA Glenn Research Center	Cleveland	OH	44135	216.433.5490	malcolm.g.robbie@grc.nasa.gov
Robertson	Brandan	NASA Johnson Space Center	Houston	TX	77058	281.483.3732	brandan.r.robertson@nasa.gov
Roche	Brian	Stein Seal Company	Kulpsville	PA	19443	215.256.0201	brianroche@steinseal.com
Ruiz	Rafael	General Electric	Cincinnati	OH	45215	513.243.5364	rafael.ruiz@ae.ge.com
Sankovic	Denis	Radian Milparts	Eastlake	OH	44095	440.946.5921	denis@milparts.net
Shaughnessy	Dennis	Pratt & Whitney	East Hartford	CT	06108	860.557.1675	dennis.shaughnessy@pw.utc.com
Sherman	Andrew	Powdermet Inc.	Euclid	OH	44117	216.404.0053	powdermet@earthlink.net
Shi	Jun	United Technologies Research Center	East Hartford	CT	06108	860.610.1539	shij@utrc.utc.com
Smallwood	Drew	The Boeing Company	Huntington Beach	CA	92648	714.896.2098	Drew.Smallwood@boeing.com
Solomon	Dan	PerkinElmer Fluid Sciences	Beltsville	MD	20705	301.902.3442	dan.solomon@perkinelmer.com
Spoth	Kevin	Honeywell - Engines & Systems	Phoenix	AZ	85034	602.231.2524	kevin.spoth@honeywell.com
Stango	Robert	Marquette Univeristy	Milwaukee	WI	53233	414.288.6972	Robert.Stango@mu.edu
Steinetz	Bruce	NASA Glenn Research Center	Cleveland	OH	44135	216.433.3302	bruce.m.steinetz@nasa.gov
Taylor	Shawn	Case Western Reserve U.	Cleveland Hts.	OH	44106	216.320.1332	smt16@cwru.edu
Taylor	Thomas	Praxair Surface Technologies	Indianapolis	IN	46224	317.240.2614	Thomas_Taylor@praxair.com
Thomas	G. Richard	Bently Pressurized Bearing Company	Minden	NV	89423	775.783.4642	richard.thomas@bpb-co.com
Thomas	Mark D.	ATK Thiokol Inc	Brigham City	UT	84302	435.863.3582	mark.thomas@atk.com
Tritz	Terry	The Boeing Company	Seattle	WA	98124	425.234.5194	terrance.g.tritz@boeing.com
Turnquist	Norm	GE Global Research Center	Niskayuna	NY	12309	518.387.5978	turnquist@crd.ge.com
Valliere	Alan	Car-Graph, Inc.	Tempe	AZ	85281	480.894.1356	avalliere@car-graph.com
Virtue	John	Pratt & Whitney	East Hartford	CT	06450	860.565.4770	virtuej@pweh.com
Watts	O. A. (Bud)	Allison Advanced Development Co.	Indianapolis	IN	46202	317.230.6726	bud.watts@aadc.com
Yun	HeeMan	NASA Glenn Research Center	Cleveland	OH	44135	216.433.6089	heeman.yun@grc.nasa.gov
Zheng	Xiaoqing	PerkinElmer	Warwick	RI	02888	401.473.2274	Xiaoqing.Zheng@PerkinElmer.com

REPORT DOCUMENTATION PAGE

Form Approved
OMB No. 0704-0188

1. AGENCY USE ONLY (*Leave blank*)	2. REPORT DATE	3. REPORT TYPE AND DATES COVERED
	October 2005	Conference Publication

4. TITLE AND SUBTITLE

2004 NASA Seal/Secondary Air System Workshop

5. FUNDING NUMBERS

WBS–22–714–70–42

6. AUTHOR(S)

Bruce M. Steinetz and Robert C. Hendricks, editors

7. PERFORMING ORGANIZATION NAME(S) AND ADDRESS(ES)

National Aeronautics and Space Administration
John H. Glenn Research Center at Lewis Field
Cleveland, Ohio 44135–3191

8. PERFORMING ORGANIZATION REPORT NUMBER

E–15144–1

9. SPONSORING/MONITORING AGENCY NAME(S) AND ADDRESS(ES)

National Aeronautics and Space Administration
Washington, DC 20546–0001

10. SPONSORING/MONITORING AGENCY REPORT NUMBER

NASA CP—2005-213655–VOL1

11. SUPPLEMENTARY NOTES

Proceedings of a conference held at Ohio Aerospace Institute sponsored by NASA Glenn Research Center, Cleveland, Ohio, November 9–10, 2004. Responsible person, Bruce M. Steinetz, organization code RSM, 216–433–3302.

12a. DISTRIBUTION/AVAILABILITY STATEMENT

Unclassified - Unlimited
Subject Categories: 37, 16, and 99 Distribution: Nonstandard

Available electronically at http://gltrs.grc.nasa.gov

This publication is available from the NASA Center for AeroSpace Information, 301–621–0390.

12b. DISTRIBUTION CODE

13. ABSTRACT ***(Maximum 200 words)***

The 2004 NASA Seal/Secondary Air System workshop covered the following topics: (i) Overview of NASA's new Exploration Initiative program aimed at exploring the Moon, Mars, and beyond; (ii) Overview of the NASA-sponsored Ultra-Efficient Engine Technology (UEET) program; (iii) Overview of NASA Glenn's seal program aimed at developing advanced seals for NASA's turbomachinery, space, and reentry vehicle needs; (iv) Reviews of NASA prime contractor and university advanced sealing concepts including tip clearance control, test results, experimental facilities, and numerical predictions; and (v) Reviews of material development programs relevant to advanced seals development. The NASA UEET overview illustrated for the reader the importance of advanced technologies, including seals, in meeting future turbine engine system efficiency and emission goals. For example, the NASA UEET program goals include an 8- to 15-percent reduction in fuel burn, a 15-percent reduction in CO_2, a 70-percent reduction in NO_x, CO, and unburned hydrocarbons, and a 30-dB noise reduction relative to program baselines. The workshop also covered several programs NASA is funding to develop technologies for the Exploration Initiative and advanced reusable space vehicle technologies. NASA plans on developing an advanced docking and berthing system that would permit any vehicle to dock to any on-orbit station or vehicle, as part of NASA's new Exploration Initiative. Plans to develop the necessary mechanism and "androgynous" seal technologies were reviewed. Seal challenges posed by reusable re-entry space vehicles include high-temperature operation, resiliency at temperature to accommodate gap changes during operation, and durability to meet mission requirements.

14. SUBJECT TERMS	15. NUMBER OF PAGES
Seals; Turbine; Clearance control, Materials; Analyses; Experimental; Design, Docking mechanism; Leakage	400
	16. PRICE CODE

17. SECURITY CLASSIFICATION OF REPORT	18. SECURITY CLASSIFICATION OF THIS PAGE	19. SECURITY CLASSIFICATION OF ABSTRACT	20. LIMITATION OF ABSTRACT
Unclassified	Unclassified	Unclassified	